

https://dspace.org/

Lithostratigraphic modelling and framework of the Karoo coal and non-bearing strata in the Waterberg coalfield, South Africa

Mavanyisi, Ntsako Salthiel Gester

2024-07

University of the Witwatersrand, Johannesburg

https://hdl.handle.net/10539/49416

Mavanyisi, Ntsako Salthiel Gester. (2024). Lithostratigraphic modelling and framework of the Karoo coal and non-bearing strata in the Waterberg coalfield, South Africa. [Master's dissertation, University of the Witwatersrand, Johannesburg]. WIReDSpace. https://hdl.handle.net/10539/49416

Downloaded from a DSpace repository. https://dspace.org/



LITHOSTRATIGRAPHIC MODELLING AND FRAMEWORK OF THE KAROO COAL AND NON–COAL BEARING STRATA IN THE WATERBERG COALFIELD, SOUTH AFRICA

By

Ntsako Salthiel Gester Mavanyisi

(0502556G)

Dissertation

Submitted in fulfilment of the requirements for the degree

Magister Scientiae

in

GEOLOGY

in the Faculty of Science, University of the Witwatersrand, Johannesburg, South Africa

July, 2024

DECLARATION

I declare that this dissertation is my own, unaided work. It is submitted for a Master of Science Degree at the University of the Witwatersrand, Johannesburg. It has never been submitted for any examination or degree at another university.



(N.S.G. Mavanyisi)

31st day of July 2024

ABSTRACT

The Waterberg Coalfield is located 340 km in the north-western part of South Africa, in Limpopo Province, north-west of Johannesburg, north of the Waterberg Mountains. It extends westwards into Botswana, joining the Kalahari Karoo Basin. The study involved 3D lithostratigraphic facies modelling, interpretations of coal seam geometry, structural interpretations, and coal and non-coal seam grid analyses (thickness and quality) at the Waterberg Coalfield. This approach presents additional information on the characteristics of the coalfield, supporting findings and theories proposed in previous research work, by bringing three-dimensional visualization and interpretation. Sparsely distributed boreholes (757), comprising lithological units, defined coal and non-coal zones with laboratory sample analyses were used as the building blocks of the 3D lithostratigraphic facies model using GEOVIA Minex™ 6.1.1 geological modelling software. The coal analyses were displayed and processed in ESRI® ArcGIS™ 10.2 software. Using these industry-recognised software applications, processing, interpretation, and presentation of the geological data was achievable. Coal and non-coal zone thicknesses, quality distributions, cross-sections depicting geometries of the sedimentary strata, and stratigraphy of the Waterberg Coalfield were created and interpreted. The bituminous coal analysed is highly shaley and of a low grade; with raw qualities on weighted average - Calorific Value: 9.77MJ/kg; Inherent Moisture: 2.06%; Ash: 45.63%; Volatile Matter: 21.59%; Fixed Carbon: 25.49%; Total Sulphur: 0.93% and Phosphorus: 0.02%. The model reveals that the Waterberg Coalfield experienced more structural disturbance than initially postulated. Post-depositional, delineated upthrow and downthrow faults 1 to 7, occurring much deeper into the Waterberg Coalfield, were identified from the cross-sections and isopach maps. Multiple step faults and folds occur throughout the coalfield, subdividing it into deeper central blocks and shallower outer edge blocks.

Keywords: Karoo Supergroup, Main Karoo Basin, Waterberg Coalfield, 3D Lithostratigraphic Facies Modelling, Lithofacies Analysis.

ACKNOWLEDGEMENTS

My sincere appreciation to:

- The Almighty God—to Him be the glory.
- My parents, Mr P.C.G. Mavanyisi and Mrs J.V. Mavanyisi, for their sacrifices in my upbringing.
- My wife Kathy, sons Muhluri and Ntlhari, and daughters Lulama and Enelo Mavanyisi for their support, love, patience, and inspiration during the time taken to complete this research.
- Prof G. Drennan, Head of School: Geoscience at Witwatersrand University, for her unprecedented support towards student affairs and guidance in the research.
- Mr Hennie van Der Berg, Former Head of Geosciences Exxaro Resources (Pty) Ltd and Mr Henk Lingenfelder, Current Head of Geosciences Exxaro Resources (Pty) Ltd., for granting permission to access and use geological information for the research.
- Mr Claris Dreyer (former Chief Coal Geologist_Grootegeluk Mine), for his great humility, training, and sharing knowledge about the Waterberg Coalfield.
- Mrs Marietjie Schalekamp (Database Manager-Coal and Coredata) from the Council for Geoscience (Pretoria), who afforded me access to borehole information, essential to the research.

CONTENTS

DECLARATION .....
ABSTRACT i
ACKNOWLEDGEMENTS ii
CONTENTS iii
LIST OF FIGURES vii
LIST OF TABLES xvi
Chapter 1 : INTRODUCTION 1
1.1. Preamble 1
1.2 Literature Review 2
1.3 Aims And Objectives of Study 4
1.4 Methodology 5
1.4.1 GEOVIA Minex™ 6.1.1 Geological Modelling Software 5
1.4.2 ESRI® ArcGIS™ 10.2 Software 6
1.5 Study Outline 7
Chapter 2 : GEOLOGY 8
2.1 Introduction 8
2.2 Location 9
2.3 Tectonic Setting 10
2.4 Structural Geology 11
2.5 Regional Geology 14
2.5.1 Karoo Supergroup 14
2.5.1.1 Main Karoo Basin 15
2.5.2 Stratigraphy of The Waterberg Coalfield 18
2.5.2.1 Waterkloof Formation 19
2.5.2.2 Wellington Formation 20
2.5.2.3 Swartrant Formation 20
2.5.2.4 Goedgedacht Formation 21
2.5.2.5 Grootegeluk Formation 21
2.5.2.6 Eendragtpan Formation 22

2.5.2.7 Greenwich Formation 22
2.5.2.8 Lisbon Formation 22
2.5.2.9 Clarens Formation 23
2.5.2.10 Letaba Formation 23
Chapter 3 : WATERBERG COALFIELD LITHOSTRATIGRAPHIC FACIES ANALYSIS AND INTERPRETATIONS 24
3.1 Introduction 24
3.2 Sedimentary Facies 24
3.3 Sample Boreholes Across The Study Area 25
3.4 Lithofacies Description and Interpretation 31
3.4.1 Sandstone lithofacies 33
3.4.1.1 Massive sandstone sub-lithofacies 33
3.4.1.2 Planar cross-bedded sandstone sub-lithofacies 35
3.4.1.3 Cross-laminated sandstone sub-lithofacies 36
3.4.2 Mudstone lithofacies 38
3.4.2.1 Multi-coloured mudstone sub-lithofacies 38
3.4.2.2 Massive mudstone sub-lithofacies 39
3.4.2.3 Horizontally laminated mudstone sub-lithofacies 41
3.4.2.4 Gritty mudstone sub-lithofacies 42
3.4.3 Siltstone lithofacies 44
3.4.3.1 Lenticular laminated siltstone sub-lithofacies 44
3.4.4 Coal lithofacies 45
3.4.4.1 Intercalated bright and dull coal sub-lithofacies 45
3.4.4.2 Coal-mudstone sub-lithofacies 47
3.4.5 Mixed facies 49
3.4.5.1 Wavy laminated sandstone-mudstone sub-lithofacies 49
3.4.5.2 Interlaminated sandstone-mudstone-coal sub-lithofacies 51
Chapter 4 : SEDIMENTARY MODELLING 53
4.1 Introduction 53
4.2 Lithostratigraphic Facies Modelling 54

4.3 Common Modelling Software Packages 58
4.5 Inverse-Distance Weighted Method (IDW)..... 62
4.6 Geomodelling Steps on Minex Modelling Software..... 62
Chapter 5 : RESULTS AND INTERPRETATIONS OF THE LITHOSTRATIGRAPHIC MODEL..... 65
5.1 Introduction..... 65
5.2 Topographic Map of The Waterberg Coalfield 65
5.3 Overburden, Coal, And Non-coal Zone, And Interbed Distribution In The Waterberg Coalfield..... 68
5.3.1 Overburden Thickness (OVB) 70
5.3.2 Coal Zone 11_Seam Thickness (CZ11) 72
5.3.3 Coal Zone 10_Seam Thickness (CZ10) 74
5.3.4 Coal Zone 9_Seam Thickness (CZ9) 76
5.3.5 Coal Zone 8_Seam Thickness (CZ8) 78
5.3.6 Coal Zone 7_Seam Thickness (CZ7) 80
5.3.7 Coal Zone 6_Seam Thickness (CZ6) 82
5.3.8 Coal Zone 5_Seam Thickness (CZ5) 84
5.3.9 Coal Zone 4_Seam Thickness (CZ4) 86
5.3.10 Mudstone 2_Interbed Thickness (MS2)..... 88
5.3.11 Coal Zone 4A_Seam Thickness (CZ4A) 90
5.3.12 Mudstone 1_Interbed Thickness (MS1)..... 92
5.3.13 Coal Zone 3_Seam Thickness (CZ3) 94
5.3.14 Sandstone 2_Thickness (SS2)..... 96
5.3.15 Coal Zone 2_Seam Thickness (CZ2) 98
5.3.16 Sandstone 1_Thickness (SS1)..... 100
5.3.17 Coal Zone 1_Seam Thickness (CZ1) 102
5.4 Geological Cross-Sections..... 104
5.4.1 Geological cross-section interpretations..... 105
5.4.2 North-south cross-sections (1; 2; 3; 4; 5) 108
5.4.3 West-east cross-sections (6; 7; 8; 9; 10)..... 118
5.5 Geological Fault Modelling..... 128

5.5.1 Fault modelling 128
5.5.2 Fault interpretation 128
5.5.3 Coal Zone 1 floor contour grid (the bottommost coal zone) 130
5.6 3D Lithostratigraphic Facies Model 131
Chapter 6 : DISCUSSION 134
6.1 Lithostratigraphy and Deposition 134
6.1.1 Swartrant Formation 134
6.1.2 Grootegeluk Formation 135
6.1.3 Eendragtpan Formation 137
6.2 Geological Cross-Sections 138
6.2.1 Evidence from north-south cross-sections (1; 2; 3; 4; 5) 139
6.2.2 Evidence from west-east cross-sections (6; 7; 8; 9; 10) 139
Chapter 7 : SUMMARY AND CONCLUSIONS 140
7.1 SUMMARY 140
7.2 CONCLUSIONS 141
REFERENCES 144
APPENDICES 156
APPENDIX A: COAL ZONES, COAL SAMPLES AND NON-COAL SAMPLES 156
APPENDIX B: RAW QUALITY DISTRIBUTION PLANS 169
APPENDIX C: ISOPACH FLOOR GRIDS FOR THE OVB AND THE COAL ZONES ACROSS 205
APPENDIX D: WATERBERG COALFIELD COLUMNAR SECTIONS ... 214

LIST OF FIGURES

Figure 2.1: Coalfields in South Africa, circled in red is the Waterberg Coalfield (modified after Hancox & Götz, 2014). 9

Figure 2.2: The Karoo Foreland Basin and other south-western Gondwanan depocentres of the Karoo age (Hancox & Götz, 2014)..... 11

Figure 2.3: Position of the Ellisras Basin and the Waterberg Coalfield on the 2326 Ellisras 1:250 000 sheet, major faults, and structural lineaments are depicted (after Fourie et al., 2014). 13

Figure 2.4: Main Karoo Basin and the Kalahari Basin in Southern Africa, in relation to the Ellisras Basin (Waterberg Coalfield, circled in red). Modified from Catuneanu et al. (2005). 15

Figure 2.5: Main Karoo Foreland Basin in relation to the Cape Fold Belt, the subduction zone and magmatic arc in the south (Nxumalo, 2011)..... 16

Figure 2.6: Lithostratigraphic units and correlation of the Main Karoo Basin and its sub-basins (Catuneanu et al., 2005). 18

Figure 2.7: The stratigraphy of the Waterberg Coalfield. 19

Figure 3.1: Udden-Wentworth grain-size scale for categorization of sedimentary rocks (Nichols, 2009)..... 25

Figure 3.2: Sample boreholes drilled from the Waterberg Coalfield..... 26

Figure 3.3: Project sample borehole CA217LQ5. 27

Figure 3.4: Project sample borehole DR213LQ3. 28

Figure 3.5: Project sample borehole PE216LQ7..... 29

Figure 3.6: Project sample borehole SN245LQ3. 30

Figure 3.7: Project sample borehole VN310LQ3. 31

Figure 3.8: Massive sandstone (Sm) sub-lithofacies comprise coarse-grained, highly competent, and tightly packed quartz grains. 34

Figure 3.9: Planar cross-bedded sandstone (Sp) sub-lithofacies, with planar-bedded mica bands across the unit. 35
Figure 3.10: Cross-laminated sandstone sub-lithofacies (Sr) showing flaser and wavy stratification across the sandstone unit. 37
Figure 3.11: Multi-coloured mudstone (Fm) sub-lithofacies is fractured and highly weathered. 38
Figure 3.12: Massive mudstone (Fm) sub-lithofacies is slightly carbonaceous. 40
Figure 3.13: Horizontally laminated mudstone (Fh) sub-lithofacies capped sharply by coal. 41
Figure 3.14: Gritty mudstone (F_d) sub-lithofacies comprise fine carbonaceous bands and lenses, closely packed quartz grains appear as sandstone grit. 43
Figure 3.15: Lenticular laminated siltstone (Fsn) sub-lithofacies comprising fine to medium-grained sandstone laminae throughout the unit. 44
Figure 3.16: Intercalated bright and dull coal sub-lithofacies appear as alternating bands across the unit. 46
Figure 3.17: Coal-mudstone (c-Fm) sub-lithofacies comprise a carbonaceous mudstone with interbedded coal bands with calcite veins. 48
Figure 3.18: Wavy laminated sandstone-mudstone (Sw) sub-lithofacies demonstrate a wavy carbonaceous mudstone across the sandstone unit. 50
Figure 3.19: Interlaminated sandstone-mudstone-coal (Sh/Fl/C) sub-lithofacies appear as intercalated units with bioturbation, commonly within the coalfield. 52
Figure 4.1: Overview of the geological modelling process (Turner & Gable, 1994). 56
Figure 4.2: Principles for the suggested modelling technique, depicted schematically (Popovs et al., 2014). 58

Figure 4.3: Borehole-surface-solid modelling steps (Caumon & Mallet, 2006)..... 64
Figure 5.1: The Waterberg Coalfield topographical map (DTM). 67
Figure 5.2: Overburden (OVB) thickness distribution across the Waterberg Coalfield. 71
Figure 5.3: Coal Zone 11 (CZ11) seam thickness distribution across the Waterberg Coalfield. 73
Figure 5.4: Coal Zone 10 (CZ10) seam thickness distribution across the Waterberg Coalfield. 75
Figure 5.5: Coal Zone 9 (CZ9) seam thickness distribution across the Waterberg Coalfield. 77
Figure 5.6: Coal Zone 8 (CZ8) seam thickness distribution across the Waterberg Coalfield. 79
Figure 5.7: Coal Zone 7 (CZ7) seam thickness distribution across the Waterberg Coalfield. 81
Figure 5.8: Coal Zone 6 (CZ6) seam thickness distribution across the Waterberg Coalfield. 83
Figure 5.9: Coal Zone 5 (CZ5) seam thickness distribution across the Waterberg Coalfield. 85
Figure 5.10: Coal Zone 4 (CZ4) seam thickness distribution across the Waterberg Coalfield. 87
Figure 5.11: Mudstone 2 (MS2) interbed thickness distribution across the Waterberg Coalfield. 89
Figure 5.12: Coal Zone 4A (CZ4A) seam thickness distribution across the Waterberg Coalfield. 91
Figure 5.13: Mudstone 1 (MS1) interbed thickness distribution across the Waterberg Coalfield. 93
Figure 5.14: Coal Zone 3 (CZ3) seam thickness distribution across the Waterberg Coalfield. 95
Figure 5.15: Sandstone 2 (SS2) thickness distribution across the Waterberg Coalfield. 97

Figure 5.16: Coal Zone 2 (CZ2) seam thickness distribution across the Waterberg Coalfield. 99
Figure 5.17: Sandstone 1 (SS1) thickness distribution across the Waterberg Coalfield. 101
Figure 5.18: Coal Zone 1 (CZ1) seam thickness distribution across the Waterberg Coalfield. 103
Figure 5.19: Horizons algorithm with cross-sectional data (adopted from Lemon & Jones et al., 2003). 105
Figure 5.20: Ten (10) most representative cross-sections constructed across the Waterberg Coalfield. 107
Figure 5.21: Cross-Section 1 depicts sympathetic block faulting concentrated between boreholes KR1919951 and DE1919952. 109
Figure 5.22: Cross-Section 2 depicts a graben structure as observed with a sudden change in elevation between the projected faults. 111
Figure 5.23: Cross-Section 3 depicts the Zoetfontein Fault with ~180m displacement, with the Daarby Fault towards the south. ... 113
Figure 5.24: Cross-Section 4 depicts a palaeo-uplift towards the south of the coalfield. 115
Figure 5.25: Cross-Section 5 depicts a palaeo-floor upliftment and deficient coal deposition by borehole ML1920052. 117
Figure 5.26: Cross-Section 6 depicts non-coal deposition in some boreholes; TG1919913 is barren of coal. 119
Figure 5.27: Cross-Section 7 depicts the undulating coal zones from the shallow western part of the deposit through to the deep central portion and to the shallow eastern part of the coalfield. 121
Figure 5.28: Cross-Section 8 depicts a palaeo-floor uplift between boreholes GG1919955 and GG1919924. 123

Figure 5.29: Cross-Section 9 depicts the Daarby Fault downthrow movement between borehole MY311LQ12 and GP1966204 with a displacement of ~360m change in elevation..... 125
Figure 5.30: Cross-Section 10 depicts surface erosion between TE1901547 and ET1901356. 127
Figure 5.31: The Waterberg Coalfield phase magnetic data depicting magnetic features (Fourie, 2014). 129
Figure 5.32: Interpreted faults (solid black lines), interpreted lineaments (dotted black lines) as depicted from cross-sections drawn across the Waterberg Coalfield. 130
Figure 5.33: Waterberg Coalfield possible faults creating a graben structure and a palaeo-high on the southeastern corner. . 131
Figure 5.34: 3D geological model of the Waterberg Coalfield visualized from different directions (A) North View, (B) South View, (C) West View, and (D) East View. Approximate structural locations (dotted red lines) creating noticeable displacements of the lithofacies. 133

Figure A 1: Sample 1B+1A 157
Figure A 2: Sample 1C 157
Figure A 3: Sample 1D 158
Figure A 4: Sample 2 158
Figure A 5: Sample 3 159
Figure A 6: Sample 4 159
Figure A 7: Sample 5 160
Figure A 8: Sample 6 160
Figure A 9: Sample 7 161
Figure A 10: Sample 8 161
Figure A 11: Sample 9 162
Figure A 12: Sample 10 162
Figure A 13: Sample 11 163

Figure A 14: Sample 12 163
Figure A 15: Sample 13 164
Figure A 16: Sample 14 164
Figure A 17: Sample 15A 165
Figure A 18: Sample 15B 165
Figure A 19: Sample 16 166
Figure A 20: Sample 17 166
Figure A 21: Sample 18 167
Figure A 22: Sample 19 167
Figure A 23: Sample 20 168
Figure A 24: Sample 21 168

Figure B 1: CZ11_Total Sulphur (TS) 169
Figure B 2: CZ11_Inherent Moisture (IM) 169
Figure B 3: CZ11_Fixed Carbon (FC) 170
Figure B 4: CZ11_Calorific Value (CV) 170
Figure B 5: CZ11_Ash (AS) 171
Figure B 6: CZ11_Volatile Matter (VM) 171
Figure B 7: CZ10_Total Sulphur (TS) 172
Figure B 8: CZ10_Inherent Moisture (IM) 172
Figure B 9: CZ10_Fixed Carbon (FC) 173
Figure B 10: CZ10_Calorific Value (CV) 173
Figure B 11: CZ10_Ash (AS) 174
Figure B 12: CZ10_Volatile Matter (VM) 174
Figure B 13: CZ9_Total Sulphur (TS) 175
Figure B 14: CZ9_Volatile Matter (VM) 175
Figure B 15: CZ9_Inherent Moisture (IM) 176
Figure B 16: CZ9_Fixed Carbon (FC) 176
Figure B 17: CZ9_Calorific Value (CV) 177
Figure B 18: CZ9_Ash (AS) 177
Figure B 19: CZ8_Volatile Matter (VM) 178

Figure B 20: CZ8_Total Sulphur (TS) 178
Figure B 21: CZ8_Inherent Moisture (IM) 179
Figure B 22: CZ8_Fixed Carbon (FC) 179
Figure B 23: CZ8_Calorific Value (CV) 180
Figure B 24: CZ8_Ash (AS) 180
Figure B 25: CZ7_Volatile Matter (VM) 181
Figure B 26: CZ7_Total Sulphur (TS) 181
Figure B 27: CZ7_Inherent Moisture (IM) 182
Figure B 28: CZ7_Fixed Carbon (FC) 182
Figure B 29: CZ7_Calorific Value (CV) 183
Figure B 30: CZ7_Ash (AS) 183
Figure B 31: CZ6_Volatile Matter (VM) 184
Figure B 32: CZ6_Total Sulphur (TS) 184
Figure B 33: CZ6_Inherent Moisture (IM) 185
Figure B 34: CZ6_Fixed Carbon (FC) 185
Figure B 35: CZ6_Calorific Value (CV) 186
Figure B 36: CZ6_Ash (AS) 186
Figure B 37: CZ5_Volatile Matter (VM) 187
Figure B 38: CZ5_Total Sulphur (TS) 187
Figure B 39: CZ5_Inherent Moisture (IM) 188
Figure B 40: CZ5_Fixed Carbon (FC) 188
Figure B 41: CZ5_Calorific Value (CV) 189
Figure B 42: CZ5_Ash (AS) 189
Figure B 43: CZ4A_Volatile Matter (VM) 190
Figure B 44: CZ4A_Total Sulphur (TS) 190
Figure B 45: CZ4A_Inherent Moisture (IM) 191
Figure B 46: CZ4A_Fixed Carbon (FC) 191
Figure B 47: CZ4A_Calorific Value (CV) 192
Figure B 48: CZ4A_Ash (AS) 192
Figure B 49: CZ4_Volatile Matter (VM) 193
Figure B 50: CZ4_Total Sulphur (TS) 193

Figure B 51: CZ4_Inherent Moisture (IM) 194
Figure B 52: CZ4_Fixed Carbon (FC) 194
Figure B 53: CZ4_Calorific Value (CV) 195
Figure B 54: CZ4_Ash (AS) 195
Figure B 55: CZ3_Volatile Matter (VM) 196
Figure B 56: CZ3_Total Sulphur (TS) 196
Figure B 57: CZ3_Inherent Moisture (IM) 197
Figure B 58: CZ3_Fixed Carbon (FC) 197
Figure B 59: CZ3_Calorific Value (CV) 198
Figure B 60: CZ3_Ash (AS) 198
Figure B 61: CZ2_Volatile Matter (VM) 199
Figure B 62: CZ2_Total Sulphur (TS) 199
Figure B 63: CZ2_Inherent Moisture (IM) 200
Figure B 64: CZ2_Fixed Carbon (FC) 200
Figure B 65: CZ2_Calorific Value (CV) 201
Figure B 66: CZ2_Ash (AS) 201
Figure B 67: CZ1_Volatile Matter (VM) 202
Figure B 68: CZ1_Total Sulphur (TS) 202
Figure B 69: CZ1_Inherent Moisture (IM) 203
Figure B 70: CZ1_Fixed Carbon (FC) 203
Figure B 71: CZ1_Calorific Value (CV) 204
Figure B 72: CZ1_Ash (AS) 204

Figure C 1: Isopach floor map for the overburden (OVB) 205
Figure C 2: Isopach Floor map for Coal Zone 11 (CZ11) 206
Figure C 3: Isopach Floor map for Coal Zone 10 (CZ10) 206
Figure C 4: Isopach Floor map for Coal Zone 9 (CZ9) 207
Figure C 5: Isopach Floor map for Coal Zone 8 (CZ8) 207
Figure C 6: Isopach Floor map for Coal Zone 7 (CZ7) 208
Figure C 7: Isopach Floor map for Coal Zone 6 (CZ6) 208
Figure C 8: Isopach Floor map for Coal Zone 5 (CZ5) 209

Figure C 9: Isopach Floor map for Coal Zone 4 (CZ4) 209
Figure C 10: Isopach Floor map for Mudstone Interburden_2 (MS2) 210
Figure C 11: Isopach Floor map for Coal Zone 4A (CZ4A) 210
Figure C 12: Isopach Floor map for Mudstone Interburden_1 (MS1) 211
Figure C 13: Isopach Floor map for Coal Zone 3 (CZ3) 211
Figure C 14: Isopach Floor map for Sandstone Interburden_2 (SS2) 212
Figure C 15: Isopach Floor map for Coal Zone 2 (CZ2) 212
Figure C 16: Isopach Floor map for Sandstone Interburden_1 (SS1) 213
Figure C 17: Isopach Floor map for Coal Zone 1 (CZ1) 213

Figure D 1: Waterberg Coalfield columnar sections boreholes 21-40 214
Figure D 2: Waterberg Coalfield columnar sections boreholes 41-80 215
Figure D 3: Waterberg Coalfield columnar sections boreholes 81-100 .. 216
Figure D 4: Waterberg Coalfield columnar sections boreholes 101-143 217

LIST OF TABLES

Table 3.1: The sedimentary lithofacies established in the Karoo Supergroup boreholes of the Waterberg Coalfield (study area). 32
Table 4.1: GEOVIA Minex™ software advantages and disadvantages 61
Table 5.1: Overburden, coal, non-coal zones, interbeds, and their *in-situ* parameters across the Waterberg Coalfield (compiled from Council for Geoscience, 2010)..... 69

Chapter 1: INTRODUCTION

1.1. Preamble

The Waterberg Coalfield is in Limpopo Province in the north-western part of South Africa, 340 km north-west of Johannesburg, north of the Waterberg Mountains. It represents an eastern continuation of the Kalahari Karoo Basin which is in Botswana (Beukes et al., 1991; Cairncross, 2001; Johnson et al., 2006).

The Waterberg Coalfield, despite green/renewable energy initiatives, will be the most essential coal source in South Africa should the remaining coal resources in the Witbank and Highveld Coalfields be depleted (Jeffrey, 2005; Fourie et al., 2009; Hancox & Götz, 2014) however, development is hampered by the finely interbedded coal-mudstone strata, structural complexity, low grade, high ash content, significant core depth, and water shortage (Prevost, 2016). The coalfield covers an insignificant area compared to other South African coalfields (Faure et al., 1996a), hosting 40% to 50% of coal deposits in South Africa (De Jager, 1983; Smith and Whittaker, 1986; Dreyer,1994; Hancox & Götz, 2014).

The coalfield spans a 2 700 km^2 region, extending ~90 km east-west and ~40 km north-south from the basement outcrops and the Palala Shear Zone east of Botswana. The Zoetfontein Fault Zone, flanked to the north by basement outcrops of Limpopo Belt, serves as the northern limit boundary. South of the Palaeoproterozoic Waterberg Group rocks is the Eenzaamheid Fault Zone, serving as a boundary. The resources within the coalfield are divided into shallow and deep zones by the Daarby Fault (Dreyer, 1994; Fourie et al., 2009; Chabedi, 2013).

This research presents the 3D lithostratigraphic facies model whereby coal seam geometry, lithological correlations, structural networks, and the lateral

and vertical distribution of coal and non-coal seam grids (Thickness and Quality) are modelled, analysed, and interpreted.

1.2 Literature Review

Research conducted in 1920 recorded the initial 20 boreholes drilled in the coalfield by the Department of Mines. According to Hancox & Götz (2014), an article by François Alwyn Venter from the Department of Mines from 1944 to 1945 is the first study to describe the lithological succession in the Waterberg Coalfield. Cillié & Visser (1945) and Cillié (1951; 1957) documented geological research from 1940 to 1950 by the Department of Mines.

Sedimentological studies on the coalfield, primarily unpublished, have been conducted (Ryan, 1966; Beukes, 1985; Siepker, 1986; Faure et al., 1996a; summarised by Brandl, 1996). The creation, development, and formation of the Grootegeluk Mine are documented (Alberts & Liebenberg, 1982).

Siepker (1986) analysed the sedimentology, stratigraphy, and depositional settings of the Karoo fill in the Ellisras sub-basin, also insights on numerous controls on sedimentary accumulation. West of the coalfield, Spears et al. (1988) described the first tonstein recorded in South African coalfields, positioning it stratigraphically in the Grootegeluk Formation (Hancox & Götz, 2014).

Beukes et al. (1991) produced the genetic stratigraphy (GIS 1–7) of the Waterberg Coalfield, with 7 increments of sedimentation. Faure et al. (1996a) provided research on the Palaeo-environments and sedimentology of the Karoo Supergroup in the Waterberg Coalfield. Faure et al. (1996b) provided numerous geochemical data from the mudstones of the Karoo Supergroup in the “Ellisras Basin” to discuss the provenance.

An extensive high-resolution aerial geophysical survey covering the Ellisras sub-basin was conducted in the Waterberg Coalfield (Fourie, 2008). The results demonstrate that the Karoo Supergroup fill was twice as thick as previously thought (Hancox & Götz, 2014).

Mtimkulu (2009) worked on a provisional basin analysis study of the Ellisras Basin using 830 boreholes. De Korte (2010) detailed how Grootegeluk Mine could meet its production targets for the metallurgical and thermal markets by using large coal beneficiation plants. Roux (2011) connected the Run of Mine (RoM) material processed at the beneficiation plants in Grootegeluk Mine with the data and analysis from the coal wash table collected from the exploration drill core.

(Chabedi, 2013) investigated the subject of mining deep coal resources and concluded that underground mining, whereby long wall mining is identified as the best method for optimum extraction. Sullivan (2013) examined the practical use of vectar processed densities from geophysical logs in demonstrating coal seam lateral continuity. Deysel (2015) examined the environmental geochemistry of the Waterberg Coalfield, aiming to determine the geological units at risk of producing acid mine drainage (AMD) upon oxidation and the environmental geochemical risk owing to elements leaching from the exposed rock and Mine products. Wagner et al. (2019) detailed the type of macerals, combined maceral-microlithotype, maximum vitrinite reflectance analyses and mean random, included palynology and etching studies on coal from four productive horizons.

1.3 Aims And Objectives of Study

The study aimed to develop a 3D lithostratigraphic facies model of the Waterberg Coalfield through lithostratigraphic modelling of the coal and non-coal bearing strata in the coalfield. The study sought to illustrate that coal deposits, with their associated structural networks (lineaments, joints, and faults) and possible intrusions, can be identified, modelled, and projected into areas with no geological data.

The idea is to demonstrate that the information (i.e., borehole data) and their characterisation in the Waterberg Coalfield can provide a reliable approach in understanding sedimentary deposition and modelling. The Waterberg Coalfield has thick and uniform stratigraphic coal zones; therefore, this approach is well-suited and fits the study.

Integrated computer-based sedimentological studies are continuously improved and updated. Pioneering geological models are known; however, there is no existing 3D lithostratigraphic facies model covering the Waterberg Coalfield. Hence this study, to simulate coal seam geometry, illustrate coal and non-coal thickness and quality distribution, and identify fault and fold locations across the coalfield while demonstrating variations in the complex bedrock geology.

The research is based on geological modelling with interpretations using *Geovia Minex™ 6.1.1 Geological Software* and *ESRI® ArcGIS™ 10.2 Software* for the Waterberg Coalfield. This work encompasses a regional study across the coalfield, applying this modern software.

1.4 Methodology

The approach to this study used all historical geological borehole data from a database of 757 boreholes (all containing lithological units, defined coal and non-coal zones, and laboratory sampled analyses); geological maps, and survey records. Five boreholes were logged and sampled in the study. The Council for Geoscience together with Exxaro Resources (Pty) Ltd provided the remaining data with records of boreholes dating back from 1944 belonging to various mining houses, exploration projects, and published literature (Venter, 1944; Cillié, 1945, 1951, 1957; Ryan, 1966; Smith, 1984; Siepker, 1986; Dreyer, 1994, Johnson et al., 1996, Dreyer, 1999; Cairncross, 2001; Johnson, 2006; Fourie, 2008, et al., 2009; De Korte, 2010).

Exploration drilling, logging, and sampling of boreholes was conducted during an exploration project at Grootegeluk Mine. The author was involved in the logging, sampling, and in correlating coal and non-coal zones of boreholes from farms Caroline 217 LQ5, Dartmoor 213 LQ3, Pentonville 216 LQ7, Swelpan 245 LQ3, and Van Der Waltspan 310 LQ3. The geological data were stored and retrieved from a geological database management system called SABLE® Xplor.

The collected data were modelled using industry-recognised software packages*, GEOVIA Minex™ 6.1.1 Geological Modelling Software* to interpret the geological data in a 1D, 2D and 3D display*,* then processed, and displayed in *ESRI® ArcGIS™ 10.2*. Boreholes were selected for stratigraphic studies and correlations for continuity and depositional environmental settings across the Waterberg Coalfield.

1.4.1 GEOVIA Minex™ 6.1.1 Geological Modelling Software

GEOVIA Minex™ 6.1.1 Geological Modelling Software (Minex) is among the leading sedimentary modelling software, using data (i.e., geophysical,

geotechnical, lithological, qualities, and structural) for coal seam correlation, structural interpretation, coal seam distribution, and analysis of stratified coal deposits. It produces high-resolution geological models depicting coal seam geometries, distributions, and depositional structures. The software uses inverse-distance weighted (IDW); nearest neighbour and kriging techniques to assimilate and interpolate point data and convert it to spatially representative continuous grids.

The basis for using Minex in this project is for structural interpretation, correlation, and gridding of the lithological and raw data analyses obtained from the drilled core. Target coal seam roof and floor elevations were gridded to produce surfaces, and isopach maps were integrated to estimate volumes between controlling surfaces, average seam thicknesses and a structural interpretation over a local and regional space.

Resource estimations were achieved by a triangulation method where sample points are linked by straight lines to form triangles. Each triangle grade is calculated using the arithmetic mean of the samples from the three corners, either as a thickness-weighted mean or by weighing the samples according to how far they are from the centre of the triangle (Shirzadi Babakan et al., 2008).

1.4.2 ESRI® ArcGIS™ 10.2 Software

ESRI® ArcGIS™ 10.2 Software (ArcGIS) is a computer-based software, supporting the gathering, storage, evaluation, and distribution of spatial data (Bolstad, 2005). The subsequent ArcGIS process was followed in the research:

- Defining the information product – the deliverables from the software were georeferenced with plans displaying information (surface infrastructure, boreholes, rivers, and the landscape) distributed spatially across the study area.

- Acquisition of the data – borehole, geometric and spatial data were collected from the Council for Geoscience, Exxaro Resources (Pty) Ltd, and from published literature for the research.
- Analysis of the data – data were displayed relative to other spatially displaced data sets of known locations in a GIS interface. Their coordinate systems were verified against points of known locations. The data were then accepted as reliable and representative for the research.
- Communication of the results – spatially created plans and maps were the outputs derived from the software and used in the research for interpretations and illustrations.

The *ESRI® ArcGIS™ 10.2 Software* desktop study includes analysing of 1:50 000 satellite images, topographical and geological maps, and aerial photos across the Waterberg Coalfield. To achieve the research goals, combined use of these software programs, Minex, and ArcGIS were applied as critical interpretation tools.

1.5 Study Outline

- Chapter 1: Provides an overview and emphasis of the study, the aims and objectives, and the methodology applied in the study.
- Chapter 2: The tectonic setting is described, followed by structural and regional geology, and stratigraphy of the Waterberg Coalfield.
- Chapter 3: The chapter details lithostratigraphic facies analysis and interpretations of the Waterberg Coalfield.
- Chapter 4: This chapter details the sedimentary modelling of lithostratigraphic facies and stratigraphic architecture.
- Chapter 5: Results are presented and interpreted.
- Chapter 6: The observations and results are discussed.
- Chapter 7: Summarises and concludes the research by emphasising crucial findings and observations.

Chapter 2: GEOLOGY

2.1 Introduction

Coal was found in the Waterberg Coalfield in 1922 during water drilling 25 km west of Ellisras Township (Alberts & Liebenberg, 1982). The coal in the Waterberg Coalfield occurs in 12 defined coal zones within the Grootegeluk and the Swartrant Formation, with varying thicknesses from millimetres to meters throughout the full stratigraphic column (Johnson et al., 2006).

The early crustal architecture of the continent controlled the Karoo Supergroup distribution in Southern Africa (SACS, 1980). The Karoo rocks cover and crops out over two-thirds (300 000 km^2) of the land surface of Southern Africa and host the most critical coal-bearing formations (Smith et al., 1993). They are preserved in basins among the ancient cratons, intra-cratonic grabens or fault blocks, on stable cratonic shelves, and rifted and down-warped continental margins (Faure et al., 1996a).

The Waterberg Coalfield forms part of the Main Karoo Basin and extends westwards to the Kalahari Karoo Basin in Botswana, part of the Gondwanan basins. These basins were developed through compression, subduction, collection, and terrane accretion along the southern margin of Gondwana (Cole, 1992; Catuneanu et al., 1998). The combined stratigraphies of these depocentres (Kalahari Karoo Basin and the Main Karoo Basin), formed from the Late Carboniferous to the Middle Jurassic, and offers the finest record of non-marine sedimentation globally (Falcon, 1986; Snyman, 1998; Hancox & Götz, 2014).

In South Africa, the Main Karoo Basin records a complete sequence of Carboniferous to Triassic strata (Cadle et al., 1993; Caincross, 2001; Johnson et al., 2006).

2.2 Location

The Waterberg Coalfield falls under Lephalale Magisterial District, in Limpopo Province, north-west of South Africa. The Permo-Carboniferous coalfield succession is part of the Karoo Supergroup. It occurs between the latitudes 27E and 28E, covering ~90 km east-west ~40 km north-south, covering 2 700 km^2 in South Africa (Figure 2.1).

It is relatively small compared to the other coalfields in South Africa (Figure 2.1), holding 44% to 50% of the *in-situ* bituminous coal deposits found in the country (De Jager, 1983; Smith & Whittaker, 1986; Dreyer, 1991; Hancox & Götz, 2014). The rocks are preserved as fault blocks in a half-graben, paralleling Limpopo Mobile Belt (Faure, 2008). The landscape of the Waterberg Coalfield is flat, covered by recent grits, gravel, and sands (Faure et al., 1996b).

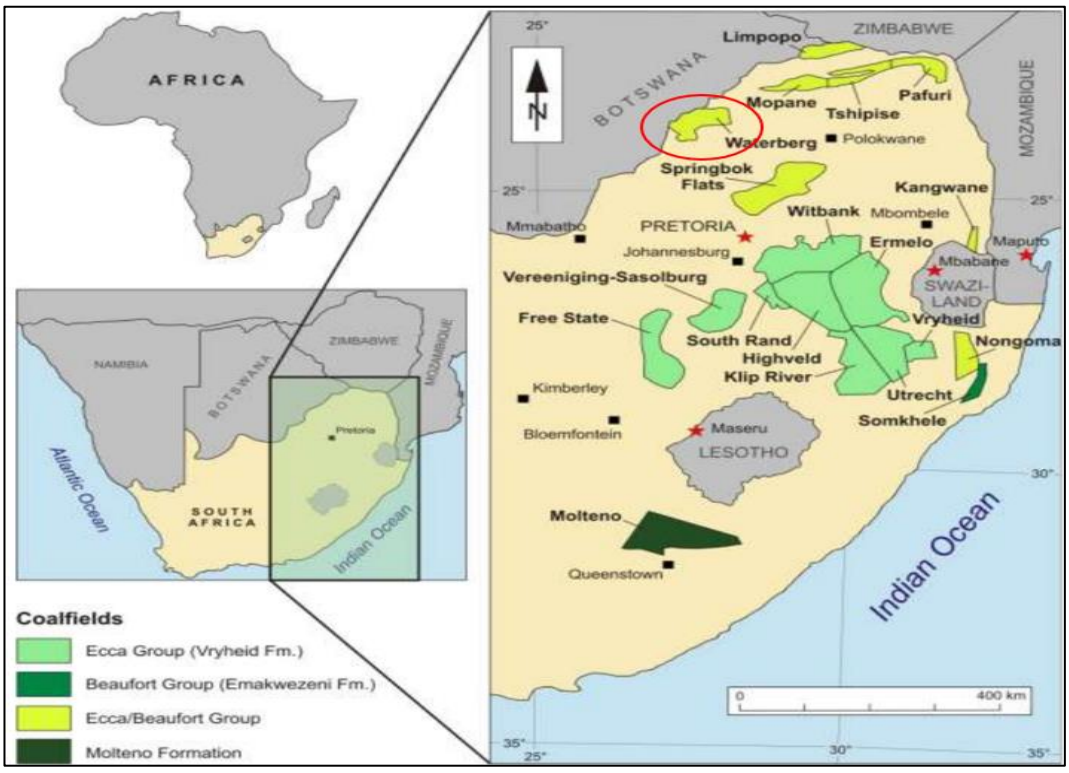

Figure 2.1: Coalfields in South Africa, circled in red is the Waterberg Coalfield (modified after Hancox & Götz, 2014).

2.3 Tectonic Setting

Pangaea was subjected to the influence of two tectonic regimes originating from the convergent (southern) and divergent (northern) borders of Gondwana. Karoo-aged basins appeared during a first-order cycle of supercontinent creation, followed by a breakup (Rust, 1975; Bumby & Guiraud, 2005; Catuneanu et al., 2005). Diverse basin types were formed across Africa because of these two tectonic regimes, with sediment accommodation space produced by tectonic and dynamic loads in the south, and rifting to the north (Catuneanu et al., 2005).

The tectonic regimes in the convergent margin of Gondwana were characterised by shallow-angle subduction of the palaeo-Pacific plate beneath the supercontinent resulting in the formation of a retroarc foreland system in South Africa and related foreland basins. The Beacon Basin in Antarctica, Bowen Basin in Australia and the Paraná Basin in South America were formed because of shallow-angle subduction of the Palaeo-Pacific plate beneath the supercontinent during the tectonic regimes along the convergent boundary of Gondwana (Catuneanu & Elango, 2001; Hancox & Götz, 2014) (Figure 2.2).

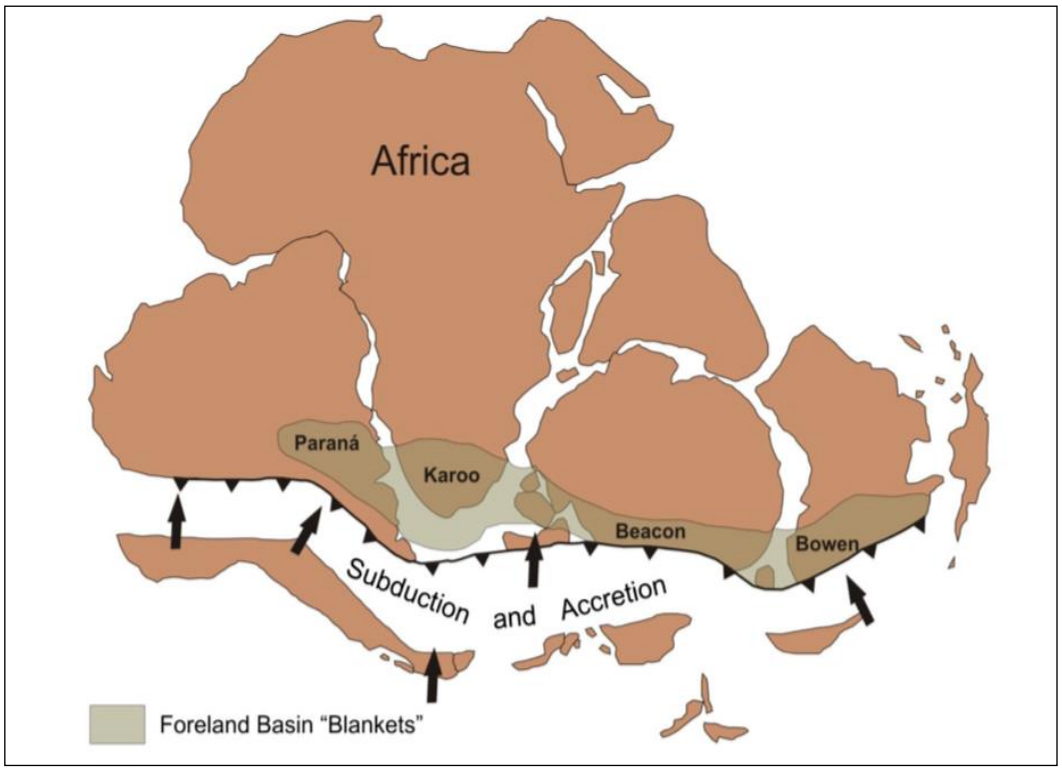

Figure 2.2: The Karoo Foreland Basin and other south-western Gondwanan depocentres of the Karoo age (Hancox & Götz, 2014).

2.4 Structural Geology

The Waterberg Coalfield is in a fault-bounded Ellisras sub-basin. The sub-basin is widely described as a graben structure or a half-graben (Fourie et al., 2009; Sullivan, 2013; Hancox & Götz, 2014). The Proterozoic Waterberg Group and Archaean Beit Bridge Complex comprise its basement, respectively (Brandl, 1996). The Constantia Suite and Bushveld Igneous Complex (Villa Nora Gabbro and Nebo granites) are developed to the northeast and east (Figure 2.3) (Fourie et al., 2009).

The Waterberg Coalfield is structurally complex; it is cross-cut by numerous east-west and northeast-southwest trending faults. It signifies a localised cratonic graben or fault block structure among ancient cratons, which became a site where the Karoo Supergroup was deposited (Falcon, 1986; Snyman, 1998; Dreyer, 1999; Faure, 2008). Four major fault zones

influenced it: the Eenzaamheid; Zoetfontein; Melinda; and the Daarby Faults (Figure 2.3).

The Eenzaamheid, Zoetfontein, Daarby, and Melinda Fault Zones control the regional fault patterns. The Daarby Fault effectively divides the coalfield into a shallow portion that may be mined as opencast and a deep portion that can be mined by an underground operation. Displacements generated by the Daarby Fault range from 240 m to 350 m (De Jager, 1976; Dreyer, 1994; Snyman, 1998; Segwabe, 2013); the juxtaposition of Clarens Formation and Ecca Group lithologies caused the exposure of Grootegeluk Formation strata at the surface to the west and Stormberg Group rocks to the east of the fault (Dreyer, 1999; Hancox & Götz, 2014).

According to Dreyer (1999), the Zoetfontein Fault was active prior and post the Karoo Supergroup deposition. Tectonic reactivation, caused partly by sediment loading, occurred during the Karoo era, controlling the sedimentation locally within the coalfield (Sullivan, 2013). Evidence suggests that the southern side of the Zoetfontein Fault experienced a syn-depositional downthrow (Smith, 1984). The Eenzaamheid and the Daarby Faults are younger than the Karoo Supergroup in the Waterberg Coalfield (Dreyer, 1994).

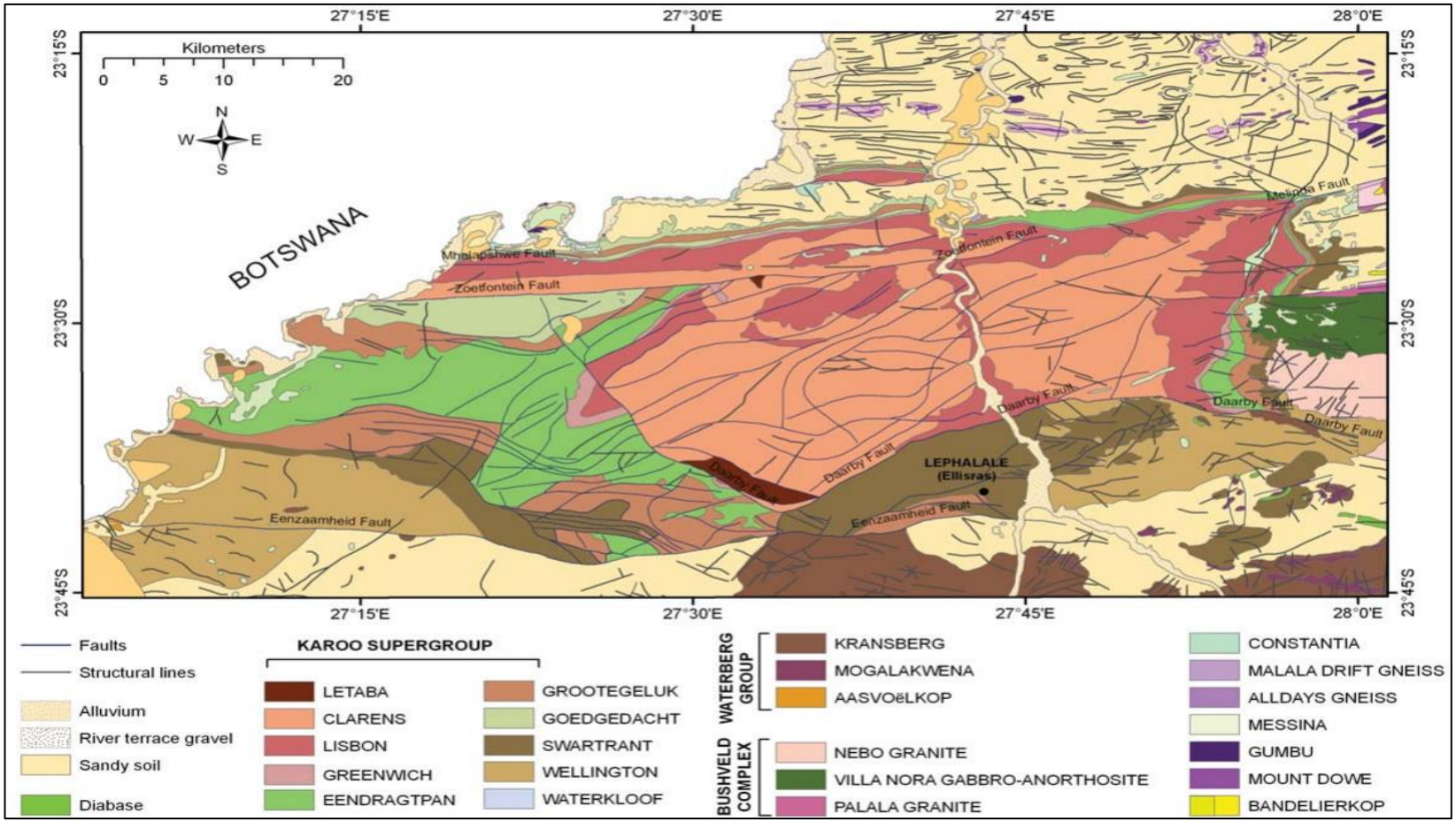

Figure 2.3: Position of the Ellisras Basin and the Waterberg Coalfield on the 2326 Ellisras 1:250 000 sheet, major faults, and structural lineaments are depicted (after Fourie et al., 2014).

2.5 Regional Geology

2.5.1 Karoo Supergroup

The Waterberg Coalfield represents an eastern continuation of the Kalahari Karoo Basin in Botswana; here, the Karoo Supergroup is best preserved (Rust, 1975; Fourie et al., 2009) (Figure 2.4). The subsidiary Karoo Basins in South Africa belong to the Main Karoo Basin. These basins are preserved in the Waterberg Coalfield, Witbank Coalfield, Highveld Coalfield, Soutpansberg/Limpopo Coalfield, and the Springbok Flats Coalfield. The coalfields occur in two major tectonic basin types: foreland and fault-bounded (intercratonic and intracratonic) rift basins (Johnson, 1991; Catuneanu et al., 1998; Snyman, 1998; Cairncross, 2001). The typical Main Karoo Basin is a stable cratonic basin, with coal seams developed on the broad flanks of the Kaapvaal Craton (Falcon, 1986; Hancox & Götz, 2014).

The Karoo Supergroup hosts major coal bearing strata in southern Africa (Falcon, 1986; Hancox & Götz, 2014). It was deposited in the Late Carboniferous to Early Jurassic (Falcon, 1986; Johnson et al., 1996; Snyman, 1998). The strata records over 100 million years of continental and marine sedimentation under different climatic regimes (Smith, 1995; Catuneanu et al., 2002; 2005).

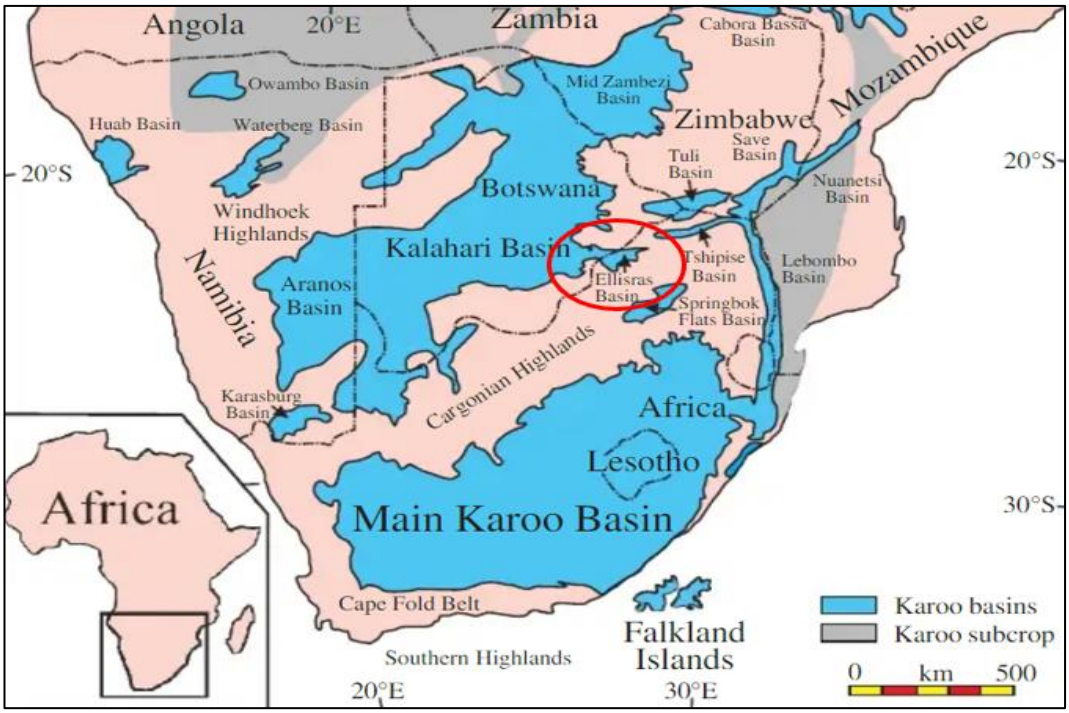

Figure 2.4: Main Karoo Basin and the Kalahari Basin in Southern Africa, in relation to the Ellisras Basin (Waterberg Coalfield, circled in red). Modified from Catuneanu et al. (2005).

2.5.1.1 Main Karoo Basin

The Main Karoo Basin which constitutes a retro-arc foreland basin is primarily underlain by a stable basement, comprising the Kaapvaal Craton in the north and the Namaqua-Natal Metamorphic Belt to the south, and is bounded along its southern margin by a fold-thrust belt (Cape Fold Belt) (Johnson et al., 2006) (Figure 2.5). This developed during the Palaeo-Pacific plate subduction phase beneath the Gondwana plate (late Palaeozoic to Early Mesozoic) (Catuneanu et al., 1998). Karoo succession accumulated within numerous tectonically controlled depositories (Smith, 1995). The volcanic rocks of the Drakensberg Group and sedimentary rocks of the Karoo Supergroup are present in the basin (Johnson et al., 1997).

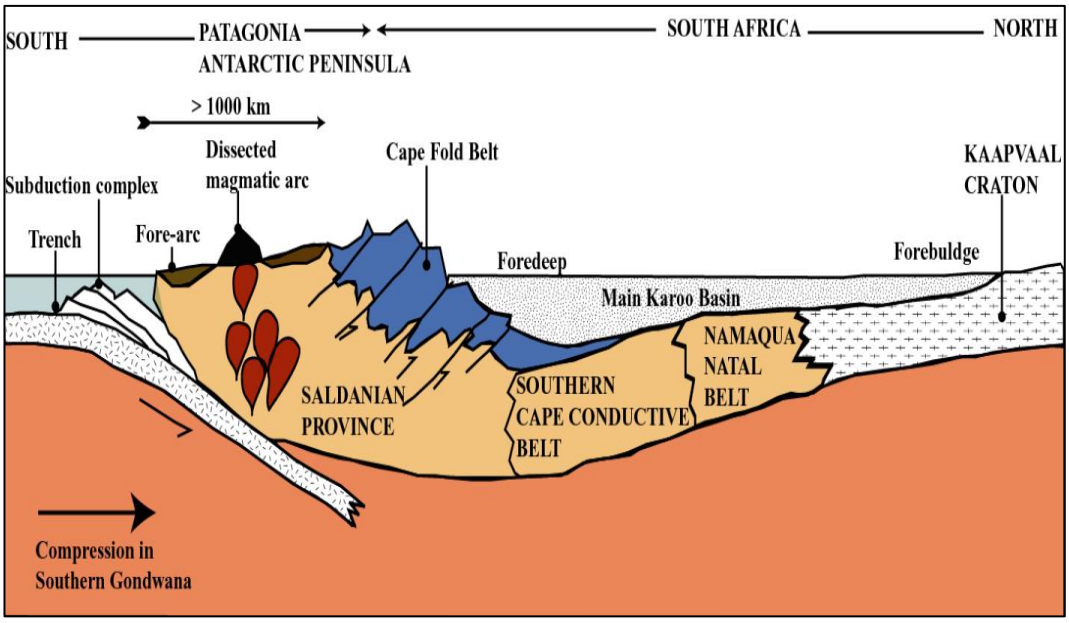

Figure 2.5: Main Karoo Foreland Basin in relation to the Cape Fold Belt, the subduction zone and magmatic arc in the south (Nxumalo, 2011).

The Main Karoo Basin has an abundant terrestrial vertebrate fossil record, distinctive plant assemblages, significant economic coal seams, large dolerite dyke and sill systems, and well-preserved glacial deposits (Johnson et al., 2006; Hancox & Götz, 2014). Based on the sedimentological characteristics of the basin, four groups have been identified, namely: the Dwyka, Ecca, Beaufort and Stormberg Groups.

Dwyka Group glacial deposits are predominantly diamictite and form the basal succession of the basin. The Permian Ecca Group overlies the Dwyka Group and comprises predominantly clastic sedimentary rocks and it has significant coal deposits. It is linked to fluvial, deltaic and lacustrine depositional environments. The Beaufort Group comprises predominantly fluvial sedimentary rocks laid down on alluvial plains and overlies the subaqueous Ecca Group (Smith et al., 1993; Johnson et al., 2006). Stormberg Group comprises the Molteno Formation (fossil-rich clastic sedimentary rocks), Elliot Formation (fluvial red beds) and Clarens

Formation (aeolian sandstone deposits) in stratigraphic succession (Smith et al., 1993; Johnson et al., 1997; Hancox and Götz, 2014).

The Molteno Formation formed predominately by bedload-dominated rivers flowing across extensive braid-plains, with rare coal, fine-grained lithofeldspathic sandstone and mudstone deposited within a fluviatile environment (Bordy et al., 2005; Bumby & Guiraud, 2005; Johnson et al., 2006; Hancox, 2014). Low and high sinuosity fluvial systems deposited the overlying argillaceous Elliot Formation (Hancox, 2000; Bordy et al., 2005). The aeolian dune complexes of the Clarens Formation were deposited due to progressive aridification (Smith et al., 1993; Johnson et al., 2006). The continental flood basalts of the Drakensberg Group are characterized by an outpouring of flood basaltic lavas which terminated the Karoo sedimentation by acting as a cap (Smith et al., 1993; Hancox and Götz, 2014).

Lithostratigraphic units from the Main Karoo Basin, Ellisras (Waterberg), Springbok Flats, Tuli, and Soutpansberg basins are correlated (Figure 2.6). These generalised vertical profiles characterise the lithostratigraphic subdivisions of the Main Karoo Basin and its sub-basins and can be traced and correlated for kilometres (Catuneanu et al., 2005).

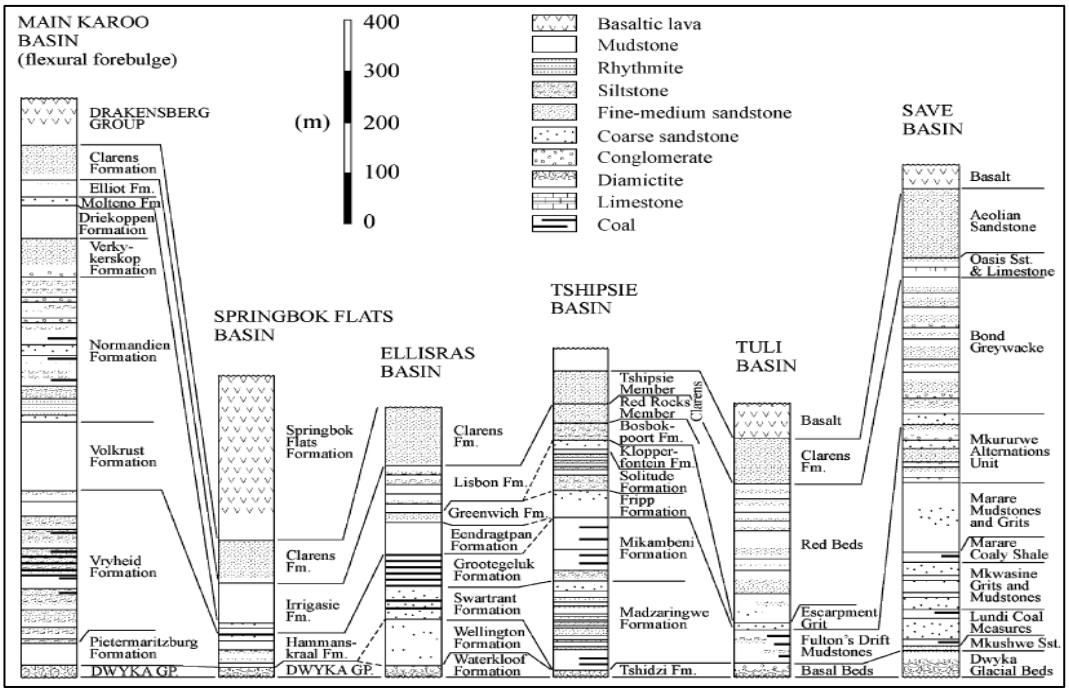

Figure 2.6: Lithostratigraphic units and correlation of the Main Karoo Basin and its sub-basins (Catuneanu et al., 2005).

2.5.2 Stratigraphy of The Waterberg Coalfield

The Waterberg Coalfield is part of the Karoo Supergroup, containing all classical stratigraphic units; therefore, a similar lithological nomenclature as that of the Main Karoo Basin is applied, except for a few arenaceous units (Johnson et al., 2006). Brandl (1996) compiled descriptions of the Waterberg Coalfield stratigraphy, depicting various formations, based on Beukes (1985); Siepker (1986); MacRae (1988) and Beukes et al. (1991). The formations overlie the Waterberg Group, from bottom-to-top, (1) Waterkloof, (2) Wellington, (3) Swartrant, (4) Grootegeluk, (5) Eendragtpan, (6) Greenwich, (7) Lisbon, (8) Clarens Formation and capped by the (9) Letaba Formation (Figure 2.7).

The formations in the Waterberg Coalfield are preserved in separate, fault-bounded depositories which are interpreted as rift basins or intracratonic thermal sag basins (Johnson et al., 1996).

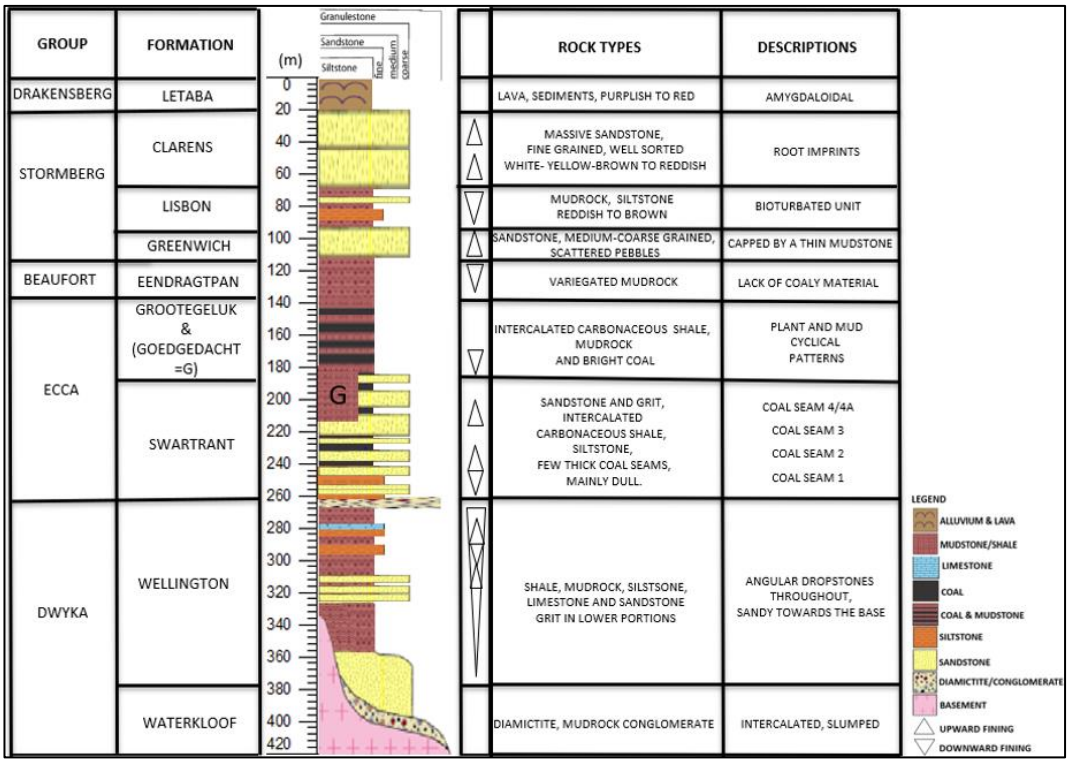

Figure 2.7: The stratigraphy of the Waterberg Coalfield.

2.5.2.1 Waterkloof Formation

The diamictite, mudstone, rhythmite, and conglomerate of the Waterkloof Formation rests unconformably on rocks from the Waterberg Group (Johnson et al., 2006). The formation is found in the western region of the coalfield and the northern and southern rims of the preserved Karoo layers. The over 9 m thick diamictite and conglomerate contains rounded and angular clasts and are interpreted as subaqueous outwash from reworked glacial tills in the north and north-eastern regions (Brandl, 1996). The over 17 m thick mudstones of the formation represent distal glaciolacustrine deposits (Mtimkulu, 2009).

2.5.2.2 Wellington Formation

The formation only developed in the southern half of the Waterberg Coalfield. It is typically 20 m to 30 m thick, reaching a maximum of 160 m to 180 m in the southwest and southeast, respectively (Johnson et al., 2006). This unit exhibits upward-coarsening cycles and becomes siltier and lighter in colour towards the top (Johnson et al., 2006; Faure, 2008). Where fully developed, the formation consists of dark-grey, horizontally laminated mudstone and siltstone that contains lenses of sandstone, small dropstones, and scattered gritstones. The laminated mudstones and siltstones are interpreted as suspension deposits developed in a sizeable body of salty or brackish stagnant water (Brandl, 1996; Johnson et al., 2006).

2.5.2.3 Swartrant Formation

Three zones of the formation have been recognised from boreholes i.e., lower, middle, and upper zones. The maximum thicknesses in the north range from 2 m to 75 m, in the east from 7 m to 50 m, and in the centre up to 130 m (Johnson et al., 2006).

Coal Zone 1, sandstone and siltstone with cross-bedding, ripple cross-laminations, flaser structures, and finer material with imprints of plant roots (*Stigmaria*) make up most of the lower zone. The depositional model includes a delta front that later developed into a delta plain for the coal deposited (Brandl, 1996).

The middle zone has a maximum thickness of 15 m of coarse-grained sandstone and a grey, horizontally laminated mudstone, with coaly shales, and the Coal Zone 2 (Faure, 2008). A glaciolacustrine environment is presumed to be the source of the overlying mudstones, with dropstones pointing to the presence of scattered icebergs (Mtimkulu, 2009).

Upper zone facies are mudstones (13.6 m to 36.4 m thick), sandstones and coal zones, erosionally overlain by 16.5 m to 30 m thick coarse, cross-bedded feldspathic sandstone. This formation represents meandering or braided streams flowing onto a floodplain or delta (Faure, 2008).

2.5.2.4 Goedgedacht Formation

This formation is only found in the northern and north-western regions of the Waterberg Coalfield (Siepker, 1986; Faure, 2008). The thickness diminishes from 80 m in the north to at least 10 m in the south, the contacts are marked in places by coal beds where it inter-fingers with the Swartrant Formation. The formation comprises mudstone units with graded bedding and angular quartz grains towards the base (Johnson et al., 2006). Mudstones are massive and are thought to reflect mudflows, with localized sandstones probably reflecting braided streams on a fan surface (Mtimkulu, 2009).

The inferred palaeo-environment follows a humid alluvial fan in a proglacial setting with retreating or stagnating glaciers to the north and the progradation of the fan to the south (Brandl, 1996).

2.5.2.5 Grootegeluk Formation

The formation thickness is 110 m in the south, 40 m to 60 m in the north and northwest, 50 m in the southeast, and 10 m to 20 m in the northeast. In the northern and central regions, the lower half of the Grootegeluk Formation interfingers with the Goedgedacht Formation, whereas in the east and far south, it conformably overlies the Swartrant Formation (Johnson et al., 2006; Faure, 2008). Mudstone and coal are all found in the formation; each cycle has a coal layer at the base with a distinct contact that grades up into mudstone. The succession has siderite lenses, concretions, nodules, calcite cleats and pyrite fracture fillings (Johnson et al., 2006, Mtimkulu, 2009).

The mudstone and coal succession probably reflects a phase of delta abandonment in a tectonically stable environment where poorly drained swamps on a floodplain gave rise to the formation of pit (Johnson et al., 2006).

2.5.2.6 Eendragtpan Formation

Except for the northeast and eastern portions of the Mokolo River, the formation transgresses onto Limpopo Belt gneisses (Faure, 2008). The formation conformably overlies the Grootegeluk Formation, and it is composed of entirely variegated mudstones, with purplish-red colours (Johnson et al., 2006). The complete lack of any vegetation or coal-like material, drastic change in the climate from wet to dry conditions is assumed to flood basin and floodplain deposition (Brandl, 1996).

2.5.2.7 Greenwich Formation

The formation is separated from the underlying Eendragtpan Formation by a sharp erosive contact in the northern, eastern, and central regions of the Waterberg Coalfield (Faure, 2008). It is a medium to coarse-grained purple-red-green-white sandstone with a thickness range of 7 m to 33 m (Johnson et al., 2006). With thin lenses of conglomerate rock and thin laminated mudstones, it is frequently cross-bedded and gritty. Upward-fining units frequently have thin mudstone caps (Brandl, 1996). The upward-fining sandstones are thought to have formed as channel deposits in a braided stream environment (Johnson et al., 2006).

2.5.2.8 Lisbon Formation

The formation is present across the Waterberg Coalfield and is consistently 100 m to 110 m thick. The formation is made up of massive red mudstones and siltstones which are fine to coarse-grained with pebble washes (Johnson et al., 2006). The mudrocks frequently contain calcareous

concretions; with fining-upwards cycles 5 m to 10 m thick (Johnson et al., 2006; Faure, 2008). *Cruziana* and *Skolithos* frequently cause bioturbation in this unit. The setting was low energy environment, on an extensive floodplain (Brandl, 1996; Johnson et al., 2006).

2.5.2.9 Clarens Formation

The formation forms prominent hills and ridges in the Waterberg Coalfield, with a maximum thickness of 130 m (Johnson et al., 2006). It comprises large, well-sorted, fine-grained sandstone that ranges in colour from cream to off-white (Johnson et al., 2006). Most of the sandstones, particularly the upper part of the formation, is interpreted as aeolian origin. While the minor coarse detrital material which can be present is thought to have been transported by small, ephemeral streams (Brandl, 1996).

2.5.2.10 Letaba Formation

The Letaba Formation is preserved in two locations, south of the Zoetfontein Fault and northeast of the Grootegeluk Mine, comprising basaltic lava (Faure, 2008). Tertiary deposits also occur near major drainages, including the Mokolo, Limpopo and Tamboti Rivers. A thick blanket of Quaternary red soil caps all the Tertiary deposits. Quaternary deposits, such as scree, unconsolidated red sands, terrace gravel, alluvium, calcrete and ferricrete, were also established (Brandl, 1996).

Chapter 3: WATERBERG COALFIELD LITHOSTRATIGRAPHIC FACIES ANALYSIS AND INTERPRETATIONS

3.1 Introduction

Lithofacies description and interpretation of sedimentary rocks identified in the Waterberg Coalfield are provided. This was achieved by studying the borehole core. The Beaufort and Ecca Group rocks were identified and studied in the research area.

The practical information from these separate lithofacies was used to interpret hydrodynamic processes and depositional environments in the study area, as each lithofacies represents a unique depositional event.

The studied 757 exploration drilling boreholes were coded based on the method of Miall (1990), (1996), and (2000) (Figure 3.3 to Figure 3.7). Based on the observations and descriptions of the drill core, five (5) lithofacies with twelve (12) sub-lithofacies were identified.

3.2 Sedimentary Facies

Sedimentology frequently uses the term “facies”, referring to distinct, observable characteristics of a sedimentary rock. These characteristics include thickness, grain size, sedimentary structures, biogenic content, colour, rock type, and geometry of the sedimentary rock (Nichols, 2009).

Associating the individual facies and facies assemblages allows for the inference and interpretation of depositional successions and depositional systems (Bhattacharya & Walker, 1992).

From the 757-borehole core, facies were identified and described. The study also analysed accessible images of the core. The Udden-Wentworth grain-size scale was applied to define and name terrigenous clastic rocks for the study (Figure 3.1). A specific range of grain sizes characterises each

clastic sediment. Sediment grains vary from small clay particles to large pebbles and boulders.

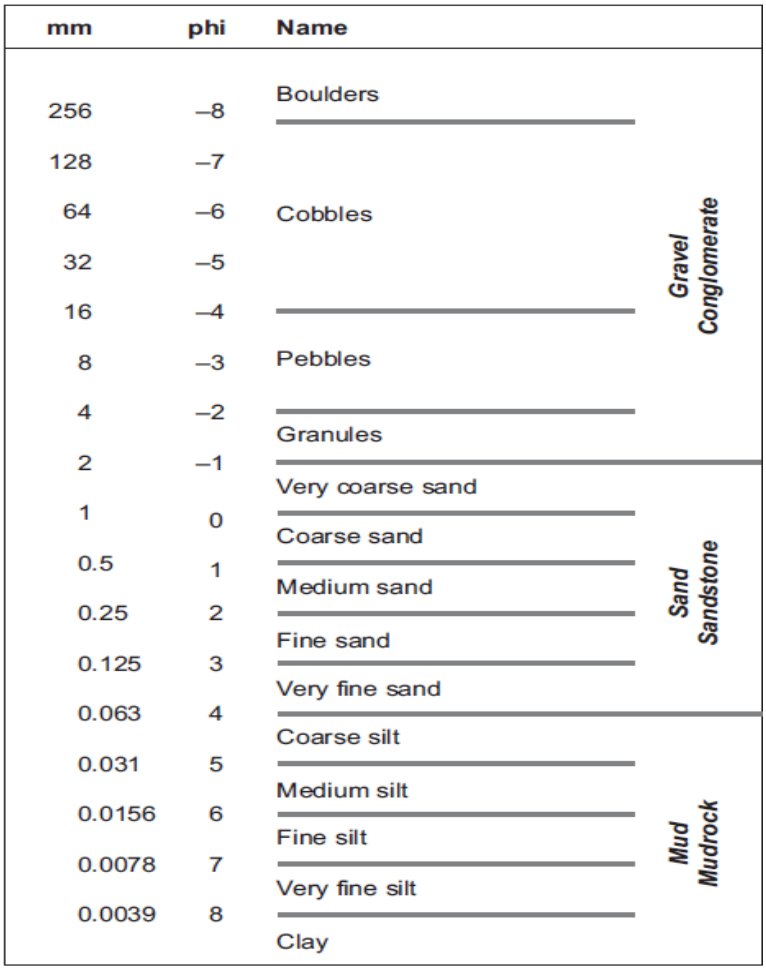

Figure 3.1: Udden-Wentworth grain-size scale for categorization of sedimentary rocks (Nichols, 2009).

3.3 Sample Boreholes Across The Study Area

Five (5) boreholes served as physical evidence for the study. Exxaro Resources (Pty) Ltd drilled the boreholes during their exploration program. The boreholes were drilled at farms Caroline 217 LQ, Dartmoor 213 LQ, Pentonville 216 LQ, Swelpan 245 LQ and Van Der Waltspan 310 LQ (Figure 3.2).

Exploration boreholes were logged, correlated, and sampled then geological information was interpreted. The Eendragtpan Formation (lower portion of Beaufort Group), Grootegeluk Formation (upper portion of Ecca Group), and Swartrant Formation (middle portion of Ecca Group) were intersected by the boreholes used for this study.

All coal samples were sent for float and sink analyses at relative densities (1.35; 1.40; 1.50; 1.60; 1.70; 1.80; 1.90; 2.00; 2.10, and 2.20). proximate, calorific value, free swelling index, total sulphur, roga index, and ash analyses were conducted.

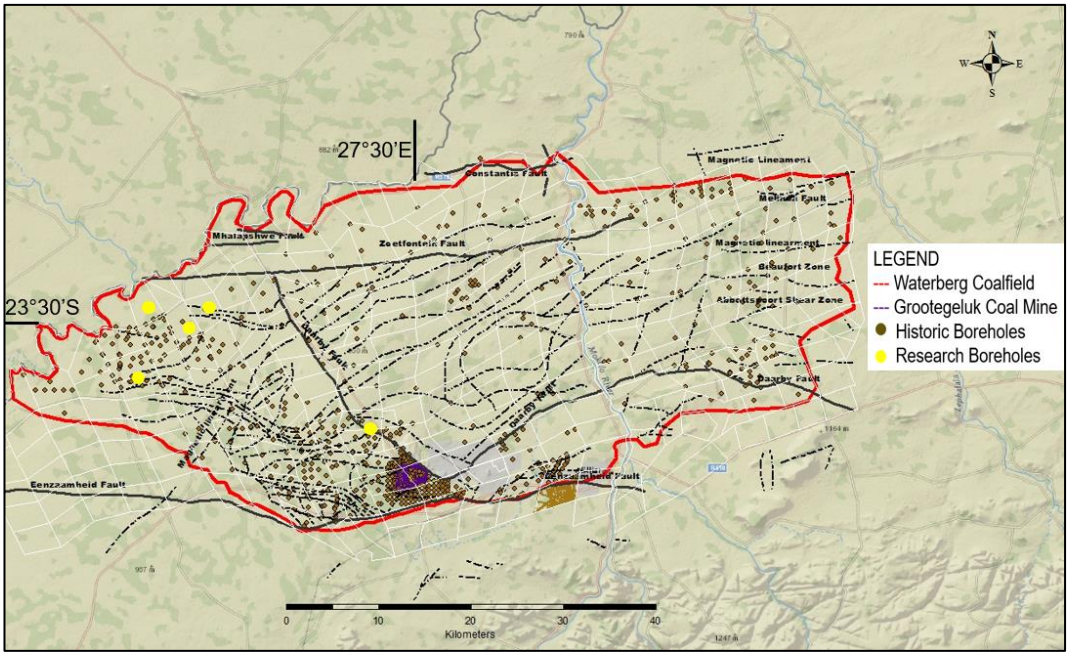

Figure 3.2: Sample boreholes drilled from the Waterberg Coalfield.

This lithofacies classification scheme uses codes of two to three characters, with a uppercase letter for grain size (S for sand; F for silt and clays; C for coal); and a lowercase indicating the texture of each lithofacies (Figure 3.3 to Figure 3.7).

Sedimentary lithofacies recognized in the study area are Massive sandstone (Sm); Ripple cross-laminated sandstone (Sr); Massive

carbonaceous mudstone (Fc); Planar cross-bedded sandstone (Sp); Horizontally laminated mudstone (Fh); Massive mudstone (Fm); Gritty mudstone (F-d); Lenticular siltstone (Fsn); Coal (C); Wavy sandstone and mudstone (Sw) and Interlaminated sandstone, mudstone, and coal (Sh/Fl/C).

A. Borehole CA217LQ5 (Farm Caroline).

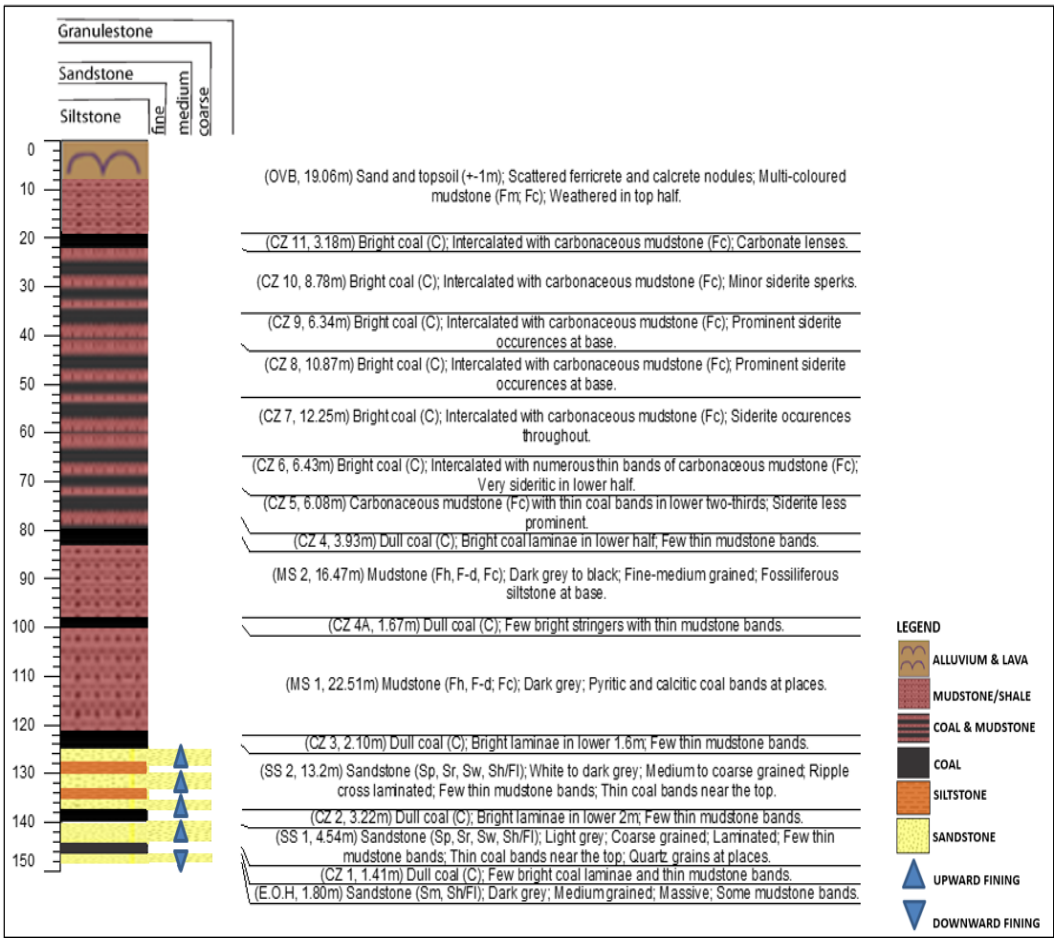

Figure 3.3: Project sample borehole CA217LQ5.

B. Borehole DR213LQ3 (Farm Dartmoor).

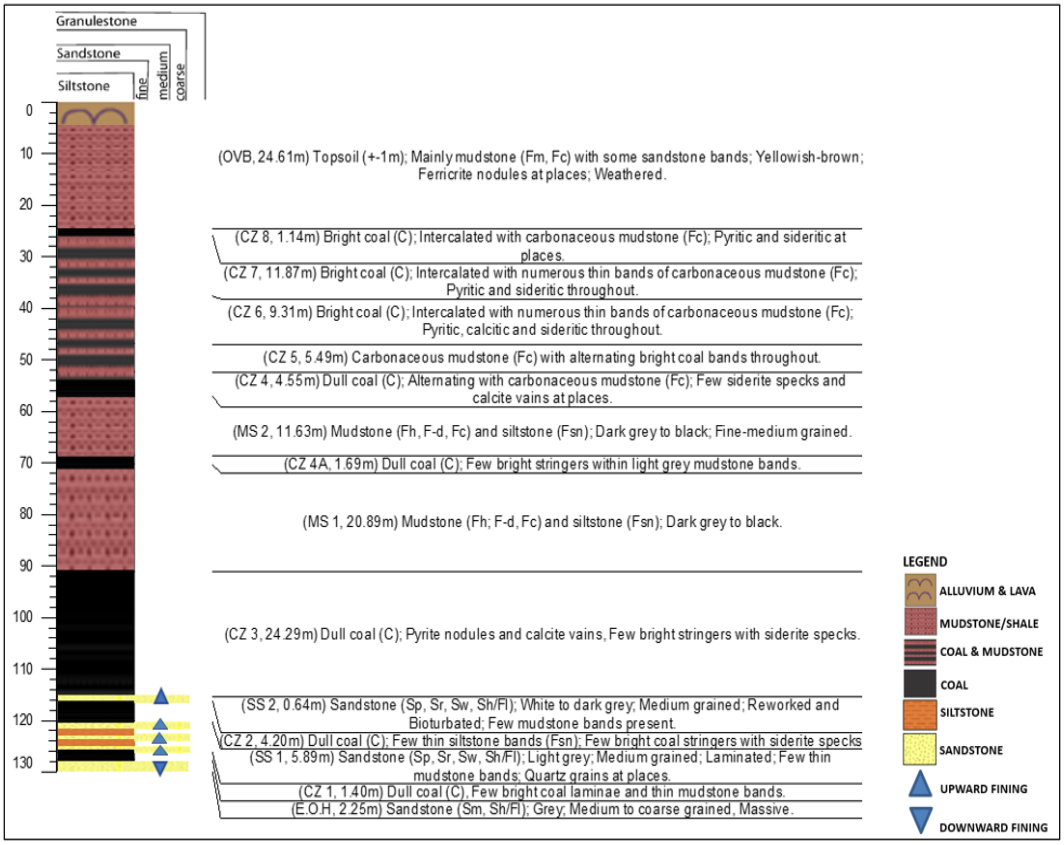

Figure 3.4: Project sample borehole DR213LQ3.

C. Borehole PE216LQ7 (Farm Pentonville).

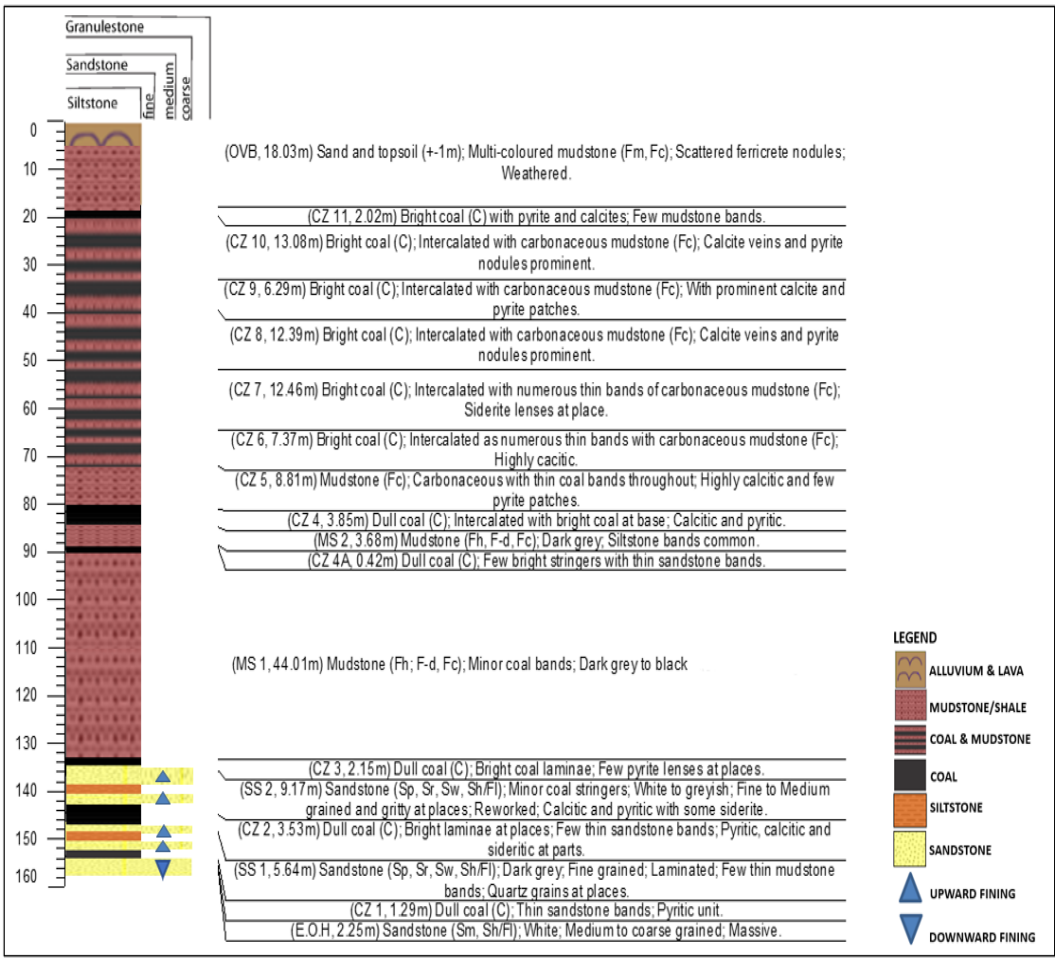

Figure 3.5: Project sample borehole PE216LQ7.

D. Borehole SN245LQ3 (Farm Swelpan).

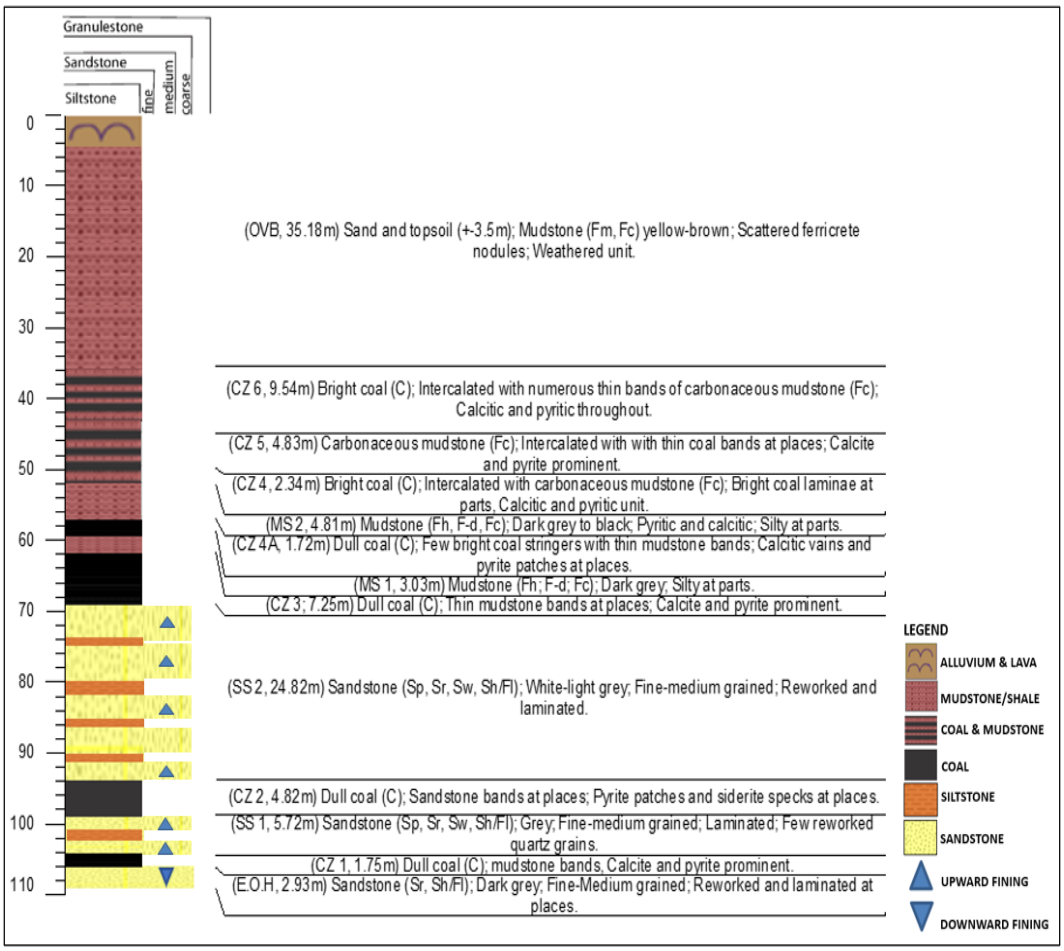

Figure 3.6: Project sample borehole SN245LQ3.

E. Borehole VN310LQ3 (Farm Van Der Waltspan).

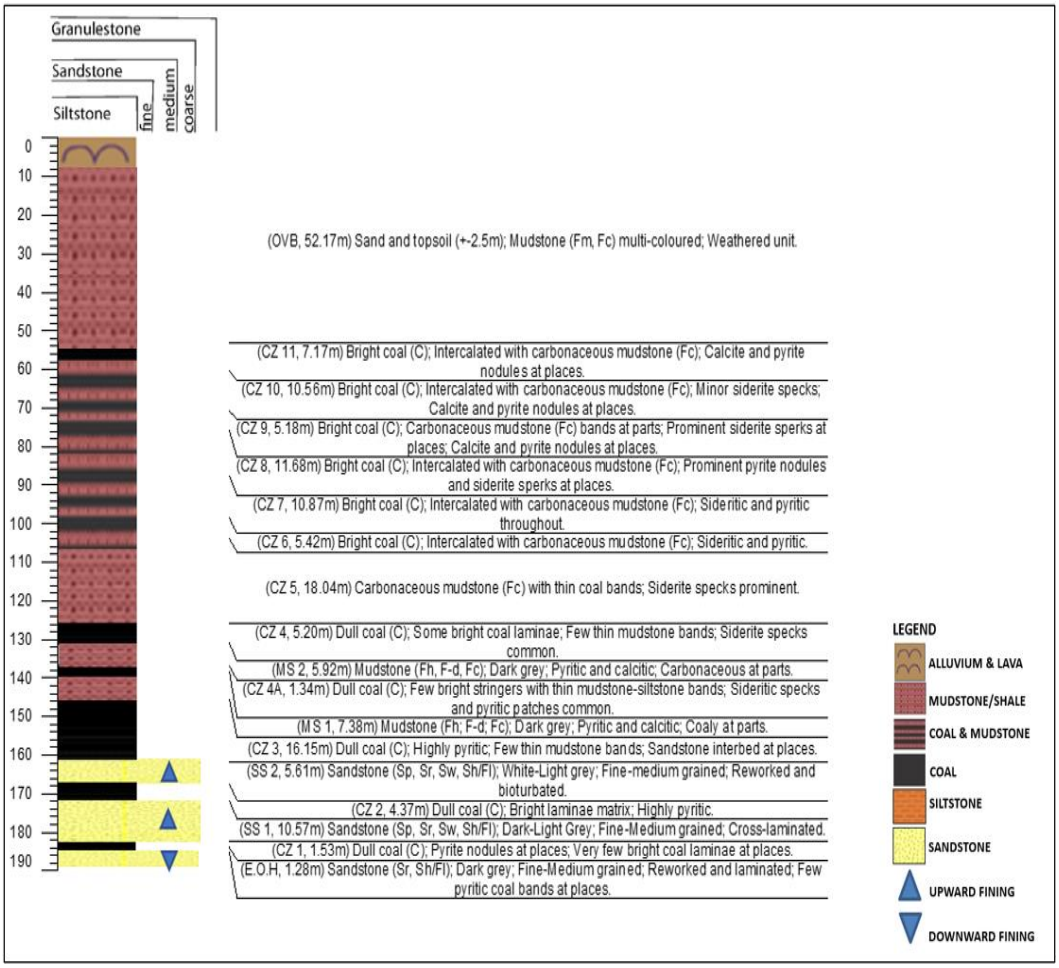

Figure 3.7: Project sample borehole VN310LQ3.

3.4 Lithofacies Description and Interpretation

The lithofacies observed are summarised (Table 3.1). The various depositional settings of the Karoo Supergroup were represented by facies associations made up of the lithofacies.

Table 3.1: The sedimentary lithofacies established in the Karoo Supergroup boreholes of the Waterberg Coalfield (study area).

Lithofacies	Sub-lithofacies	Description	Facies code description
Sandstone	Massive sandstone	Well cemented and consolidated sandstone. Colour: White to light grey. Grain size: Fine to coarse grained.	**Sm** (Massive sandstone)
	Planar cross-bedded sandstone	Sand, medium to coarse with grouped planar cross-beds. Colour: Light grey to white. Grain size: Fine to medium grained.	**Sp** (Planar cross-bedded sandstone)
	Cross-laminated sandstone	Sand, fine to medium grained with ripple cross-laminations. Colour: Light grey to white. Grain size: Fine to medium grained.	**Sr** (Ripple cross-laminated sandstone)
Mudstone	Massive mudstone	Muddy and highly weathered throughout. Colour: Red-green-purple. Grain size: Very fine grained.	**Fm** (Massive mudstone)
		Muddy, silty at places. Colour: Grey to dark grey. Grain size: Very fine grained.	
	Horizontally laminated mudstone	Horizontally laminated mudstone. Colour: Light grey. Grain size: Fine grained.	**Fh** (Horizontally laminated mudstone)
	Carbonaceous mudstone	Massive but faintly laminated carbonaceous mudstone or organic-rich mudstone. Colour: Grey to Dark grey. Grain size: Fine grained.	**Fc** (Massive carbonaceous mudstone)
	Gritty mudstone	Poorly sorted mudstone with quartz grains in the matrix. Colour: Dark grey, white at places owing to the quartz. Grain size: Fine to coarse grained.	**F-d** (Gritty mudstone)
Siltstone	Lenticular laminated siltstone	Silt with sandstone lenticular laminations. Colour: Grey to light grey. Grain size: Fine to very fine grained.	**Fsn** (Lenticular siltstone)

Lithofacies	Sub-lithofacies	Description	Facies code description
Coal	Bright and dull coal	Highly carbonaceous unit with vitrinite and inertinite contents. Coal stringers may alternate with shaley material. Colour: Dark grey to black.	**C** (Coal)
Mixed	Wavy sandstone-mudstone	Wavy laminated sandstone with mudstone drapes at places. Colour: Light grey to grey. Grain size: Very fine to medium.	**Sw** (Wavy Sandstone and mudstone)
	Interlaminated sandstone-mudstone-Coal	Alternating laminations of sandstone and mudstone with coal layers throughout. Colour: Light grey to dark grey. Grain size: Fine to very fine.	**Sh/Fl/C** (Interlaminated Sandstone, mudstone and coal)

Modified from (Rust, 1978); (Miall, 1990, 1996, & 2000).

3.4.1 Sandstone lithofacies

3.4.1.1 Massive sandstone sub-lithofacies

- **Description**

Massive sandstone (Sm) sub-lithofacies is consolidated and micaceous, occasionally containing pyrite nodules. The massive sandstone is characterised by cream white to pure white feldspathic granules in a coarse-grained sandstone (Figure 3.8) consisting primarily of quartz grains. Towards the base of the unit, upward-fining sequences were described with erosive contacts.

This unit is highly competent and occurs across the coalfield. The lithofacies exhibits no sedimentary structure nor contains any fossils. The grains are tightly packed, and a matrix is almost absent.

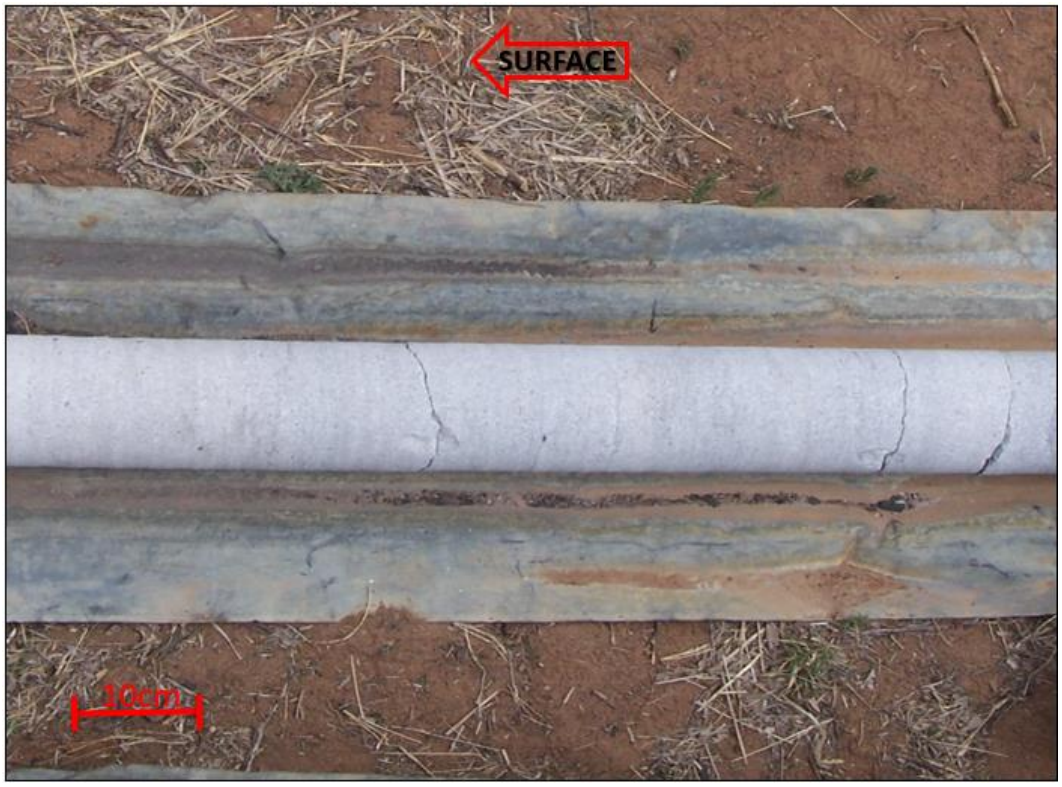

Figure 3.8: Massive sandstone (Sm) sub-lithofacies comprise coarse-grained, highly competent, and tightly packed quartz grains.

- **Interpretation**

The massive and unstructured sandstone unit was likely formed by brief, rapidly fluidised sand flows triggered by highly water-saturated, unconsolidated coarse-grained sand in streams (Tavener-Smith, 1982; Johnson et al., 2006). The investigated core demonstrates no evidence of bioturbation, the coarse-grained character prevents any biogenic alteration. Homogeneous settling of sediments may have developed owing to debris flow processes (Cairncross, 1986).

The massive sandstone sub-lithofacies commonly occurs within the Swartrant Formation in the study area.

3.4.1.2 Planar cross-bedded sandstone sub-lithofacies

- **Description**

Planar cross-bedded sandstone (Sp) sub-lithofacies observed comprises light grey to white, fine to medium sized grains. The unit is defined by the moderately sorted sandstone with thin micaceous bands and a silty matrix, forming the cross-bedding structure (Figure 3.9).

The examined drilled core revealed both upward-fining and upward-coarsening sequences, representing the lithofacies. When the lithofacies changes to another, erosive contacts are more frequent than gradational contacts.

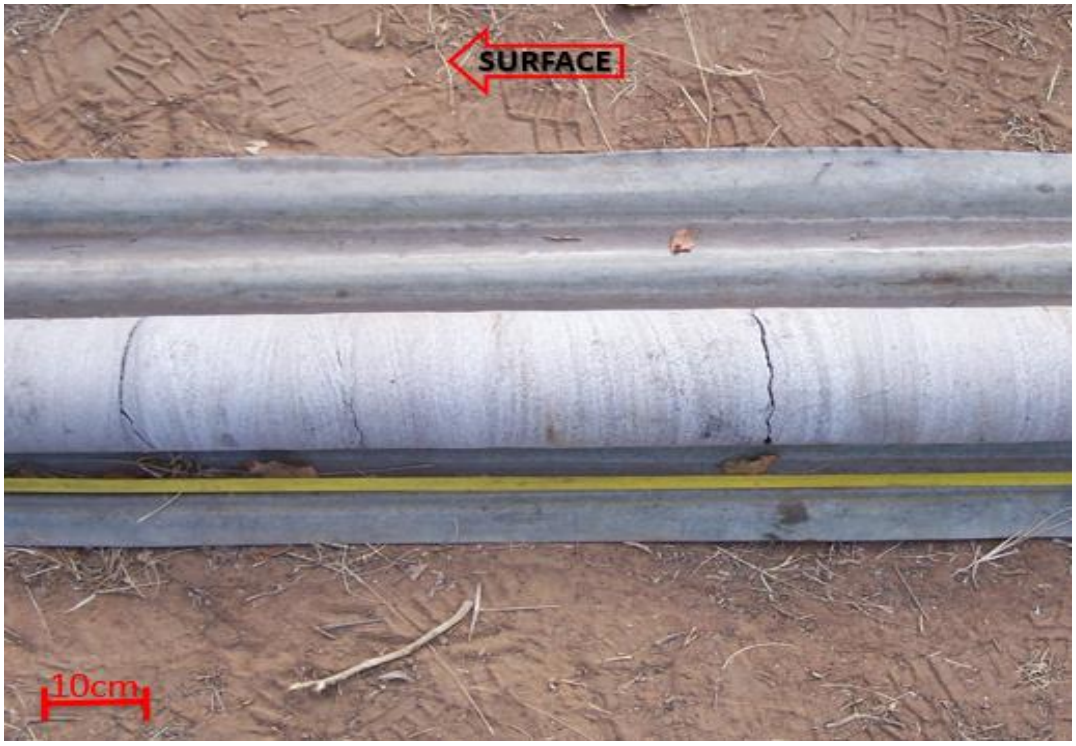

Figure 3.9: Planar cross-bedded sandstone (Sp) sub-lithofacies, with planar-bedded mica bands across the unit.

- Interpretation

Planar cross-bedding formed as 2-Dimensional, straight-crested dunes migrating downstream (Harms et al., 1982; Holland et al., 1989). The bedforms develop in the lower flow regime of a unidirectional current at relatively high flow velocities (Prothero & Schwab, 1996). The finer-grained material formed in a low energy environment, whereas the coarser-grained formed in a high energy environment (Tavener-Smith, 1982). The intercalation of these sedimentary strata indicates fluctuating current velocity (Uys, 2007).

The planar cross-bedded laminated sandstone sub-lithofacies is common in the Swartrant Formation in the study area.

3.4.1.3 Cross-laminated sandstone sub-lithofacies

- Description

Fine-grained cross-laminated sandstone (Sr) comprises light grey to white sandstone. The cross-laminated facies is moderately sorted, with finer grain sizes (Figure 3.10). Often, the cross-laminated sandstone units are upward fining.

Lower contacts of the finer upward-fining units are usually erosive, with a thin gravel at the base of the unit. Feldspar grains occur in the sandstone more prominently in the coarser units. Slightly carbonaceous siltstone laminations alternate with the sandstone units, showing flaser and wavy stratification across the sandstone unit.

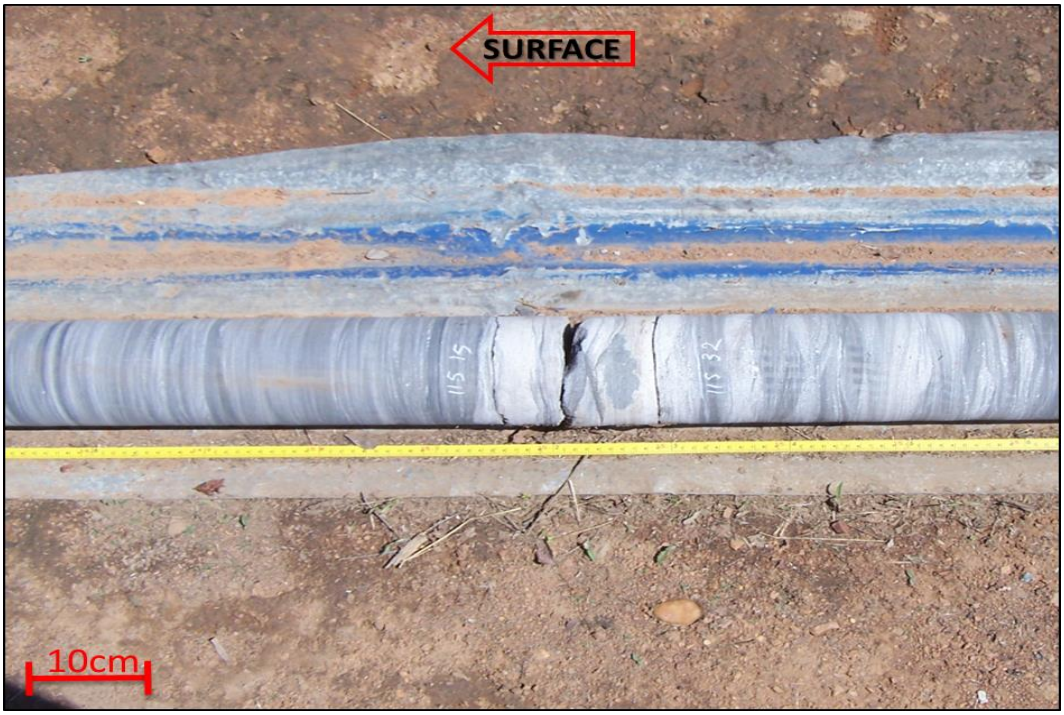

Figure 3.10: Cross-laminated sandstone sub-lithofacies (Sr) showing flaser and wavy stratification across the sandstone unit.

- Interpretation

Cadle (1993) remarked that small-scale oscillation-ripple lamination suggests that wave processes were an essential factor in reworking fine-grained sand. Small-scale cross-laminated sandstone commonly represents the migration of current ripples. These ripples are formed due to reduced water depth, velocity, and grain size.

A flat lamination that changes to a cross-lamination with minor ripples indicates that energy levels were declining; therefore, these transitions represent events associated with waning storms (Tavener-Smith, 1982). The cross-laminated sandstones suggest deposition on top of the bars in abandoned channel and floodplain conditions during periods of reduced discharge by vertical accretion or shallow water flow conditions (Malaza, 2014).

The cross-laminated sandstone sub-lithofacies commonly occurs within the Swartrant Formation in the study area.

3.4.2 Mudstone lithofacies

3.4.2.1 Multi-coloured mudstone sub-lithofacies

- Description

The multi-coloured mudstone (Fm) sub-lithofacies, occurs as a highly fractured and weathered unit, becomes silty in the bottom third of the succession. Red to purple towards the top, ranging from grey to blueish-grey, devoid of carbonaceous or organic-rich material. This unit was identified in the upper parts of the boreholes studied (Figure 3.11).

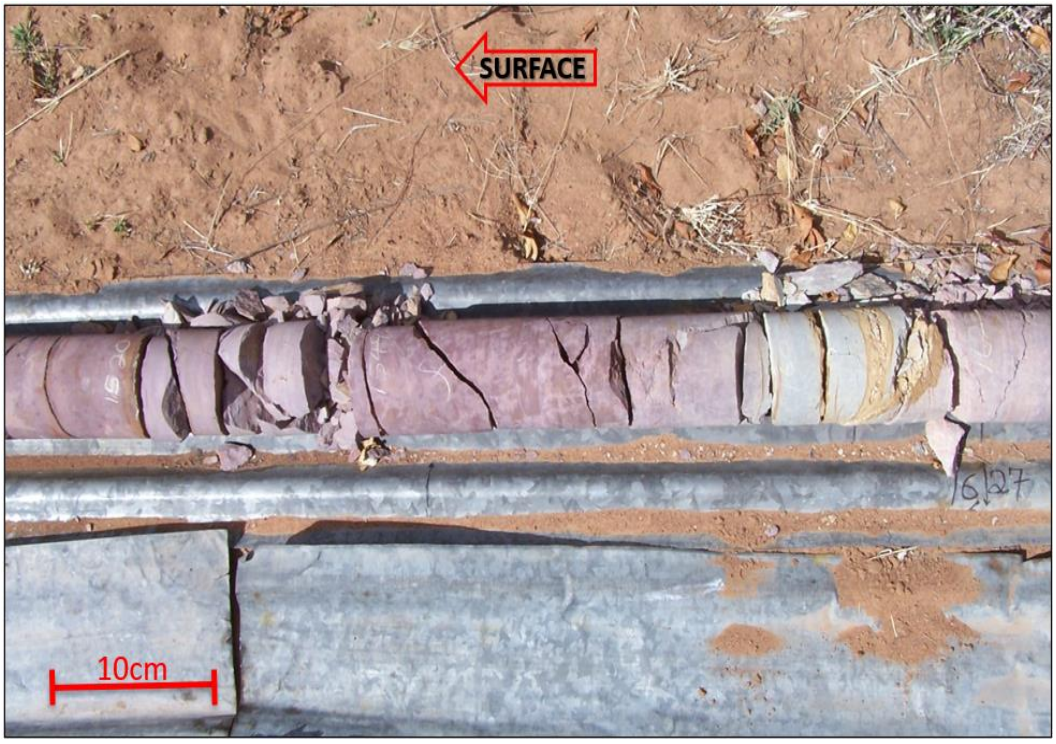

Figure 3.11: Multi-coloured mudstone (Fm) sub-lithofacies is fractured and highly weathered.

- Interpretation

The multi-coloured mudstone lacks vegetation or coal-like particles; it is assumed to have formed in a floodplain deposit (Faure, 1996b; Brandl, 1996; Johnson et al., 2006). Sedimentological studies suggest freshwater for the Beaufort Group mudstones deposition (Beukes, 1985; Siepker, 1986). It is hypothesized that substantial organic material may have been deposited in the Beaufort Group mudstones, but the material was later removed as a result of degradation after deposition (Faure et al., 1996b).

The multi-coloured massive mudstone sub-lithofacies typically occurs within the Eendragtpan Formation in the study area.

3.4.2.2 Massive mudstone sub-lithofacies

- Description

The massive mudstone (Fm) sub-lithofacies, occurs as massive or slightly laminated black, dark grey and grey carbonaceous or organic-rich mudstone, identified in most boreholes studied (Figure 3.12). The unit remains directly below Coal Zone 4 and is fine-grained and slightly carbonaceous.

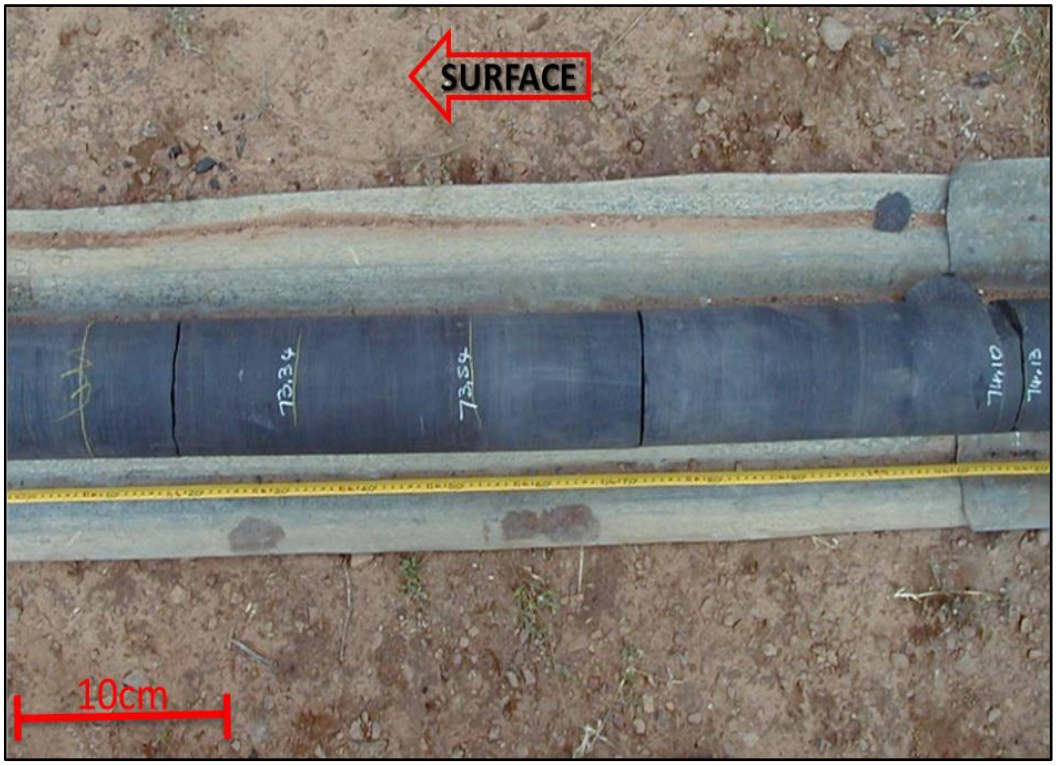

Figure 3.12: Massive mudstone (Fm) sub-lithofacies is slightly carbonaceous.

- Interpretation

This massive mudstone may have also formed during the flocculation process when particles of silt and carbonaceous clay gets clumped together because of the electrostatic attraction of materials with opposing charges (Sabah & Erkom, 2006).

Dark mudstone demonstrates a closer association with the organic-rich material deposited away from water movements in floodplain areas with quieter water and lower energy. The mudstone was deposited in low-energy environment strongly influenced by organic accumulation (Tavener-Smith, 1982).

The massive mudstone sub-lithofacies commonly occurs within the Grootegeluk Formation in the study area.

3.4.2.3 Horizontally laminated mudstone sub-lithofacies

- Description

The horizontally laminated mudstone (Fh) sub-lithofacies comprises slightly carbon-rich light grey carbonaceous laminations with faint siltstone laminations across the unit (Figure 3.13). The facies contain plant fossil remains (*Glossopteris* species) that can be observed in some units (Siepker, 1986; MacRae, 1989). Coal units that contain pyrite and calcite sharply capping the mudstone facies are frequent.



Figure 3.13: Horizontally laminated mudstone (Fh) sub-lithofacies capped sharply by coal.

- Interpretation

The repeated presence of silty laminations throughout the units demonstrates periods when slack water conditions prevailed, allowing fine sediments to settle in suspension in shallower channels (Tavener-Smith,

1982). The vertical or lateral grain sizes are likely because of the sediments being deposited in a floodplain environment with frequent variations in energy conditions. This unit may have formed in an environment with a decrease in the build-up of organic material, yet with an increased supply off sediments (Faure, 1996b; Malaza et al., 2014).

The horizontally laminated mudstone sub-lithofacies commonly occurs within the Swartrant Formation in the study area.

3.4.2.4 Gritty mudstone sub-lithofacies

- Description

Gritty mudstone (F_d) sub-lithofacies comprise angular grit – coarse – or fine quartz grains “floating” in a dark grey matrix of carbonaceous mudstone (Figure 3.14). The ratio of quartz grains to the carbonaceous mudstone matrix varies significantly, from 1 mm to 1 cm in size. The quartz grains appear as dropstones within a reworked unit, and highly carbonaceous wavy lenses occur throughout the unit.

At places, the sub-lithofacies is highly silty to sandy, indicating higher rates of sedimentation and settling. The Goedgedacht Formation comprises mudstone units with graded bedding and angular quartz grains (sand to pebble size range) towards the base, which are mostly capped by a thin bright coal.

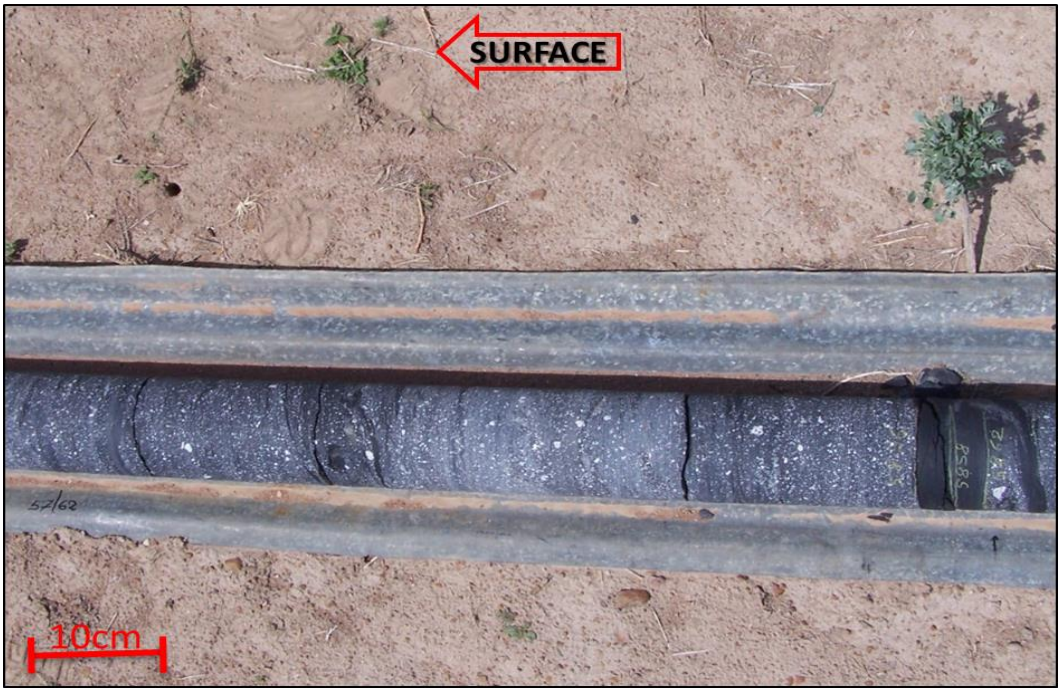

Figure 3.14: Gritty mudstone (F_d) sub-lithofacies comprise fine carbonaceous bands and lenses, closely packed quartz grains appear as sandstone grit.

- Interpretation

The gritty mudstone is thought to have formed from high viscosity mudflows of a humid alluvial fan which developed in a proglacial environment (Johnson et al., 2006). The coarse-grained sandstone grit within the mudstone indicates higher energy levels associated with storm events (Tavener-Smith, 1982; Faure et al., 1996b).

The gritty mudstone sub-lithofacies commonly occurs within the Goedgedacht Formation in the study area.

3.4.3 Siltstone lithofacies

3.4.3.1 Lenticular laminated siltstone sub-lithofacies

- Description

The lenticular laminated siltstone (Fsn) sub-lithofacies displaces lenticular sandstone horizontal laminae throughout the core. That appears as fissile, often micaceous, slightly carbonaceous, and light grey (Figure 3.15). Throughout the siltstone unit, lenses have deformed shapes, and the sandstone laminae are frequently disrupted. A sharp, abrupt transition into coal facies follows the light grey siltstone on both ends of the unit.



Figure 3.15: Lenticular laminated siltstone (Fsn) sub-lithofacies comprising fine to medium-grained sandstone laminae throughout the unit.

- Interpretation

According to Prothero & Schwab (1996), the siltstone lenticular laminae in the siltstone matrix are formed by the slow, steady suspension settling of silt and mud in a medium energy pro-delta environment. The laminae are noticeable as there is a high concentration of feldspars and quartz on the bedding surfaces.

In an environment dominated by the suspension settling of mud and silt under a passive hydrodynamic regime, settling of the fine-grained sediments is encouraged. When there is a scarcity of sand, this sub-lithofacies forms (Winter, 1985).

The lenticular laminated siltstone sub-lithofacies commonly occurs within the Swartrant Formation in the study area.

3.4.4 Coal lithofacies

3.4.4.1 Intercalated bright and dull coal sub-lithofacies

- Description

The intercalated bright and dull coal sub-lithofacies has a vitreous to sub-vitreous lustre and range from dull to lustrous black (Figure 3.16). Occasionally, vitrinite-rich bright coal has calcite veins, pyrite nodules, and siderite nodules described as granular or gritty. Sedimentary structures range from structureless to thinly laminated, the lustrous coal often has conchoidal fractures.

Quartz occurs in the coal as scattered grains, lenses, cavity-fill, and aggregates and are associated with dull, inertinite-rich coal. Calcite occurs primarily as cleats and pyrite as lenses in the bright, vitrinite-rich coal.

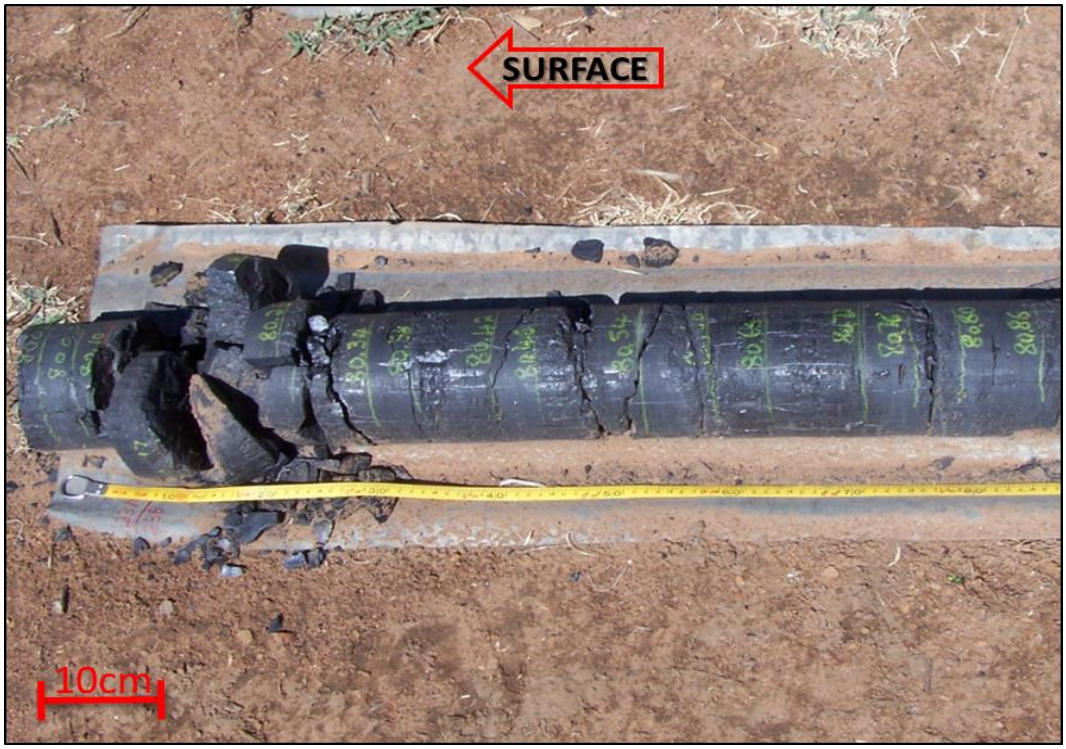

Figure 3.16: Intercalated bright and dull coal sub-lithofacies appear as alternating bands across the unit.

- Interpretation

Coal forms through organic vegetation accumulation, burial, and coalification in a marsh or waterlogged swamp environments (Falcon, 1986). The alternating bright, dull coal and carbonaceous mudstone in this sub-lithofacies indicate microcycles consisting of alternating laminations (0.1 m – 0.2 m) of exinite, vitrinite, mudstone, and organic silt.

Interpretation of the coal facies is that the swamp environment gradually changed from tranquil to more active but not destructive phase, exposing the peat to more reduction in an acidic environment, resulting in pyrite formation and siderite. This might have been brought on by an increase in oxygen in the atmosphere and a drop in water level (Siepker, 1986; Faure et al., 1996a). Siderite suggests a reducing freshwater environment with low Eh conditions (Brandl, 1996).

The unit comprising the intercalating bright and dull coal sub-lithofacies commonly occur within the Grootegeluk Formation in the study area.

3.4.4.2 Coal-mudstone sub-lithofacies

- Description

The coal-mudstone (c-Fm) sub-lithofacies comprises carbonaceous mudstone and coal bands with pyrite nodules and calcite cleats (Figure 3.17). The coal and mudstone facies occasionally have an erosive sandstone and carbonaceous siltstone which cuts through the unit. The unit comprises coal bands which exhibit a sharp basal contact grading into the mudstones.

The coal is dark black to shiny black, whereas the mudstones range from dark, highly carbonaceous rocks to a light and slightly carbonaceous type. The coal may occasionally grade into carbonaceous shale or shaly coal. Based on the proportions of coal and mudstone thicknesses, the coal-mudstone sequence demonstrates micro to macro cyclic repetitions.

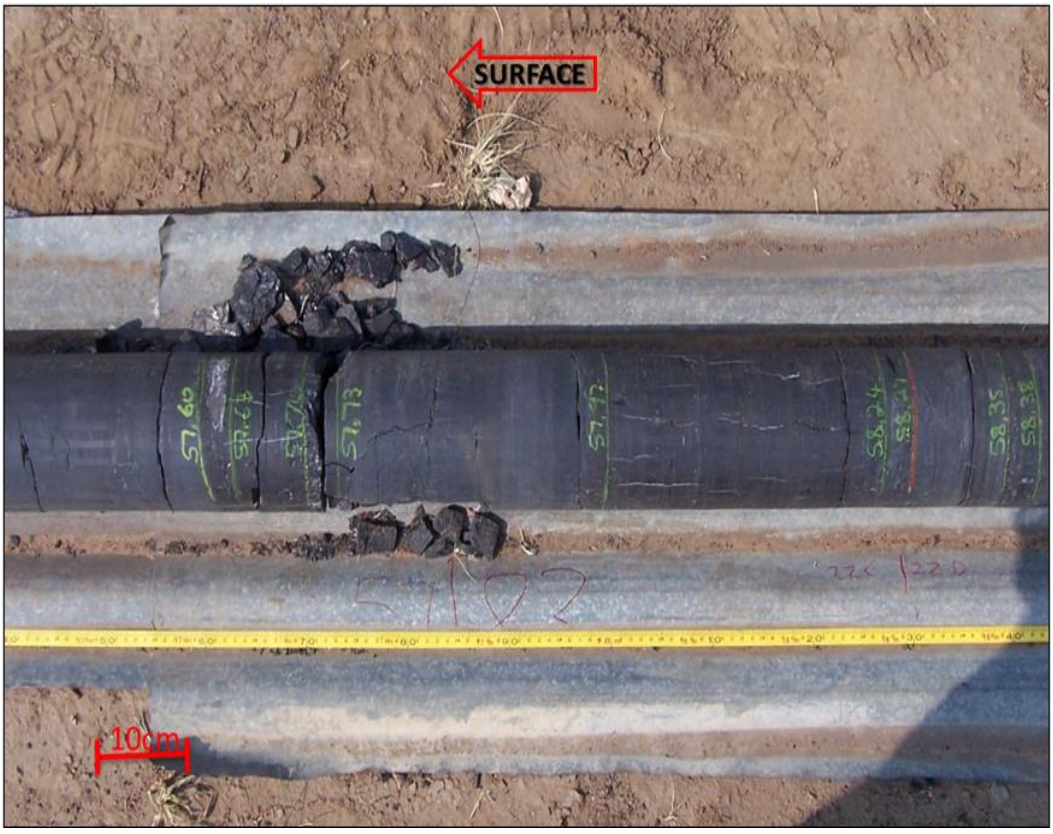

Figure 3.17: Coal-mudstone (c-Fm) sub-lithofacies comprise a carbonaceous mudstone with interbedded coal bands with calcite veins.

- Interpretation

The coal-mudstone succession formed during a stage of delta abandonment in a stable tectonic environment where poorly drained swamps on a floodplain elicited the formation of tundra-type peat. Periodic fluctuations of the water table forming the cyclicity of plant material accumulation and mud deposition (Beukes, 1985; 1991). Grootegeluk Formation's lower coal-mudstone, contains higher amounts of inertinite, developed in a poorly drained proximal floodplain environment, whereas the upper portions of the formation, is rich in vitrinite formed in a well-drained distal floodplain facies (Siepker, 1986; Beukes et al., 1991).

The thicker coal seams represent periods when deposition and subsidence were balanced (Faure et al.,1996b). According to Faure et al. (1996b), the coal-mudstone succession repeated nature, lateral continuity of cycles, and the proportions of ash and maceral in the sequence suggest allogenic and authigenic controls may have contributed to the formation of these sub-lithofacies.

The unit comprising the coal-mudstone sub-lithofacies unit commonly occurs within the Grootegeluk Formation in the study area.

3.4.5 Mixed facies

3.4.5.1 Wavy laminated sandstone-mudstone sub-lithofacies

- Description

The wavy laminated sandstone-mudstone (Sw) sub-lithofacies comprise fine to medium granular sandstones and wavy laminated mudstone throughout the sandstone unit (Figure 3.18). Mudstone is found cross cutting the sandstone unit.

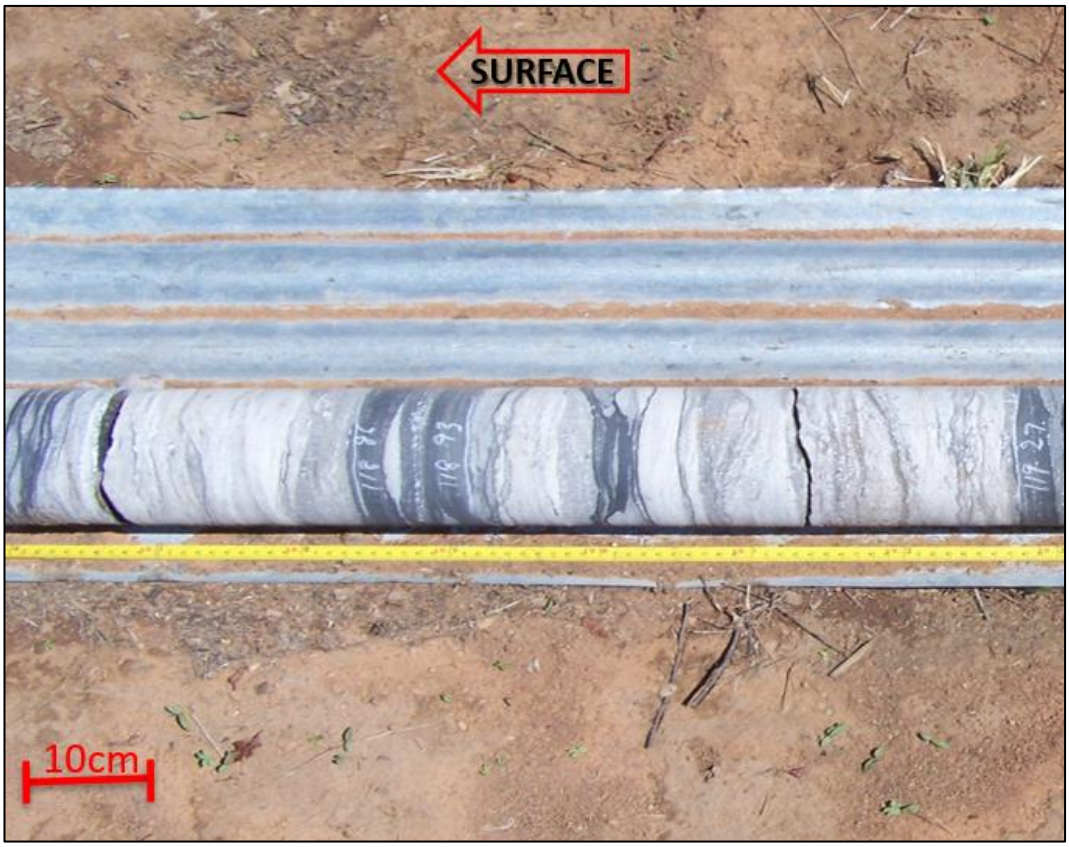

Figure 3.18: Wavy laminated sandstone-mudstone (Sw) sub-lithofacies demonstrate a wavy carbonaceous mudstone across the sandstone unit.

- Interpretation

Wavy laminated sandstone-mudstone sub-lithofacies imply that sand and mud were available during deposition and that quiet periods interspersed with stream flow (Siepker, 1986; Faure et al., 1996a). During the transportation and deposition of sand grains in the current flow, the mud settled as energy fell into the system. When the flow rate decreased, the mud material created waves and settled in the sandstone matrix. The wavy lamination is formed when sand is deposited into the trough while ripples migrate across a muddy substrate, suggesting the presence of more mud-sized particles in the suspension (Prothero & Schwab, 1996).

Small ripple structures, dark in appearance are probably owing to mud draped on depositional surfaces following suspension settling under storm conditions (Travener-Smith, 1982).

The unit comprising the wavy laminated sandstone-mudstone sub-lithofacies commonly occurs within the Swartrant Formation in the study area.

3.4.5.2 Interlaminated sandstone-mudstone-coal sub-lithofacies

- Description

Interlaminated sandstone-mudstone-coal (Sh/Fl/C) sub-lithofacies comprise fine to medium-grained, dark grey mudstone, poorly sorted sandstone, and black coal laminations (Figure 3.19). Alternating laminations with bioturbation of these units are evident in the core analysed, indicating consistency throughout the coalfield.

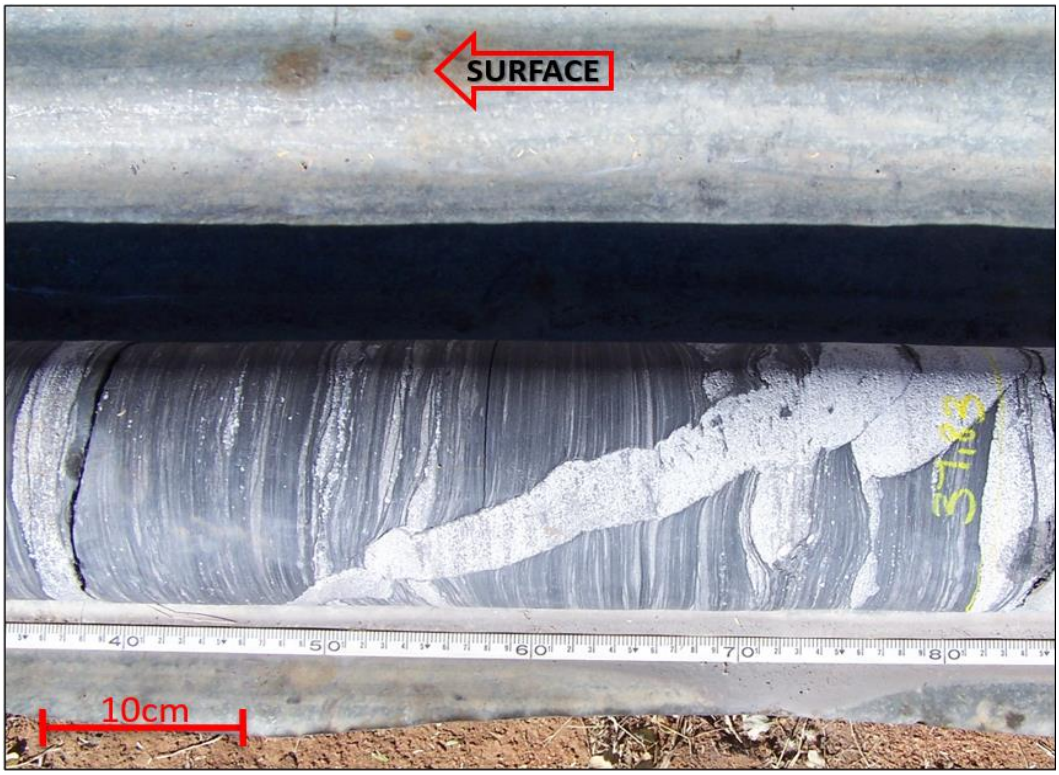

Figure 3.19: Interlaminated sandstone-mudstone-coal (Sh/Fl/C) sub-lithofacies appear as intercalated units with bioturbation, commonly within the coalfield.

- Interpretation

The intercalated sandstone, mudstone, and coal sub-lithofacies of the Swartrant Formation suggests that the basin subsided as it filled (Faure et al., 1996b). Low energy conditions occurred during deposition (Holland et al., 1989). The sandstone, mudstone, and coal succession's repetitive nature illustrate the lateral persistence of cycles. The intercalations of the sedimentary strata suggest that the current velocities fluctuated between high and low, while *Cruziana* and *Skolithos* frequently caused bioturbation. The mudstone-sandstone-coal unit has formed as a crevasse-splay deposit, as infills in small channels, and in small, isolated swamps (Brandl, 1996).

The unit comprising the interlaminated sandstone-mudstone-coal sub-lithofacies was allocated to the Swartrant Formation in the study area.

Chapter 4: SEDIMENTARY MODELLING

4.1 Introduction

The foundation for this 3D lithostratigraphic facies model in this research is based on information derived from 757 boreholes drilled across the Waterberg Coalfield. Data were collected from multiple sources involved in coal exploration in the study area. These external parties were the Council for Geoscience, Anglo American Coal Corporation of South Africa (Pty) Ltd, the Department of Irrigation, Exxaro Resources (Pty) Ltd, Gold Fields Mining and Development (Pty) Ltd, ISCOR (Pty) Ltd, SHELL South Africa (Pty) Ltd, South African Coal, Oil and Gas Corporation (Pty) Ltd, and Ingwe Coal Corporation (Pty) Ltd.

Several 3D modelling software packages have satisfied the demand for a precise and accurate depiction of subsurface conditions in the past decades. These software packages are called geoscientific information systems (GSIS) (Turner, 1991; Berg et al., 2011; Zhu et al., 2012). The geoscience industry needs this interactive system for developing spatial and spatiotemporal geological models of the earth's crust (Kelk, 1991). This research employed GSISs to illustrate a "layer-cake" method, creating a 3D lithostratigraphic facies model based primarily on borehole data.

Cross-sections, 2-Dimension (2D), 3-Dimension (3D), and isopach maps of the Karoo Supergroup in the Waterberg Coalfield were created using the lithostratigraphic information obtained from exploration boreholes. The 2D and 3D lithostratigraphic facies model development aimed at providing data on the geological distribution of lithological units, facies associations, depositional settings, and stratigraphic architecture. The 3D lithostratigraphic facies model created, include a mandatory suite of data sets: (1) the Digital Terrain Model (DTM) of land surface topography; (2) Borehole Logs; (3) Surficial and Subsurface Geological Maps; (4) Structural Maps; (5) Geometry Data, such as infrastructure.

4.2 Lithostratigraphic Facies Modelling

A lithostratigraphic facies model is an idealised facies sequence defined by a sedimentary environment based on rock and sediment studies over time (Maliva, 2016). All sediment characteristics resulting from the depositional environment where the sedimentary unit was formed are represented by lithofacies (Miall, 2000). In this research, the identified lithofacies occurring in the Waterberg Coalfield were used as contact zones for geological modelling. The 3D lithostratigraphic facies model created can be called a deterministic model, although conventional techniques, such as polygonal, triangular, sectional, random stratified gridding, and contouring methods, are known and used techniques to infer correlations and develop an understanding of stratal geometry (Overeem, 2008).

This modelling strategy enables the representation of geological objects, such as fault networks, sedimentary lithofacies, and several other sedimentary structures. The intrinsic challenges such as complex subsurface, low data density, irregular data distribution, and diverse data sources, constrained the effectiveness of GEOVIA Minex™ Software during this study.

This lithostratigraphic sedimentary modelling method is intended to create a “layer cake” model (Turner, 2006). Creating a geologically plausible model that is accurate and precise from drilled core data is challenging. When modelling, the modeller considers the influence of missing strata, and provides a method for dealing with unique geological structures, pinch-outs, intrusions, and lenses (Zhu et al., 2012).

Critical work in this geological modelling process was the determination of strata interfaces using borehole data for stratigraphic correlation. This then defined the primary function of the geological modelling software which is to integrate the borehole and geometric data into continuous stratigraphic

information, displayed on a computer with a specific data structure (Huang et al., 2014).

Computers and computerised methods result in predicting sedimentary facies distribution and geometry of sedimentary basins; therefore, it is becoming a valuable device in geological studies (Gratacós et al., 2009). Figure 4.1, illustrates typical steps followed in a geological modelling process. Spatial and property data are two categories of unprocessed data collected from various sources.

Geometry modelling entails two steps: (1) Developing an appropriate geometric representation of the geological “framework”, and (2) Subdividing or “discretisation” of this framework. This connection is defined by the horizontal arrow connecting discretisation and analytical computation to visualisation and interpretation of the geological model (Turner & Gable, 1994).

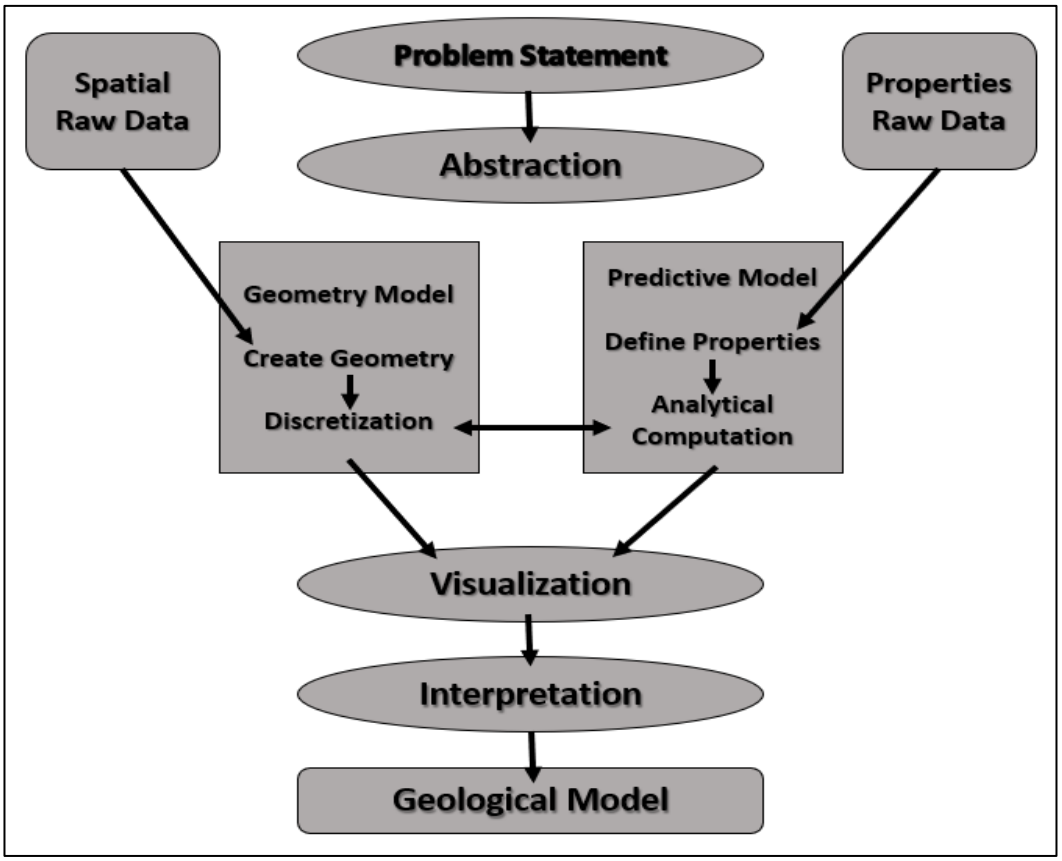

Figure 4.1: Overview of the geological modelling process (Turner & Gable, 1994).

In a sedimentary basin, a dominant geometrical shape is sequential, while faults and intersections of strata complicate the stacking of sedimentary strata (Popovs et al., 2014). A strata can be categorised as “complete” or “missing” with regards to their integrity and spatial distribution; for example, one spreads continuously over each region or discontinuously intersecting with other strata (Turner, 2006; Zhu et al., 2012).

Popovs et al. (2014) remark that “the model framework is established on apparent, well-organised depositional sequences”, dividing sedimentary strata by adherence to tectonic sequences to satisfy the requirements of a geological structure. Stacking the available base surfaces and reconstructing erosion interfaces creates the model. Erosion surfaces must be considered when comparing the thickness of an overlaying layer

because the same displacement must be represented in the erosion surface if the overlaying layer is faulted (Figure 4.2A).

Based on borehole data describing the deposited strata, sedimentary layer geometry is determined for each tectonic sequence. The proper layer topography is generated by gradually adding modelled slices to the space between the base and erosion surfaces; therefore, known fault displacements are transferred from base surfaces to the influenced layer sequence, consequently topography of sedimentary layers is logically coherent (Figure 4.2B). A layer is topographically similar to the underlaying layer if the thickness is unknown but can be identified (4th layer in Figure 4.2C). The void between the underlaying layer and the unconformity can be filled to produce the layer volume (Popovs et al., 2014).

A. Building the model outline;

B. Building sedimentary layers with known thicknesses;

C. Building sedimentary layers with unknown thicknesses.

Geological layer boundaries are indicated by boreholes BH 1, BH 2 and BH 3; vertical lines indicate faulting; dashed lines indicate actual surfaces; and dotted lines indicate erosional surfaces (Popovs et al., 2014).

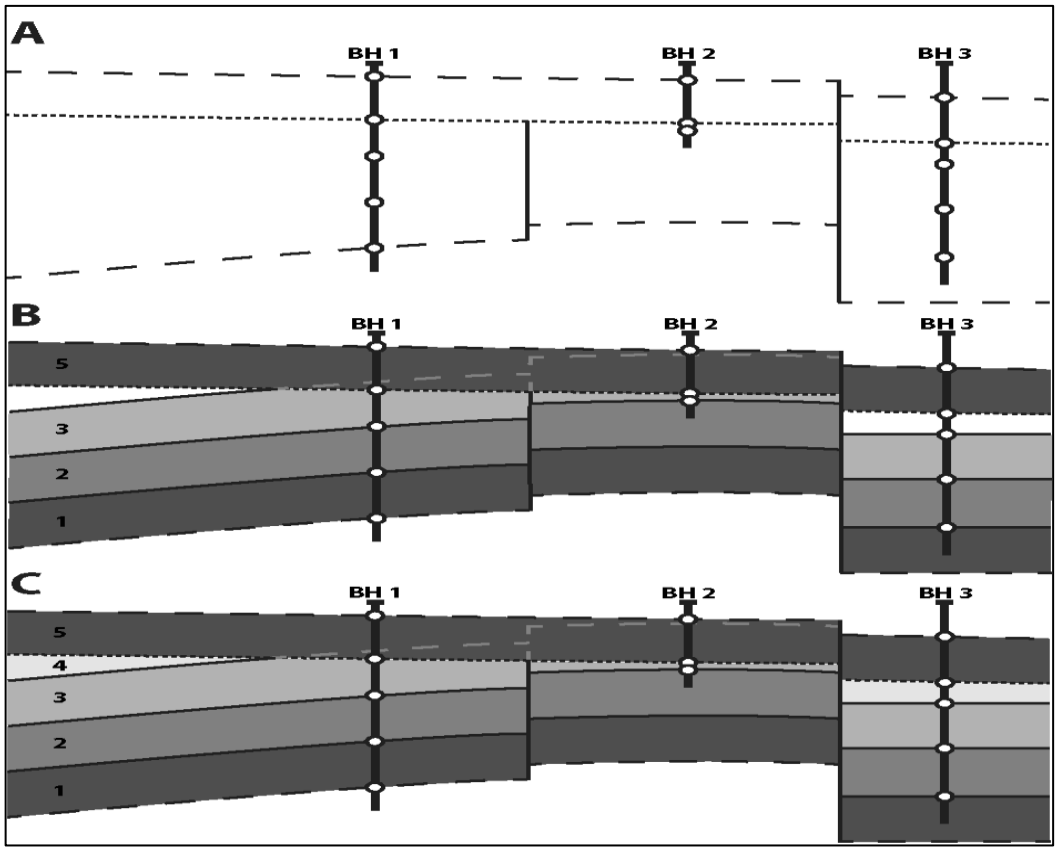

Figure 4.2: Principles for the suggested modelling technique, depicted schematically (Popovs et al., 2014).

4.3 Common Modelling Software Packages

There is a plethora of modelling software packages used for building geological models, including and not limited to (1) GEOVIA Minex; (2) 3D Geomodeller; (3) ESRI ArcGIS; (4) EarthVision; (5) Gocad; (6) GSI3D; (7) Multilayer-GDM; (8) GeoVisionary, (9) Isatis, (10) Move; (11) Petrel; (12) Rockworks; (13) SKUA; (14) Surfer; (15) Surpac; (16) Vulcan; (17) Leapfrog; (18) GemPy (19) BGS Groundhog Desktop; (20) Minescape and (21) Datamine.

Software programs can be utilized in geological modelling. Some software uses standard interpolation algorithms such as Natural Neighbor, Near Dense; Radial Basis Function, Minimum Curvature, Local Polynomial,

Polynomial Regression, Modified Shepard's Method, Triangulation using Linear Interpolation, and Inverse Distance Weighting methods to create geological surfaces (grids), while others use sophisticated geostatistical methods, including kriging and co-kriging (Shirzadi Babakan et al., 2008).

Primarily, two categories of geological models must be understood. The most typical kind delineates map unit distribution. The limits of these models imprecisely describe distributing material characteristics. The other typical model-form explicitly delineates the potential distribution of material qualities inside deposits, delineating the deposits' boundaries. These models are typically used as input to flow simulation models, incorporating plausible petrophysical parameter distributions, such as permeability and porosity (Berg et al., 2011).

Geo-modellers visualise their data at different stages of modelling to understand the conceptual geological framework.

4.4 GEOVIA Minex™ Modelling Software

GEOVIA Minex™ software is a recognised global leader in integrated geology and mining solutions mainly for stratified deposits. Minex ensures resources are precisely and accurately evaluated. The software uses all available data (i.e., geophysical, geotechnical, qualities, lithology, and structural data) to model and interpret the deposit.

In Minex geomodelling—the growth algorithm technique is preferred for interpolation. Minex follows the method of 'ECS Growth Technique' for triangulation to compute grids for stratigraphic layer deposits such as coal, Kriging and Inverse Distance Weighted methods are meant for more sophisticated models.

In the study, Minex was used as the main software of choice, for it is familiar; it was the only available software accessible; it has a proven record for

accuracy, precision, and compelling geological interpretations on stratified coal deposits. Other modelling software could not be used or tested for this research owing to their high licencing costs and inaccessibility. (Table 4.1) emphasises the motivators for choosing the software. The GEOVIA Minex™ software capabilities are as follows:

- Creates accurate geological models, which include coal seam thickness, roof and floor, quality gridding and cross-sections;
- Creates accurate models of inclined or curved faults in standard or reverse fault environments;
- Models complete coal wash curves for yield, ash, and other coal analyses and simulate plant processes by area or scheduled time;
- Useful in coal resource and reserves reporting;
- Capable of variogram modelling, which helps in identifying the best variograms for the data;
- Validates geological data by jack-knifing to ensure confidence in the accuracy of the geological models;
- Capable of contouring, cross sectioning, 2D and 3D borehole displaying, statistics, and histogram analysis.

A lithostratigraphic “layer-cake” model was created using Minex, modelling sedimentary settings by first building contact surfaces of strata, stacking the strata interfaces in the stratigraphy, and then describing the zones between them as geological units.

Exploration borehole information was used in the lithostratigraphic and structural model. The model comprises gridded roof and floor surfaces for the sampled zones defined from the exploration boreholes. Each roof and floor elevation of the zones are obtained from the boreholes’ sample elevations, resulting in roof and floor elevation data (Z-coordinate values) at the various borehole locations (X- and Y-coordinates). These zones’ roof

and floor elevations are then modelled in 2D - 3D for interpolation and extrapolation to form continuous grid data (25 m x 25 m grid cells).

"Gridding produces a regularly spaced, rectangular array of Z values from irregularly spaced XYZ data." Gridding uses extrapolation or interpolation of the data values to produce Z values at each grid node (Shirzadi Babakan et al., 2008).

Table 4.1: GEOVIA Minex™ software advantages and disadvantages

Advantages	Disadvantages
Saves Time – Mine design made easier	Financially costs more per licence
Helps In Making Better Decisions – Speed and accuracy over the entire process	It is not intuitive and requires some experience with other similar software
Improves Communication – Better interpretation of data with powerful visualisation devices and graphical displays	Surface grids sometimes crosscuts and create geologically impossible settings
Achieves Greater Accuracy – Tight integration with the stratigraphic model	If the z-collar is not aligned to the datum, this may lead to stratigraphic unit off-sets and zone mismatches
It has advanced and flexible devices for designing 3D geomodels and resource estimation	Wrong-referenced (XYZ) coordinates of borehole points may lead to boreholes being wrongly plotted and may paint a wrong picture of the information interpreted.

4.5 Inverse-Distance Weighted Method (IDW)

As a first rule, the IDW method should be used when the point set is dense for adequate analysis. The technique uses a linear-weighted combination sample point set to determine cell values. The weight assigned is a function of the separation between the input point and the location of the output cell. IDW is a deterministic spatial interpolation method. The overarching goal in this method is that the attribute values of any pair of points are related, and their similarity is inversely related to the distances between them (Shirzadi Babakan et al., 2008; Zhu et al., 2012; Shahbeik et al., 2014).

4.6 Geomodelling Steps on Minex Modelling Software

The geology modelling module is an integrated borehole database and geological modelling package for stratigraphic deposits. The module allows data (borehole collars, lithology, quality, geophysical, geotechnical etc.) to interpret the coal seams (Caumon et al., 2006; Zhu et al., 2012).

Minex modelling and new fault interpretation devices have been combined to support a single modelling process. The accuracy of faulting is achieved by detailed 3D conceptual modelling of the fault surfaces and fault blocks. Borehole-Surface-Solid method (Caumon et al., 2006) was followed in building the lithostratigraphic facies model for this research, as in Figure 4.3.

- Step 1: Identify the exact location of the coalfield as well as borehole XYZ coordinates.
- Step 2: Code the identified strata i.e., CZ1: Coal Zone Number 1; SS1: Sandstone Number 1; MS1: Mudstone Number 1.
- Step 3: Subdivide borehole data into a series of scatter points to see best fit trends.
- Step 4: Align top and bottom surfaces of each stratum to coincide horizontally.

- Step 5: Apply IDW interpolation technique to infer the elevations of surfaces.
- Step 6: Identify the types of all missing strata based on the top and bottom surfaces' elevations.
- Step 7: Intersect the TIN (Triangulated Irregular Network) surfaces in order to modify the elevations for the various types of missing stratum and their control strata.
- Step 8: Connect the top and bottom TINs with the corresponding control surfaces and heights of each missing stratum.
- Step 9: Manage the interfaces between the missing layers to their adjacent layers to ensure the consistency of all surfaces.
- Step 10: Build a reliable model by looking at the topological connections between each surface and each stratum.
- Step 11: Lastly, use the modelling output for spatial analysis and 3D visualization.

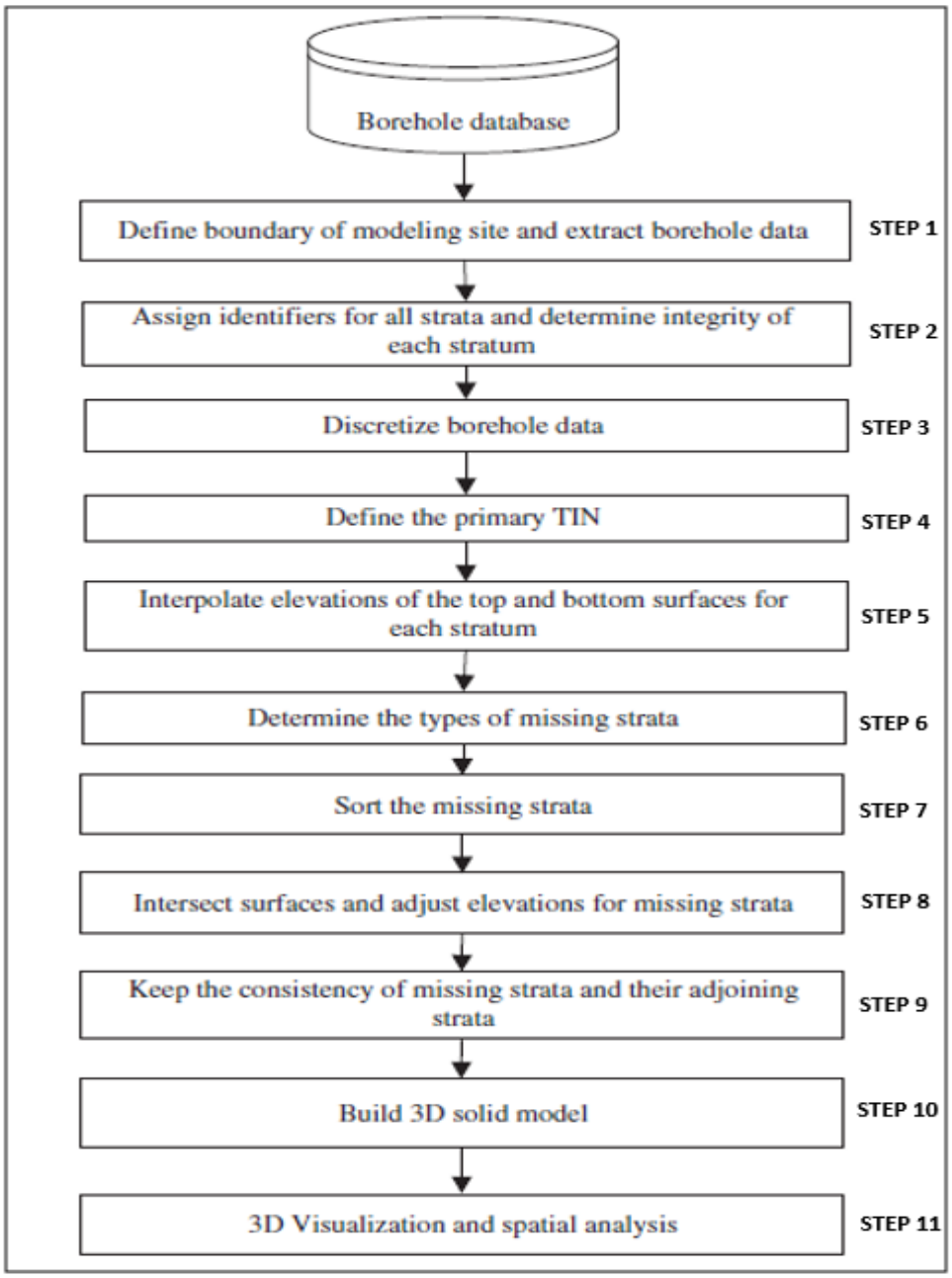

Figure 4.3: Borehole-surface-solid modelling steps (Caumon & Mallet, 2006).

Chapter 5: RESULTS AND INTERPRETATIONS OF THE LITHOSTRATIGRAPHIC MODEL

5.1 Introduction

A 3D lithostratigraphic facies model covering the Waterberg Coalfield was created to enable sedimentary basin interpretations and for the modelled grids to be visualised in an interactive platform. The model includes contour grids and cross-sections generated from surfaces identified to indicate thicknesses, quality distributions, and geometry for the coal and non-coal zones (CZ1 to OVB).

The data set used for the model comprises (1) collar; (2) lithology; (3) zones; and (4) raw coal analyses. From this data set, contour grid extrapolations were derived from drill hole surfaces and coal zone contacts. Data from the logs were digitised, and the lithology was numerically coded.

Borehole correlation to identify the zones and assign them to formations was done on all the 757 boreholes (Appendix A, Appendix D). Overburden (OVB) was assigned to the Eendragtpan Formation; coal zones 11 to 5 were assigned to the Grootegeluk Formation; coal and non-coal zones 4 to 1 were assigned to the Swartrant Formation. The ability to consistently apply correlation rules throughout the modelled area primarily determined the accuracy and precision of the model.

5.2 Topographic Map of The Waterberg Coalfield

The Digital Terrain Model (DTM) used in this research was provided by the Council for Geoscience, indicating a surface boundary and an elevation datum. Borehole z-collars were checked against it as a reference; any z-coordinate out by 1 m either above or below the DTM was rejected.

According to DTM interpretations, the locations around Mokolo River has the lowest topography in the Waterberg Coalfield area, whereas the highest

is along the Waterberg Mountains (Figure 5.1). With its wide confluence with Limpopo River, and the Mokolo River drainage channel, which flows in the north, is evident. The sandstone “koppies” of the Waterberg Group are associated with the higher elevated areas in the extreme south and south-east. Karoo rock outcrops, structure the central areas with moderate elevations. Height above mean sea level varies between 850 m and 950 m.

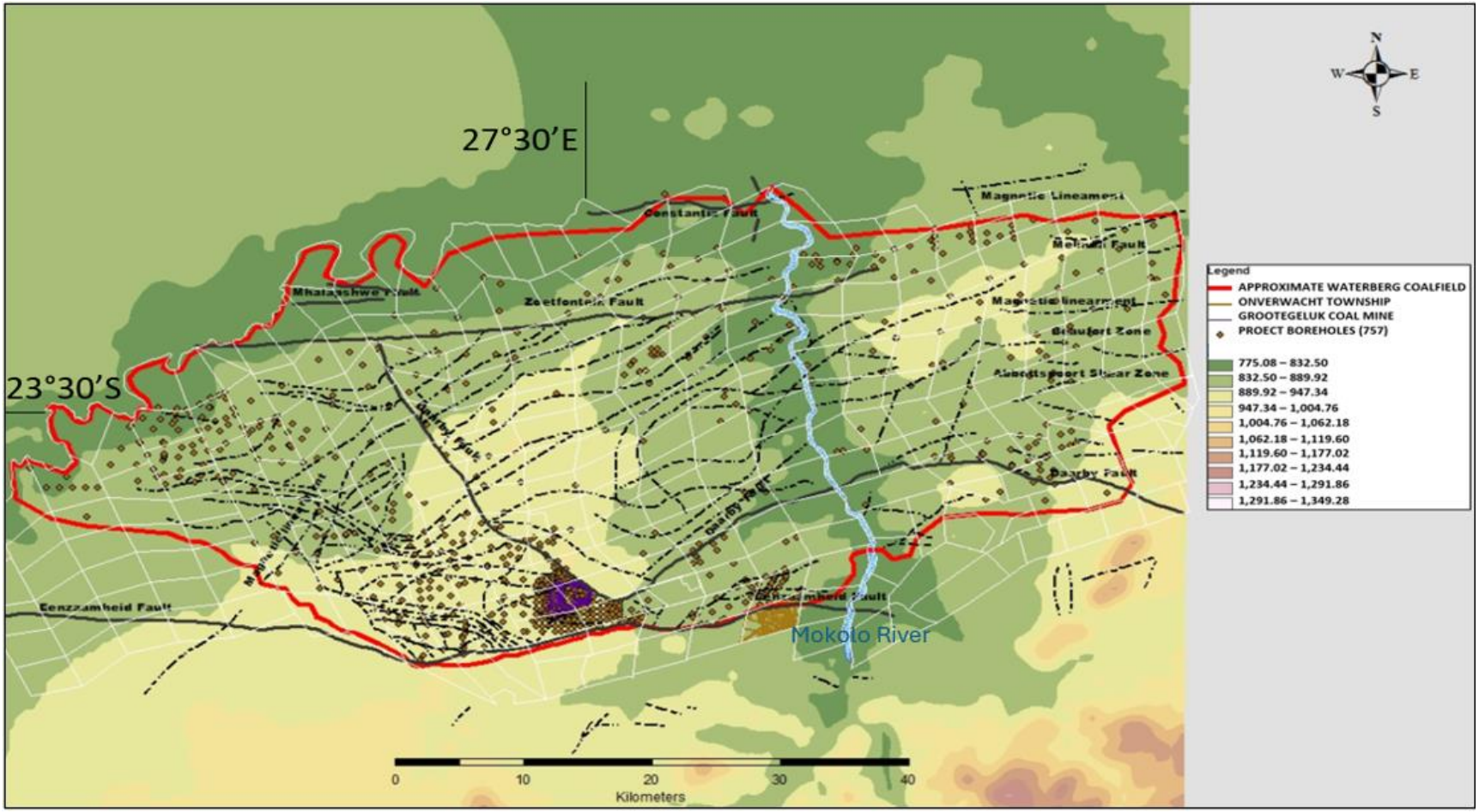

Figure 5.1: The Waterberg Coalfield topographical map (DTM).

5.3 Overburden, Coal, And Non-coal Zone, And Interbed Distribution In The Waterberg Coalfield

The Grootegeluk Formation (±55 m thick) comprises intercalated bright coal and mudstone layers. It has a coal-mudstone assemblage repetition that is so well-developed that it may be separated into seven distinct sedimentary cycles or zones (Zones 11 and 5) (Jeffrey, 2005). This formation is classified as a Thick Interbedded Seam Deposit Type (SANS 10320, 2004).

The Swartrant Formation (±50 m thick) consists of sandstone and carbonaceous shale that are interspersed with dull coal seams that range in thickness from 1.5 m to 9 m. It is classified as a Multiple Seam Deposit Type (SANS 10320, 2004). The Swartrant Formation has five coal zones, the majority of which are dull coal, with some bright coal developing near the base of coal zones 1, 2, 3, and 4 (Table 5.1).

Thickness and quality grids were created representing the coal, non-coal zones, interbeds, and overburden (OVB) (Appendix B); Coal Zone 11 (CZ11); Coal Zone 10 (CZ10); Coal Zone 9 (CZ9); Coal Zone 8 (CZ8); Coal Zone 7 (CZ7); Coal Zone 6 (CZ6); Coal Zone 5 (CZ5); Coal Zone 4 (CZ4); Mudstone 2 (MS2); Coal Zone 4A (CZ4A); Mudstone 1 (MS1); Coal Zone 3 (CZ3); Sandstone 2 (SS2); Coal Zone 2 (CZ2); Sandstone 1 (SS1) and Coal Zone 1 (CZ1) across the Waterberg Coalfield.

Table 5.1 represents the data output generated from the created geological model. The data are from the 757 boreholes, indicating the associated zones and samples, *in-situ* tons, average thicknesses, coal percentage content, waste thickness and raw analyses. This geostatistical information is generated from grids interpolated over a digitised area of influence across the coalfield. A grid is a linked spatial data structure, defining space as a display of equal-size cells arranged in rows and columns (Childs, 2004).

Table 5.1: Overburden, coal, non-coal zones, interbeds, and their *in-situ* parameters across the Waterberg Coalfield (compiled from Council for Geoscience, 2010).

SUPERGROUP	GROUP	FORMATION	ZONES	SAMPLES (Coal & Non-Coal)		*In-Situ* Tons (Gt)	AVERAGE THICKNESS (m)	Coal %	Waste Thick (m)	AS	CV	FC	IM	P_2O_5	RD	TS	VM
KAROO	BEAUFORT	EENDRAGTPAN	OVB	-		-	123.93	-	-	-	-	-	-	-	-	-	-
	ECCA	GROOTEGELUK	CZ11	1A-1D		5.59	6.07	38.33	26.16	54.15	9.90	17.98	2.08	0.00	2.50	1.10	20.22
			CZ10	2-6		12.72	8.72	53.86	5.08	46.07	10.50	24.45	2.22	0.00	1.74	1.26	23.05
			CZ9	7-9		7.76	6.08	48.34	1.87	46.34	10.91	24.19	2.24	0.00	1.86	1.31	23.72
			CZ8	10-14		9.40	8.44	42.82	2.31	46.51	10.19	24.68	2.16	0.00	1.86	0.85	22.81
			CZ7	15-18		9.08	8.92	39.94	2.93	45.66	9.00	22.58	1.94	0.00	1.86	0.69	23.74
			CZ6	19-21		4.57	6.34	32.17	3.42	43.99	10.56	27.45	1.96	0.00	1.86	0.89	23.16
			CZ5	22A-22E		6.21	11.06	21.97	5.02	46.72	8.56	25.09	1.91	0.02	1.88	0.96	22.23
		SWARTRANT	CZ4	23A-23C		10.96	5.02	99.13	14.85	55.68	7.18	17.74	1.80	0.04	1.65	0.85	17.51
			MS2	23AS-23BS*		-	4.36	-	80.69	-	-	-	-	-	2.21	-	-
			CZ4A	24		3.61	2.47	96.37	24.05	44.24	6.82	31.04	1.98	0.05	1.80	0.95	19.12
			MS1	24S*		-	15.35	-	31.38	-	-	-	-	-	2.45	-	-
			CZ3	25-29		8.43	4.92	96.41	27.34	37.62	10.57	28.48	2.18	0.03	1.59	0.69	19.78
			SS2	25S*		-	5.20	-	37.92	-	-	-	-	-	2.49	-	-
			CZ2	30-31		6.77	4.16	98.22	4.29	31.99	12.46	45.31	2.15	0.01	1.52	1.01	21.72
			SS1	30S*		-	7.08	-	62.07	-	-	-	-	-	2.50	-	-
			CZ1	32		2.86	1.74	98.54	20.05	30.21	11.55	34.60	1.87	0.01	1.52	1.09	21.30
				Weighted Averages		87.98	6.69	62.72	10.09	45.26	9.80	25.80	2.06	0.01	1.79	0.97	21.60

COAL ANALYSES **(1) AS:** *Ash (%);* **(2) CV:** *Calorific Value (MJ/kg);* **(3) FC:** *Fixed Carbon (%);* **(4) IM:** *Inherent Moisture (%);* **(5) P_2O_5:** *Phosphorus (%);* **(6) RD:** *Relative Density (g/cm^3);* **(7) TS:** *Total Sulphur (%);* **(8) VM:** *Volatile Matter (%).*

* Interburden Waste

5.3.1 Overburden Thickness (OVB)

The overburden, which belongs to the Eendragtpan Formation averages 123.93 m, with a min of 0.40 m and a max thickness of 450 m (Figure 5.2). It comprises topsoil and sand with sporadic calcrete and ferricrete nodules, massive and weathered brown-yellow-purple-red mudstone towards the top, and light grey mudstone with bright coal streaks on the lower half.

In this study area, the overburden thickens inwards towards the centre of the coalfield, and the thickness ranges from 85.20 m to 426 m. The OVB isopach map demonstrates some relatively thick deposition (~213 m) in the central portion of the deposit where the bedrock is deeper, where sand and gravel are mapped at the land surface.

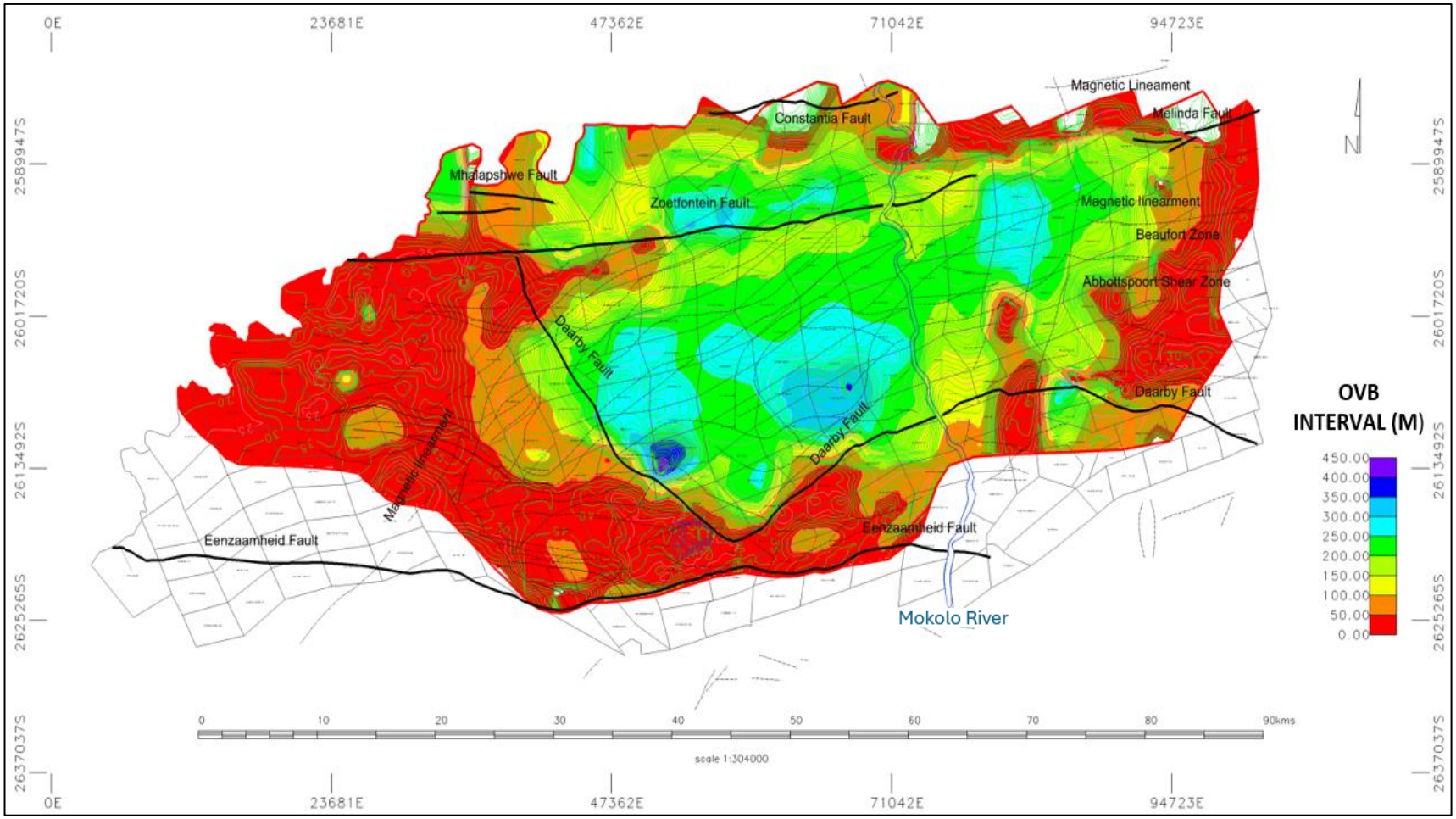

Figure 5.2: Overburden (OVB) thickness distribution across the Waterberg Coalfield.

5.3.2 Coal Zone 11_Seam Thickness (CZ11)

Coal Zone 11 (coal samples 1A-1D; non-coal samples 1BS-1DS) (Appendix A), which belongs to the Grootegeluk Formation averages 6.07 m, with a min of 0.19 m and a max of 55 m. A thickness of up to 55 m occurs and is maintained to less than 10 m across the coalfield. In the northern part, and in the north-eastern portion of the coalfield the thickness is less than 5 m. An anomaly thickness of between 15 m and 55 m can be observed at the central parts of the coalfield (Figure 5.3).

It comprises bright coal interbedded with grey mudstone and carbonaceous lenses, with 38.33% *in-situ* coal content. At Grootegeluk Mine, the coal zone produces semi-soft coking coal (10% Ash) at yields between 32-34% and power station coal. The coal is processed through Grootegeluk 1 (GG1) and Grootegeluk 6 (GG6)—two-stage wash plants (Chabedi & Mhlongo, 2018). Raw qualities: Calorific Value_9.90Mj/kg; Inherent Moisture_2.08%; Ash_54.15%; Volatile Matter_20.22%; Fixed Carbon_17.98%; Total Sulphur_1.10% (Council for Geoscience, 2010; Table 5.1).

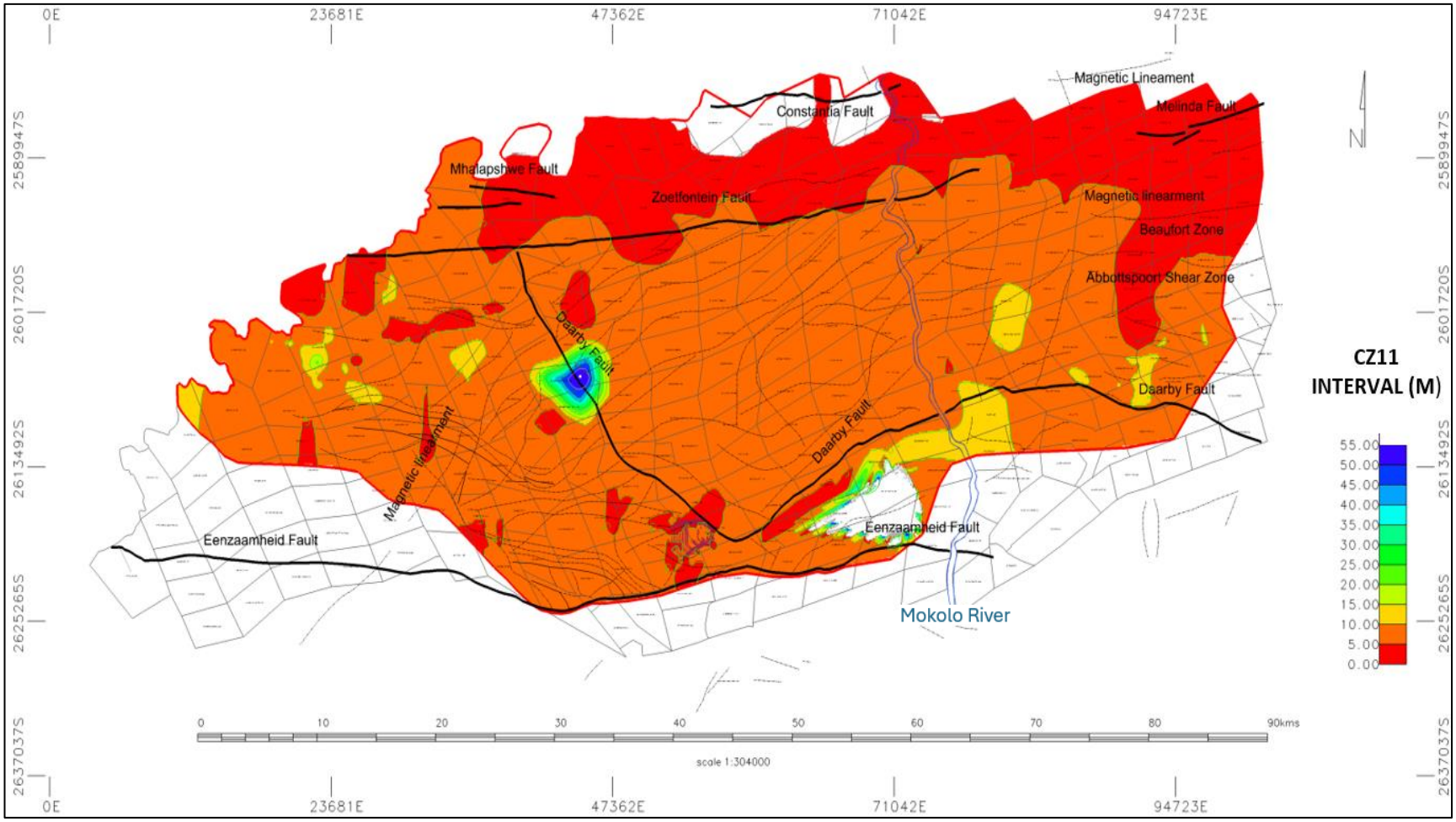

Figure 5.3: Coal Zone 11 (CZ11) seam thickness distribution across the Waterberg Coalfield.

5.3.3 Coal Zone 10_Seam Thickness (CZ10)

Coal Zone 10 (coal samples 2-6; non-coal samples 2S-6S) (Appendix A), which belongs to the Grootegeluk Formation averages 8.72 m, with a min of 0.80 m and a max thickness of 25 m. A thickness of up to 25 m occurs and is maintained at less than 20 m across the coalfield. The northern part, beyond the Zoetfontein Fault and on the north-eastern portion of the coalfield a 10 m thickness generally occurs. Anomaly thicknesses of between 15 m and 25 m can be observed towards the eastern part of the coalfield (Figure 5.4).

The coal zone comprises carbonaceous mudstone interbedded with bright coal, carbonaceous lenses, a trace of siderite, and thick mudstone plies in the bottom half, with 53.86% *in-situ* content. At Grootegeluk Mine, the coal zone produces semi-soft coking coal (10% Ash) at yields between 32-34% and power station coal. The coal is processed through Grootegeluk 1 (GG1) and Grootegeluk 6 (GG6)—two-stage wash plants (Chabedi & Mhlongo, 2018). Raw qualities: Calorific Value_10.50Mj/kg; Inherent Moisture_2.22%; Ash_46.07%; Volatile Matter_23.05%; Fixed Carbon_24.45%; Total Sulphur_1.26% (Council for Geoscience, 2010; Table 5.1).

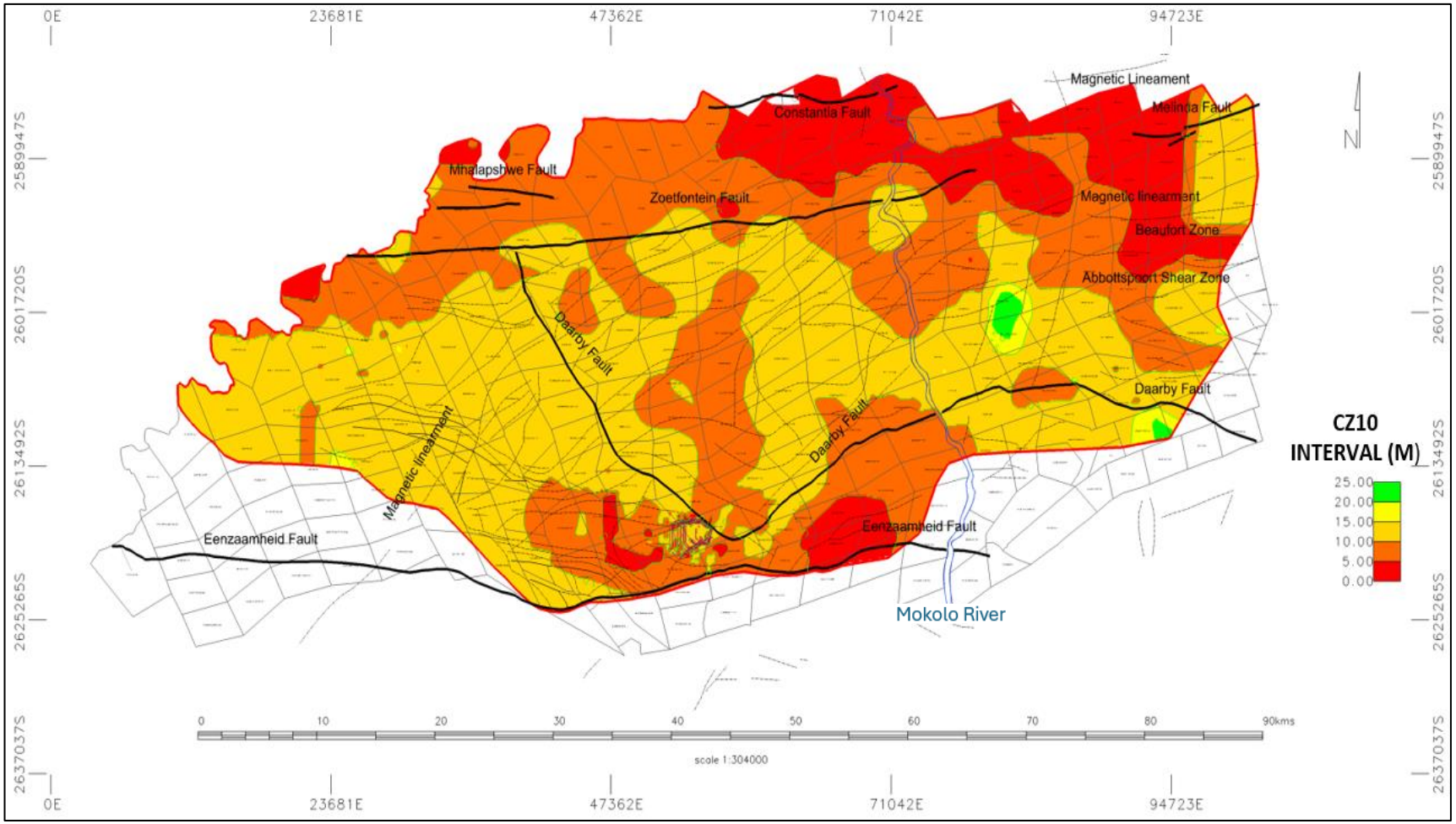

Figure 5.4: Coal Zone 10 (CZ10) seam thickness distribution across the Waterberg Coalfield.

5.3.4 Coal Zone 9_Seam Thickness (CZ9)

Coal Zone 9 (coal samples 7-9; non-coal samples 7S-9S) (Appendix A), which belongs to the Grootegeluk Formation averages 6.08 m, with a min of 0.94 m and a max thickness of 20 m. A thickness of up to 20 m occurs and is maintained to less than 10 m across the coalfield. The north-eastern portion of the coalfield as well as in a few places, the thickness is less than 5 m. It is only at random places where the thickness range between 15 m and 20 m (Figure 5.5).

The zone comprises a thick basal coal seam, carbonaceous shale/mudstone, and bright coal with noticeable siderite at the base, with 48.34% *in-situ* coal content. At Grootegeluk Mine, the coal zone produces semi-soft coking coal (10% Ash) at yields between 32-34% and power station coal. The coal is processed through Grootegeluk 1 (GG1) and Grootegeluk 6 (GG6)—two-stage wash plants (Chabedi & Mhlongo, 2018). Raw qualities: Calorific Value_10.91Mj/kg; Inherent Moisture_2.24%; Ash_46.34%; Volatile Matter_23.72%; Fixed Carbon_24.19%; Total Sulphur_1.31% (Council for Geoscience, 2010; Table 5.1).

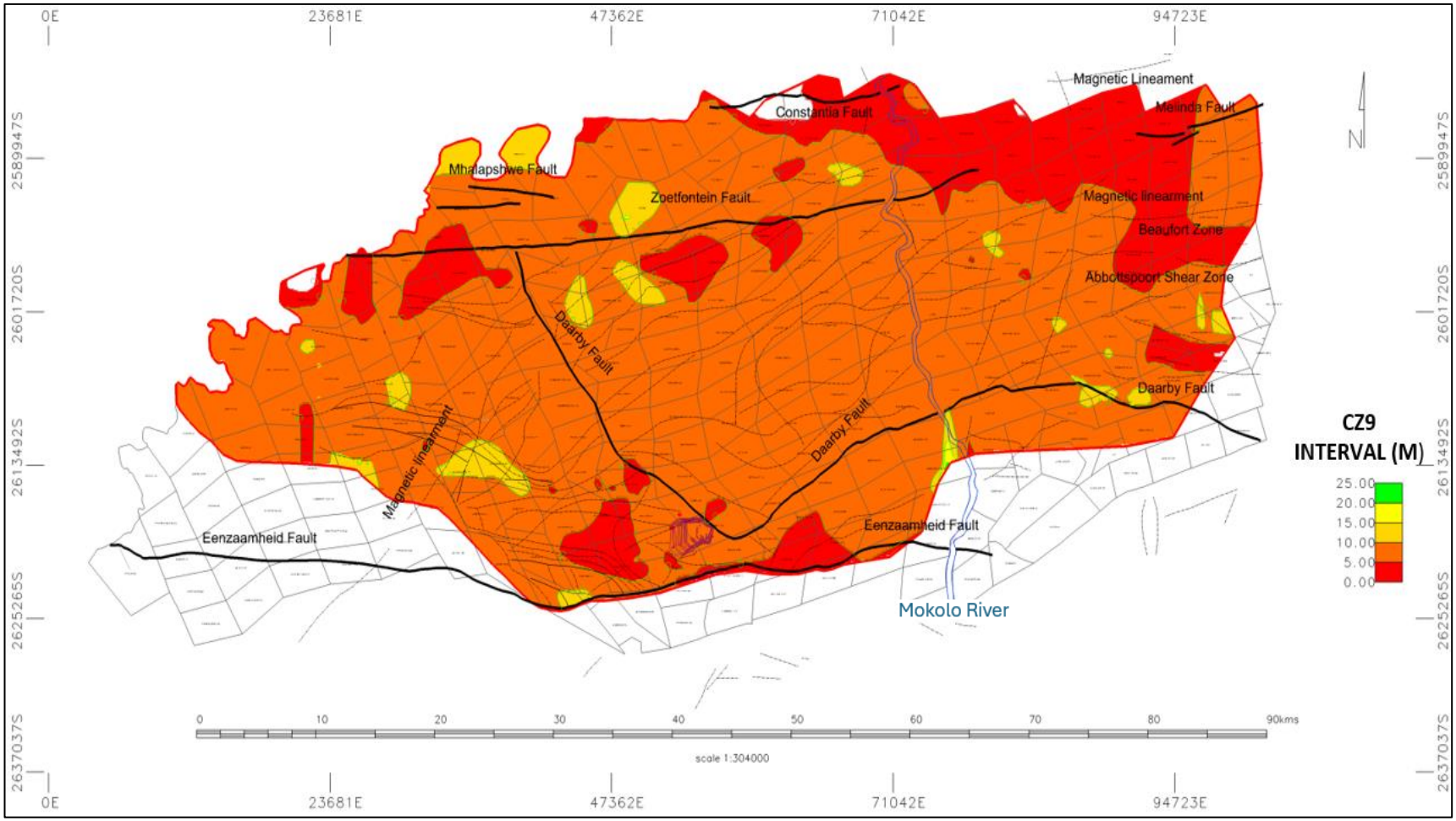

Figure 5.5: Coal Zone 9 (CZ9) seam thickness distribution across the Waterberg Coalfield.

5.3.5 Coal Zone 8_Seam Thickness (CZ8)

Coal Zone 8 (coal samples 10-14; non-coal samples 10S-14S) (Appendix A), which belongs to the Grootegeluk Formation averages 8.44 m, with a min of 0.13 m and a max thickness of 30 m. A thickness of up to 30 m occurs and is maintained to less than 20 m across the coalfield. The northern part, beyond the Zoetfontein Fault and on the north-eastern portion of the coalfield has a thickness of less than 5 m. The central portion is up to 10 m, while the eastern and western portions range between 10 m and 30 m in thickness (Figure 5.6).

The zone has thick coal seams at the base, interbedded with carbonaceous shale/mudstone and bright coal with prominent siderite, with 42.82% *in-situ* coal content. At Grootegeluk Mine, the coal zone produces semi-soft coking coal (10% Ash) at yields between 32-34% and power station coal. The coal is processed through Grootegeluk 1 (GG1) and Grootegeluk 6 (GG6)—two-stage wash plants (Chabedi & Mhlongo, 2018). Raw qualities: Calorific Value_10.19Mj/kg; Inherent Moisture_2.16%; Ash_46.51%; Volatile Matter_22.81%; Fixed Carbon_24.68%; Total Sulphur_0.85% (Council for Geoscience, 2010; Table 5.1).

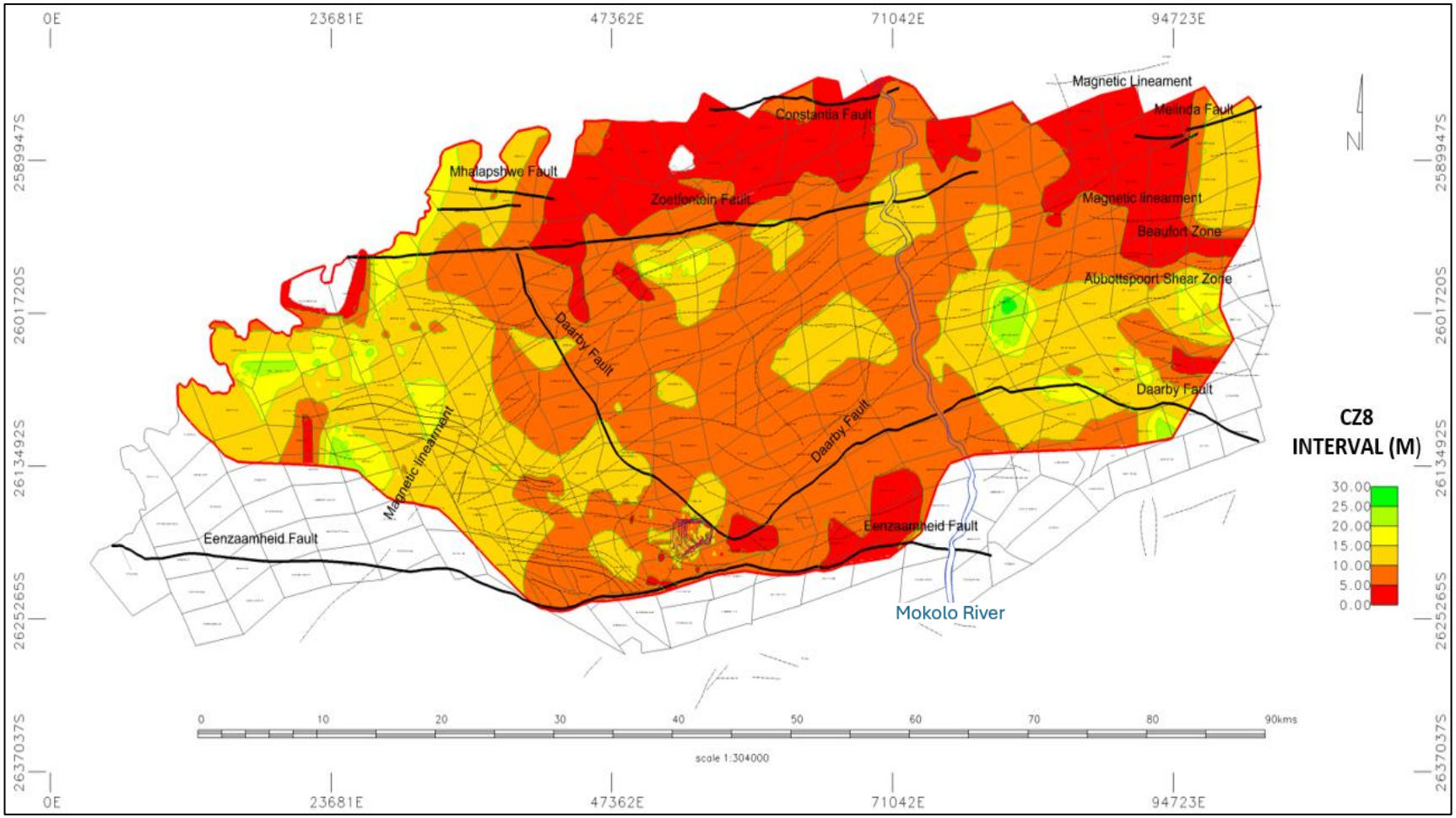

Figure 5.6: Coal Zone 8 (CZ8) seam thickness distribution across the Waterberg Coalfield.

5.3.6 Coal Zone 7_Seam Thickness (CZ7)

Coal Zone 7 (coal samples 15A, 15B-18; non-coal samples 15AS, 15BS-18S) (Appendix A), which belongs to the Grootegeluk Formation averages 8.92 m, with a min of 0.48 m and a max thickness of 35 m. A thickness of up to 35 m occurs and is maintained to less than 20 m across the coalfield. At isolated areas in the northern part, beyond the Zoetfontein Fault and on the north-eastern portion of the coalfield the thickness is generally less than 5 m. The southern and western portions increase in thickness to 20 m, while the eastern portion range between 20 m and 35 m in thickness (Figure 5.7).

The zone has bright sideritic coal, interlayered with carbonaceous shale and mudstone, interlaminated in nature, with 39.94% *in-situ* coal content. At Grootegeluk Mine, the coal zone produces semi-soft coking coal (10% Ash) at yields between 32-34% and power station coal. The coal is processed through Grootegeluk 1 (GG1) and Grootegeluk 6 (GG6)—two-stage wash plants (Chabedi & Mhlongo, 2018). Raw qualities: Calorific Value_9.00Mj/kg; Inherent Moisture_1.94%; Ash_45.66%; Volatile Matter_23.74%; Fixed Carbon_22.58%; Total Sulphur_0.69% (Council for Geoscience, 2010; Table 5.1).

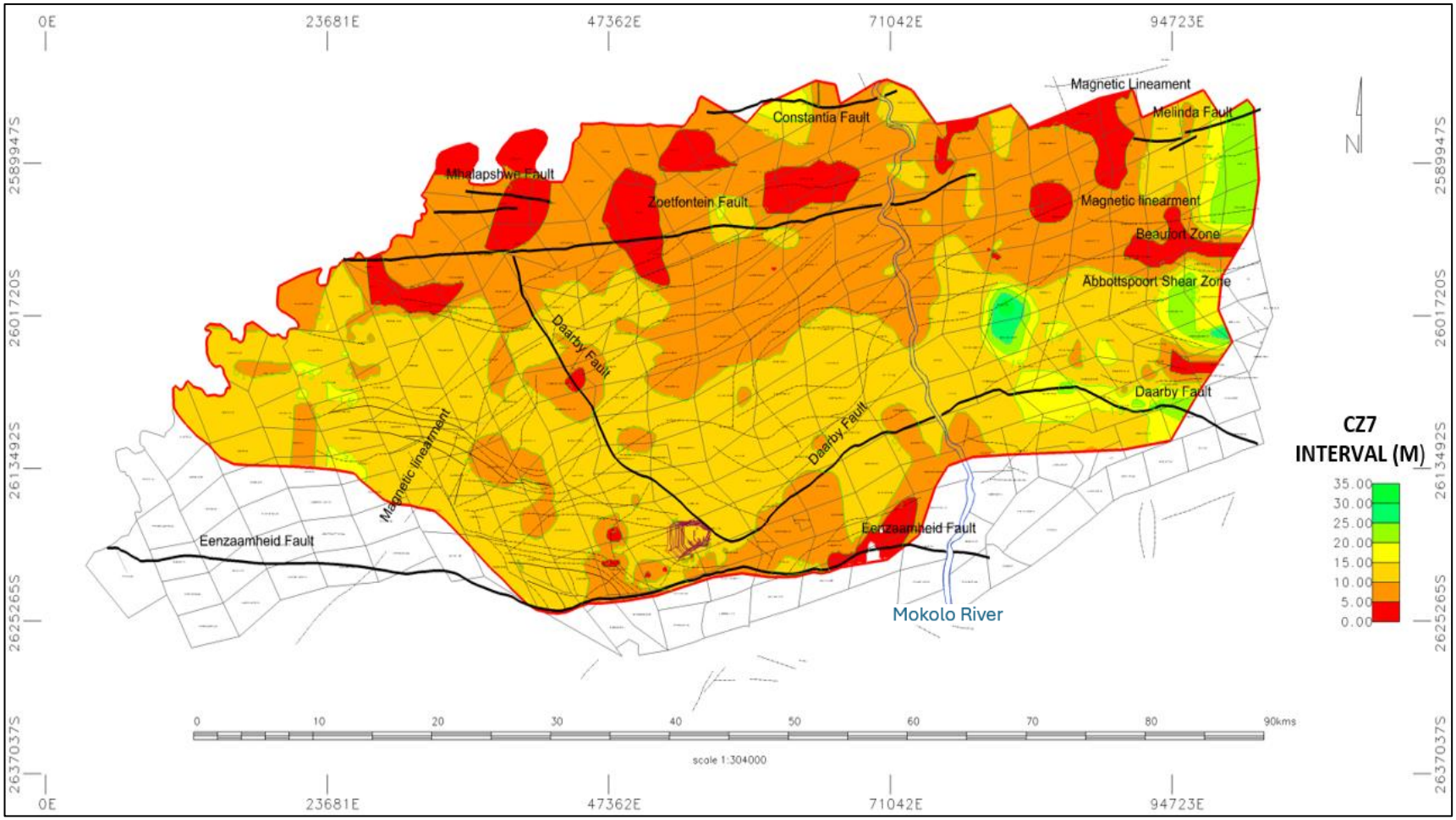

Figure 5.7: Coal Zone 7 (CZ7) seam thickness distribution across the Waterberg Coalfield.

5.3.7 Coal Zone 6_Seam Thickness (CZ6)

Coal Zone 6 (coal samples 19-21; non-coal samples 19S-21S) (Appendix A), which belongs to the Grootegeluk Formation averages 6.34 m, with a min of 0.27 m and a max thickness of 30 m. A thickness of up to 30 m occurs and is maintained to less than 10 m across the coalfield. At isolated areas across the coalfield the thickness is generally less than 5 m. The central and eastern portions increase in thickness ranging between 10 m to 30 m in thickness (Figure 5.8).

The zone comprises carbonaceous shale/mudstone interlaminated with bright coal that is extremely sideritic at the base, with 32.17% *in-situ* coal content. At Grootegeluk Mine, the coal zone produces semi-soft coking coal (10% Ash) at yields between 32-34% and power station coal. The coal is processed through Grootegeluk 1 (GG1) and Grootegeluk 6 (GG6)—two-stage wash plants (Chabedi & Mhlongo, 2018). Raw qualities: Calorific Value_10.56Mj/kg; Inherent Moisture_1.96%; Ash_43.99%; Volatile Matter_23.16%; Fixed Carbon_27.45%; Total Sulphur_0.89% (Council for Geoscience, 2010; Table 5.1).

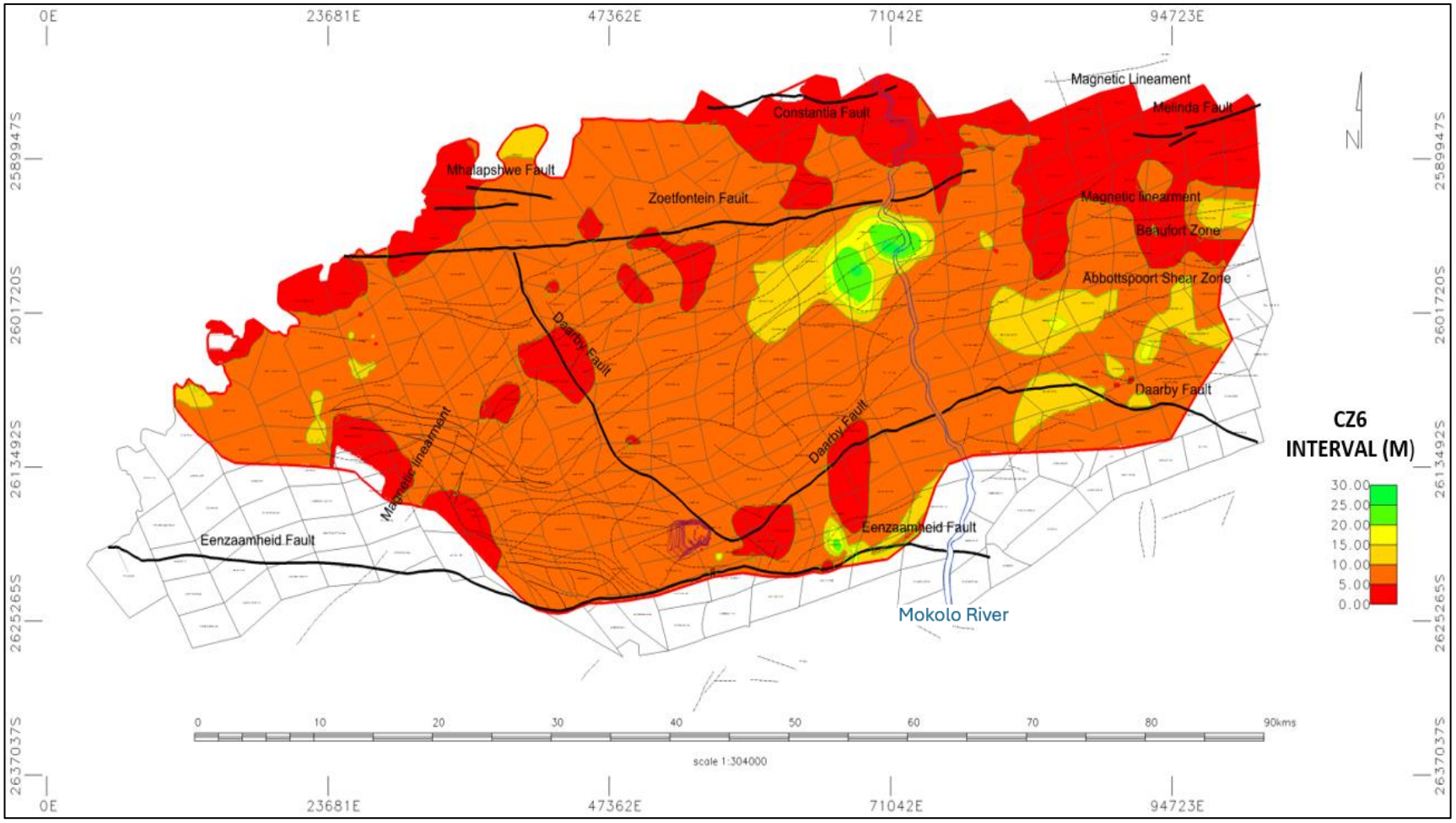

Figure 5.8: Coal Zone 6 (CZ6) seam thickness distribution across the Waterberg Coalfield.

5.3.8 Coal Zone 5_Seam Thickness (CZ5)

Coal Zone 5 (coal samples 22A-22E; non-coal samples 22AS-22FS) (Appendix A), which belongs to the Grootegeluk Formation averages 11.06 m, with a min of 0.65 m and a max thickness of 40 m. A thickness of up to 40 m occurs and is maintained to less than 20 m across the coalfield. The central portion ranges between 10 m and 25 m. At isolated areas in the northern part, beyond the Zoetfontein Fault and on the north-eastern and south-western portions thickness is generally less than 10 m. An anomaly thickness of between 25 m and 40 m occur in the eastern portion of the coalfield (Figure 5.9).

The zone comprises 2.5 m of coal-rich shale and carbonaceous mudstone, with thin coal laminae in the lower two-thirds and less noticeable siderite content, with 21.97% *in-situ* coal content. At Grootegeluk Mine, high phosphorus coking coal, and power station coal at yields between 32-34% are produced. The coal is processed through Grootegeluk 2 (GG2) and Grootegeluk 8 (GG8)—single-stage wash plants (Chabedi & Mhlongo, 2018). Raw qualities: Calorific Value_8.56Mj/kg; Inherent Moisture_1.91%; Ash_46.72%; Volatile Matter_22.23%; Fixed Carbon_25.09%; Total Sulphur_0.96% (Council for Geoscience, 2010; Table 5.1).

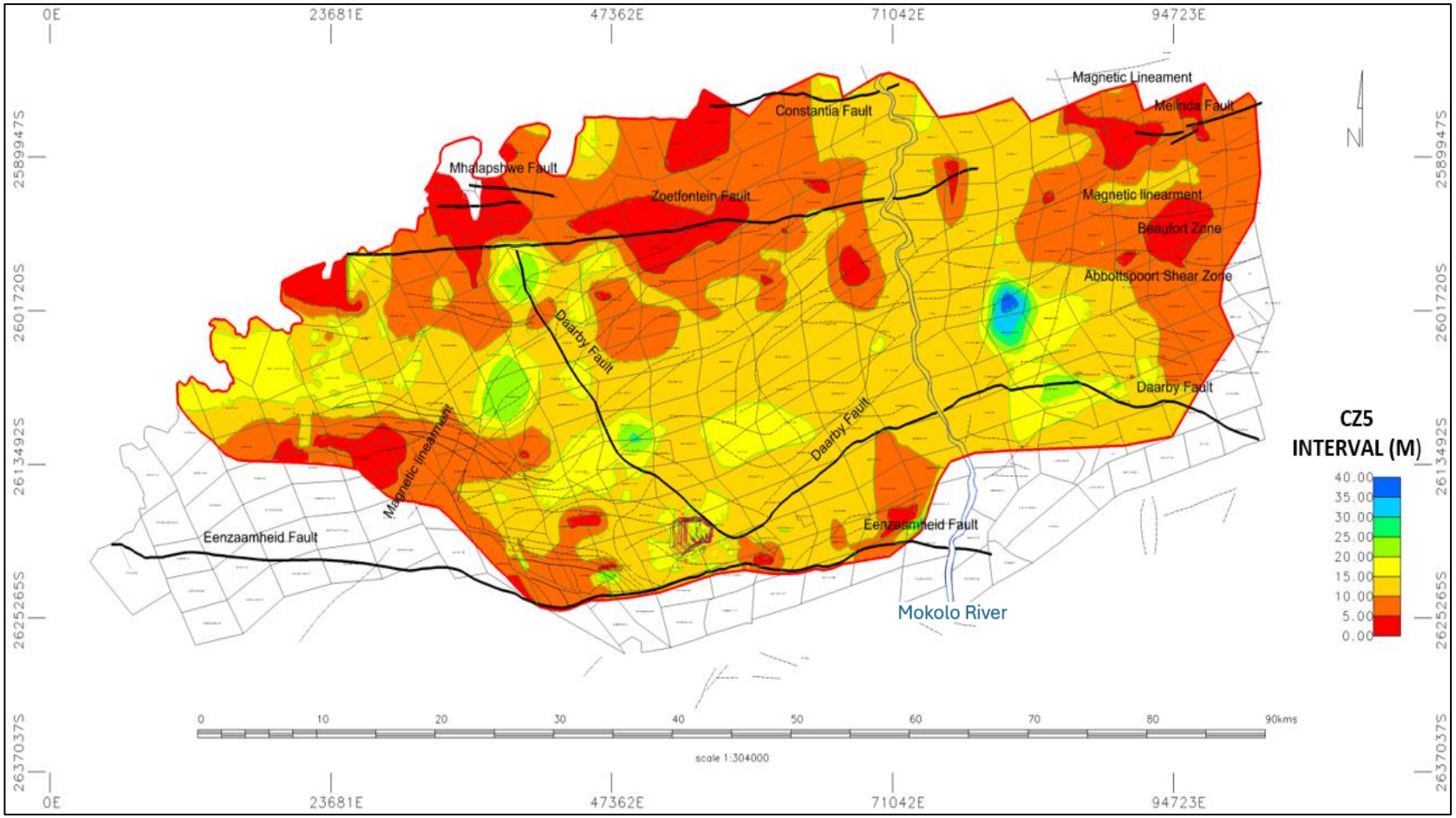

Figure 5.9: Coal Zone 5 (CZ5) seam thickness distribution across the Waterberg Coalfield.

5.3.9 Coal Zone 4_Seam Thickness (CZ4)

Coal Zone 4 (coal samples 23A-23C) (Appendix A), which belongs to the Swartrant Formation averages 5.02 m, with a min of 0.07 m and a max thickness of 45.88 m. A thickness of up to 45.88 m occurs and is maintained to less than 10 m across the coalfield. At isolated areas in the northern and eastern parts, the thickness is generally more than 15 m. An anomaly thickness of between 30 m and 45.88 m can be observed at the central part of the coalfield (Figure 5.10).

The zone contains thin shale bands and bright coal interlaminated with dull coal at the base, with 99.13% *in-situ* coal content. The coal zone produces blend coking coal at yields between 10-12%. At Grootegeluk Mine, the coal is processed through Grootegeluk 3 (GG3) and Grootegeluk 7 (GG7), dry crush and screening plants (Chabedi & Mhlongo, 2018). Raw qualities: Calorific Value_7.18Mj/kg; Inherent Moisture_1.80%; Ash_55.68%; Volatile Matter_17.51%; Fixed Carbon_17.74%; Total Sulphur_0.85% (Council for Geoscience, 2010; Table 5.1).

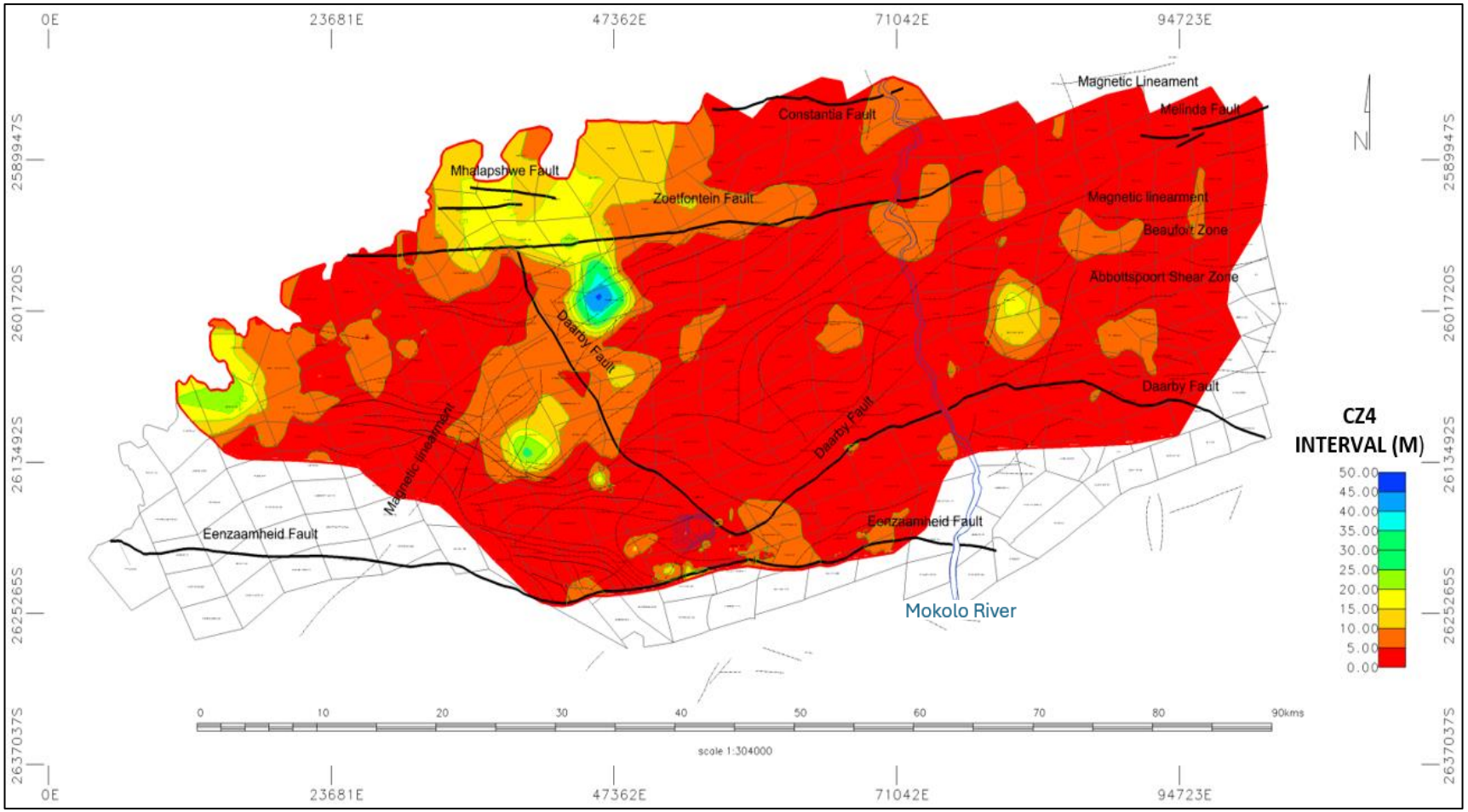

Figure 5.10: Coal Zone 4 (CZ4) seam thickness distribution across the Waterberg Coalfield.

5.3.10 Mudstone 2_Interbed Thickness (MS2)

Mudstone 2 (non-coal samples 23AS, 23BS) (Appendix A), which belongs to the Swartrant Formation averages 4.36 m, with a min of 0.64 m and max of 29.96 m. An anomaly thickness of up to 55 m occurs and is maintained to less than 20 m across the coalfield. At an isolated area in the northern part, the thickness is generally more than 20 m. There was no data interpolated at the north-eastern part of the coalfield, therefore there is no thickness range (i.e., white patches depicting low level of confidence) (Figure 5.11).

It comprises a dark grey mudstone, with 1 m fossiliferous bearing siltstone at the base. No traces of coal or shale within this unit. The distribution plan indicates sandstone thickening towards the northwest. North-eastern portion of the coalfield is devoid of this interbed.

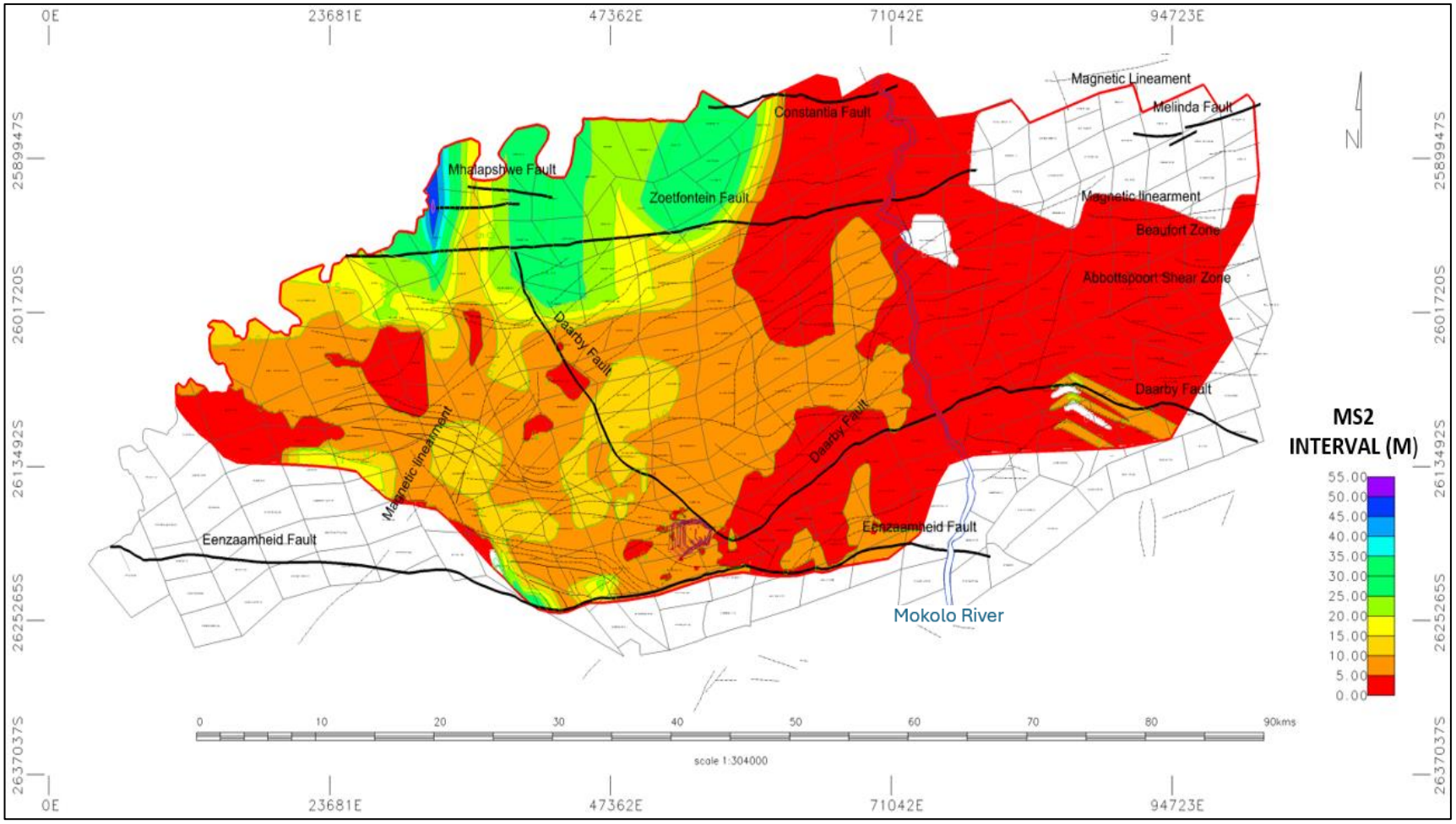

Figure 5.11: Mudstone 2 (MS2) interbed thickness distribution across the Waterberg Coalfield.

5.3.11 Coal Zone 4A_Seam Thickness (CZ4A)

Coal Zone 4A (coal sample 24) (Appendix A), which belongs to the Swartrant Formation averages 2.47 m, with a min of 0.18 m and max thickness of 25 m. A thickness of up to 25 m occurs and is maintained at less than 5 m across the coalfield. At isolated areas in the central parts, the thickness is generally more than 10 m. There was no data interpolated at the southern part of the coalfield, therefore there is no thickness range (i.e., white patches depicting low level of confidence) (Figure 5.12).

The zone comprises a few thin bright coal laminae, dull coal and mudstone bands, with 96.37% *in-situ* coal content. The coal zone produces blend coking coal at yields between 10-12%. At Grootegeluk Mine, the coal is processed through Grootegeluk 2 (GG2) and Grootegeluk 8 (GG8) single-stage wash plants (Chabedi & Mhlongo, 2018). Raw qualities: Calorific Value_6.82Mj/kg; Inherent Moisture_1.98%; Ash_44.24%; Volatile Matter_19.12%; Fixed Carbon_31.04%; Total Sulphur_0.95% (Council for Geoscience, 2010; Table 5.1).

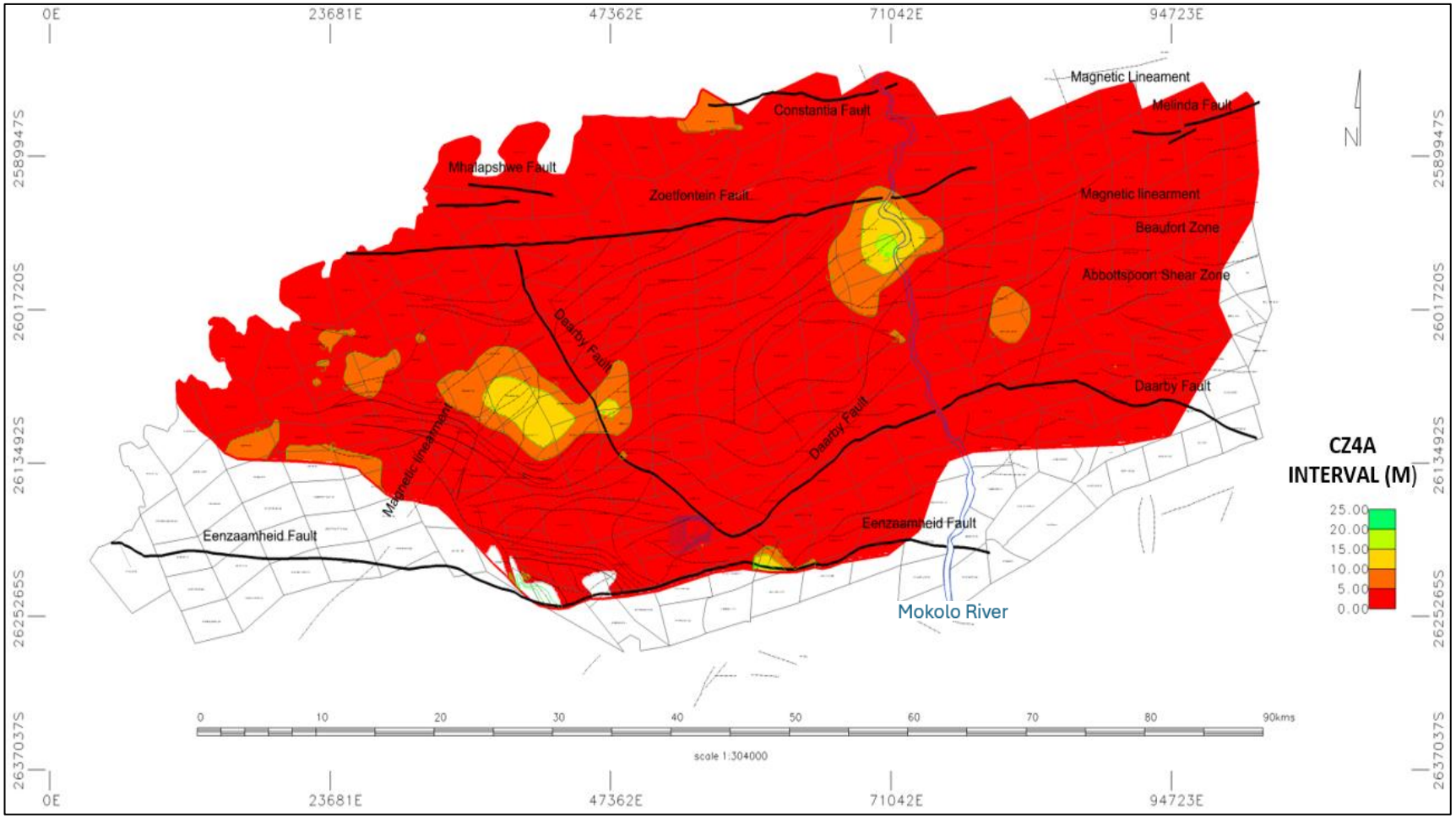

Figure 5.12: Coal Zone 4A (CZ4A) seam thickness distribution across the Waterberg Coalfield.

5.3.12 Mudstone 1_Interbed Thickness (MS1)

Mudstone 1 (non-coal sample 24S) (Appendix A), which belongs to the Swartrant Formation averages 15.35 m, with a min of 0.45 m and max of 60 m. A thickness of up to 60 m occurs and is maintained to less than 35 m across the coalfield. The western portion thickens to more than 20 m, while thinning to less than 20 m towards the eastern part of the coalfield. There was no data interpolated at the south-eastern part of the coalfield, therefore there is no thickness range (i.e., white patches depicting low level of confidence) (Figure 5.13).

It was distinctively identified in most boreholes as comprising dark grey carbonaceous or organic-rich mudstone. The unit thickens towards the northern part and thins towards the southern part of the coalfield. In some areas, it does not occur, as in the south-eastern part of the coalfield.

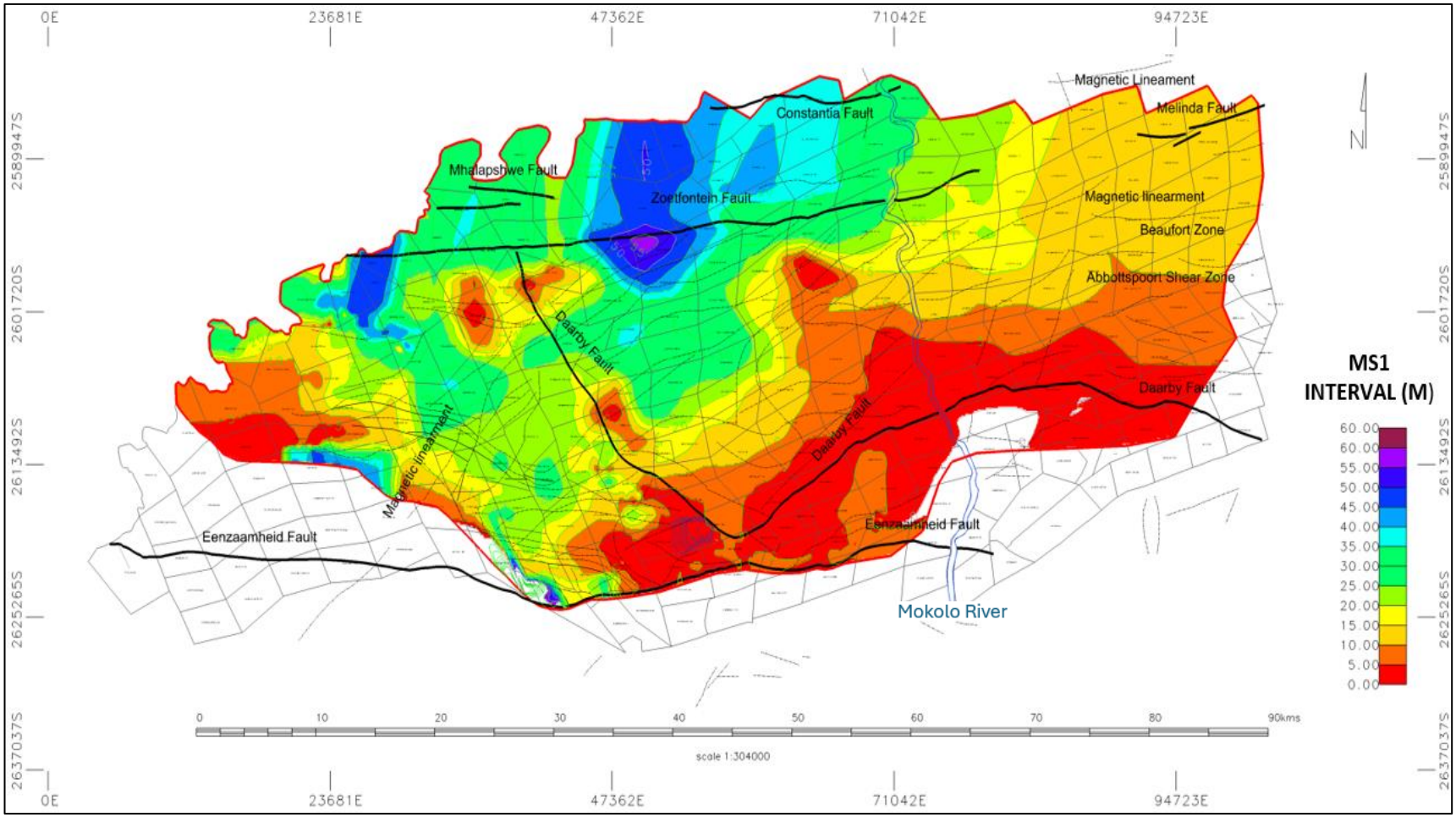

Figure 5.13: Mudstone 1 (MS1) interbed thickness distribution across the Waterberg Coalfield.

5.3.13 Coal Zone 3_Seam Thickness (CZ3)

Coal Zone 3 (coal samples 25-29; non-coal sample 25S) (Appendix A), which belongs to the Swartrant Formation averages 4.92 m, with a min of 0.19 m and a max thickness of 25 m. A thickness of up to 25 m occurs and is maintained to less than 20 m across the coalfield. The western portion thins to less than 5 m, and in other portions across the coalfield. Isolated portions of between 10 m and 20 m also occur (Figure 5.14).

The zone comprises dull coal, some bright coal laminae, and a few thin shale bands in the bottom 1.6 m, with 96.41% *in-situ* coal content. The upper part has a high phosphorus content, while the lower part has a medium phosphorus content. At Grootegeluk Mine, the coal zone produces power station coal; metallurgical coal and pulverised coal injection products (10% Ash) at yields between 10-12%.

The coal is processed through Grootegeluk 3 (GG3) and Grootegeluk 7 (GG7), dry crush and screening plants; also, through Grootegeluk 4 (GG4) and Grootegeluk 5 (GG5), single-stage beneficiation plants (Chabedi & Mhlongo, 2018). Raw qualities: Calorific Value_10.57Mj/kg; Inherent Moisture_2.18%; Ash_37.62%; Volatile Matter_19.78%; Fixed Carbon_28.48%; Total Sulphur_0.69% (Council for Geoscience, 2010; Table 5.1).

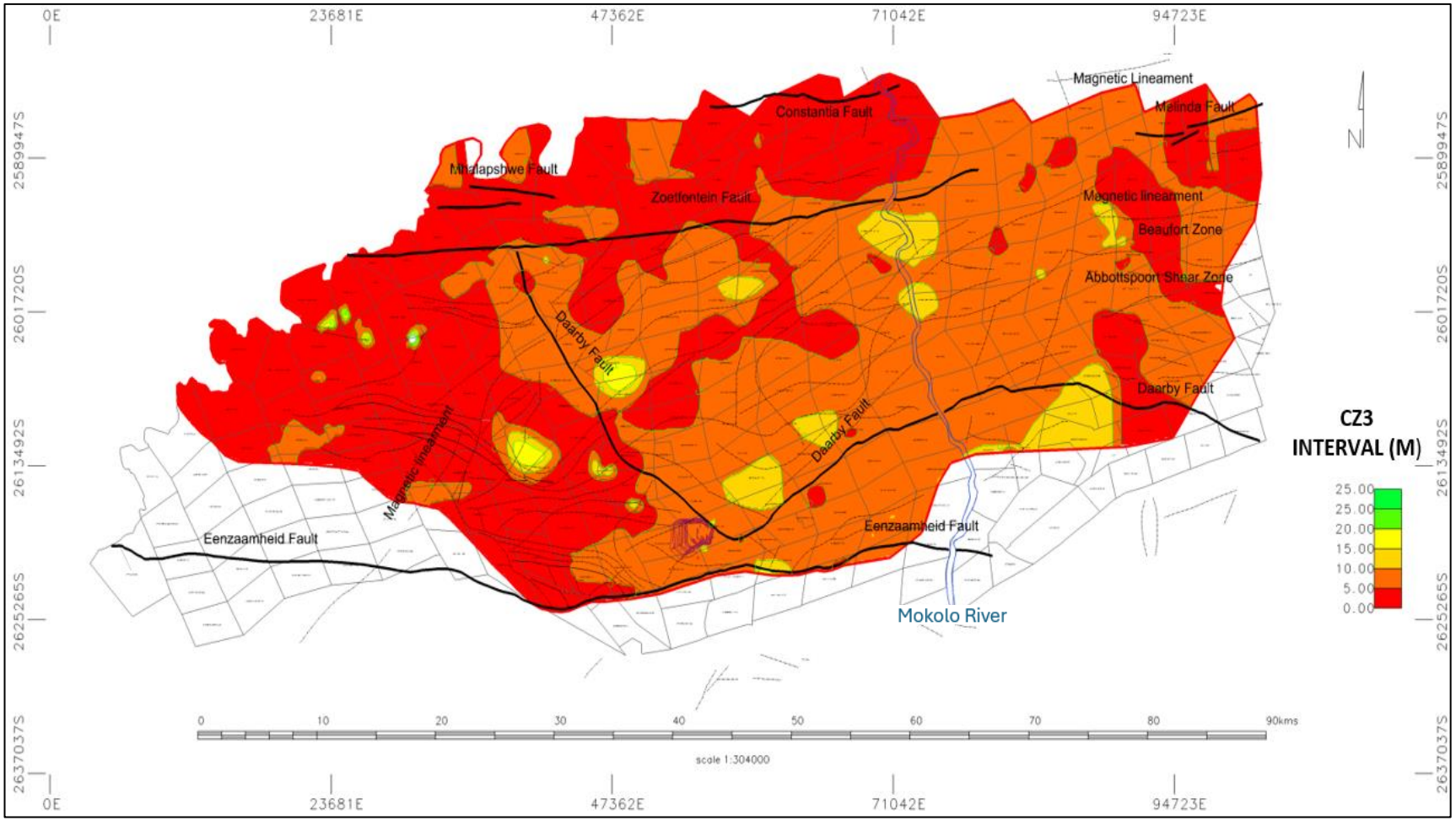

Figure 5.14: Coal Zone 3 (CZ3) seam thickness distribution across the Waterberg Coalfield.

5.3.14 Sandstone 2_Thickness (SS2)

Sandstone 2, which belongs to the Swartrant Formation averages 5.20 m, with a min of 0.47 m and max of 50 m. A thickness of up to 50 m occurs and is maintained to less than 10 m across the coalfield. At isolated areas in the northern and eastern parts, the thickness is generally more than 10 m. There was no data interpolated at the southern and south-eastern parts of the coalfield, therefore there is no thickness range (i.e., white patches depicting low level of confidence) (Figure 5.15).

Medium to coarse-grained sandstone is found, with thin mudstone bands and a few thin coal laminae near the top. The sandstone is moderately sorted, with considerable crossbedding defined by smaller grain sizes.

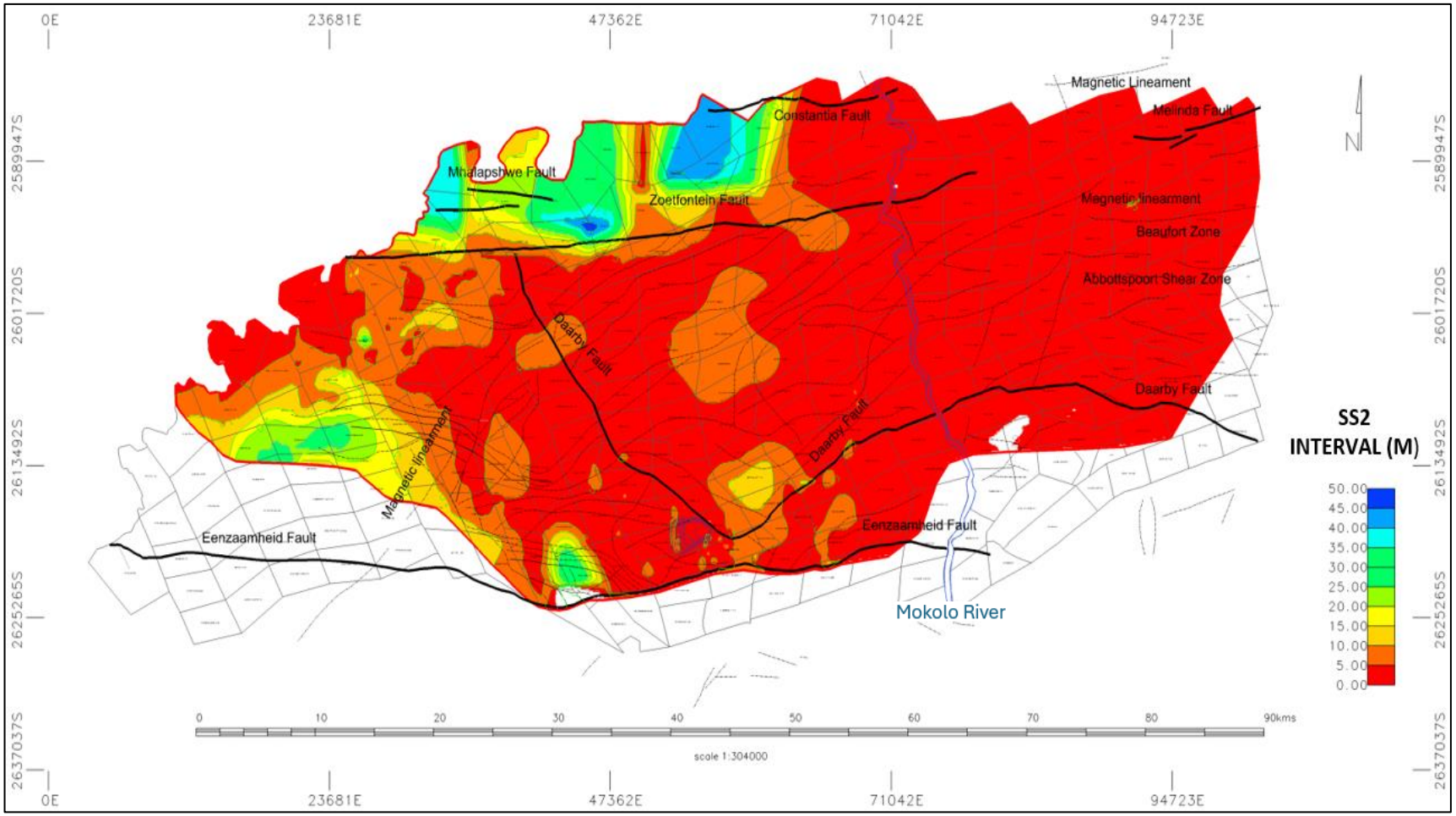

Figure 5.15: Sandstone 2 (SS2) thickness distribution across the Waterberg Coalfield.

5.3.15 Coal Zone 2_Seam Thickness (CZ2)

Coal Zone 2 (coal samples 30A, 30B-31) (Appendix A), which belongs to the Swartrant Formation averages 4.16 m, with a min of 0.07 m and a max thickness of 20 m. A thickness of up to 20 m occurs and is maintained to less than 10 m across the coalfield. At an isolated area in the eastern part of the coalfield, the thickness range between 10 m and 20 m. There was no data interpolated at some of the northern parts of the coalfield, therefore there is no thickness range (i.e., white patches depicting low level of confidence) (Figure 5.16).

The zone contains bright coal laminae and dull coal found in the bottom 2 m, with low ash, and a 98.22% *in-situ* coal content. At Grootegeluk Mine, the coal zone produces blend coking coal at yields between 10-12%. The coal zone produces metallurgical coal and pulverised coal injection products (10% Ash) at yields between 10-12%. The coal is processed through Grootegeluk 4 (GG4) and Grootegeluk 5 (GG5), single-stage beneficiation plants (Chabedi & Mhlongo, 2018). Raw qualities: Calorific Value_12.46Mj/kg; Inherent Moisture_2.15%; Ash_31.99%; Volatile Matter_21.72%; Fixed Carbon_45.31%; Total Sulphur_1.01% (Council for Geoscience, 2010; Table 5.1).

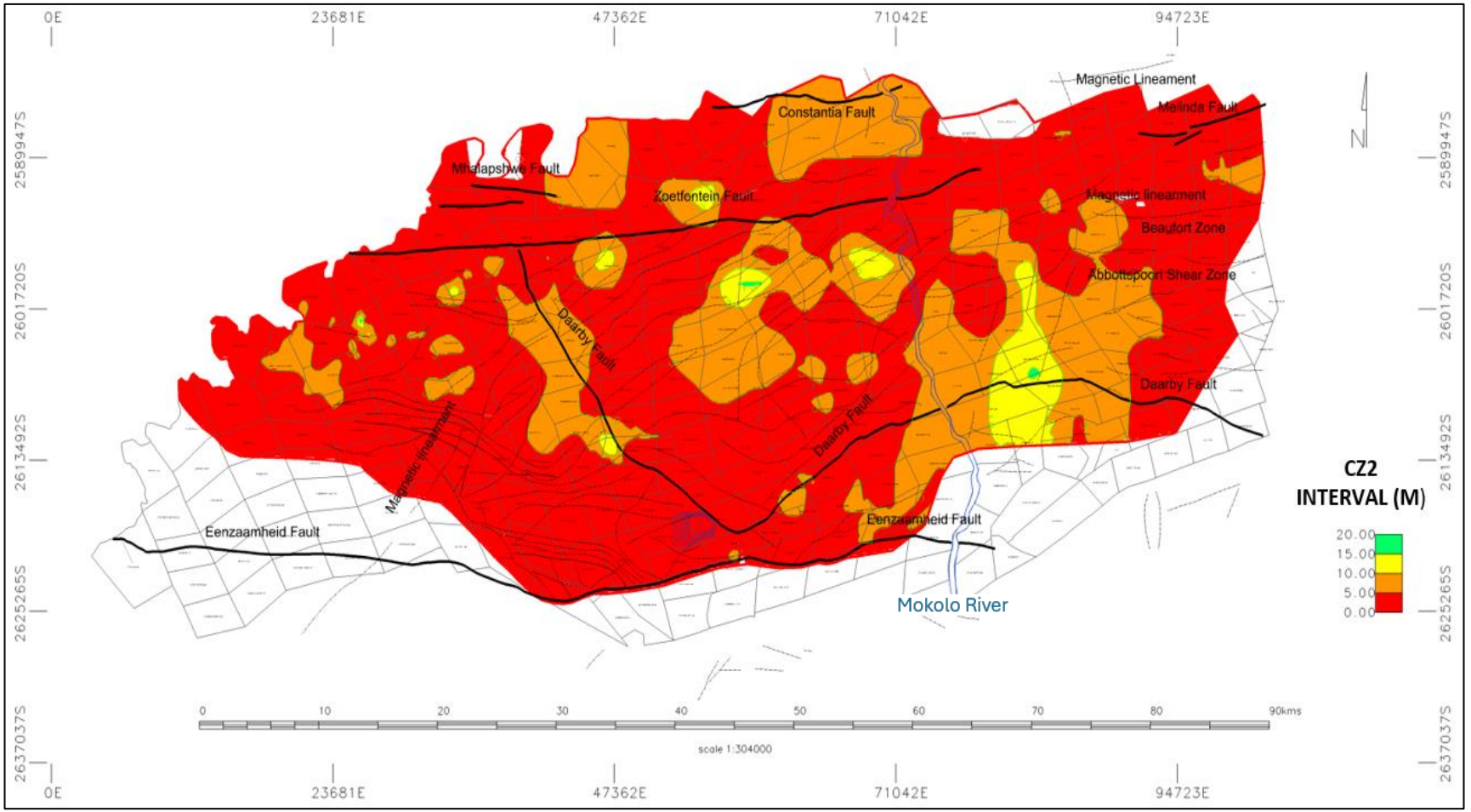

Figure 5.16: Coal Zone 2 (CZ2) seam thickness distribution across the Waterberg Coalfield.

5.3.16 Sandstone 1_Thickness (SS1)

Sandstone 1, which belongs to the Swartrant Formation averages 7.08 m, with a min of 0.24 m and a max of 30 m. A thickness of up to 30 m occurs and is maintained to less than 10 m across the coalfield. The unit thins towards the north-western portion of the coalfield but maintains a constant thickness in most parts of the deposit. At isolated areas across the coalfield, the thickness generally ranges between 10 m and 20 m (Figure 5.17).

The coarse-grained sandstone unit has a few shale bands and laminae towards the top. This massive sandstone is made up of quartz grains with very coarse-grained feldspathic granules that range from white to light creamy white. The grains are tightly packed, and the matrix is almost absent. This unit is highly competent and occurs across the coalfield.

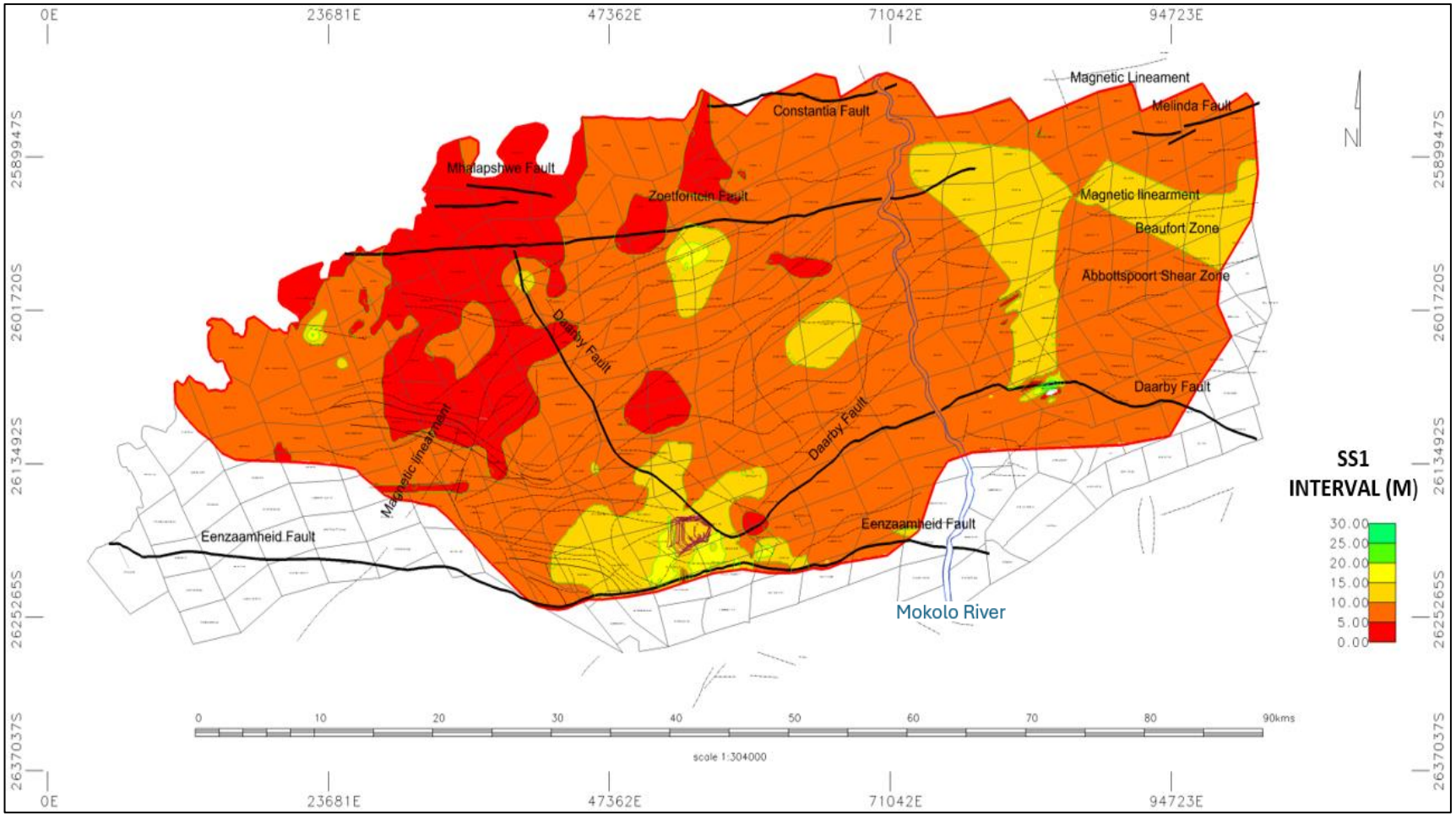

Figure 5.17: Sandstone 1 (SS1) thickness distribution across the Waterberg Coalfield.

5.3.17 Coal Zone 1_Seam Thickness (CZ1)

Coal Zone 1 (coal sample 32) (Appendix A), which belongs to the Swartrant Formation averages 1.74 m, with a min of 0.12 m and a max thickness of 7 m. A thickness of up to 7 m occurs and is maintained to less than 4 m across the coalfield. In the eastern part of the coalfield, the thickness increases above 2 m, while thinning towards the northern and eastern parts of the coalfield. At isolated areas, anomaly thicknesses between 4 m and 7 m can be observed across the coalfield (Figure 5.18).

It comprises thin shale bands and dull coal with few coal laminations throughout, with 98.34% *in-situ* coal content. The coal zone can produce blend coking coal at yields between 10-12%, but owing to high stripping ratios, the unit is not mined. Raw qualities: Calorific Value_11.55Mj/kg; Inherent Moisture_1.87%; Ash_30.21%; Volatile Matter_21.30%; Fixed Carbon_34.60%; Total Sulphur_1.09% (Council for Geoscience, 2010; Table 5.1).

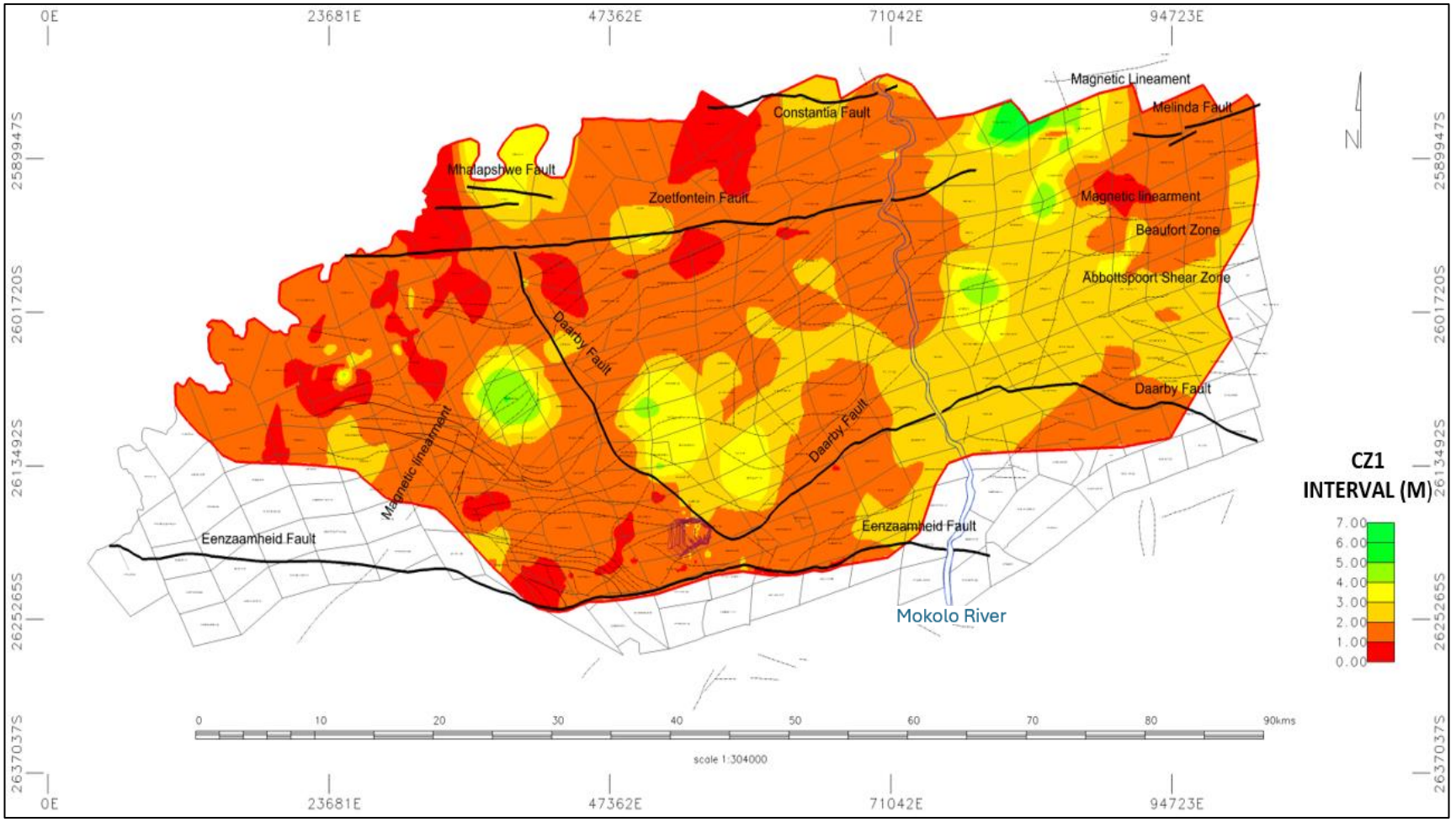

Figure 5.18: Coal Zone 1 (CZ1) seam thickness distribution across the Waterberg Coalfield.

5.4 Geological Cross-Sections

Using 3D graphics and georeferenced platforms, a series of cross-sections were constructed using 2D vertical working planes from selected data points, correlations along predetermined planes through the coalfield using Geovia Minex^{TM} Software. The section presents interfaces, such as fault lines, strata or rock boundaries, and coal zone boundaries, by outlining the intersecting line between the section and the geological body as contour lines of varied lengths (Zhang et al., 2010). For the Waterberg Coalfield model, 70 cross-sections were created, from the 70 only 10 of the most representative cross-sections (5 North-South; 5 East-West) were used for interpretations.

Stratigraphic correlations using cross-sections offer a straightforward method to simplifying geological heterogeneity (Lemon & Jones et al., 2003). The consistency to apply a set of correlation criteria across the model region determines the validity of the model. Interpretations are deterministic; therefore, the possibility exists of varying stratigraphic correlations and interpretation of one section to another section and across model iterations.

The cross-section method is demonstrated in (Figure 5.19), with scattered boreholes (Figure 5.19A). User-defined cross-section that indicates the thicknesses of the horizons that corresponds to Horizon 3 (Figure 5.19:B). (Figure 5.19:C) demonstrates a cross-section through the solids produced by the algorithm when applied to the contacts of the borehole. The created solids have a continuous layer called Horizon 3. (Figure 5.19:D) demonstrates a cross-section through the solids produced by adding user-defined cross-sections to the horizon IDs at the drill contacts. The cross-section in (Figure 5.19:D) accurately reproduces the user-defined cross-section (Figure 5.19:B) (Lemon & Jones et al., 2003).

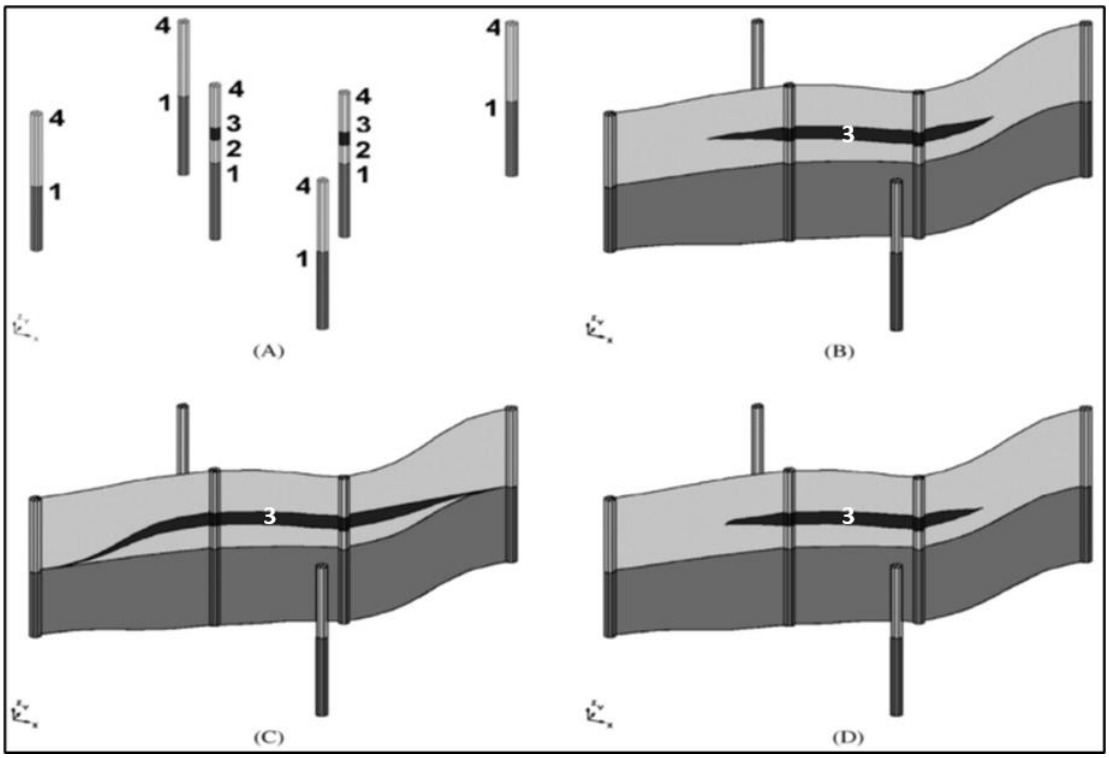

Figure 5.19: Horizons algorithm with cross-sectional data (adopted from Lemon & Jones et al., 2003).

(A) Boreholes with allocated layer intervals;

(B) Cross-section;

(C) Cross-section through solids created without defined intervention;

(D) Cross-section through solids created with user-defined intervention.

5.4.1 Geological cross-section interpretations

In the Waterberg Coalfield, strata are categorised as “complete” or “missing”. In the study area, a full stratum is continuously distributed across the coalfield. Its top and bottom intervals are a completely curved surface with no “voids”. A missing stratum is discontinuously distributed in the study area. Either a continuous curved surface with one or more “voids” makes

up its top or bottom interface or a combination of multiple disconnected continuous curved surfaces (Zhu et al., 2012).

Missing strata in sedimentary systems are divided into three types for this study: Type 1, Type 2, and Type 3, depending on their stratigraphic settings and structural characteristics:

- Type 1: Non-deposition frequently causes these missing strata.

Top surface of the underlying stratum controls the geometrical boundaries of the missing stratum because, according to Zhu et al. (2012), the missing stratum of Type 1 results from an endogenic geological event on earth.

- Type 2: Erosion frequently causes these missing strata.

Missing strata typically result from exogenic geological processes, including weathering denudation and river erosion; therefore, the bottom surface of the underlying layer determines its geometrical boundaries.

- Type 3: Superposition, combination of non-deposition and erosion causes missing stratum.

Every stratum has a constant upper interface and a lower interface, both the upper and the lower interface are located at the same x, y coordinates but with the top interface having a higher elevation (z value).

North-south cross-sections (1; 2; 3; 4; 5); east-west cross-sections (6; 7; 8; 9; 10) (Figure 5.20) were used for the research as they represent and cover most parts of the Waterberg Coalfield.

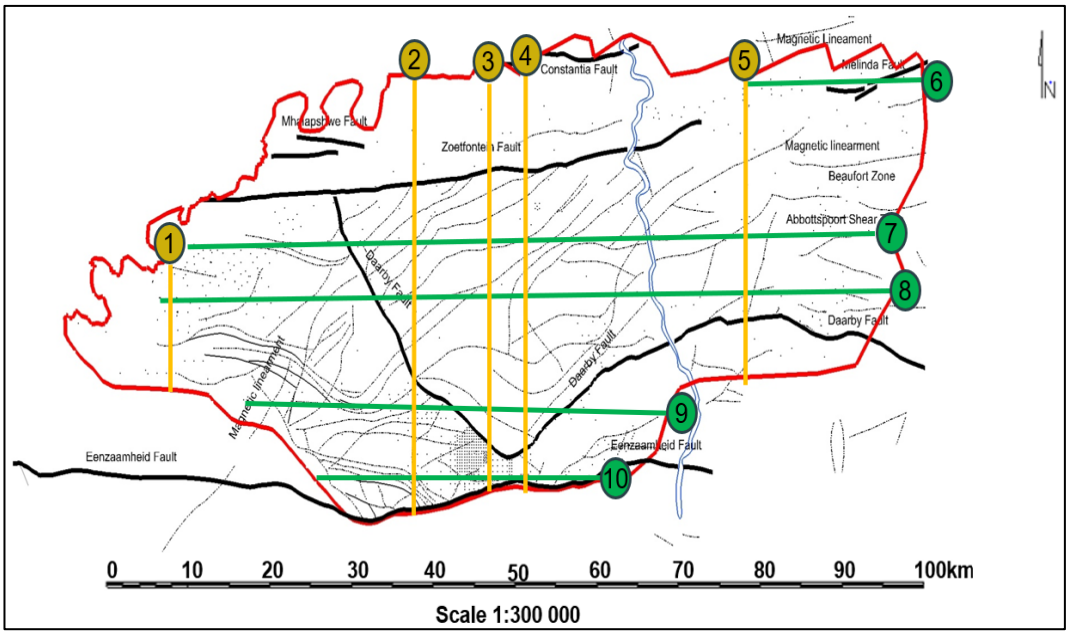

Figure 5.20: Ten (10) most representative cross-sections constructed across the Waterberg Coalfield.

The final cross-section interpretation involves packing the basal surfaces of each unit in a stratigraphically coherent manner. The basal surfaces may intersect during the stacking process. Various intersections are often conceivable:

- Upper unit was deposited against the relief of the lower unit, where it clips the lower unit.
- Upper unit has eroded the lower units; the upper unit clips the lower units.
- Intersection, an artefact of the interpolation process between two conformable units, is removed in this case by adjusting the basal surfaces of the two units.

Cross-sections showing surfaces of strata have been used to depict the successions of geological strata in the subsurface. Cross-sections depict a single plane cutting through the ground and give the sense of geological

structure and continuity in the third dimension, although inaccurately represented in 3D nature of the geology (Zhu et al., 2012).

5.4.2 North-south cross-sections (1; 2; 3; 4; 5)

- Cross-Section 1

Cross-Section 1 was created across the Waterberg Coalfield in a north-south direction at a 9.33 km distance (Figure 5.21). The overburden thickness ranges between 10 m and 40 m from the surface. A complete stratigraphic column is evident along the cross-section, demonstrating the Grootegeluk and the Swartrant Formations' full successions. Evidence of anticlinal structures developing into block faulting is observed between boreholes KR1919951 and DE1919952. Coal zones pinch towards borehole SN245LQ1 as the overburden thickens to 35 m.

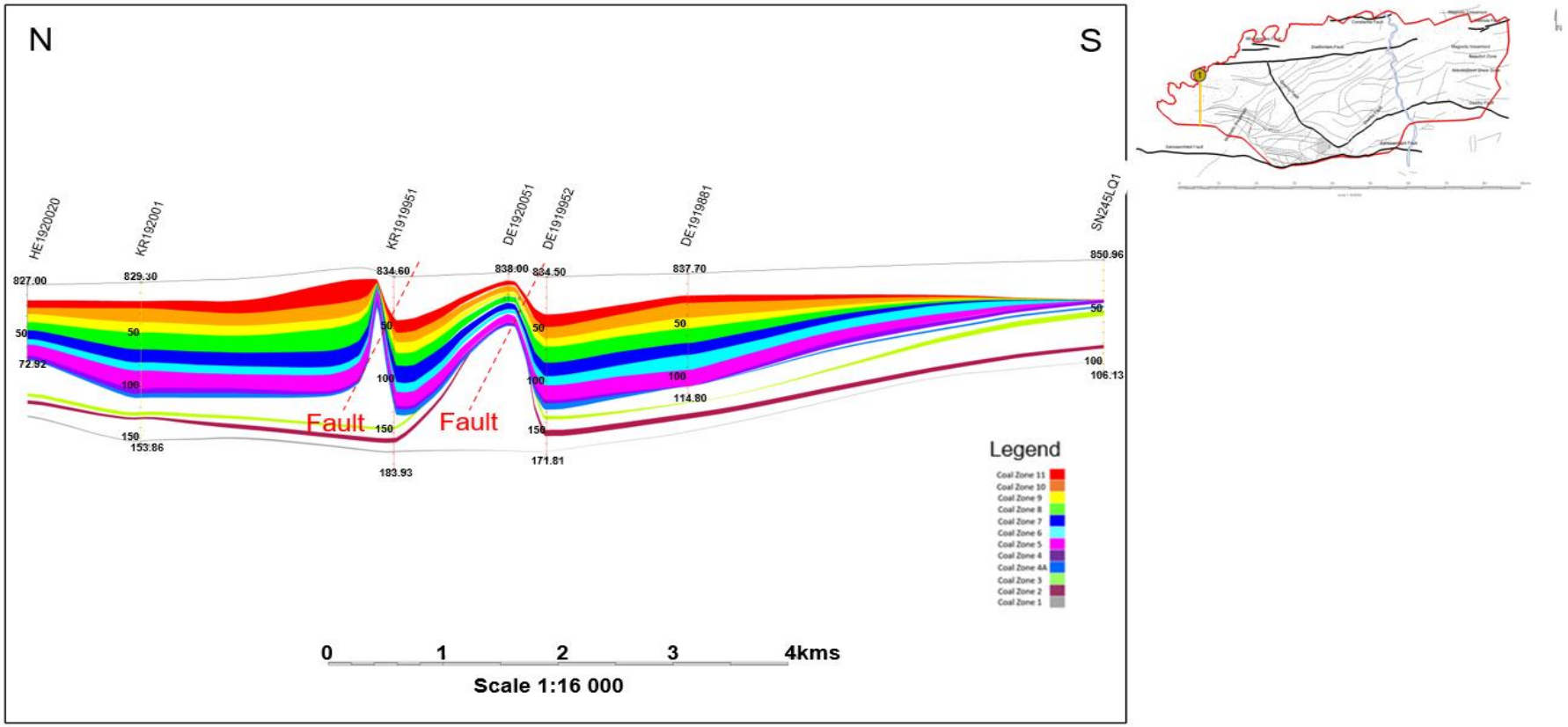

Figure 5.21: Cross-Section 1 depicts sympathetic block faulting concentrated between boreholes KR1919951 and DE1919952.

- Cross-Section 2

Cross-Section 2 was created across the Waterberg Coalfield in a north-south direction at a 63.33 km distance (Figure 5.22). The overburden thickness ranges between 50 m and 300 m from the surface. A complete stratigraphic column is evident along the cross-section and demonstrates evidence of a graben structure observed between borehole DM1977149 and VN310LQ5. Zoetfontein, Daarby, and Eenzaamheid Faults are interpreted on the cross-section.

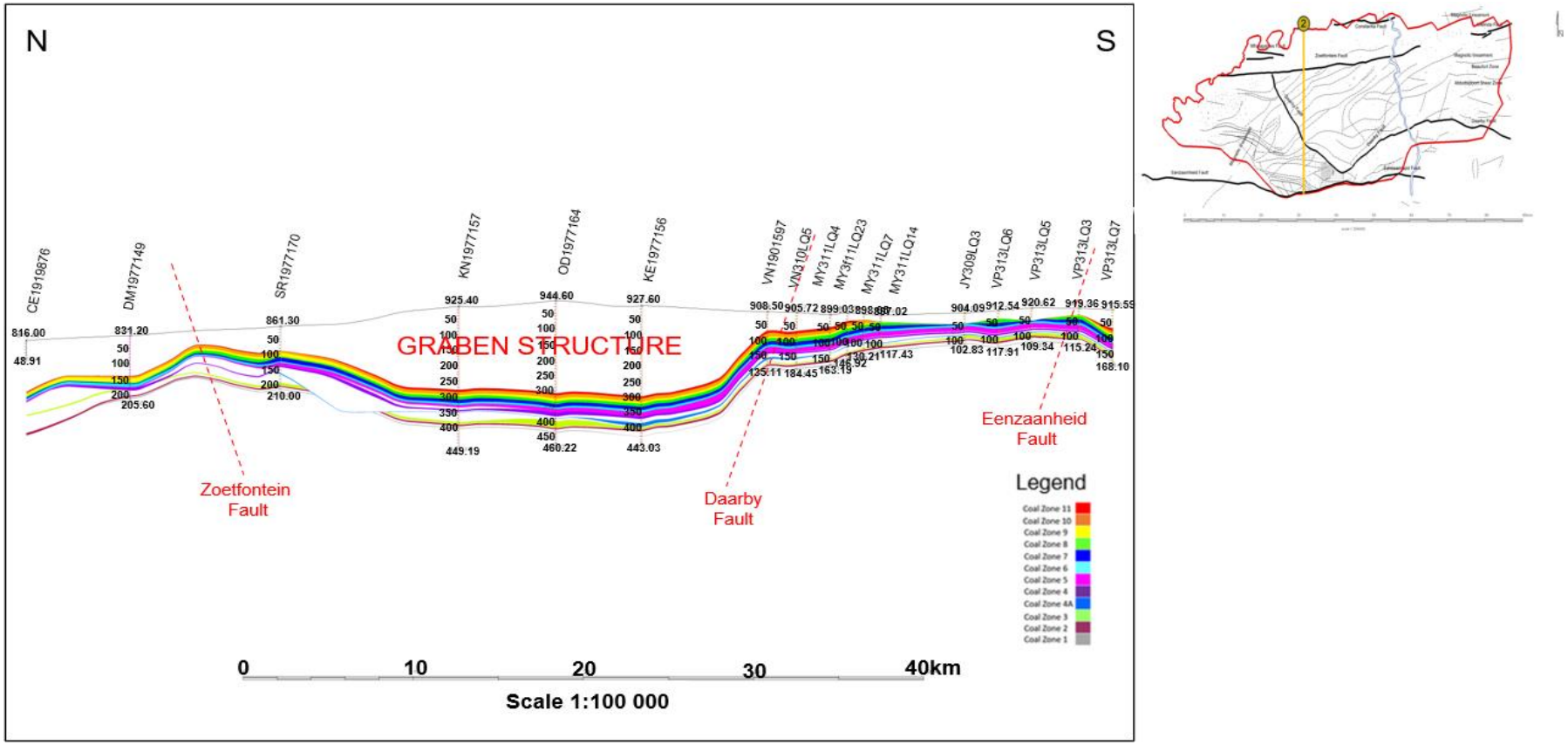

Figure 5.22: Cross-Section 2 depicts a graben structure as observed with a sudden change in elevation between the projected faults.

- Cross-Section 3

Cross-Section 3 was created across the Waterberg Coalfield in a north-south direction at a 43.64 km distance (Figure 5.23). The overburden thickness ranges between 50 m and 300 m from the surface. The Upper Ecca coal zones are prominent throughout. Coal Zones 1, 2 and 3 appear disturbed towards the north. The coal zones form a basin structure at the centre, flat-lying, and undulates from borehole MN1977161 to the north. Suggestive evidence exists of structural changes in this part of the Waterberg Coalfield, typical upthrow movement of the Zoetfontein Fault from north to south, upthrow movement of the Daarby Fault towards the south.

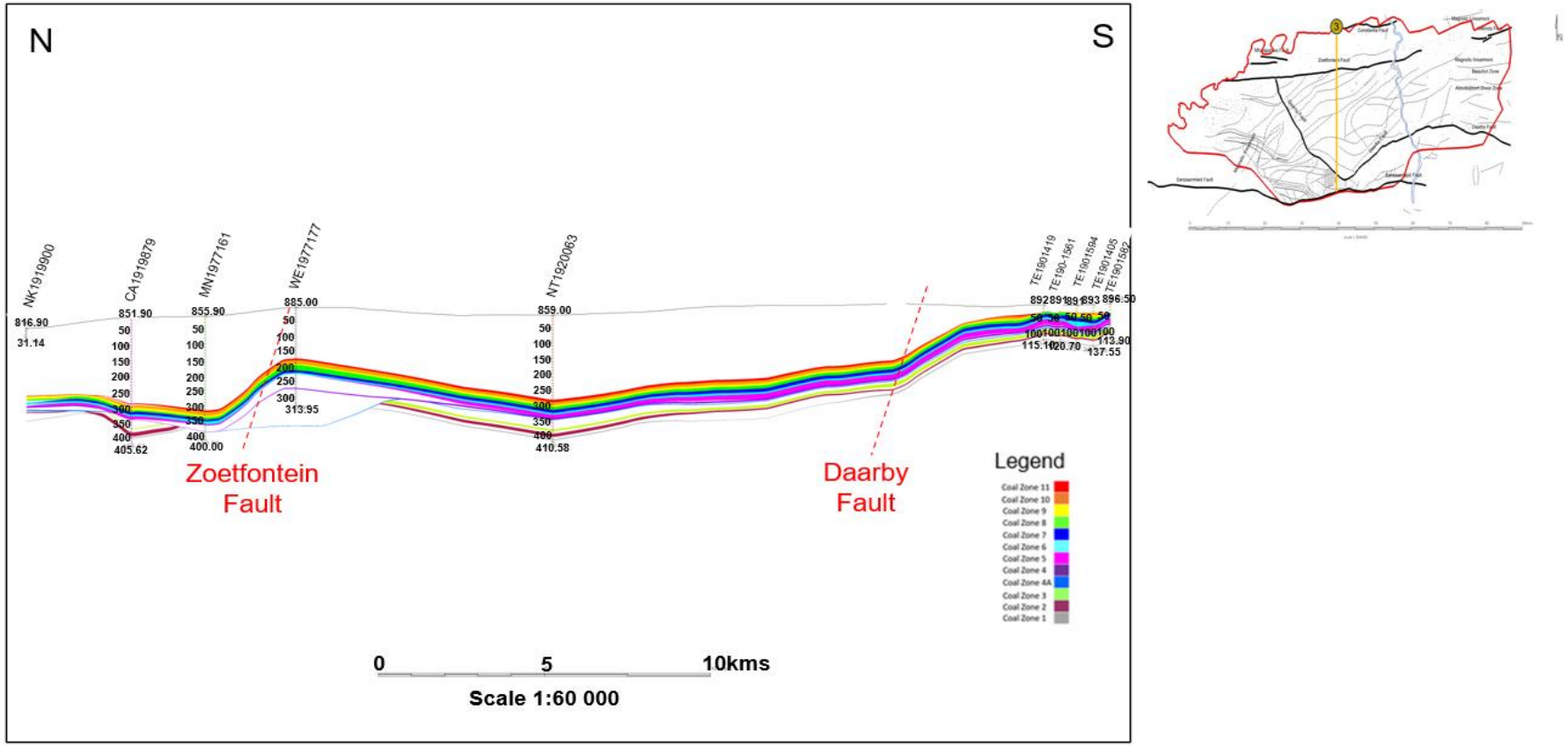

Figure 5.23: Cross-Section 3 depicts the Zoetfontein Fault with ~180m displacement, with the Daarby Fault towards the south.

- Cross-Section 4

Cross-Section 4 was created across the Waterberg Coalfield in a north-south direction at a 63.64 km distance (Figure 5.24). The overburden thickness ranges between 30 m and 350 m from the surface. Only at the central part of the coalfield is a complete stratigraphic column evident along the cross-section. Coal zones have been eroded or were not deposited between borehole GD5 and NN1901410. A synclinal structure may have formed owing to faulting and thrusting. The coal zones further undulate across the cross-section, with an up-dip towards borehole GD4. Between boreholes AE1920065 and GD4, there is evidence of Daarby faulting and palaeo-floor uplift of the Waterberg and pre-Waterberg Group rocks that unconformably underlies the Ecca Group rocks.

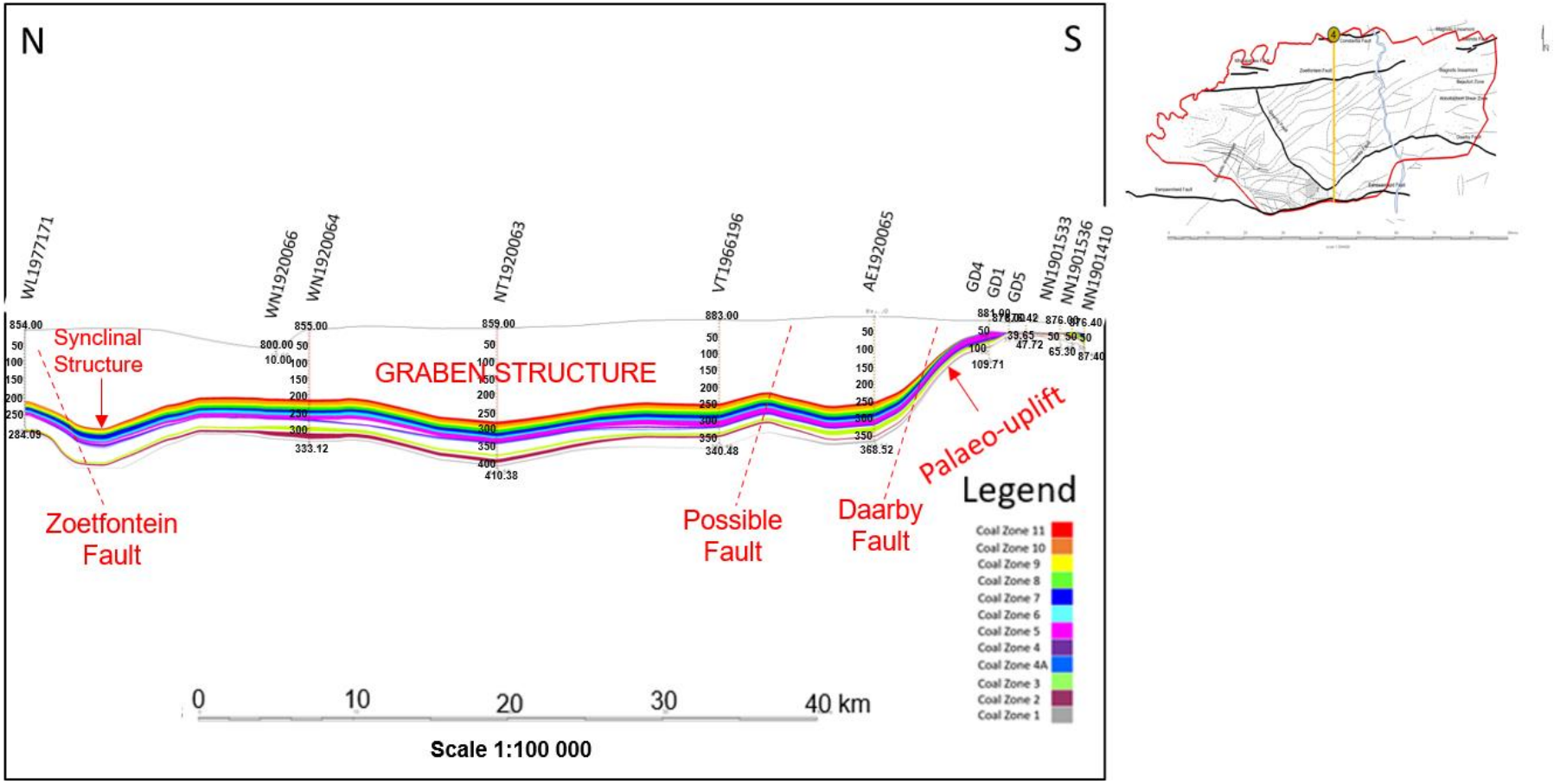

Figure 5.24: Cross-Section 4 depicts a palaeo-uplift towards the south of the coalfield.

- Cross-Section 5

Cross-Section 5 was created across the Waterberg Coalfield in a north-south direction at a 63.64 km distance (Figure 5.25). The overburden thickness ranges between 5 m and 300 m from the surface. The central part of the coalfield demonstrates much deeper coal and a complete stratigraphic column along the cross-section. Upthrow owing to the Zoetfontein Fault is evident between borehole ZO1919922 and FD1919981 as there is a drastic change in elevation from 300.00 m to 200.00 m above mean sea level over a horizontal distance of 5.60 km. The Daarby Fault contributed to palaeo-floor upliftment of the pre-Waterberg rocks (Nebo Granites and Villa Nora Gabbro) of Bushveld age that uncomformibly underlies the Ecca Group rocks at borehole ML1920052. With a change in the zone's elevations from 334.06 m to 26.58 m above mean sea level over a horizontal distance of 20.00 km.

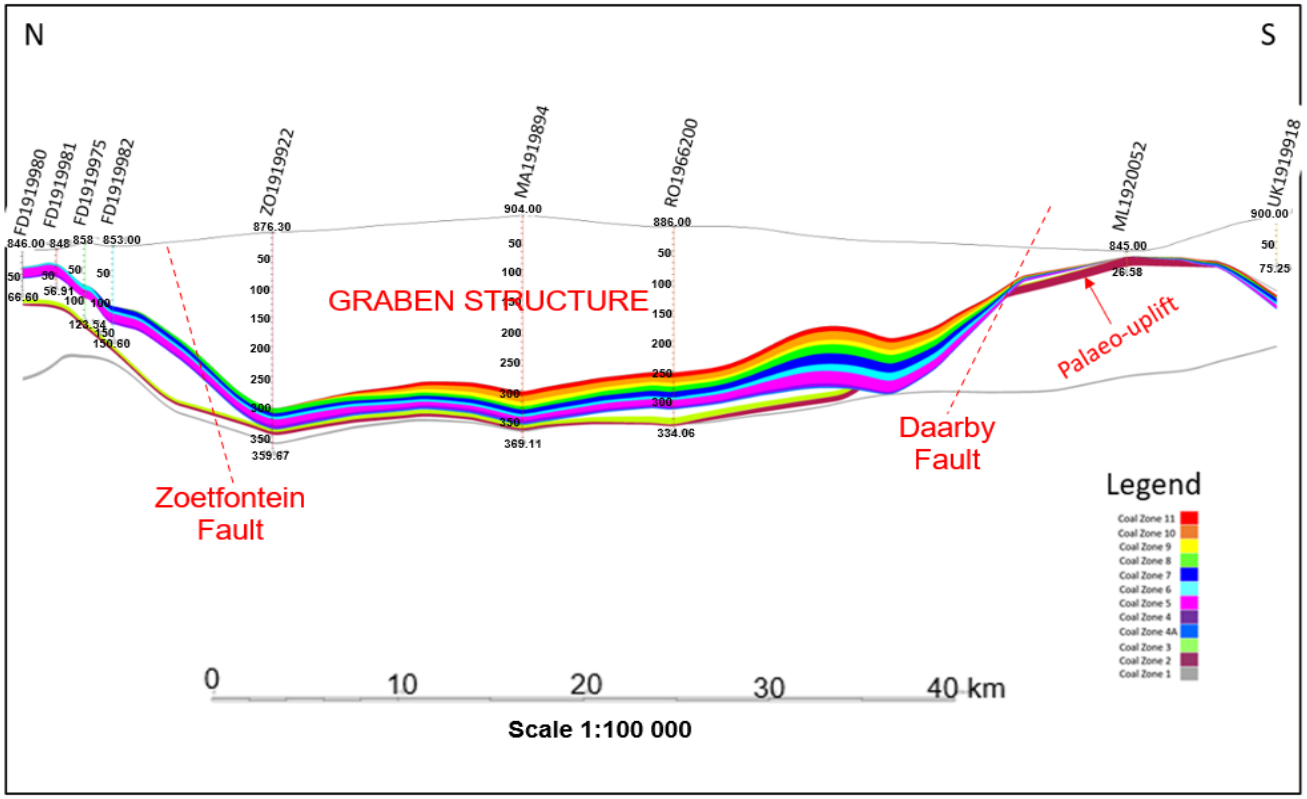



Figure 5.25: Cross-Section 5 depicts a palaeo-floor upliftment and deficient coal deposition by borehole ML1920052.

5.4.3 West-east cross-sections (6; 7; 8; 9; 10)

- Cross-Section 6

Cross-Section 6 was created across the Waterberg Coalfield in a west-east direction at a 20 km distance (Figure 5.26). The overburden thickness ranges between 2 m and 100 m from the surface. The cross-section demonstrates coal zones cross-cutting each other, and with poor coal deposition. The Swartrant Formation only occurs between boreholes TG1919912 and FD1919980, where CZ1, CZ2 and CZ3 were deposited. Only CZ5 and CZ6 were deposited from the Grootegeluk Formation, and CZ7 to CZ11 were not deposited at the far northern part of the coalfield as depicted in this cross-section. Exogenic geological processes such as weathering denudation and erosion may have influenced such conditions. The undulation of the coal zones is evident as the seams follow the palaeo-floor geometry that undulates.

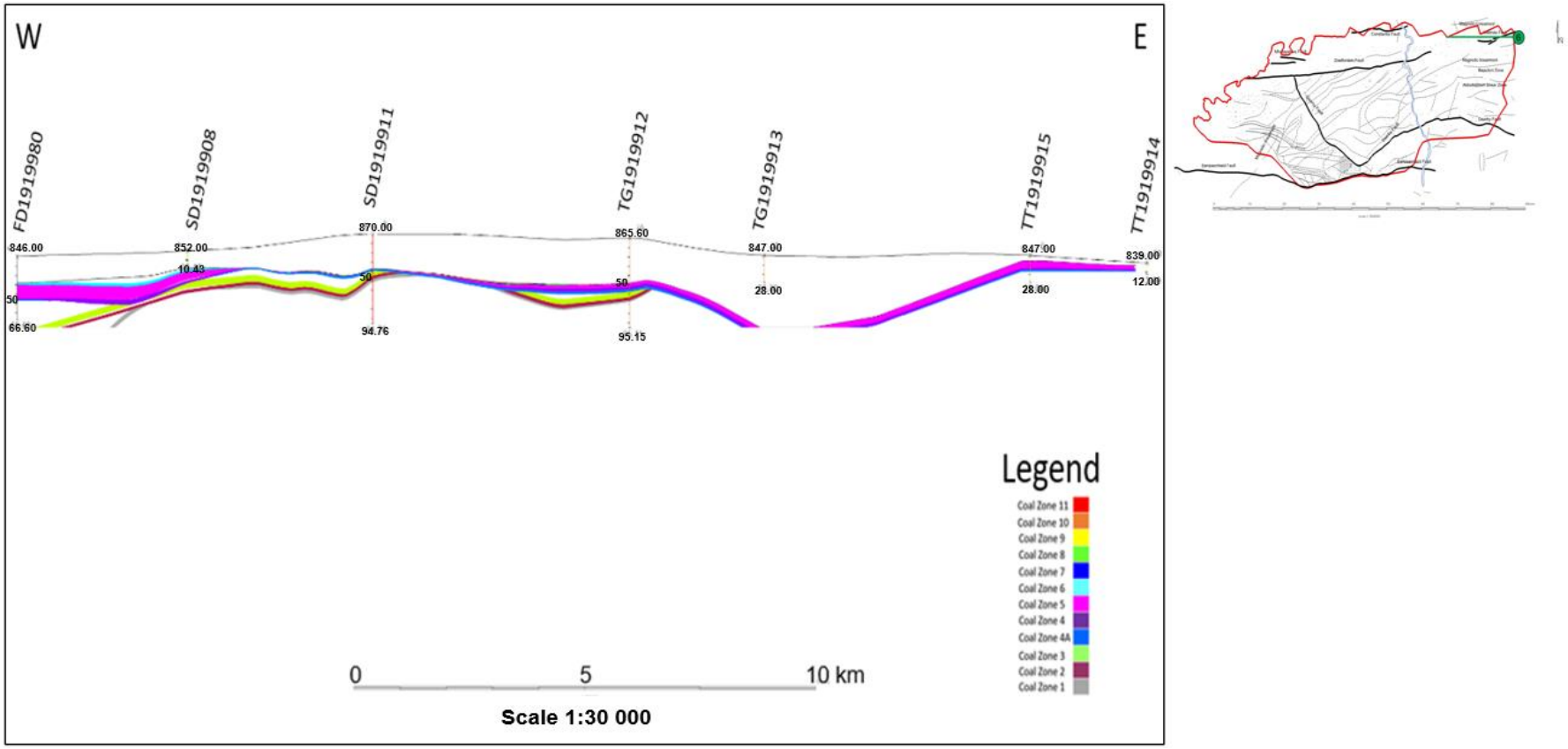

Figure 5.26: Cross-Section 6 depicts non-coal deposition in some boreholes; TG1919913 is barren of coal.

- Cross-Section 7

Cross-Section 7 was created across the Waterberg Coalfield in a west-east direction at a 56 km distance (Figure 5.27). The overburden thickness ranges between 10 m and 250 m from the surface. The cross-section demonstrates faulting, folding, and coal zones that are highly undulating. Thinning of the coal zones is observed between borehole DR213LQ1 and GR3014764 and at borehole RE1920038. This variability in coal zone thickness is mainly directly related to the accumulation of organic material during deposition. The coal zones occur much deeper at the centre of the cross-section; as well as thinning from east to west across the coalfield.

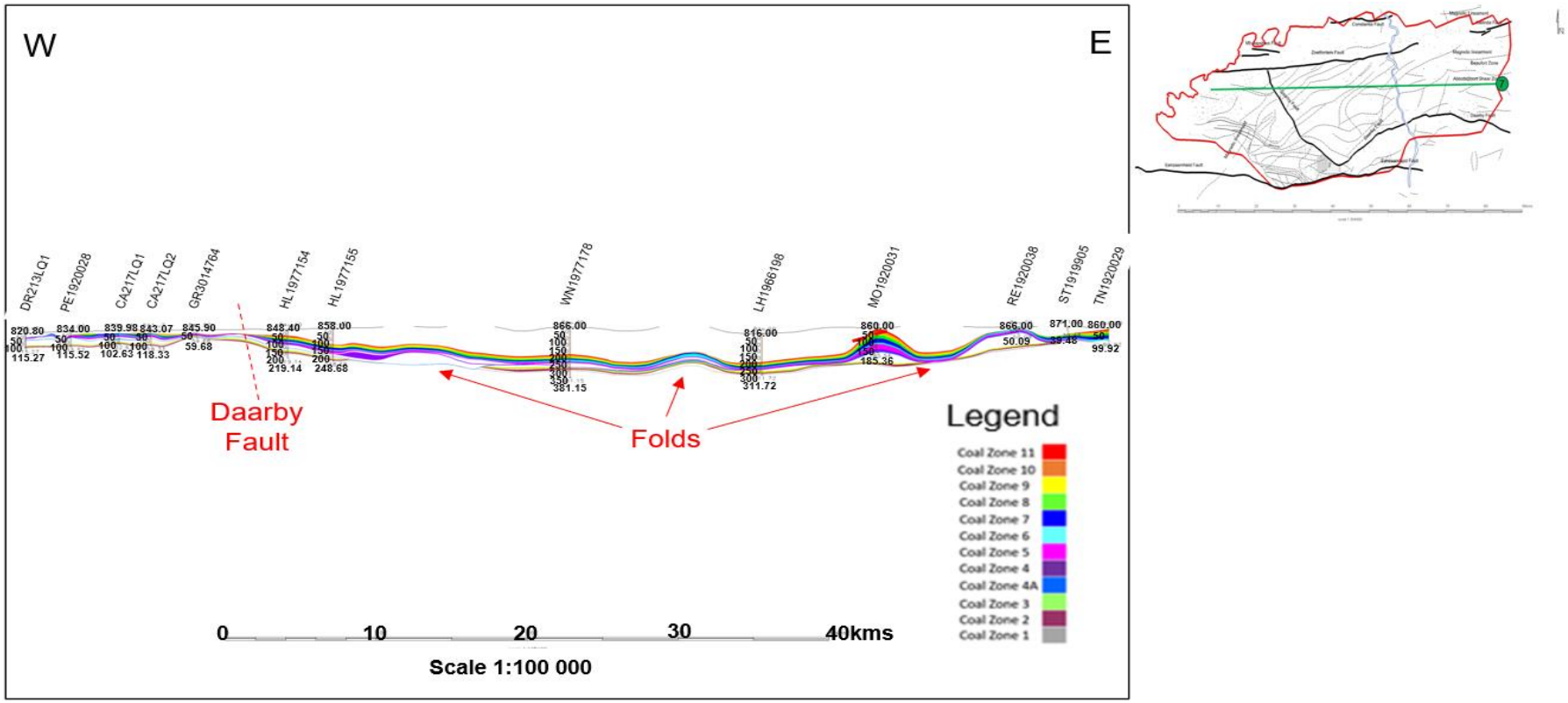

Figure 5.27: Cross-Section 7 depicts the undulating coal zones from the shallow western part of the deposit through to the deep central portion and to the shallow eastern part of the coalfield.

- Cross-Section 8

Cross-Section 8 was created across the Waterberg Coalfield in a west-east direction at a 46.67 km distance (Figure 5.28). The overburden thickness ranges between 10 m and 300 m from the surface. The cross-section demonstrates undulating coal zones and a possible fault with 150 m to 200 m displacement with variable thicknesses across the cross-section. A complete stratigraphic column is evident along the cross-section, demonstrating the Grootegeluk and the Swartrant Formation. The central part of the cross-section occurs much deeper, 200 m to 300 m below surface. Coal zone undulation is also observable across the cross-section, as an indication that the pre-Karoo sediments are not flat-lying and can drastically up and down dip as well as form folds.

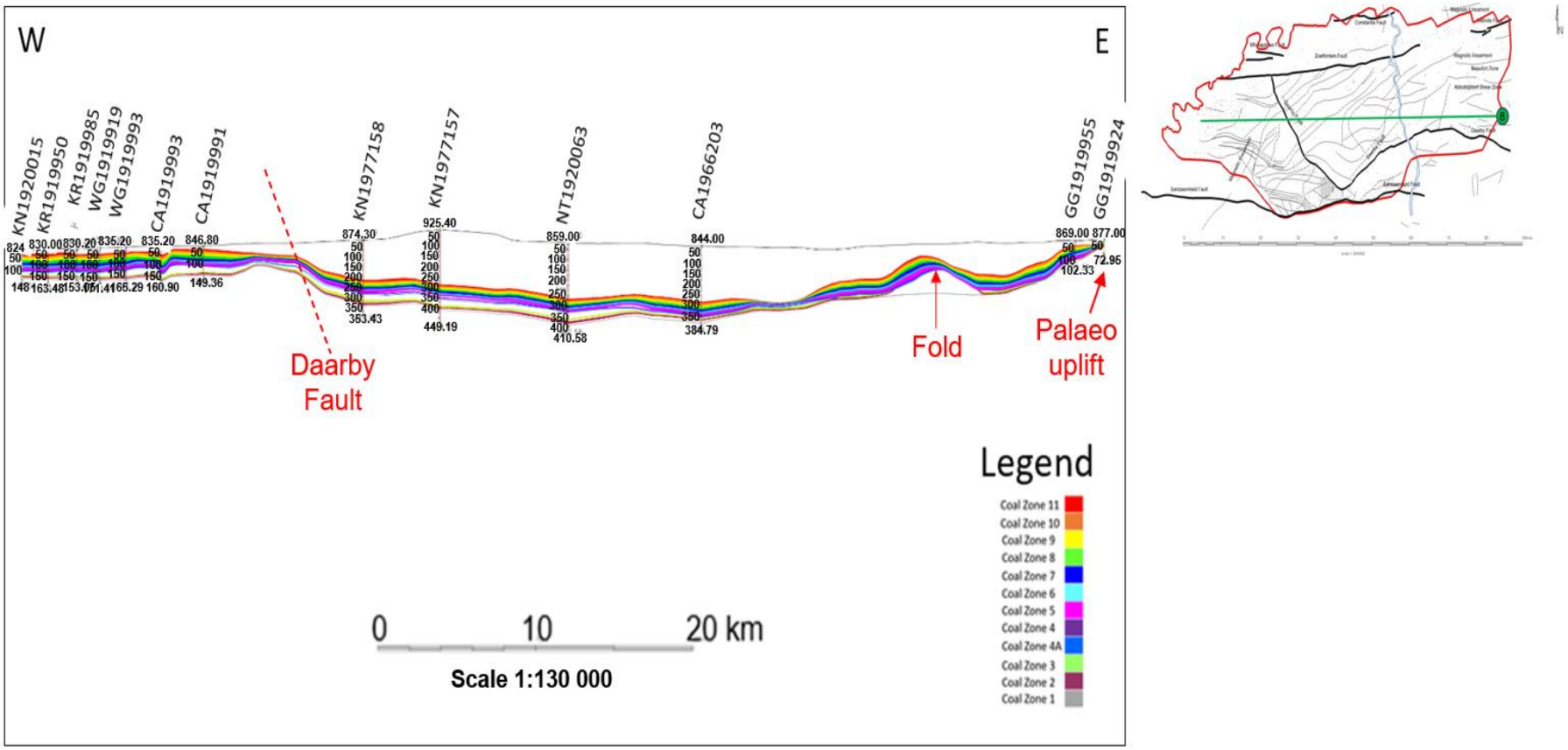

Figure 5.28: Cross-Section 8 depicts a palaeo-floor uplift between boreholes GG1919955 and GG1919924.

- Cross-Section 9

Cross-Section 9 was created across the Waterberg Coalfield in a west-east direction at a 35 km distance (Figure 5.29). The overburden thickness ranges between 10 m and 450 m from the surface. The far western and eastern parts of the coalfield demonstrate poor deposition of the coal, only CZ5, CZ4, CZ4A and CZ3 are traceable in these areas. There are possible multiple step faults between boreholes MY311LQ12 and ZN1901386 depicted by the zigzag change in elevation of the zones from 825.61 m to 473.00 m above mean sea level across 20 km. Between boreholes MY311LQ12 and GP1966204 a 360 m displacement is evident, indicating the Daarby Fault downthrow movement, followed by a set of normal and strike-slip faults. Between borehole DN3035218 and HK267LQ1, coal zones thin out and undulates. This is evidence of non-deposition and post-depositional erosion, primarily on the upper zones from the Grootegeluk Formation.

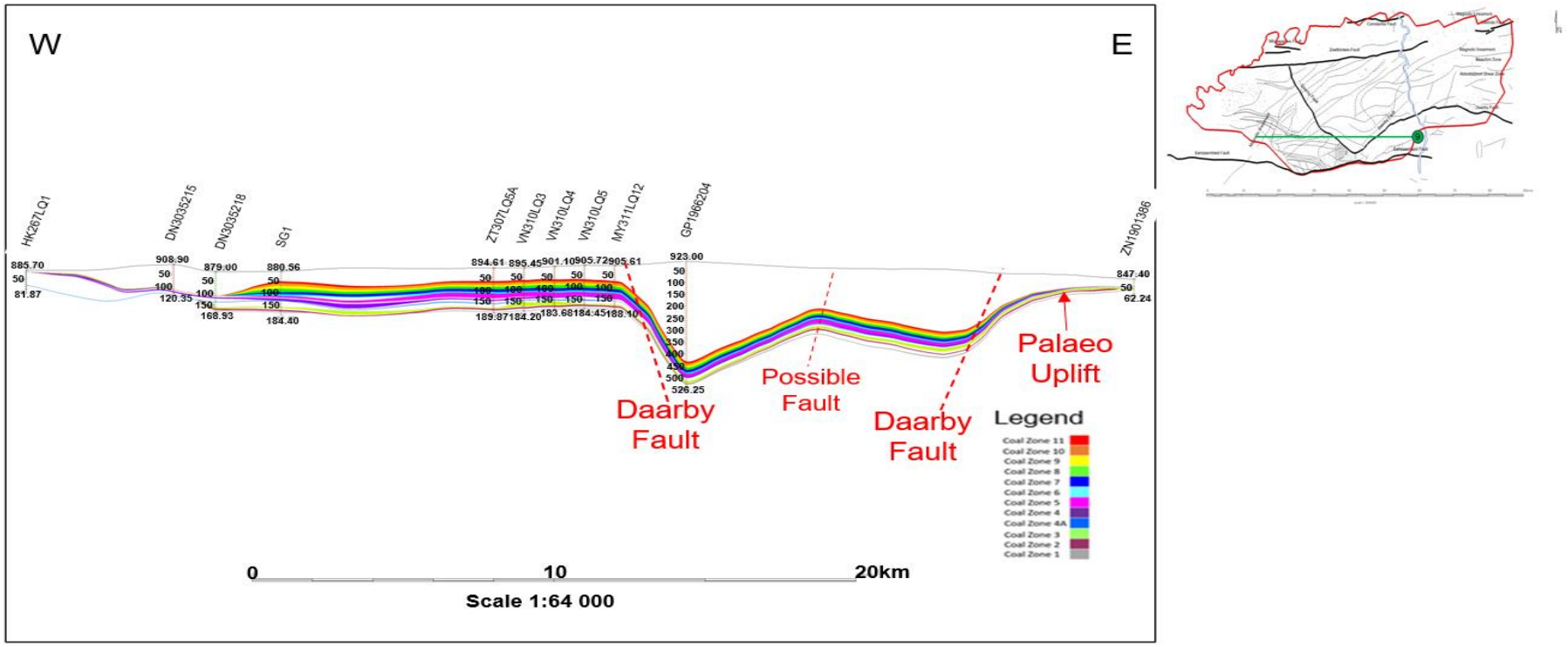

Figure 5.29: Cross-Section 9 depicts the Daarby Fault downthrow movement between borehole MY311LQ12 and GP1966204 with a displacement of ~360m change in elevation.

- Cross-Section 10

Cross-Section 10 was created across the Waterberg Coalfield in a west-east direction at a 28 km distance (Figure 5.30). The overburden thickness ranges between 10 m and 40 m from the surface. The cross-section demonstrates a complete succession at the centre; undulation is moderate while thinning and coal zone discontinuity is evident. Erosion of the coal zones can be observed between boreholes TE1901547 and ET1901356 from the Grootegeluk Formation. This subsequent erosion is most commonly by fluvial channels. Coal zones appear shallower and thicker on the cross-section, 10 m – 20 m from the surface but thins towards the west of the coalfield.

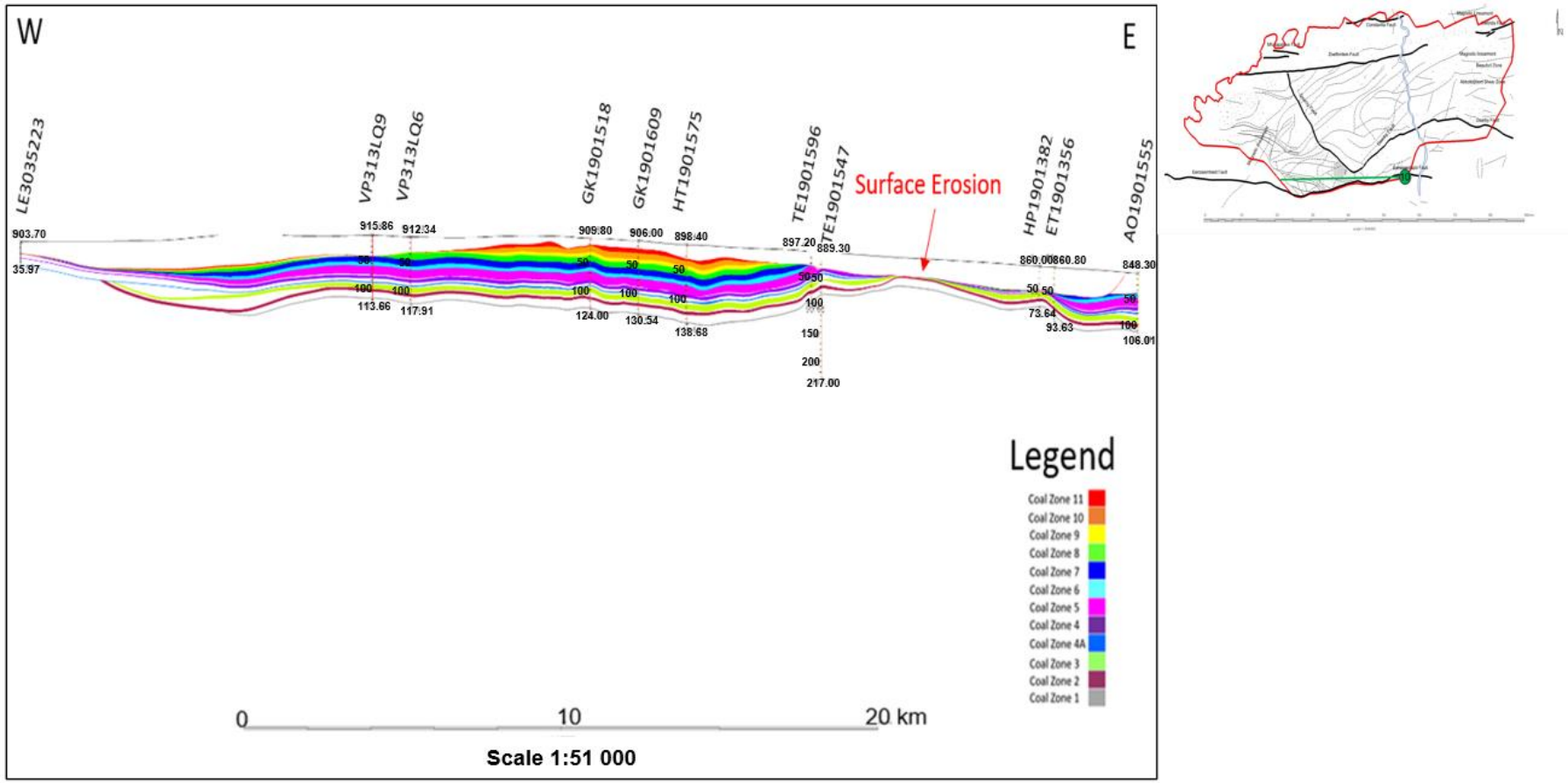

Figure 5.30: Cross-Section 10 depicts surface erosion between TE1901547 and ET1901356.

5.5 Geological Fault Modelling

Researchers have created a variety of methods to include fault data by extrapolating the geometry of the fault from basic fault information, such as the position, strike, dip, and slide (Che & Jia, 2019). By assessing fault zones and fault geometry based on borehole data and dip, the faults are represented as horizontal planes on the gridded surface. The upper and lower surfaces will then be displayed with discontinuities or displacement to represent a fault.

5.5.1 Fault modelling

Two subsequent aspects should be considered regarding fault modelling:

(i) Fault geometry

Faults are identified from their potential field because fault interpolation utilizes fault orientation data as gradients and fault traces as data points. The associated isosurface taken from the potential fault field defines the geometry of the fault (Calcagno et al., 2007).

(ii) Fault boundary

Faults can be finite; therefore, their extent should be specified. Their boundaries are circular or elliptic as it is uncommon to have actual observations specifying the tip line of a fault. The fault extent is thought to be determined by the point at which the potential-field isosurface intersects a sphere of a given radius centred on the information identifying the fault (Calcagno et al., 2007).

5.5.2 Fault interpretation

Fault locations with corresponding displacements were traced from structural geology maps. Interpreting the aeromagnetic map and the

borehole data of the research area were used to create the structural maps used for modelling.

An airborne electromagnetic survey reveals that the Waterberg Coalfield experienced more structural disturbance (faulting) than was initially thought (Fourie, 2009) (Figure 5.31). Many lineaments and faults crosscut the coalfield, subdividing it into separate blocks. Additional ground-based geophysical surveys could be required to identify some faults with weak magnetic signatures to determine their location and, consequently, the displacement of deeper coal strata.

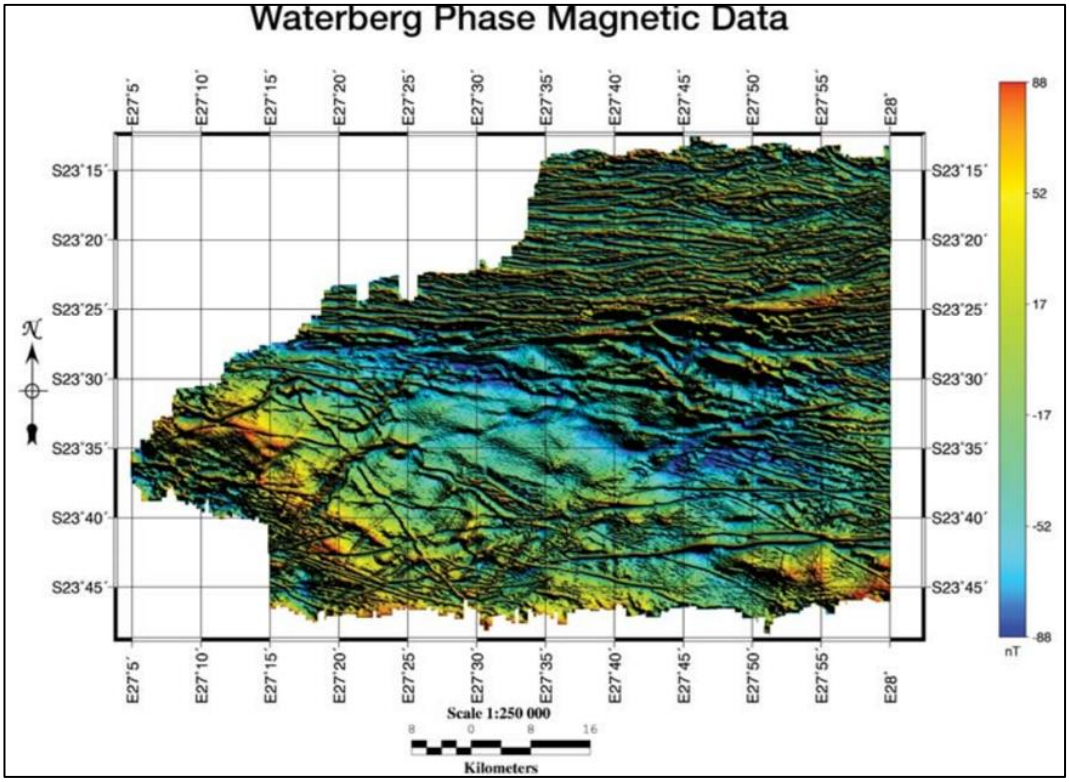

Figure 5.31: The Waterberg Coalfield phase magnetic data depicting magnetic features (Fourie, 2014).

The main data source for modelling the faults are the locations and displacements of the faults summarised in structural maps. Fault occurrences are displayed as line data (polyline) (Figure 5.32).

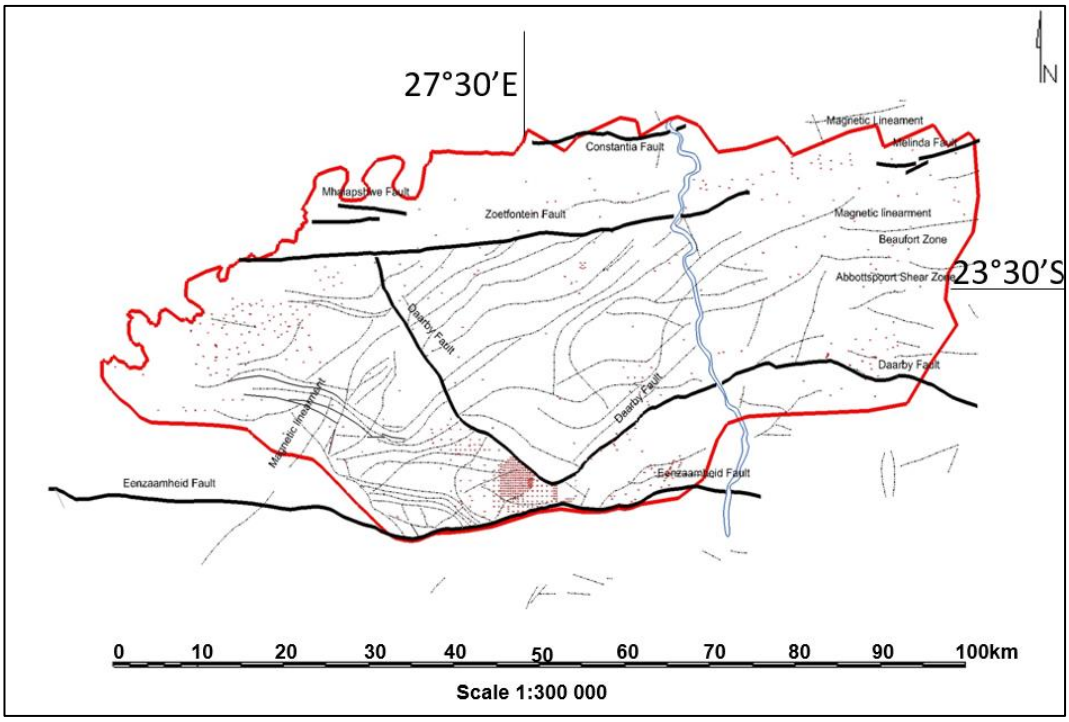

Figure 5.32: Interpreted faults (solid black lines), interpreted lineaments (dotted black lines) as depicted from cross-sections drawn across the Waterberg Coalfield.

5.5.3 Coal Zone 1 floor contour grid (the bottommost coal zone)

Geological fault modelling demonstrates that the floor contour grid for the bottommost coal zone (Figure 5.33) (Appendix C) indicates possible new faults or an extension of existing faults (Fault 1, 2, 3, 4, 5, 6, and 7) that lie beneath the strata across the Waterberg Coalfield, such as the Zoetfontein Fault possibly connecting with Malinda Fault to the east (Fault 1) and with the Mhalapshwe Fault to the west (Fault 7) of the coalfield. The faults have displacements that range between 50 m and 360 m across the deposit. The faults confirm the graben structure, and the possibility of multiple structures emphasised by other researchers (Siepker, 1986; Dreyer, 1994 and Faure, 2008).

The coalfield is divided into shallow outer margins and deep central regions by the sinuous-shaped Daarby Fault, which has a vertical displacement of ~250 m (Figure 5.33).

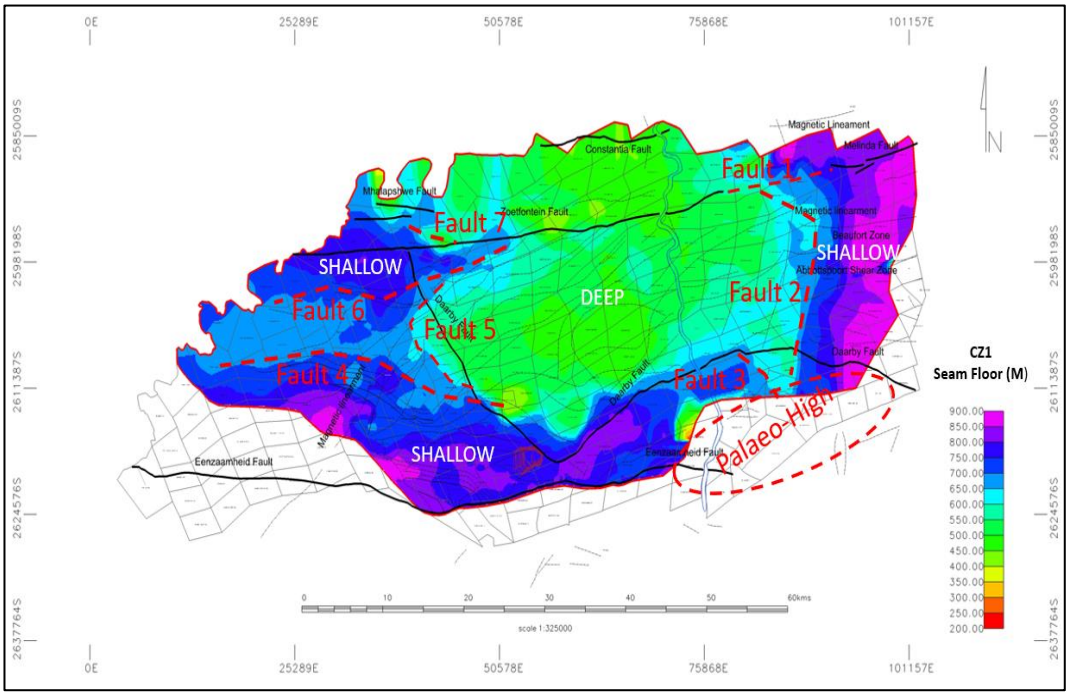

Figure 5.33: Waterberg Coalfield possible faults creating a graben structure and a palaeo-high on the southeastern corner.

5.6 3D Lithostratigraphic Facies Model

The 3D lithostratigraphic facies model displays the spatial distribution of the lithofacies deposited in the Waterberg Coalfield, OVB from the Eendragtpan Formation, CZ11 to CZ5 from the Grootegeluk Formation, and CZ4 to CZ1 from the Swartrant Formation. In this study, the geological model was based on a set of 757 boreholes to create a stacked-grid model, whereby the top and bottom grid surfaces were used to create a high-resolution 3D geological model, 93 m * 32 m * 787 m (x, y, z) axis. The digital terrain models (DTM), roof and floor grid surfaces of coal and non-coal zones were triangulated, interpolated, and then combined to create a 3D solid model on a 25 m * 25 m grid resolution. With this 3D solid model, thickness (coal and

non-coal strata), dip of the formations and structural information were depicted.

3D geological model visualized towards the north, south, west, and east directions (Figure 5.34). The surface topography is undulatory, high lying (red, orange, and yellow colours) in the eastern and south-western portions. Low lying (purple, blue, and green colours), towards the northern edges and at the central portion of the coalfield (Figure 5.34A). Boreholes appear below the surface topography as reference points of information, with lithostratigraphic facies illustrated across the coalfield (Figure 5.34B). The bottommost floor grid also marks the end-of-hole for the boreholes.

The geology across the coalfield is consistent, with a northward dip that is uniform and lateral; however, the Grootegeluk Formation was poorly deposited towards the north-eastern portion of the coalfield. The impact of geological structures to the lithology can also be observed as displacements and discontinuities across the coalfield (Figure 5.34C). Major faults, such as the Daarby Fault ~250 m upthrow, Zoetfontein ~180 m upthrow, and the Eenzaamheid Fault ~360 m downthrow moved the lithology (Figure 5.34D). The E-W graben structure represents the depositional centres of the Karoo Supergroup succession in the Waterberg Coalfield. Post depositional fault movements crosscutting the coalfield created multiple step-faults and a graben or half-graben structure during the reactivation of major regional faults such as the Daarby and the Zoetfontein Faults.

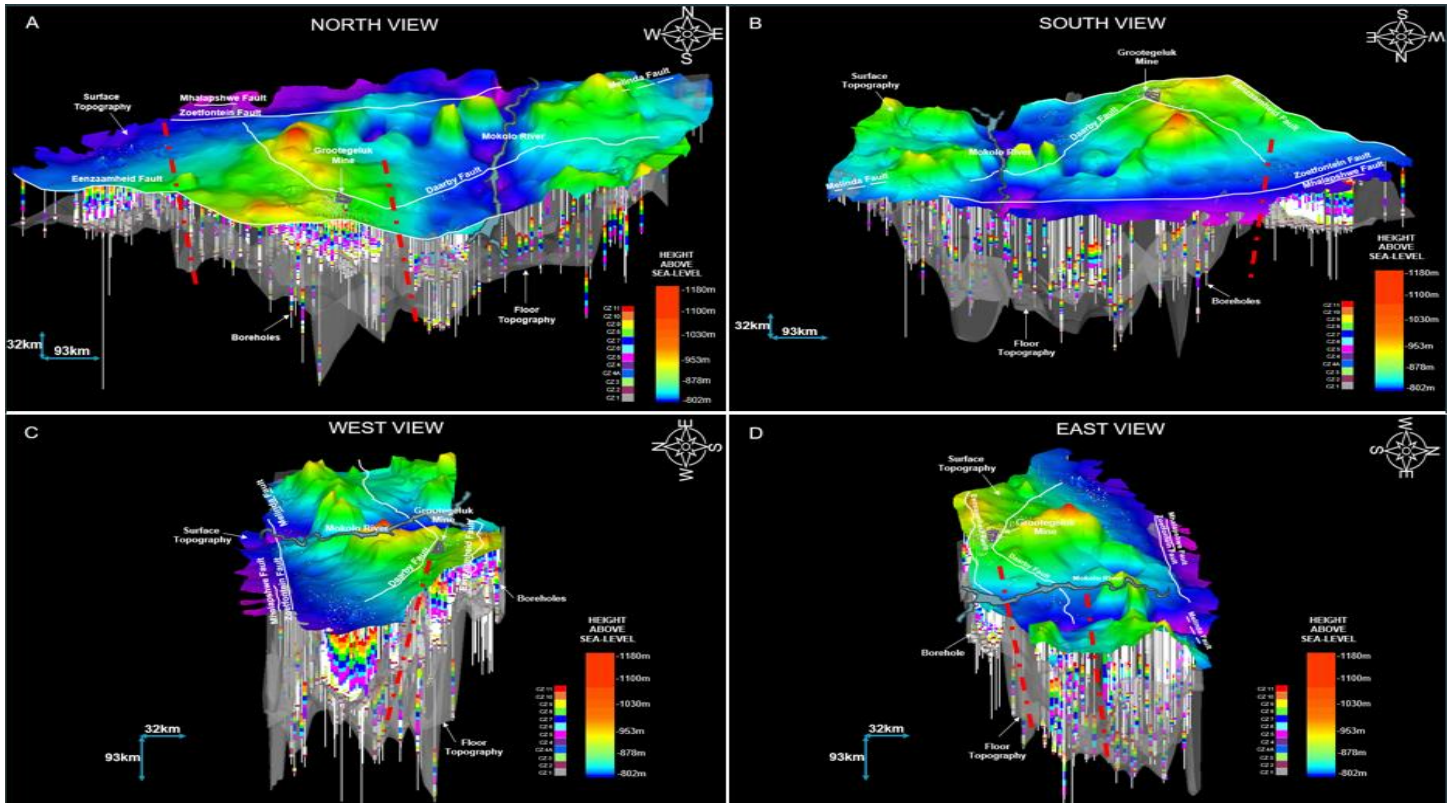

Figure 5.34: 3D geological model of the Waterberg Coalfield visualized from different directions (A) North View, (B) South View, (C) West View, and (D) East View. Approximate structural locations (dotted red lines) creating noticeable displacements of the lithofacies.

Chapter 6: DISCUSSION

6.1 Lithostratigraphy and Deposition

The 3D lithostratigraphic facies model presented in this research demonstrates the spatial distribution of the horizons from the Permo-Carboniferous Waterberg Coalfield (Figure 5.34). The coalfield's stratigraphic column was divided into seventeen (17) coal and non-coal zones (Table 5.1) identified from bottom-to-top as belonging to the Swartrant Formation (CZ1, SS1, CZ2, SS2, CZ3, MS1, CZ4A, MS2, and CZ4) Grootegeluk Formation (CZ5, CZ6, CZ7, CZ8, CZ9, CZ10 and CZ11) and the Eendragtpan Formation (OVB).

6.1.1 Swartrant Formation

The formation comprises dull coal, mudstone, and sandstone. Four non-coal zones (MS1, MS2, SS1 and SS2) and five coal zones are defined (CZ4; CZ4A; CZ3; CZ2 and CZ1) (Figure 2.7). Due to changes in the depositional environment and lateral facies changes, significant variation in thickness and quality across the coalfield characterises these zones. Noticeable differences are established between the Grootegeluk and the Swartrant Formation (Figure 3.3 to Figure 3.7); this is indicative of change in depositional environment, from lower to higher energy (occurrence of gritstone and sandstone units in this formation); climatic change and change in vegetation (change in coal type) over geological time.

Boreholes used in this 3D lithostratigraphic facies model intersected the top part of the Swartrant Formation, intersecting Coal Zone 4 to 1 (Figure 3.3 to Figure 3.7). This formation remains below the Grootegeluk Formation. Maximum thicknesses in the north ranges from 100 m to 350 m; in the east from 50 m to 100 m; in the central portion to 150 m (Figure 5.10 to Figure 5.18). The formation maintains a consistent thickness averaging 5.59 m across the coalfield (Table 5.1); the thickest unit is the MS1, which is 15 m

thick. The deterioration and disappearance of some lower coal zones is indicated by some stratigraphic units thinning towards the north and north-eastern margins of the coalfield (CZ2 and CZ1) (Figure 5.26). The lateral lithofacies distribution may suggest sediment influx from an eastern direction.

Coal from the Swartrant Formation is generally poor when looking at the weighted average raw qualities: Calorific Value_9.56Mj/kg; Inherent Moisture_1.97%; Ash_41.22%; Volatile Matter_19.56%; Fixed Carbon_30.69%; Total Sulphur_0.95% and Phosphorus_0.03% (Table 5.1). As a result, the coal is used as blend coking coal at Grootegeluk Mine. The Swartrant Formation primarily supplements power station, metallurgical, and pulverised coal injection products.

In the Swartrant Formation, coarse sandstone channel deposits, delta plain gritstone, and the delta front coarse sandstones are capped by CZ1. Fluvial channel deposits with an east-west trend, ranging in texture from coarse to sandy, are deposited on top of this unit. CZ2 and CZ3 accumulated as the interruptions of the fluviatile conditions occur. Complex units of sandstone (Figure 3.8 to Figure 3.10), mudstone (Figure 3.12), siltstone (Figure 3.15), and coal (Figure 3.17), dominate in this formation. These were formed from proximal floodplain development, alternating among the emergence of channels, splays, mudflows, and periods of fine carbonaceous mud and peat formation (CZ4 and CZ4A).

6.1.2 Grootegeluk Formation

The Grootegeluk Formation occurs between the Swartrant and the Eendragtpan Formations, it comprises bright coal intercalated with mudstone cycles and sub-cycles (Figure 2.7), making seven coal zones—CZ11; CZ10; CZ9; CZ8; CZ7; CZ6 and CZ5, with variable organic contents. The coal-mudstone cycles are preserved mainly throughout the Waterberg Coalfield and are laterally persistent (Figure 5.3 to Figure 5.8). Decrease in

depth is directly proportional to the decrease in vitrinite content in the coal and mudstone zones; also, the decrease in depth increased in RD (Table 5.1) this is due to the heavier silty material settling at the basement.

Boreholes used in this 3D lithostratigraphic facies model intersected the entire formation, from top-to-bottom, intersecting Coal Zones 11 to 5 (Figure 3.3 to Figure 3.7). The bright coal intercalated with mudstone unit occurs throughout the coalfield. The formation maintains a consistent thickness averaging 7.95 m across the coalfield, thickens in the north, and thins towards the east (Figure 5.3 to Figure 5.9). Compared to the grey-to-white mudstones higher in the formation, black-to-grey mudstones in the basal parts are more carbonaceous (Figure 3.16), indicating that more organic material were buried beneath the upper mudstones. The deposit becomes muddier with ascending height as sub-cycles with downwardly decreasing coal-to-mudstone ratios were observed (Figure 3.17).

The coal quality analyses shows that the sedimentological conditions changed gradually upward in the formation (Table 5.1: coal percentage increasing upwards). Higher vitrinite and higher ash content are characteristics of the vitrinite-rich upper Grootegeluk Formation. The higher ash in the coal in the upper parts of (CZ10, 9, 8 and 7) of the formation (Table 5.1) directly relate to the higher proportions in the mudstones with thinner high vitrinite coal bands.

Coal from the Grootegeluk Formation is generally of lower grade as depicted by the weighted average raw qualities: Calorific Value_9.99Mj/kg; Inherent Moisture_2.09%; Ash_46.84%; Volatile Matter_22.87%; Fixed Carbon_23.90%; Total Sulphur_0.93% and Phosphorus_0.03% (Table 5.1). As a result, coal from the Grootegeluk Formation gets beneficiated for semi-soft coking coal and thermal coal at Grootegeluk Mine. Owing to the coal-mudstone intercalation in this formation, a double-stage beneficiation process derives value from this low-grade coal.

From the borehole logs (Figure 3.3 to Figure 3.7), the succession has siderite lenses, concretions, calcite, and pyrite fracture fillings and nodules. The organically rich high vitrinite coal seams occur mostly with globular pyrite, mostly in Coal Zone 11 to 9 (analytically indicated by high total sulphur; Table 5.1). Spherulitic siderites occur throughout the coal zones of the Grootegeluk Formation, and within carbonaceous mudstones. Spherulitic siderite— are primarily found in coal seams and mudstones rich in organic matter. In bright, high vitrinite coal seams in the top section of the formation, calcite occasionally occurs as cleats and/or lenses (Figure 3.16). In CZ4 and CZ5, phosphate occurs in higher concentration compared to other zones (Table 5.1).

The intercalated coal (dull lustrous to bright) and carbonaceous mudstone of the Grootegeluk Formation (Figure 3.16) suggest that the basin subsided as it filled in a backswamp depositional environment. Sandstone layers or channels are absent within the formation, suggesting very low-energy conditions.

6.1.3 Eendragtpan Formation

The Eendragtpan Formation overlies the Grootegeluk Formation (Figure 2.7). It consists of alluvial sand and multi-coloured mudstones that are variably coloured and turns silty in the bottom third of the succession. Granular siderite occurs within this formation. The multi-coloured Beaufort Group mudstones (Figure 3.11), indicates that the mudstones underwent chemical alteration.

Boreholes in this 3D lithostratigraphic facies model intersected the bottom part of the formation and were classified as the overburden (OVB) (Figure 3.3 to Figure 3.7). It maintains an average thickness of 123.93 m (Table 5.1), which thickens towards the centre of the coalfield from 85.20 m to 426 m (Figure 5.2). The thickest deposition (~213 m) is central, indicating the areas where the deepest bedrock lies; therefore, forming the graben or half-

graben structure with the effect from the Daarby and the Zoetfontein Faults. The western and eastern edges of the coalfield maintain a maximum thickness of 50 m, which gradually increase inwards into the basin (Figure 5.2).

Other researchers postulates that the multi-coloured mudstones may have previously accumulated significant organic material; however, the material was later degraded and destroyed. Evidence from the borehole core indicates that the Eendragtpan Formation mudstones lack coal and carbonaceous material, which confirms that these mudstones may have formed in a distant, well-drained floodplain depositional environment.

6.2 Geological Cross-Sections

3D lithostratigraphic facies model of the Waterberg Coalfield area reveals a high concentration of crosscutting faults and lineaments, as affirmed in (Figure 5.34). The lineaments and faults dissect the coalfield on east-west and northeast-southwest trends. Stratigraphic correlations using a cross-section approach offer a simplified method of depicting geological heterogeneity and identifying displacements (Figure 5.19: illustrates the cross-section approach).

An increased depositional thickness of the Karoo Supergroup in the study area is ~300 m in the central parts, thinning to ~50 m on the western, and ~20 m in the eastern parts of the coalfield (Figure 5.24). The fault-bounded graben may indicate post and syn-sedimentary tectonism and sedimentation. Fault movement cuts throughout the Permian Ecca Group, which is evident from the Grootegeluk Formation to the Swartrant Formation which indicates post-depositional faulting (Figure 5.21; Figure 5.23; Figure 5.25 and Figure 5.29).

6.2.1 Evidence from north-south cross-sections (1; 2; 3; 4; 5)

The cross-section (Figure 5.21) reveals anticlinal structures developing into block faulting and folding. A graben structure is identifiable in (Figure 5.22) with thicker zones in the central part, trending towards the northern and southern edges of the coalfield. Evidence of structural changes in parts of the Waterberg Coalfield exists; typical upthrow and downthrow movements are evident (Figure 5.23). The central part of the coalfield demonstrates much deeper coal and a complete stratigraphic column along the cross-sections. Palaeo-floor upliftment in the east of the coalfield is attributed to the influences of the Daarby Fault and the higher elevated pre-Waterberg Group rocks (Nebo Granites and Villa Nora Gabbro) of Bushveld age that uncomfortably underlies the Ecca Group rocks (Figure 5.25).

6.2.2 Evidence from west-east cross-sections (6; 7; 8; 9; 10)

The upper zones in the Ecca Group were poorly deposited in the northern edge of the coalfield (Figure 5.26; Figure 5.34); only CZ5 was deposited—CZ6 to CZ11 were not deposited as depicted in this cross-section (Figure 5.26). This is evidence of non-deposition and/or post-depositional erosion, primarily on the upper zones of the Grootegeluk Formation (Figure 5.29). Coal zones occur much shallower and thin towards the western edge (Figure 5.28). Coal zones occur as a complete succession in the central portions of the coalfield, moderately undulating while thinning and revealing discontinuities at places (Figure 5.22 to Figure 5.25). Erosion of the coal zones can be observed (Figure 5.30), which can be attributed to fluvial channels. A 360 m downthrow movement of the Eenzaamheid Fault is a significant displacement in the coalfield, as a contributor to the graben structure. This variability in coal zone thickness is mainly directly related to the accumulation of organic material during deposition.

Chapter 7: SUMMARY AND CONCLUSIONS

7.1 SUMMARY

The research attempted to produce a 3D lithostratigraphic facies model that would help in understanding the depositional setting; structural footprint; lithological thicknesses, coal qualities, and geometry of the zones within the Waterberg Coalfield. Through using lithofacies defined cross-sections and seam distribution plans, the model extrapolated and assessed the probability of overburden, coal zones, and non-coal zone thicknesses, top and base contour trends; however, primary limitations of this model remained.

The main challenges with this 3D lithostratigraphic facies model were, uncertainty due to the complex geology in the study area, density of data, data irregularity, and varied interpolation techniques applied. The cross-sections were also challenging to interpret in locations with considerable low number of boreholes. This was due to the unrealistic scales on the cross-sections, as boreholes occurred too far apart. Variances in isolated borehole data caused the cross-sections to produce unrealistic subsurface interpretations as data are scarce.

Grid creation applied an Inverse-distance weighted (IDW) technique to interpolate thicknesses and qualities. This interpolation technique proved most effective and provided realistic lateral distributions. The grids were smoother and more realistic in areas with dense borehole information. In areas with a fewer borehole number, the software could not extrapolate to create a grid but instead left a void to indicate that there were not enough reference data points, therefore low level of confidence.

Overall, the validity and integrity of the 3D lithostratigraphic facies model mainly depended on the quantity, quality, data distribution, and the technical ability of modelling and interpretation with Geovia Minex^{TM} Software.

The model did provide the best possible representation of geological features at the Waterberg Coalfield, given the available data and software modelling limitations, interpretation of subsurface geometry and deposition were possible.

7.2 CONCLUSIONS

Geovia Minex™ software has enabled a way that geoscientific data gets displayed and interpreted to produce integrated geoscientific information across the Waterberg Coalfield. However, an acknowledgement of the limitations of the data from which the model was based to create a greater level of realism were highlighted, mainly to assist in the differentiation between observed and conjectural information.

Structural complex areas are more concentrated on the elevated outer-edges of the coalfield as observed by a high concentration of lineaments and block structures depicted on the airborne electromagnetic survey. These micro-faults and micro-folds were influenced by a massive ~250 m downthrow of the sinuous-shaped Daarby Fault on the western and the southern parts of the coalfield, and another ~180 m upthrow from the Zoetfontein Fault on the north of the coalfield. Thicker overburden material over the central parts of the coalfield may have increased sediment loading-related subsidence, contributing towards the faults' reactivation.

Deeper coal in the central part of the coalfield is of low grade and too expensive for mining when considering the current coal economics. The overburden material is too thick, it averages 123.93 m, with a maximum thickness of 424.55 m. However, the coal seams could be used to produce chars, briquettes, activated carbon and carbon reductants as well as supercritical pulverized coal injection, fluidized bed combustion, gasification, and coalbed methane.

The modelled borehole data illustrate additional structures and linear features identified within the Waterberg Coalfield, interpolated Fault 1, 2, 3, 4, 5, 6, and 7. This was observed from the abrupt changes in the Z-collars of the surface grids and major changes in elevation across the cross-sections. As emphasised, the magnetic signatures of most structures are weak, owing to thick cover or because they are weathered. Many non-magnetic structures in the study area remain undetected, however, the 3D lithostratigraphic facies model has indicated that the coalfield is highly structurally complex. A definite correlation exists between the aeromagnetic survey and the presented model on the structural influence the Waterberg Coalfield experienced. Both allude to a highly disturbed, structurally bound coalfield with more geological structures occurring much deeper.

The model deduced that the major controlling factors in thickness of the zones and lateral continuity in the Waterberg Coalfield are controlled by differential compaction and subsequent erosion—shallow Coal Zone 11, was affected by surface erosion. While deeper Coal Zones 1 and 2 were most affected by fluvial channels (SS1 and SS2), where the peat was overlain by sandstone. Thinner coal zones are mainly capped by sandstones that may have contributed to the erosion; however, where coals are overlain by mudstone which represents low-energy setting in a floodplain environment, they appear thicker as the mudstone may have created a shielding layer from subsequent erosion (e.g., Coal Zones 3 and 4). Missing coal zones typically were affected by exogenic geological processes such as weathering denudation and erosion. Coal Zones 5 to 10 overall thicknesses emanate from densely vegetated backswamps with high organic matter deposition. Isopach maps and cross-sections illustrate this possibility also on a broader scale.

The 3D lithostratigraphic facies model confirms that the Zoetfontein Fault was active post the deposition of the Karoo Supergroup, trending north-west into the Kalahari Karoo Basin and may be connected to the Melinda Fault

in the east, the Mhalapswe Fault in the west of the coalfield. The Eenzaamheid and the Daarby Faults, are younger than the Karoo Supergroup, as their displacements are post-depositional. The Daarby Fault trends north-west and changes direction at 90º towards the Zoetfontein Fault. It holds a downthrow displacement of between 150 m and 250 m, and separates the deposit into shallower opencast mineable western and eastern portions and a deeper underground mineable north-western portion where coal occurs at over 300 m below the surface. Evidence exists of a palaeo-high upliftment between the Daarby Fault and the Eenzaamheid Fault on the south-eastern part of the coalfield.

It is further confirmed that the Waterberg Coalfield was created in a structurally deformed area, with step block faulting, and lineaments crosscutting in an east-west and northeast-southwest direction. This is apparent as the strata east of the coalfield are significantly uplifted; an upthrow Daarby Fault also contributed to the condition.

This developed 3D lithostratigraphic facies model concurs with the current understanding of the structural geology, with more major faulting postulated, well-defined coal characteristics (e.g., lateral extent, thicknesses, and qualities), and with much more coal still available for exploitation from the Waterberg Coalfield; however, only through extensive beneficiation can value be derived from this low-grade bituminous coal. Grootegeluk Mine, currently requires 10 large individual plants to beneficiate the coal into multiple products. This approach serves as a blueprint model towards extracting value from such a coal deposit.

REFERENCES

Alberts B.C. and Liebenberg B.F. 1982. The Geology and Mining of the Northern Transvaal Coal Deposits. In: Glen H.W. (Ed.). Proc. 12th CMMI congress, Johannesburg. 101-110.

Berg, R.C., Mathers, S.J., Kessler, H., and Keefer, D. A. 2011. Synopsis of Current Three-dimensional Geological Mapping and Modeling in Geological Survey Organization; Champaign, Illinois: Illinois State Geological Survey, Circular 578, www.isgs.illinois.edu.

Beukes, N.J. 1985. Sedimentologie van die Ellisrassteenkoolveld. Finale verslag, WNNR, KWP, NGP: Steenkoolgeologieprojek. (Report to the CSIR Coal Geology Project), 15 pp.

Beukes, N.J., Siepker, E.H., & Naudé, F. 1991. Genetic stratigraphy of the Waterberg Coalfield. Ext. Abstr. Conference on South African's Coal Resources, Witbank. 6-9 November.

Bhattacharya, J.P., Walker, R.G. 1992. Deltas. In: R.G. Walker, N.P. James (Editors). Facies Models: Response to Sea Level Change. Geological Association of Canada, 157–177.

Boggs, S. (Jr.)., 2006. Principles of sedimentology and stratigraphy, (4th edition). Prentice Hall, Upper Saddle River, New Jersey, 662 pp.

Bolstad, P. 2005. GIS fundamentals: A first text on geographic information systems, 2nd Edition, White Bear Lake, Minnesota. 412 pp.

Bordy, E.M. & Catuneanu, O. 2002. Sedimentology of the lower Karoo Supergroup fluvial strata in the Tuli Basin, South Africa. Journal of African Earth Sciences, 35, 503-521.

Bordy, E.M., Hancox, P.J., & Rubidge, B.S. 2005. The contact of the Molteno and Elliot formations through the main Karoo Basin, South Africa:

a second-order sequence boundary. South African Journal of Geology, 108, 351-364.

Bordy, E.S., Knoll, F., Bumby, A., 2010. New data on the palaeontology and sedimentology of the Lower Jurassic Lisbon Formation (Karoo Supergroup), Ellisras Basin, South Africa. Neues Jahrbuch für Geologie und Paläontologie Abhandlungen, DOI: 10, 1-11.

Brandl, G. 1996. Ellisras (Explanation Sheet 2326, 1:250 000). Council for Geoscience. Geological Survey of South Africa.

Bumby, A.J. 2000. The geology of the Blouberg Formation, Waterberg and Soutpansberg Groups in the area of Blouberg Mountain, Northern Province, South Africa. Ph. D Geology thesis, University of Pretoria, Pretoria, 350 pp.

Bumby, A.J. & Guiraud, R. 2005. The geodynamic setting of the Phanerozoic basin of Africa. Journal of African Earth Sciences 43, 1-12.

Cadle, A.B., Cairncross, B., Cristie, A.D.M., & Roberts, D.L. 1993. The Karoo Basin of South Africa: type basin for coal-bearing deposits of southern Africa. Int. Journal of. Coal Geology, 23, 117-157.

Cairncross, B., 1986. Depositional environments of the Vryheid Formation in the east Witbank Coalfield: a framework for coal seam stratigraphy, occurrence and distribution. Ph.D. Thesis (unpublished). University of Witwatersrand, South Africa, 232 pp.

Cairncross, B. 2001. An overview of the Permian (Karoo) coal deposits of southern Africa. Journal of African Earth Sciences 23, 529–562.

Calcagno, P., Chil`es, J.P., Courrioux, G., & Guillen, A. 2007. Geological modelling from field data and geological knowledge, Part I – Modelling method coupling 3D potential-field interpolation and geological rules, Physics of the Earth and Planetary Interiors.

Caumon, G. & Mallet, J.L. 2006. 3D Stratigraphic models: representation and stochastic modelling. Int. Assoc. for Mathematical Geology XIth International Congress Université de Liège – Belgium. S14-08.

Catuneanu, O., Hancox, P.J., & Rubidge, B.S. 1998. Reciprocal flexural behaviour and contrasting stratigraphies: a new basin model for the Karoo retroarc foreland system, South Africa. Basin Research 10, 417-439.

Catuneanu, O. & Elango, H.N. 2001. Tectonic control on fluvial styles: the Balfour Formation of the Karoo Basin, South Africa. Sedimentary Geology, 140, 291-313.

Catuneanu, O., Hancox, P.J., Cairncross, B., & Rubidge, B.S. 2002. Foredeep submarine fans and forebulge deltas: orogenic offloading in the underfilled Karoo Basin. Journal of African Earth Sciences 35, 489–502.

Catuneanu, O., Wopfner, H., Eriksson, P.G., Cairncross, B., Rubidge, B.S., Smith, R.M.H., & Hancox, P.J. 2005. The Karoo basins of south-central Africa. Journal of African Earth Sciences, 43, 211-253.

Chabedi, C.K. 2013. Analysis of Technical Factors for Underground Mining of Deep Waterberg Coal Resources. Unpublished MSc Thesis, University of the Witwatersrand, South Africa, 149 pp.

Chabedi, K. & Mhlongo, S. 2018. Mining of the Waterberg - a Unique Deposit Requiring Innovative Solutions. International Journal of Georesources and Environment. IJGE 2018 4(3), 127-132.

Che, D and Jia, Q. 2019. Three-Dimensional Geological Modeling of Coal Seams Using Weighted Kriging Method and Multi-Source Data. [Online]. Available: https://ieeexplore.ieee.org/stamp/stamp.jsp?arnumber=8808857

Childs, C. 2004. Interpolating Surfaces in ArcGIS Spatial Analyst. ArcUser, July-September 32-35.

Cillié, J.F. & Visser, H.N., 1945. Waterberg coalfield: Records of boreholes, 21-40. Bull. geol. Surv. S. Afr., 16, 132 pp.

Cillié, J.F. 1951. Waterberg coalfield: Records of boreholes, 41-100. Bull. geol. Surv. S. Afr., 21, 381 pp.

Cillié, J.F. 1957. Waterberg coalfield: Records of boreholes, 101-143. Bull. geol. Surv. S. Afr., 23, 276 pp.

Cole, D.I. 1992. Evolution and development of the Karoo Basin. In: M.J. De Wit and I.G.D. Ransome (Editors) Inversion Tectonics of the Cape Fold Belt, Karoo and Cretaceous Basins of Southern Africa, Balkema: Rotterdam, The Netherlands, 87-99.

Council for Geoscience. 2010. Assay Coal Analysis: Blend coking coal and PowerStation Coal (Unpublished Reports). Pretoria: Council for Geoscience.

De Jager, F.S.J. 1976. Coal. In: Coetzee, C.B. (Ed.), Mineral Resources of the Republic of South Africa. Handbook of the Geological Survey of South Africa, 7, 478 pp.

De Jager, F.S.J. 1983. The Geology of the Springbok Flats, Waterberg, Soutpansberg and Limpopo Coal Fields (With an Addendum on the Geology of the Komatipoort Coal Field). Unpublished Report, South African Geological Survey Pretoria 1983-0120, 11 pp.

De Korte, J. 2010. Beneficiation of Waterberg Coal, Johannesburg: Unpublished.

Deysel, L.M. 2015. Environmental geochemistry of the Waterberg Coalfields. Institute for Groundwater Studies, University of the Free State, South Africa. Unpublished Ph.D. Thesis, University of the Free State Bloemfontein, South Africa, 290 pp.

Dreyer. J. C. 1991. Waterberg Coalfield: Geology, resources, mining and products. In: Conference on South Africa's coal resources, Geological Society South Africa (Abstracts). Witbank, 6-9 Nov.

Dreyer, C., 1994. Total utilization of the coal resource: the Grootegeluk experience. In: C. Anhaeusser, ed. Proceedings XVth CMMI Congress. South African Institute of Mining and Metallurgy, Johannesburg, South Africa, 153 - 164.

Dreyer, J.C. 1999. Selective mining and beneficiation at Grootegeluk Coal Mine Waterberg Coalfield. Unpublished.

Eriksson, P.G. 1986. Aeolian dune and alluvial fan deposits in the Clarens Formation of the Natal Drakensberg. Transactions of the Geological Society of South Africa 89, 389–394.

Falcon, R.M.S. 1986. The coalfields of southern Africa: an introduction. In: Anhaeusser, C. R., Maske, S. (Eds.), Mineral Deposits of Southern Africa, vol. II. Geological Society of South Africa, Johannesburg, 1875–1878.

Faure, F., Willis, J.P., & Dreyer, C.J. 1996a. The Grootegeluk Formation in the Waterberg Coalfield, South Africa: Facies, Palaeo-environment and thermal history- evidence from organic and clastic matter. International Journal of Coal Geology, 29, 147-186.

Faure, K., Armstrong, R.A., Harris, C., Willis, J.P., 1996b, Provenance of mudstones in the Karoo Supergroup of the Ellisras Basin, South Africa: Geochemical evidence. Journal of African Earth Sciences 23, 189–204.

Fourie, C.J.S. 2008. Waterberg Airborne Geophysics: Acquisition and Preliminary Results. Report no. CSIR/NRE/MIN/ER/2008/0073A, document no: 16109 © CSIR. Technical Editor: M. van Schoor.

Fourie, C.J.S., Henry G, Marè., 2009. The structure of the Karoo-age Ellisras Basin in Limpopo Province, South Africa in the light of new airborne geophysical data: a preliminary report. 11th SAGA Biennial Technical Meeting and Exhibition Swaziland. 16-18 September, 27-32.

Fourie, C.J.S., Henry, G., Maré, L.P., 2014. The structure of the karoo-age Ellisras basin in Limpopo Province, South Africa, in the light of new airborne geophysical data. South African Journal of Geology, 117, 193-221.

Gratacós, O., Bitzer, K., Cabrera, L., & Roca, E. 2009. SIMSAFADIM-CLASTIC: A new approach to mathematical 3D forward simulation modelling for terrigenous and carbonate marine sedimentation. Geologica Acta, 7, 3, 311-322.

Hancox, P.J. 2000. The Continental Triassic of South Africa. Zentralblatt für Geologie und Paläontologie, Teil I, 1998, 1285-1324.

Hancox, P.J. & Götz, A.E. 2014. South Africa's coalfields — A 2014 perspective. International Journal of Coal Geology 132, 170–254.

Harms, J.C., Southard, J.B. and Walker, R.G., 1982. Structures and sequences in clastic rocks. Society of Economic Paleontologists and Mineralogists Short Course Notes, 9, Calgary, 249 p.

Holland, M.J., Cadle, A.B., Pinheiro, R. and Falcon, R.M.S., 1989. Depositional Environments and coal petrography of the Permian Karoo Sequence: Witbank Coalfield, South Africa. International Journal of Coal Geology, 11, 143-169.

Huang, M., Depeng, L., & Xianyong, H. 2014. A Stratigraphic Modelling Method based on Borehole Data. IJCSI International Journal of Computer Science Issues, 11, Issue 2, No 1. 5 pp.

Jeffrey, L.S. 2005. Challenges associated with further development of the Waterberg Coalfield. Journal of South Africa. Inst. Min. Metall. 106, 453–457.

Johnson, M.R., van Vuuren, C.J., Hegenberger, W.F., Key, R., & Shoko, U. 1996. Stratigraphy of the Karoo Supergroup in southern Africa: An overview. Journal of African Earth Sciences, 23(1), 3-15.

Johnson, M.R., Van Vuuren, C.J., Visser, J.N.J., Wickens, H. deV., Christe, A.D.M., Roberts, D.L. 1997. The foreland Karoo Basin, South Africa. In: R.C. Selley (Editor). African Basins-Sedimentary Basins of the World. Elsevier, Amsterdam, 269-317.

Johnson, M.R., Van Vuuren, C.J., Visser, J.N.J., Cole, D.I., Wickens, H., de, V., Christie, A.D.M., Roberts, D.L., & Brandl, G. 2006. Sedimentary rocks of the Karoo Supergroup. In: Johnson, M.R., Anhaeusser, C.R., Thomas, R.J. (Eds.), The Geology of South Africa, Geological Society of South Africa, Johannesburg/Council for Geoscience, Pretoria, 461–499.

Kelk, B. 1991. 3D modelling with geoscientific information systems: the problem. In: AK Turner (ed) Three-Dimensional Modelling with Geoscientific Information Systems, NATO ASI Publications, Series C-354, Kluwer Academic Publishers, Dordrecht, The Netherlands, 29-38.

Lemon, A.M. & Jones, N.I. 2003. Building solid models from boreholes and user-defined cross sections. Computers and Geosciences 29 (5), 547-555.

MacRae, C.S. 1988. Palynostratigraphic correlation between the lower Karoo Sequence and the Waterberg and Pafuri coal-bearing basins and the Hammanskraal plant macrofossil locality, Republic of South Africa. Memoir/Memorie 75. Geological Survey. 217 pp.

MacRae, C.S. 1989. Palynostratigraphic identification of an unconformity in borehole KNP 7 from the north-eastern part of the Soutpansberg Coalfield

(Permian Period), South Africa. South African Journal of Geology, 92, 3, 261-271.

Malaza, N. 2014. Basin analysis of the Soutpansberg and Tuli Coalfields, Limpopo Province of South Africa. Ph. D Geology thesis, University of Fort Hare, South Africa, 380 pp.

Maliva, R.G. 2016. Aquifer Characterization Techniques. Springer International Publishing Switzerland. Hydrogeology, 978-1007.

Miall, A.D. 1990. Principles of Sedimentary Basin Analysis. 2nd edition. Springer-Verlag, New York Inc., 668 pp.

Miall, A.D. 1996. The Geology of Fluvial Deposits: Sedimentary Facies, Basin Analysis and Petroleum Geology. Berlin: Springer Verlag, 598 pp.

Miall, A.D. 2000. Principles of Sedimentary Basin Analysis, (3rd edition). Springer-Verlag, Berlin-Heidelberg, 616 pp.

Mtimkulu, M.N. 2009. A Provisional Basinal Study of the Waterberg–Karoo, South Africa. MSc dissertation, University of Pretoria, South Africa (http://upetd.up.ac.za/thesis/ available/etd-08172010-191251/).

Nichols, G. 2009. Sedimentology and Stratigraphy. Blackwell Science Ltd. 354 pp.

Nxumalo, V. 2011. Stratigraphy and basin modelling of the gemsbok Sub-basin (karoo supergroup) of Botswana and Namibia. MSc dissertation, University of the Witwatersrand, Johannesburg, 198.

Overeem, I. 2008. Geological Modelling: Introduction. Community Surface Dynamics Modelling System University of Colorado at Boulder. 20 pp.

Popovs, K., Saks, T., & Jātnieks, J. 2014. A comprehensive approach to the 3D geological modelling of sedimentary basins: example of Latvia, the

central part of the Baltic Basin. Estonian Journal of Earth Sciences, 64, 2, 173–188.

Prevost, X. 2016. Waterberg Coalfield Reserves and Production. Sunday Times_30-10-2016.

Prothero, D.R. & Schwab, F. 1996. Sedimentary Geology. An Introduction to Sedimentary Rocks and Stratigraphy. New York: W.H. Freeman and Company, 575 pp.

Reading, H.G. 1986. Sedimentary environments and facies, (2nd edition). Blackwell Scientific Publications, Oxford, London, 615 pp.

Roux, L. 2011. Optimal yield and cut density – Prediction of semi soft coking coal and powerstation coal in the Waterberg Coalfield, Limpopo Province. Unpublished MSc Thesis. University of the Witwatersrand, Johannesburg, 228 pp.

Rust, I.C. 1975. Tectonic and sedimentary framework of Gondwana basins in southern Africa. In: K.S.W. Campbell (Editor). Gondwana Geology (3rd Gondwana Symposium). Australian National University Press, Canberra, pp. 537–564.

Rust, B.R. 1978. A classification of alluvial channel systems. In: MIALL, A.D. (ed.) Fluvial sedimentology. Canadian Society of Petroleum Geologists. Calgary. Memoirs. 5, 187-198.

Ryan, P.J. 1966. The basin analysis of the Waterberg Coalfield. Unpubl. Rep. Geol. Surv. S. Africa, 1966-0169 (confidential), 59 pp.

Sabah, E. & Erkom, Z.E. 2006. Interaction mechanisms of flocculants with coal waste slurry. Fuels, 85, 350-359.

SANS 10320 :2004. 2004. South African guide to the systematic evaluation of coal resources and coal reserves. Standards South Africa, Pretoria.

Shahbeik, S., Afzal, P., & Moarefvand, P. 2014. Comparison between ordinary kriging (OK) and inverse distance weighted (IDW) based on estimation error. Case study: Dardevey iron ore deposit, NE Iran. Saudi Society for Geosciences. Arab Journal Geosciences 7:3693–3704.

Shirzadi Babakan, A., Mesgari, M.S., & Karimi, F. 2008. Evaluation of gridding methods for various regions with different elevations. Map India 2008, February 6-8, 2008, India Expo Center, Greater Noida, India.

Siepker, E. H. 1986. Genetiese stratigrafie en sedimentologie van die Opeenvolging Karoo in die westelike and noordelike deel van die Waterbergsteenkoolveld. – Unpublished M.Sc. thesis, Rand Afrikaans University, Johannesburg. – 177 pp.

Smith, R.A. 1984. The lithostratigraphy of the Karoo Supergroup in Botswana. Botswana Geological Survey Department Bulletin, 26, 184-205.

Smith, D.A.M. & Whittaker, R.R.L.G. 1986. The coalfields of southern Africa: an introduction. In: Anhaeusser, C.R., Maske, S. (Eds.), Mineral Deposits of Southern Africa, vol. II. The Geological Society of South Africa, pp. 1875–1878.

Smith, R.M.H., Eriksson, P.G., & Botha, W.J. 1993. A review of stratigraphy and sedimentary environments of the Karoo-aged basins of southern Africa. Journal of African Earth Sciences, 16, 143-169.

Smith, R.A. 1995. Changing fluvial environments across the Permian-Triassic boundary in the Karoo Basin, South Africa and possible causes of tetrapod extinctions. Palaeoecology, 117, 81-104.

Snyman, C.P. 1998. Coal. In: Wilson, M.G.C., Anhaeusser, C.R. (Eds.), The Mineral Resources of South Africa. Handbook, 16. Council for Geoscience, South Africa, pp. 136–205.

South African Committee for Stratigraphy (SACS), 1980. Stratigraphy of South Africa. Part 1 (Comp. L.E. Kent). Lithostratigraphy of the Republic of South Africa, South West Africa/Namibia and the Republics of Bophuthatswana, Transkei and Venda. Handbook of the Geological Survey of South Africa 8, 1–690.

Spears, D.A., Duff, P., McL, D., & Caine, P.M. 1988. The West Waterberg Tonstein, South Africa. Int. J. Coal Geol. 9, 221–233.

Sullivan, J.H. 1995. The Geology of the Coal-bearing Rocks of the Karoo Sequence in the Tshikondeni Mine Area, Northern Transvaal. Unpublished MSc Thesis, University of Pretoria, Pretoria, 169 pp.

Sullivan, J.H. 2013. The practical application of vectar processed densities in providing the lateral continuity of coal zones and samples in the Ellisras Basin, South Africa in support of effective Mineral Resource adjudication. PhD Thesis, University of Pretoria, Pretoria, 296 pp.

Tavener-Smith, R. 1982. Prograding coastal facies associations in the Vryheid Formation (Permian) at Effingham quarries near Durban, South-Africa, Sediment. Geol., 32: 111-140.

The SAMREC Code, 2016. The South African Code for the reporting of Exploration results, mineral resources and mineral reserves (2016 and previous editions available). www.samcode.co.za.

Thorleifson, L.H., Berg, R.C., & Russell, H.A.J. 2010. “Geological mapping goes 3-D in response to societal needs.” GSA Today, no. 8 (August 2010): 27-29.

Turner, A.K. 1991. Three-Dimensional Modelling with Geoscientific Information Systems. NATO ASI Publications, Series C-354, Kluwer Academic Publishers, Dordrecht, The Netherlands, 443 pp.

Turner, A.K. & Gable, C.W. 1994. A review of geological modelling. Colorado School of Mines, Golden, National Laboratory, Los Alamos.

Turner, A. 2006. Challenges and trends for geological modelling and visualization. Bulletin of Engineering Geology and the Environment, 65, 109–127.

Uys, J. 2007. Lithostratigraphy, depositional environments and sedimentology of the Permian Vryheid Formation (Karoo Supergroup), Arnot North, Witbank Coalfield, South Africa. MSc. Dissertation, Johannesburg, University of Johannesburg, 127 pp.

Venter, F.A., 1944. Waterberg coalfield, records of boreholes 1-20: Bulletin of the Geological Survey of South Africa, 15, 106 pp.

Wagner, N.J., Eble, C.F., Hower, J.C., & Falcon, R.M. 2019. Petrology and palynology of select coal samples from the Permian Waterberg Coalfield, South Africa. University of Johannesburg, Johannesburg, 204 pp.

Winter, M.F. 1985. Lower Permian paleoenvironments of the Northern Highveld Coalfield and their relationship to the character of the coal seams. Unpublished Ph.D. Thesis, University of the Witwatersrand, South Africa, 254 pp.

Zhang, B., Wu, X., & Wang, L. 2010. The Preliminary Research of Feature-based 3D Geological Modeling, China. 2nd Conference on Environmental Science and Information Application Technology.

Zhu, L., Zhang, C., Li, M., Pan, X., & Sun, J. 2012. Building 3D solid models of sedimentary stratigraphic systems from borehole data: an automatic method and case studies. Engineering Geology, 127, 1–13.

APPENDICES

APPENDIX A: COAL ZONES, COAL SAMPLES AND NON-COAL SAMPLES

Smaller samples, or sub-cycles, of the coal and non-coal zones were created and are correlated from borehole to borehole.

FORMATION	COAL ZONE	COAL SAMPLES	NON-COAL SAMPLES
VOLKSRUST	11	1A to 1D	1BS to 1DS
	10	2 to 6	2S to 6S
	9	7 to 9	7S to 9S
	8	10 to 14	10S to 14S
	7	15A, 15B to 18	15AS, 15BS to 18S
	6	19 to 21	19S to 21S
	5	22A to 22E	22AS to 22ES & (22FS)*
VRYHEID	4	23A to 23C	(23AS & 23BS)*
	4A	24	(24S)*
	3	25 to 29	25S
	2	30A, 30B to 31	
	1	32	

* Samples that are not part of Coal Zones and is interburden waste

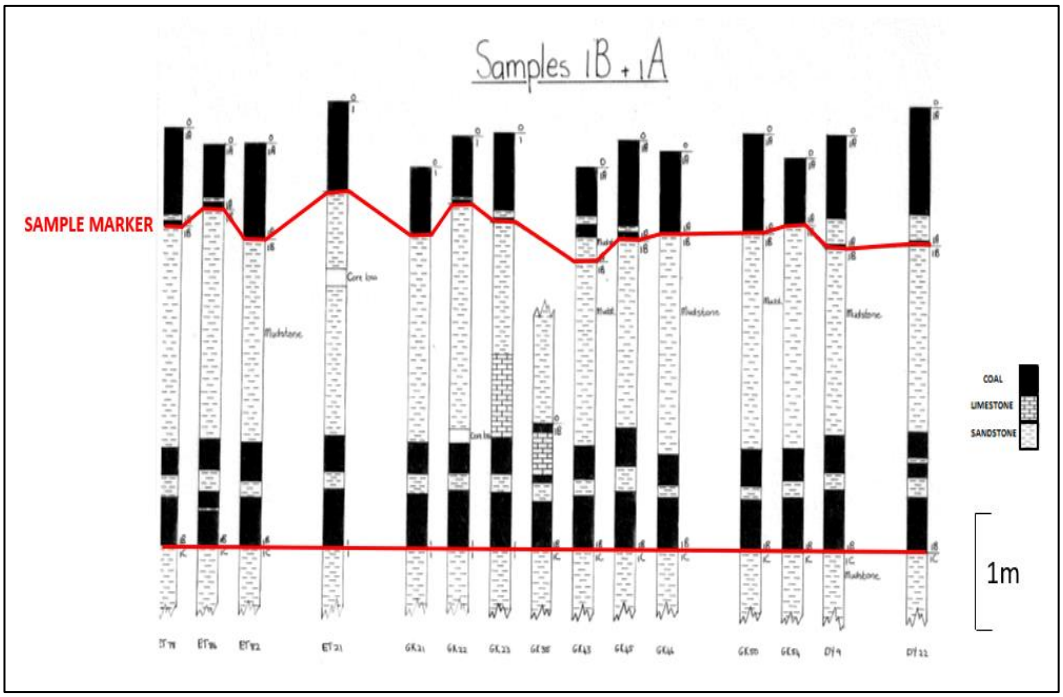

Figure A 1: Sample 1B+1A

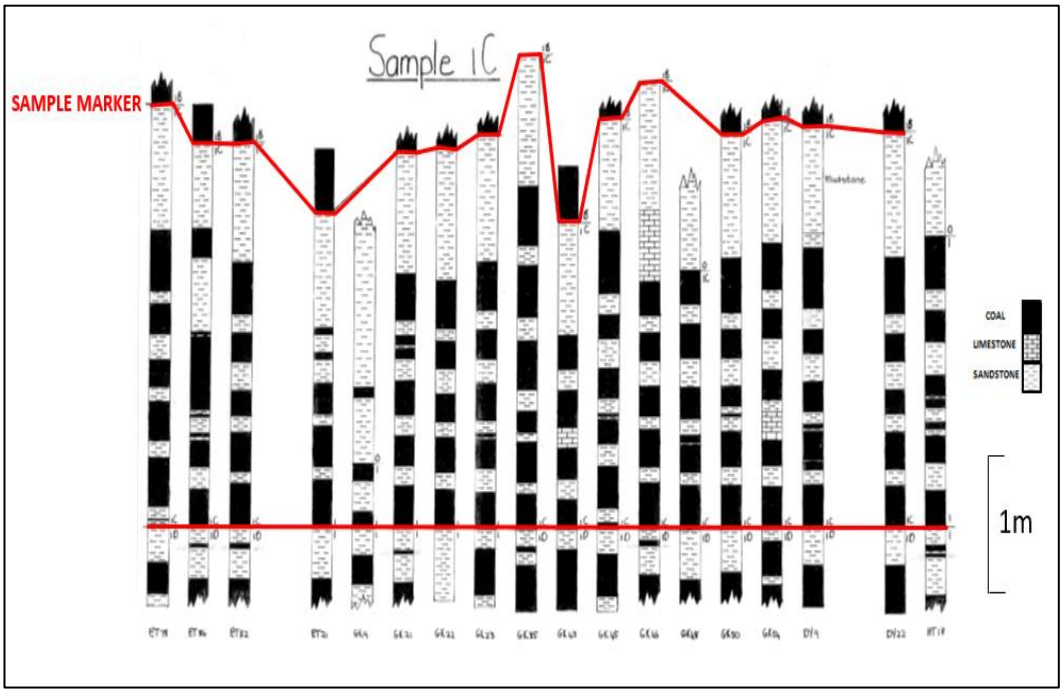

Figure A 2: Sample 1C

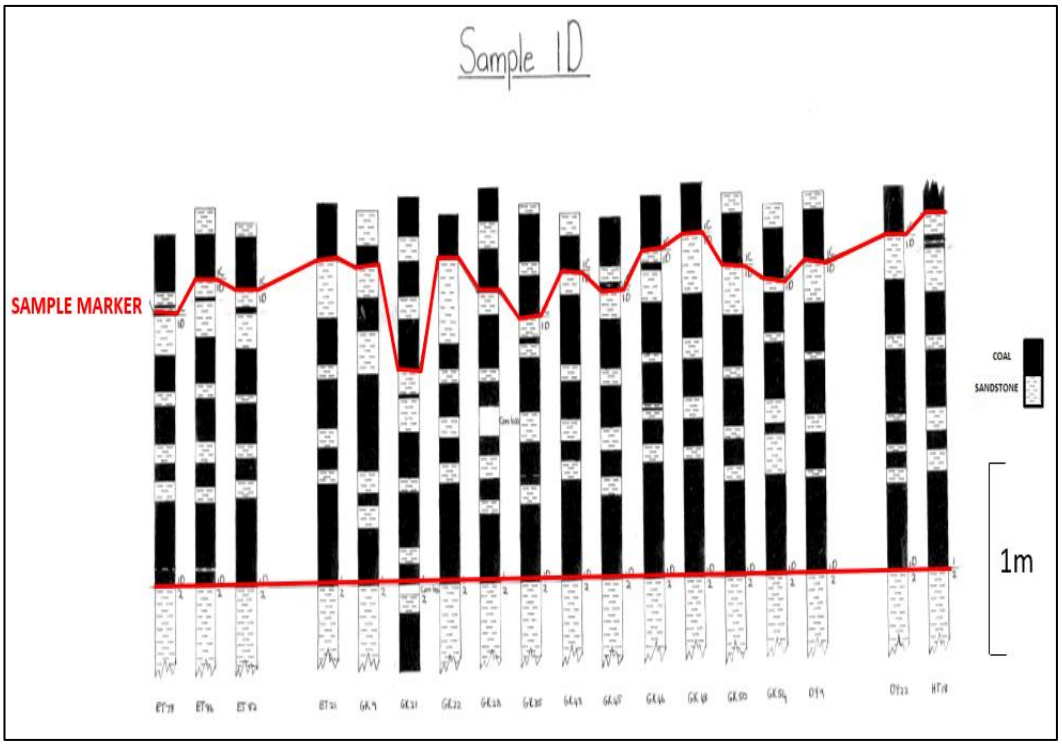

Figure A 3: Sample 1D

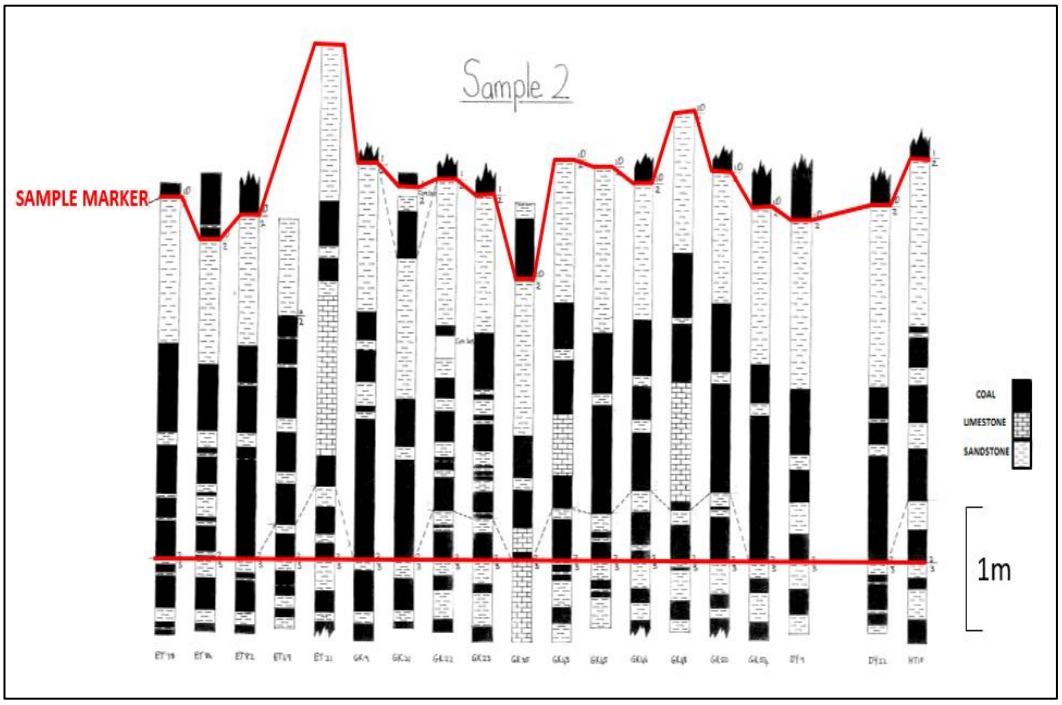

Figure A 4: Sample 2

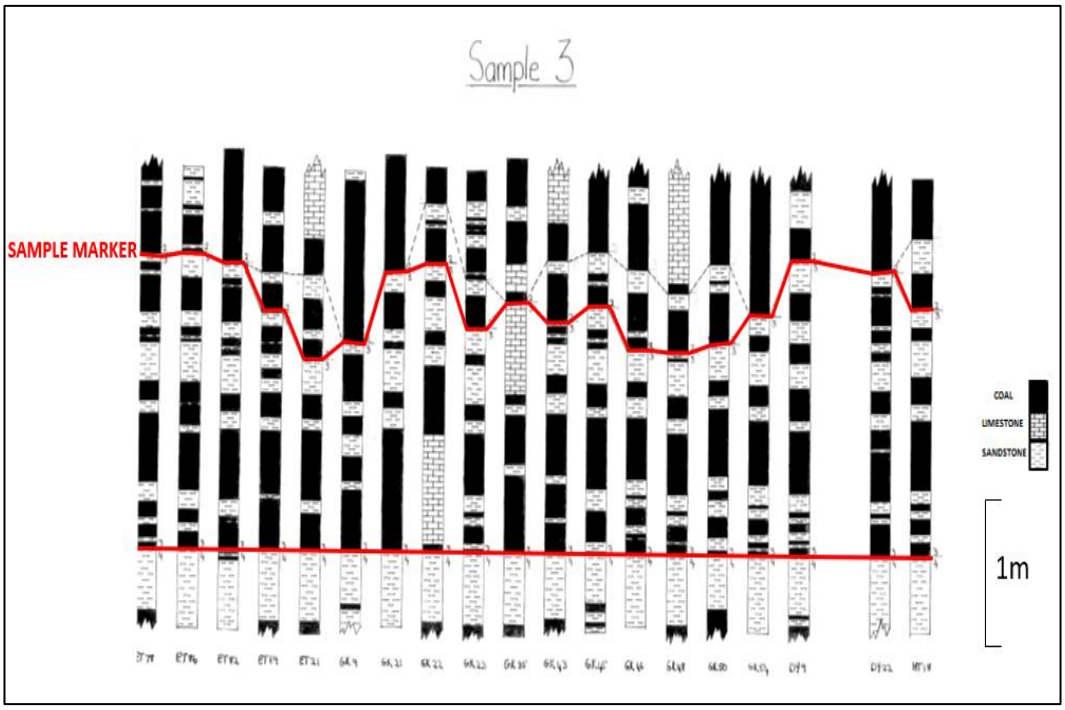

Figure A 5: Sample 3

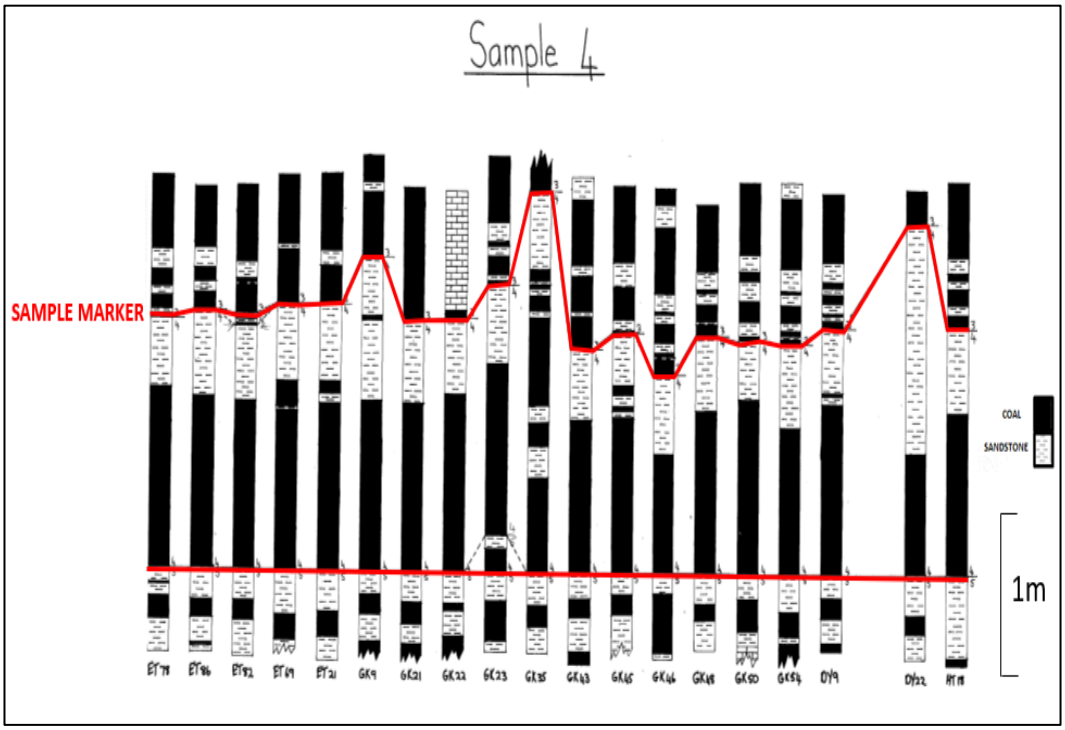

Figure A 6: Sample 4

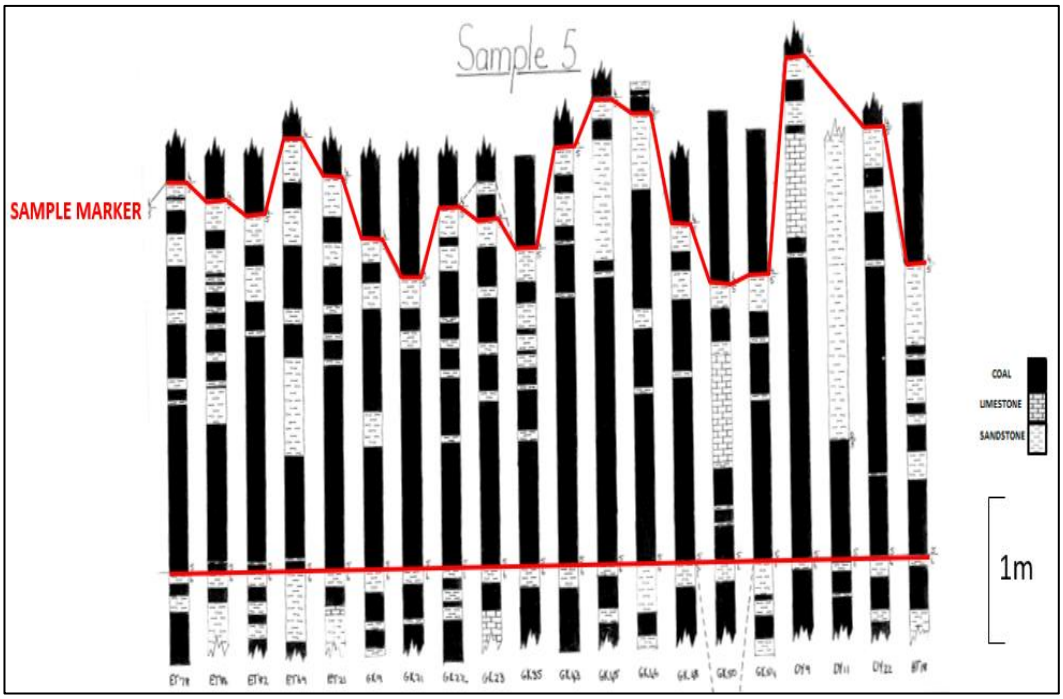

Figure A 7: Sample 5

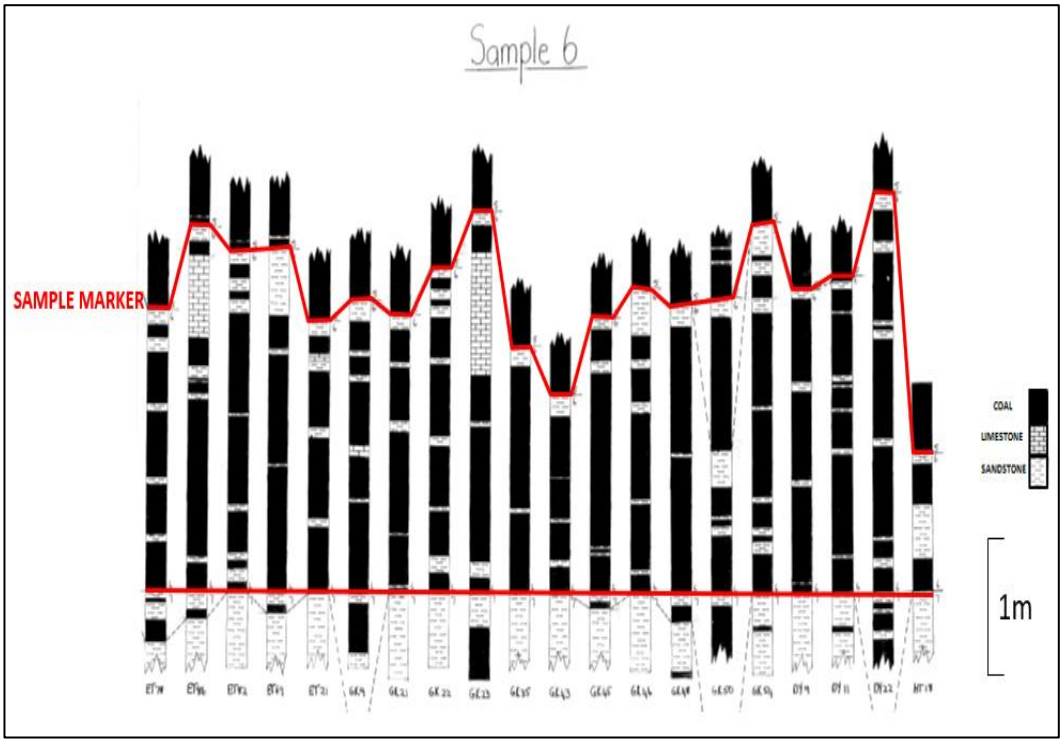

Figure A 8: Sample 6

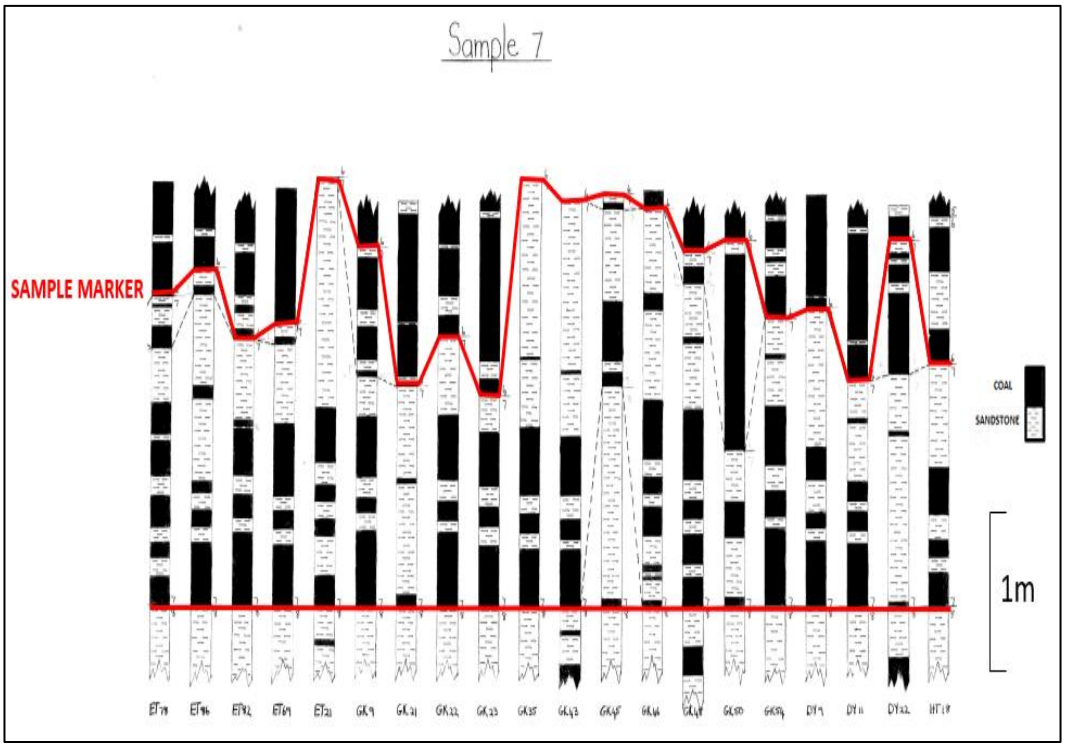

Figure A 9: Sample 7

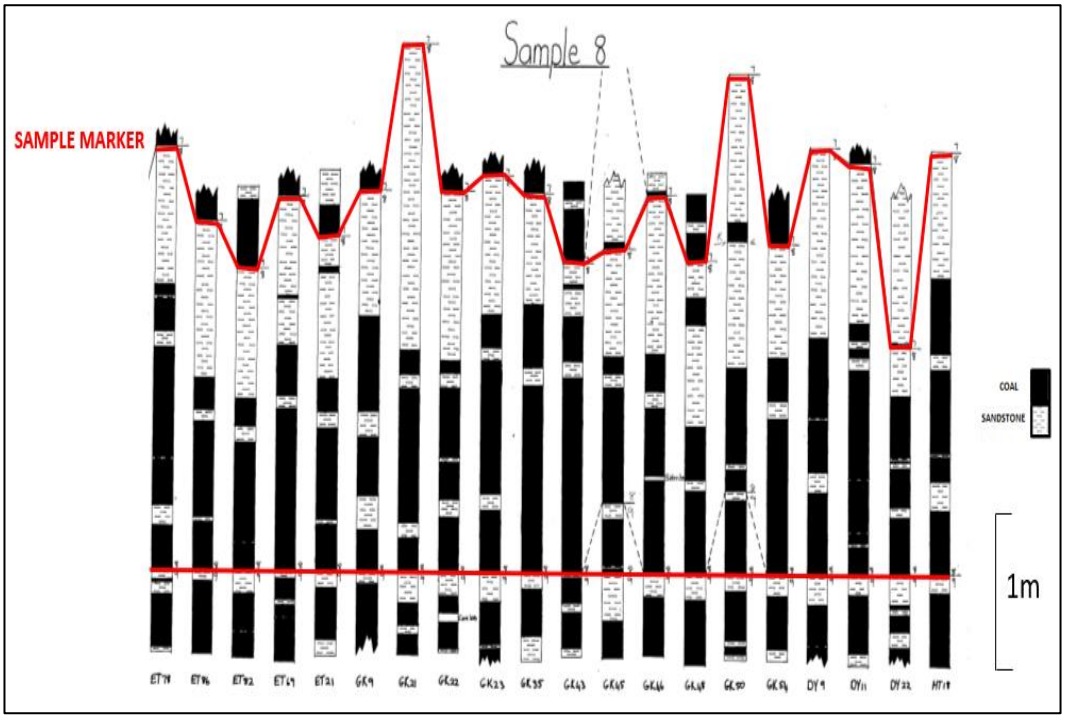

Figure A 10: Sample 8

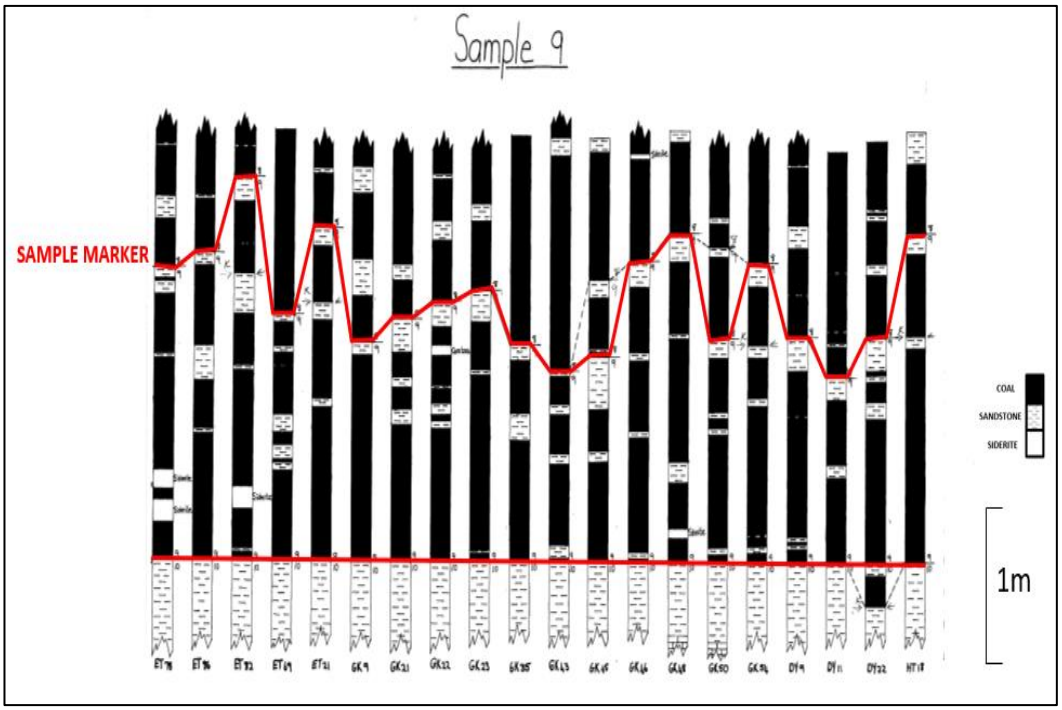

Figure A 11: Sample 9

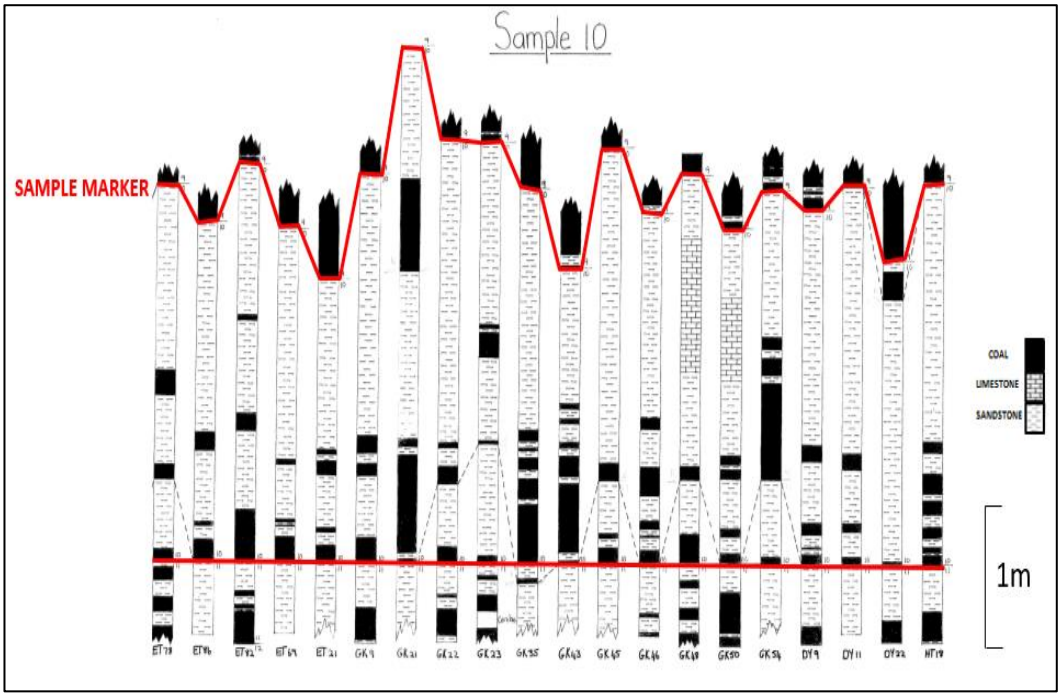

Figure A 12: Sample 10

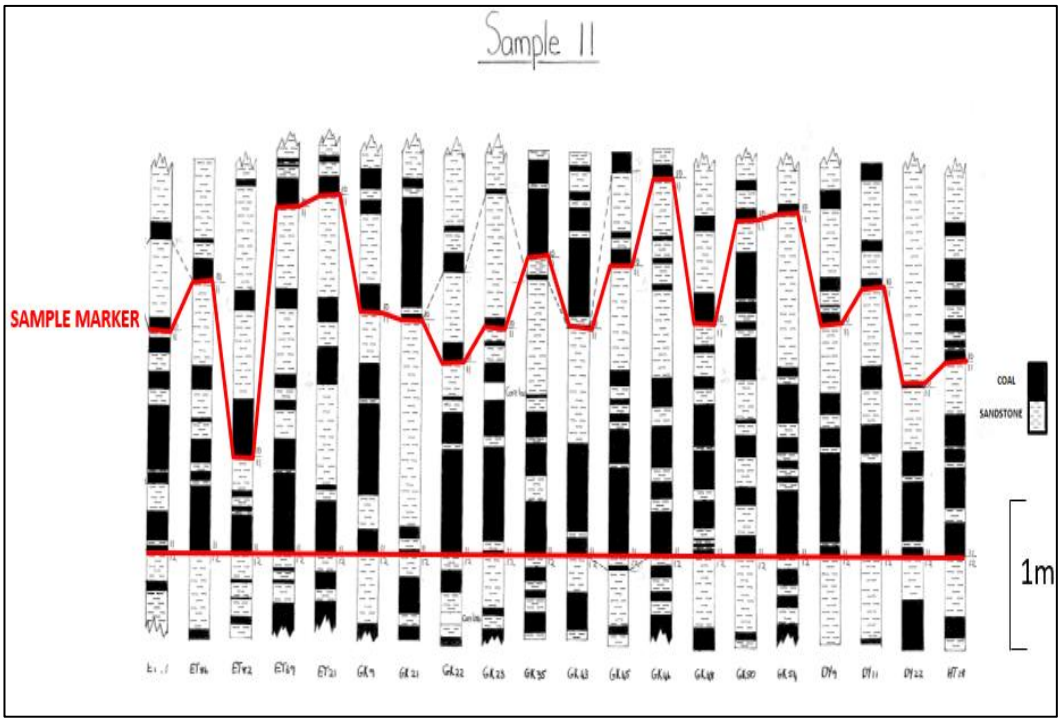

Figure A 13: Sample 11

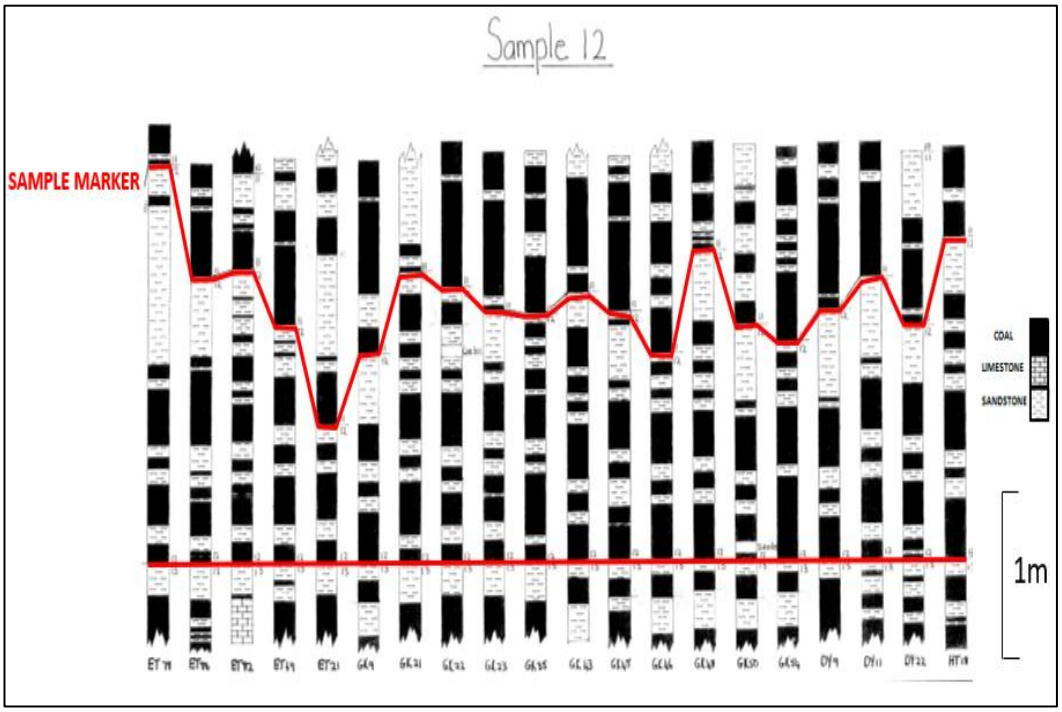

Figure A 14: Sample 12

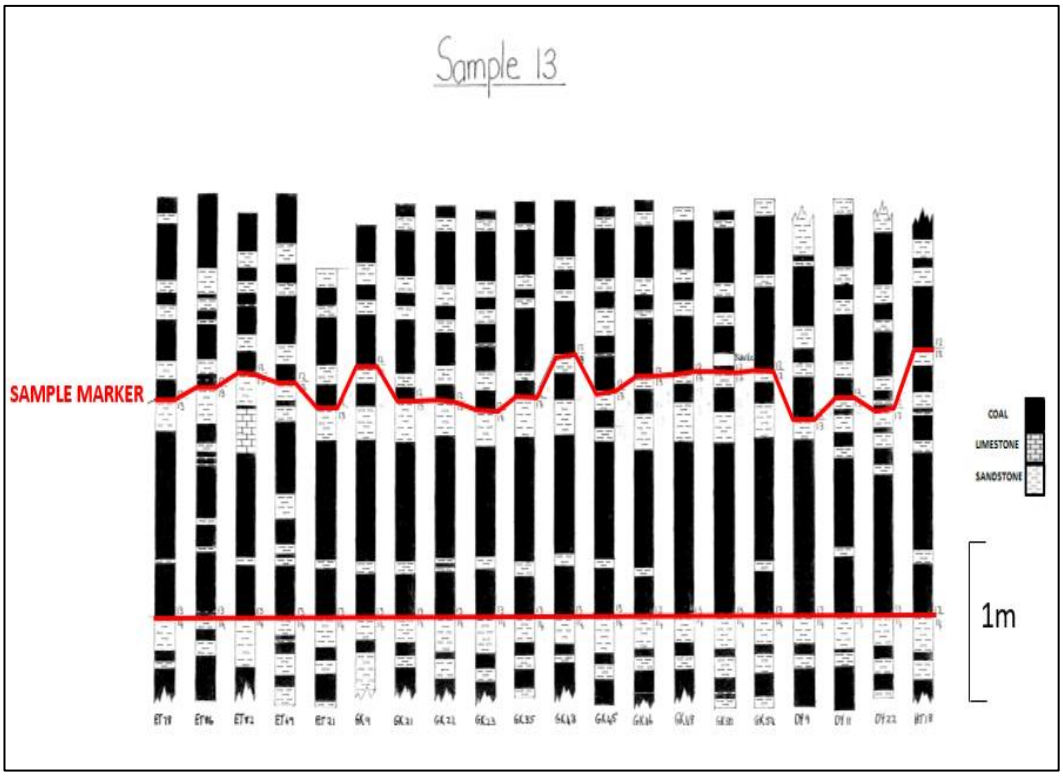

Figure A 15: Sample 13

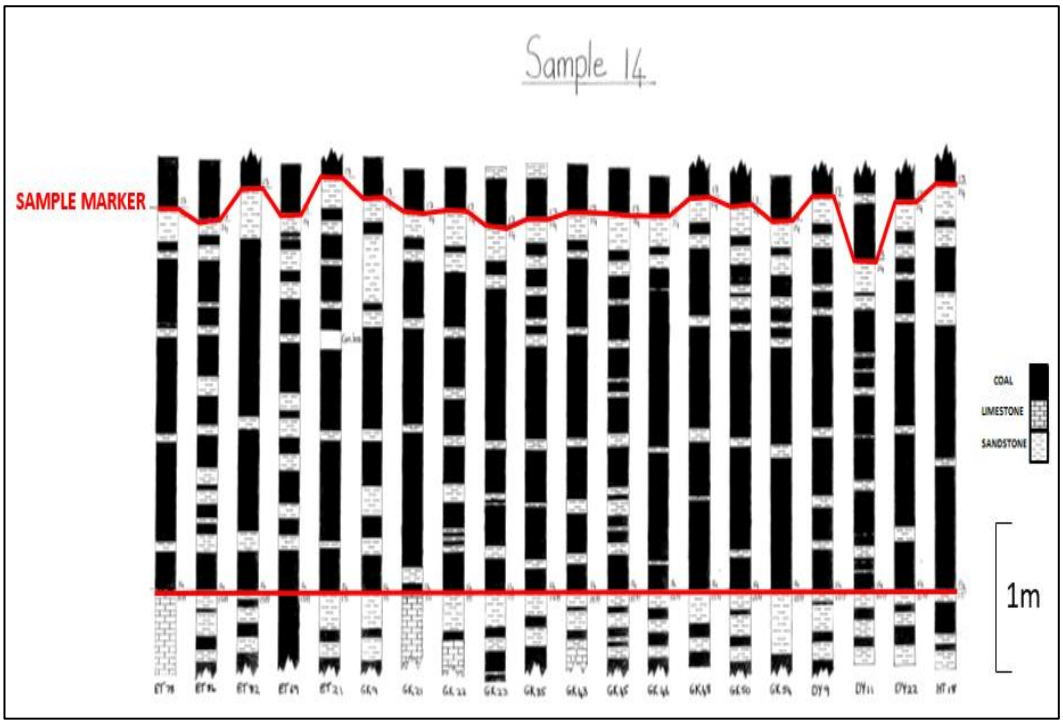

Figure A 16: Sample 14

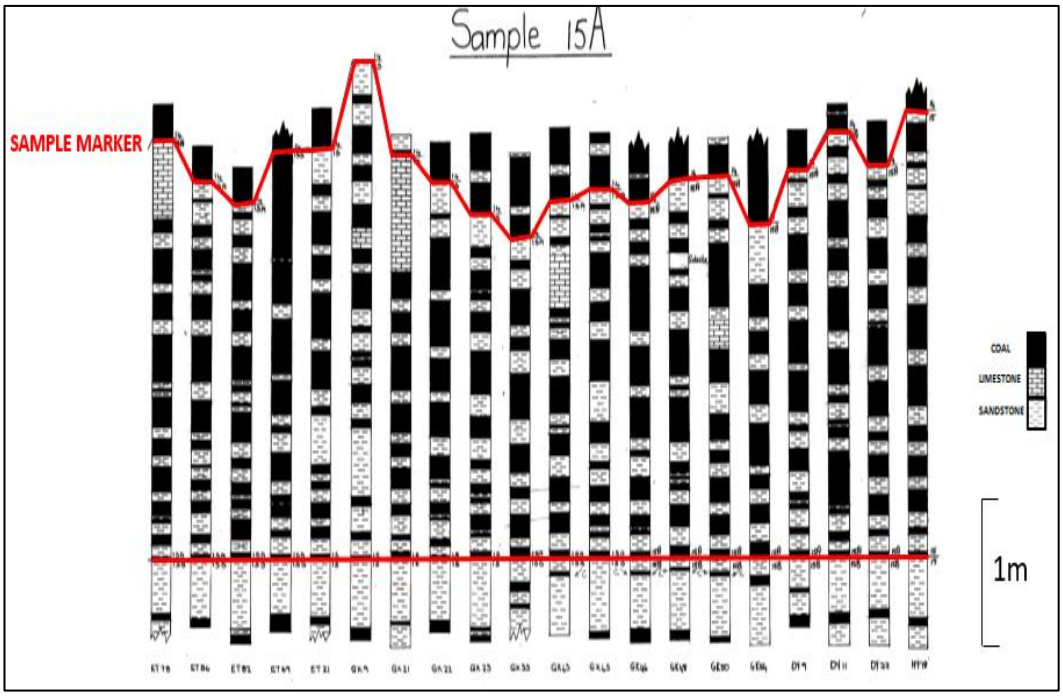

Figure A 17: Sample 15A

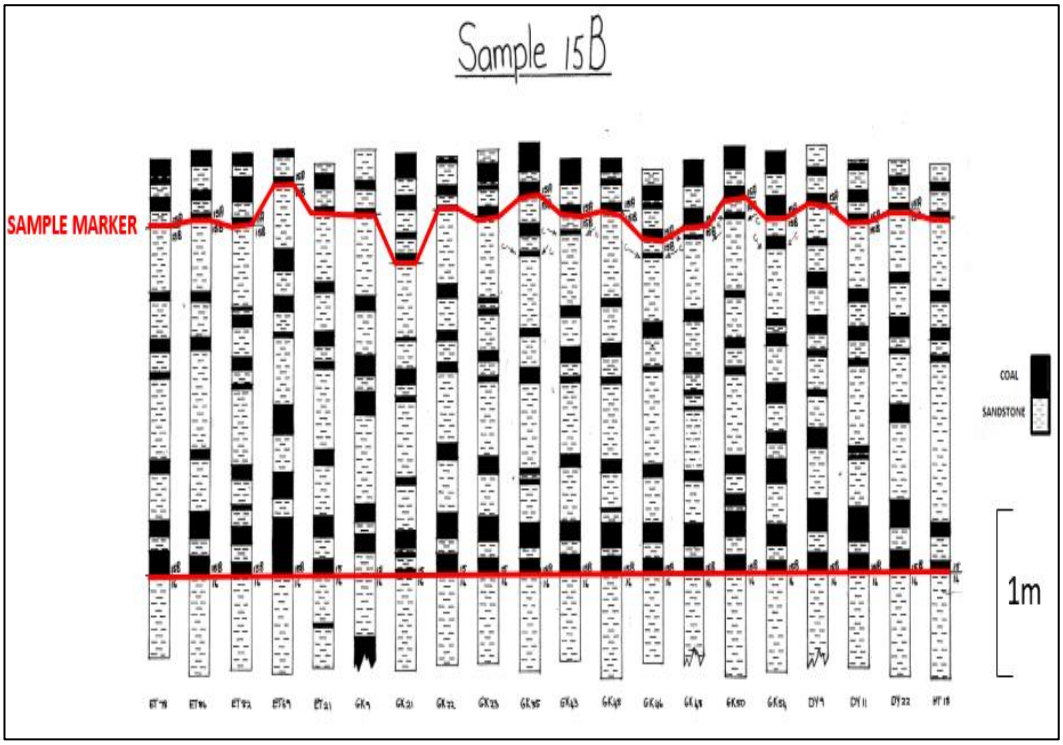

Figure A 18: Sample 15B

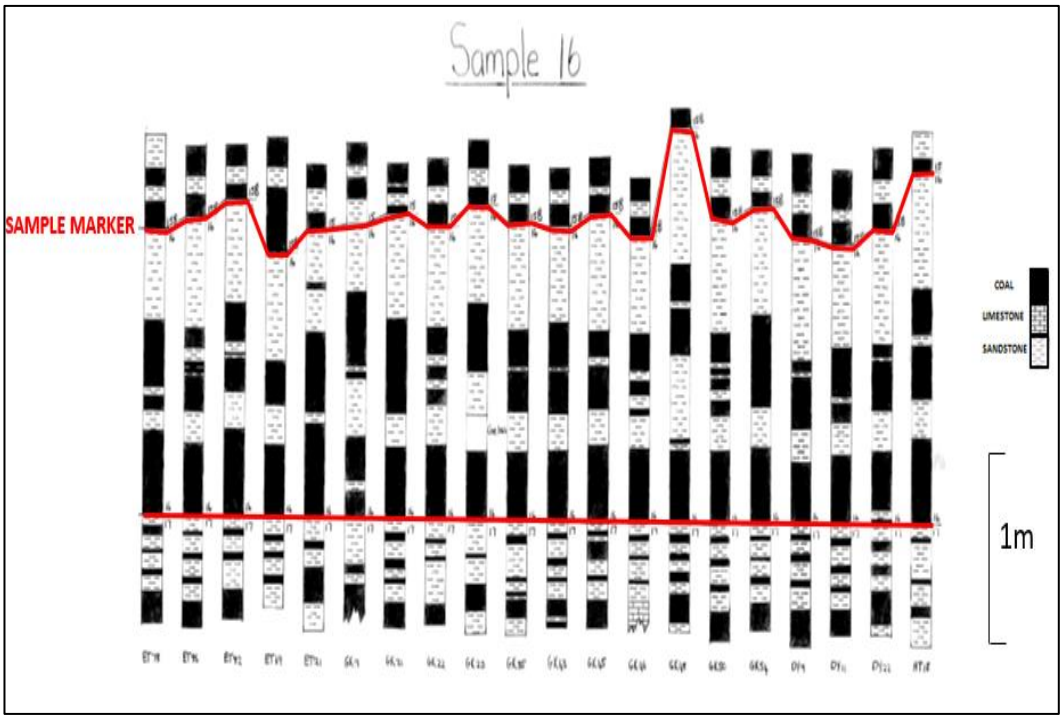

Figure A 19: Sample 16

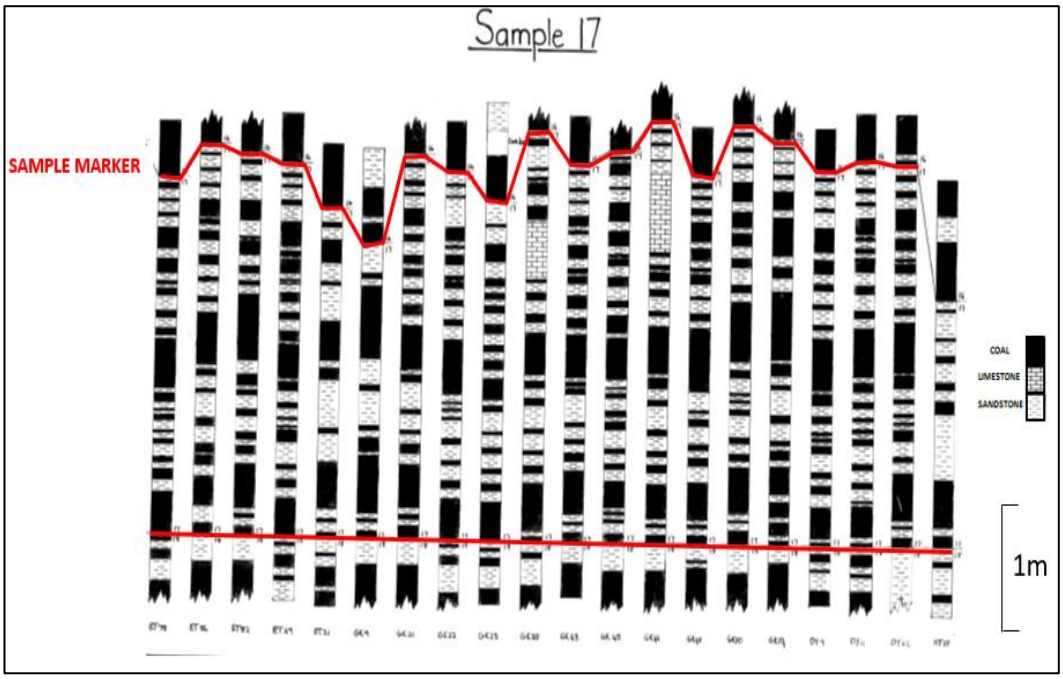

Figure A 20: Sample 17

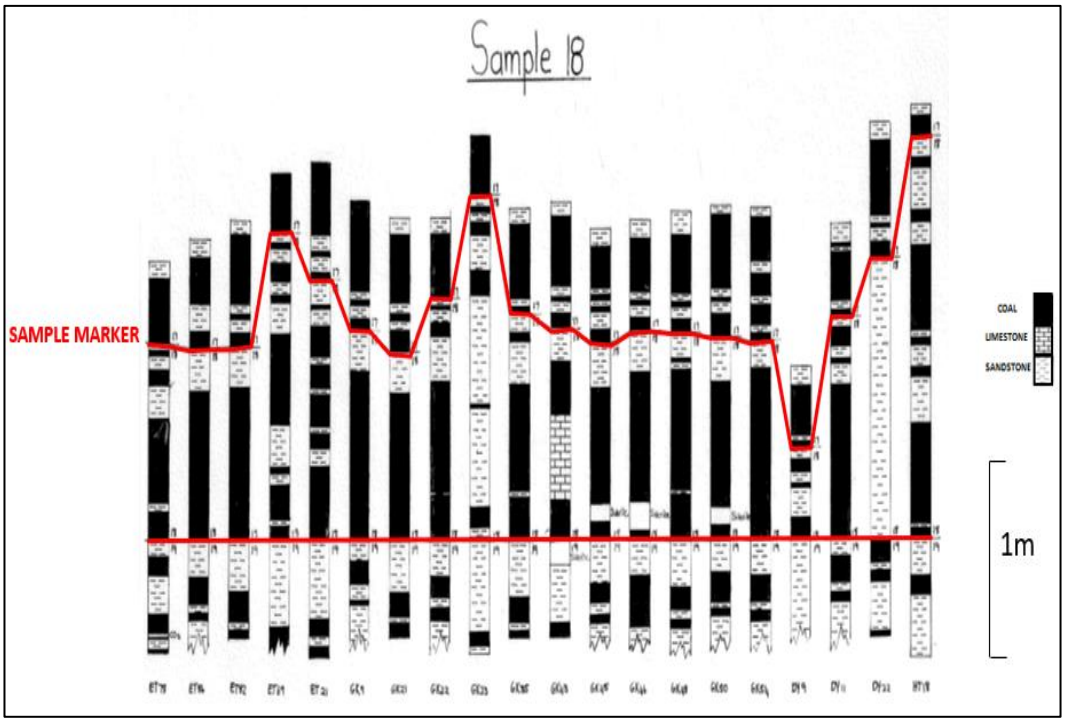

Figure A 21: Sample 18

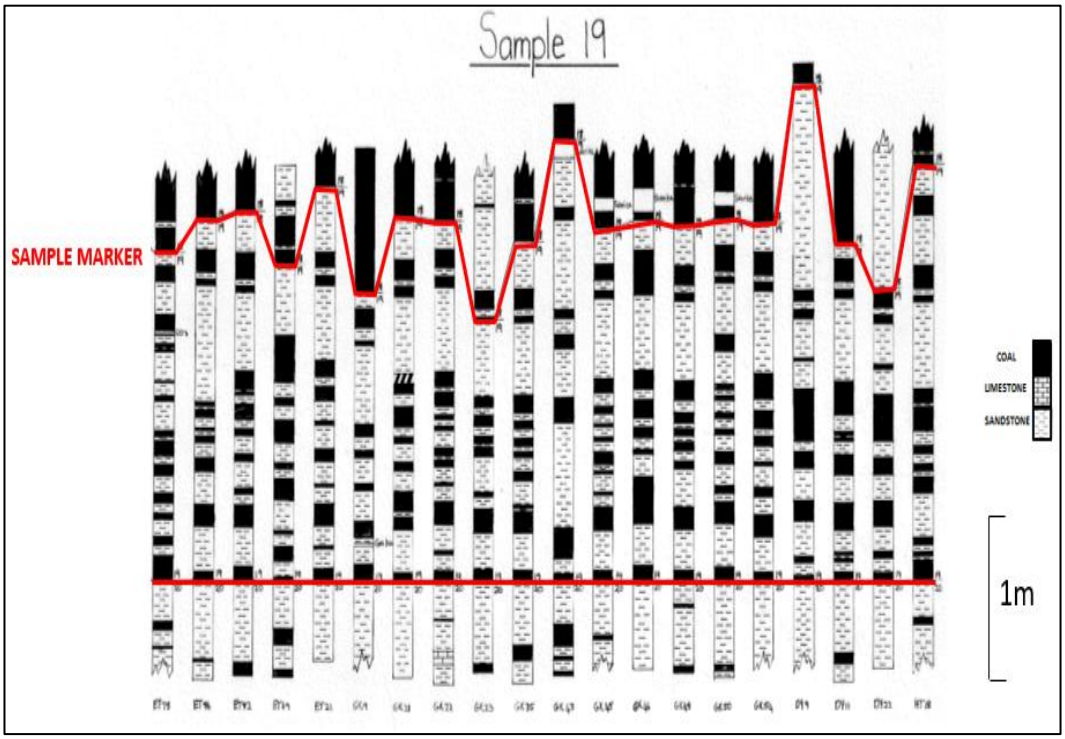

Figure A 22: Sample 19

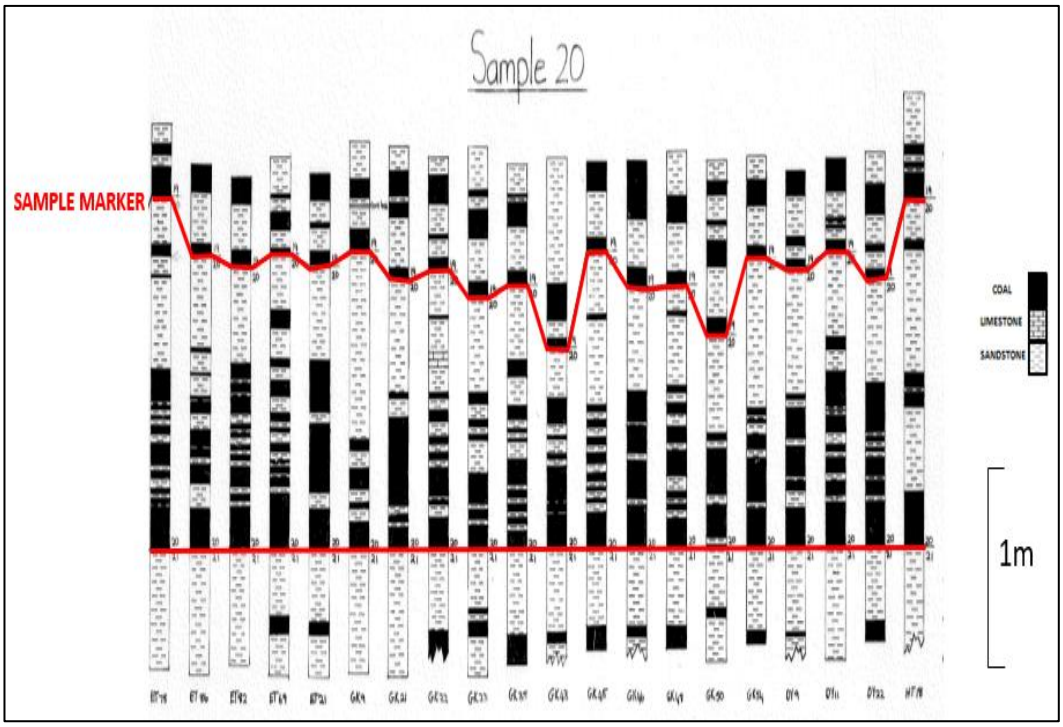

Figure A 23: Sample 20

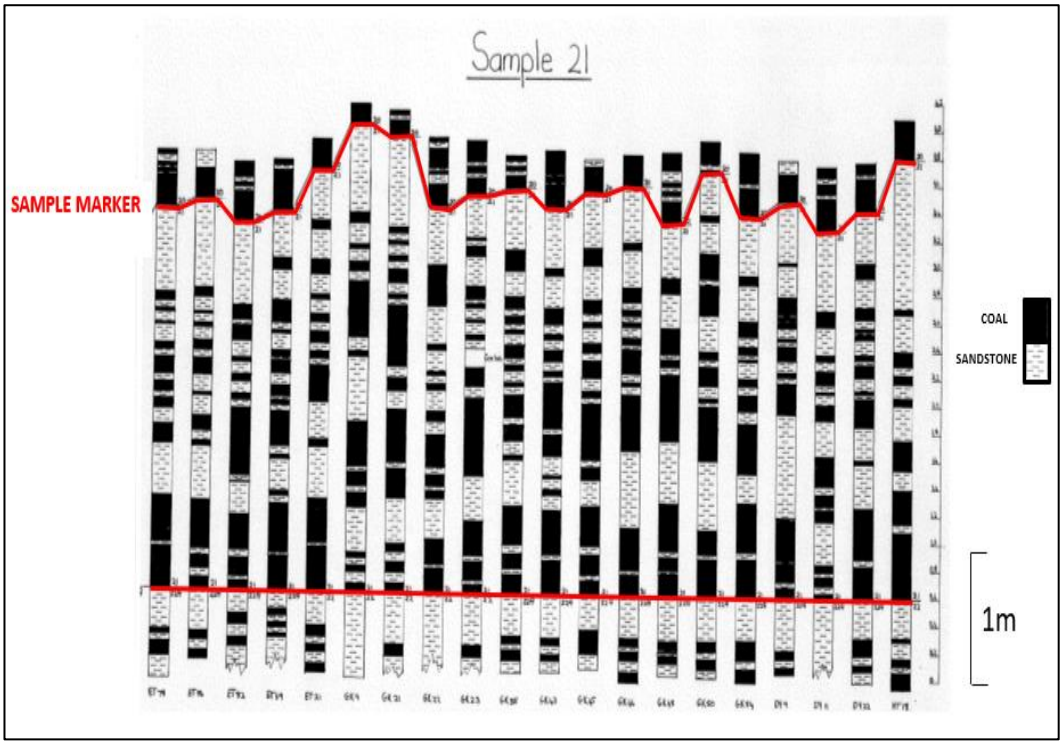

Figure A 24: Sample 21

APPENDIX B: RAW QUALITY DISTRIBUTION PLANS

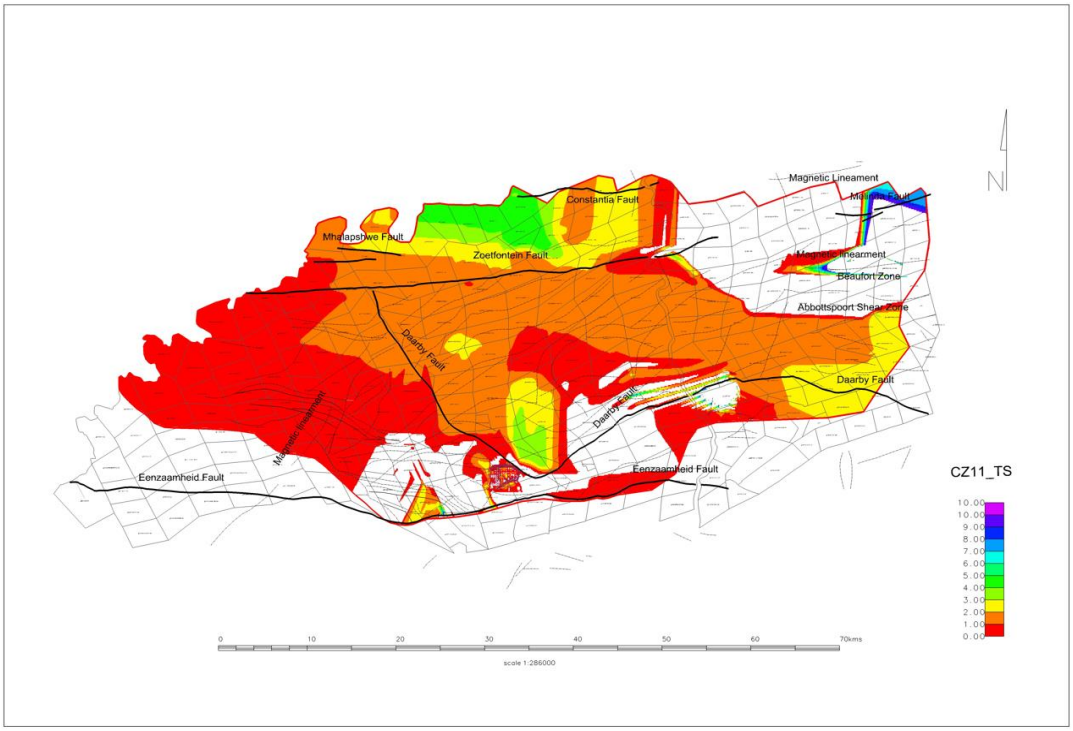

Figure B 1: CZ11_Total Sulphur (TS)

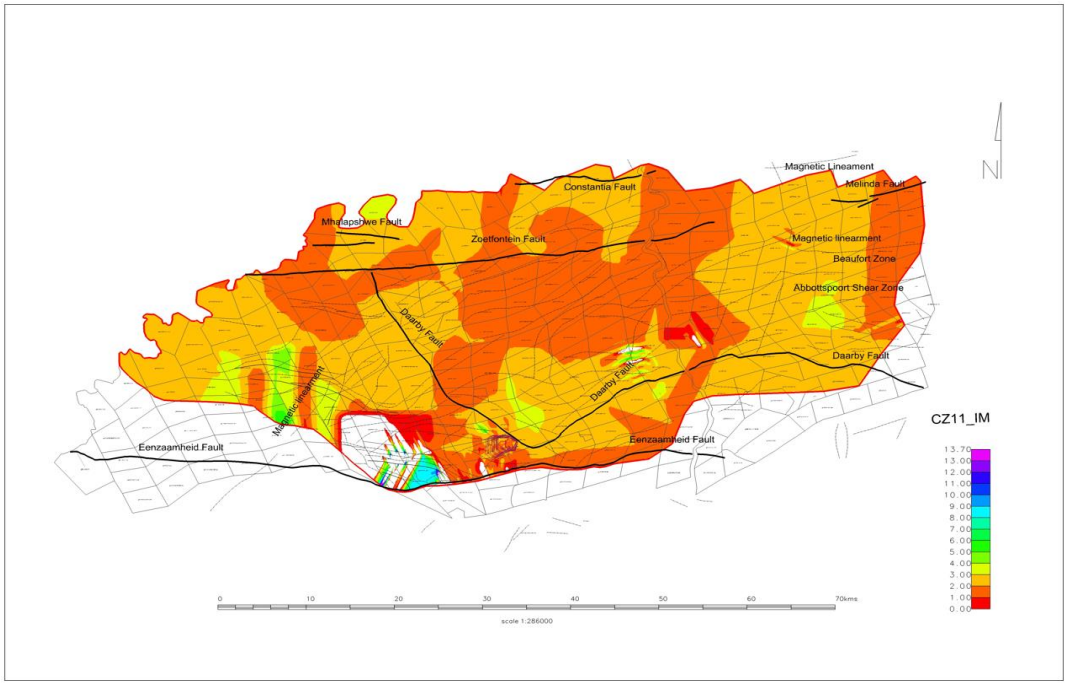

Figure B 2: CZ11_Inherent Moisture (IM)

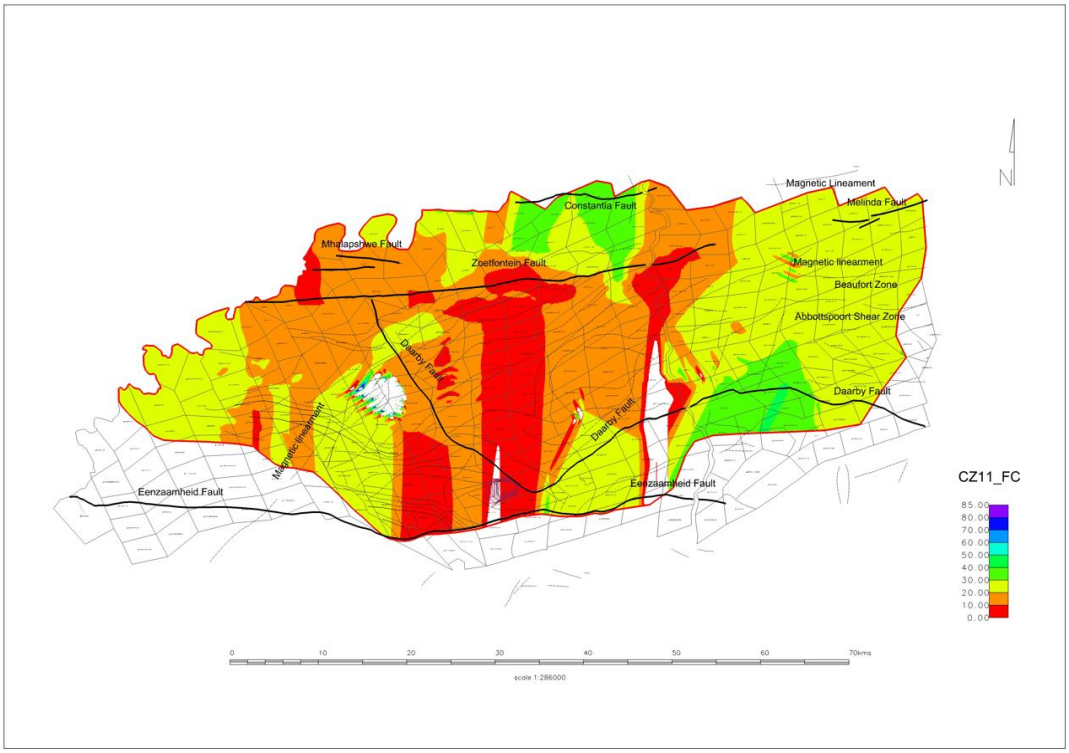

Figure B 3: CZ11_Fixed Carbon (FC)

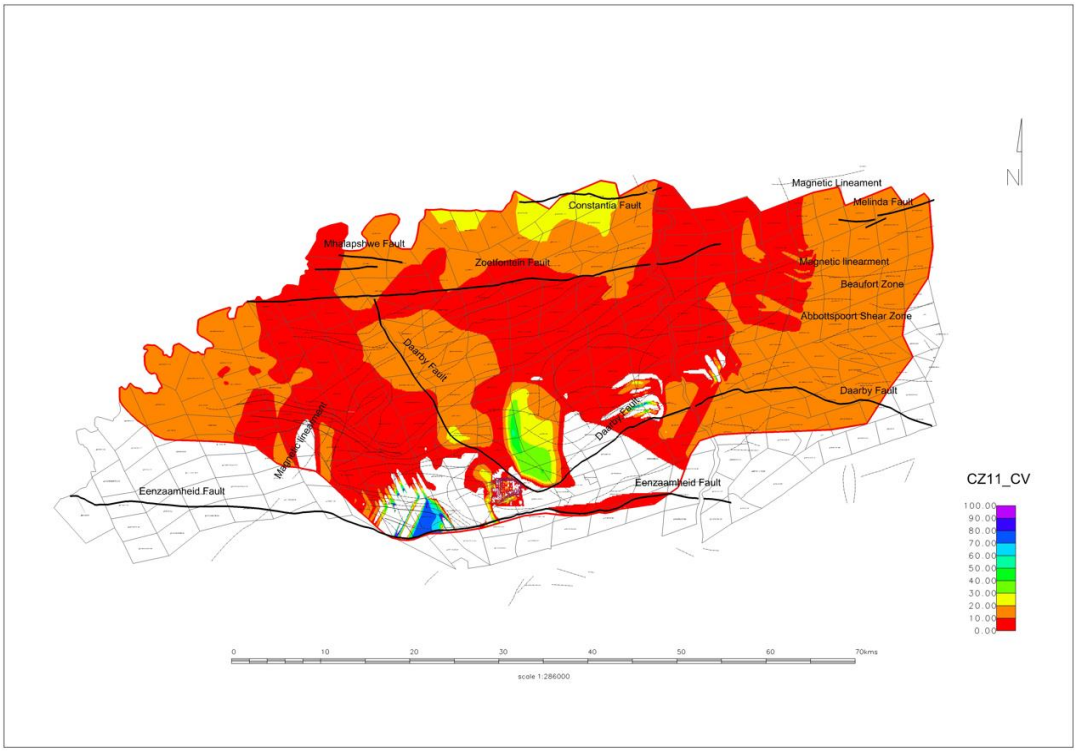

Figure B 4: CZ11_Calorific Value (CV)

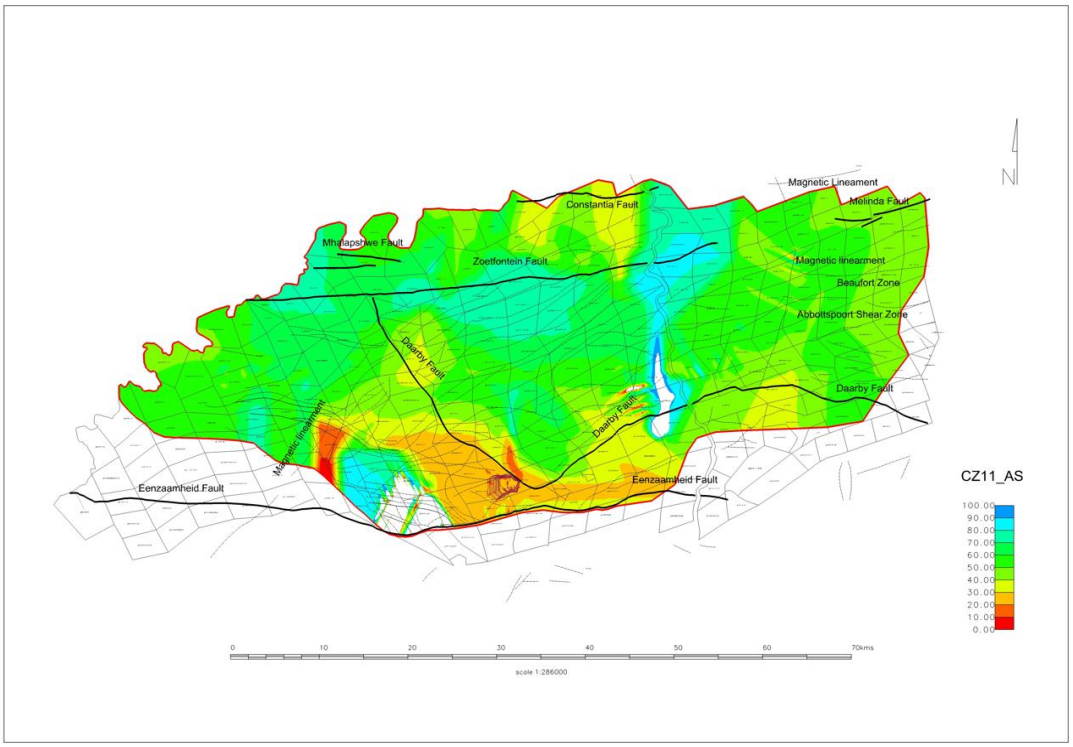

Figure B 5: CZ11_Ash (AS)

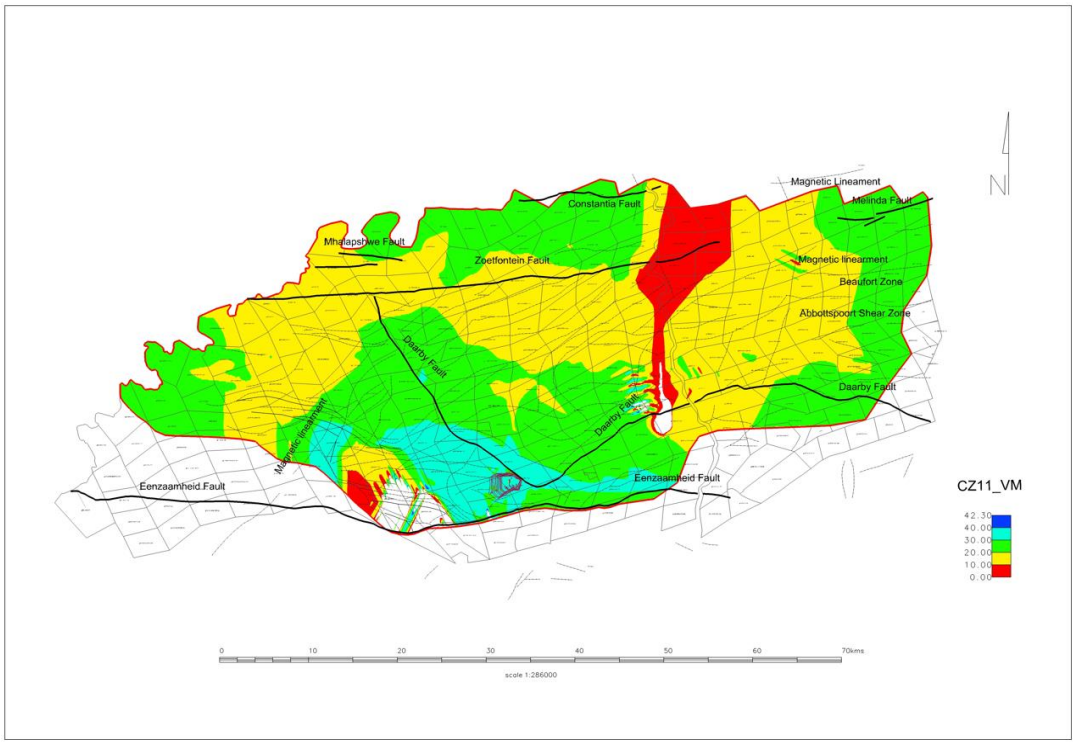

Figure B 6: CZ11_Volatile Matter (VM)

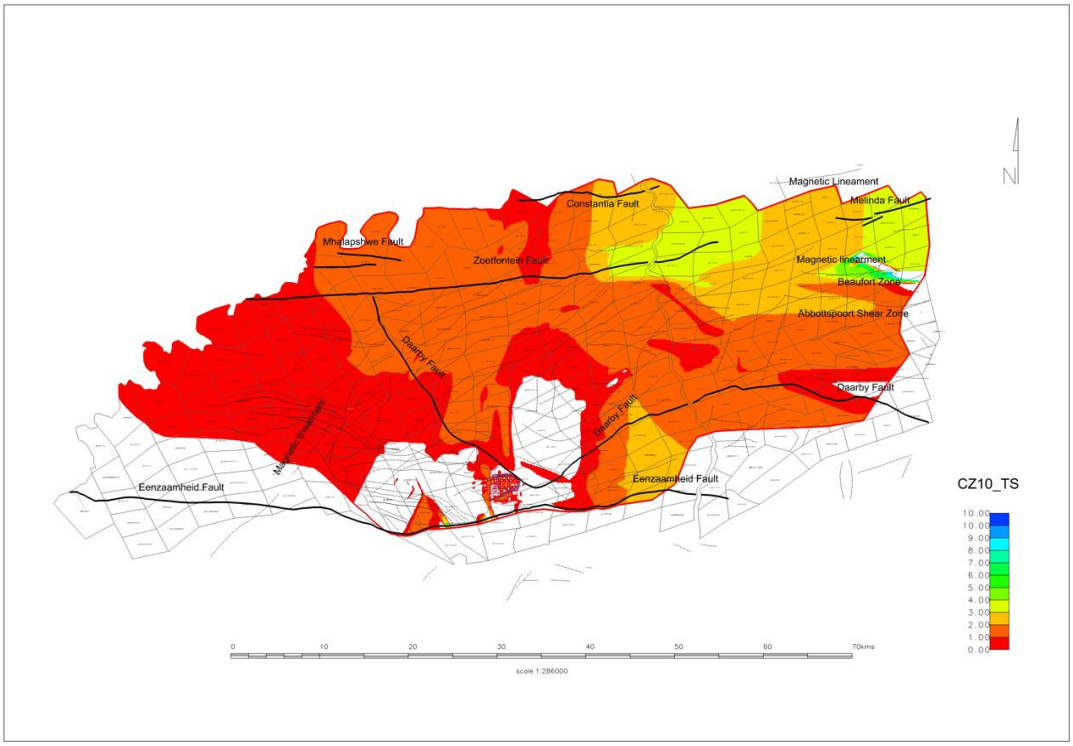

Figure B 7: CZ10_Total Sulphur (TS)

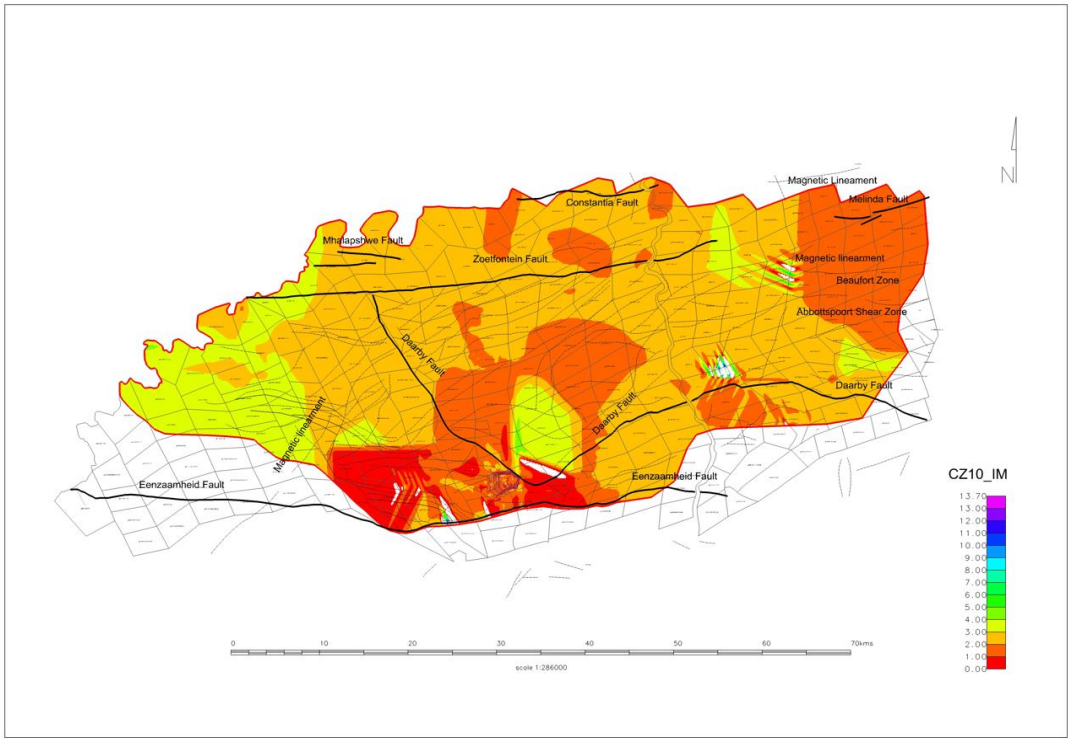

Figure B 8: CZ10_Inherent Moisture (IM)

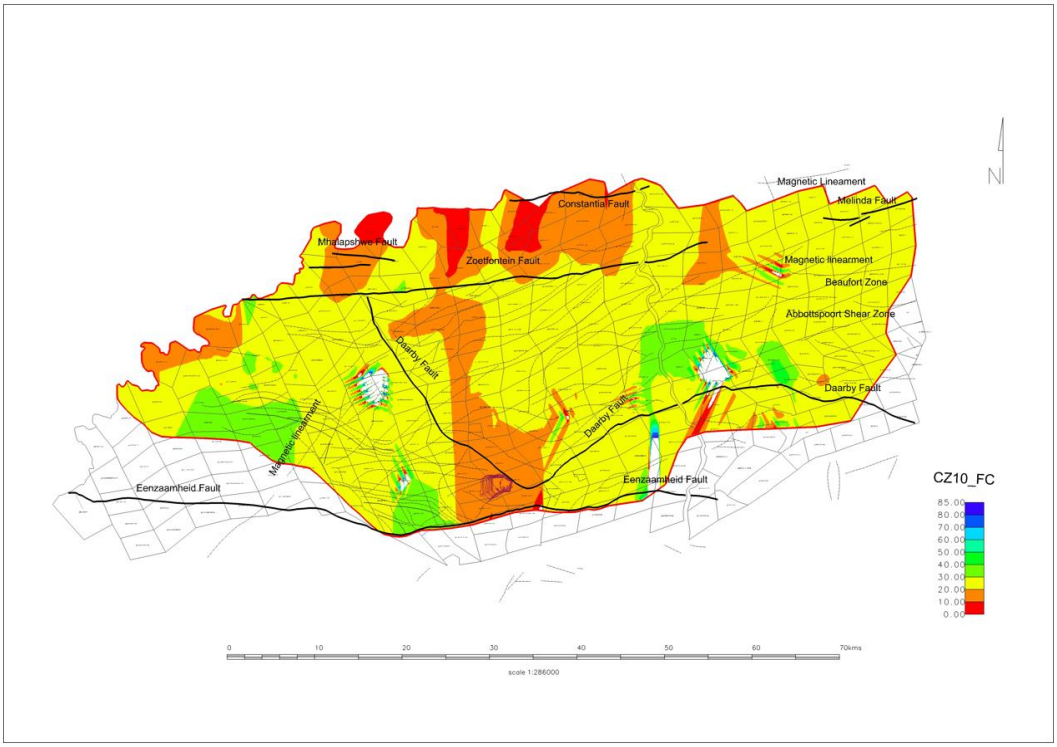

Figure B 9: CZ10_Fixed Carbon (FC)

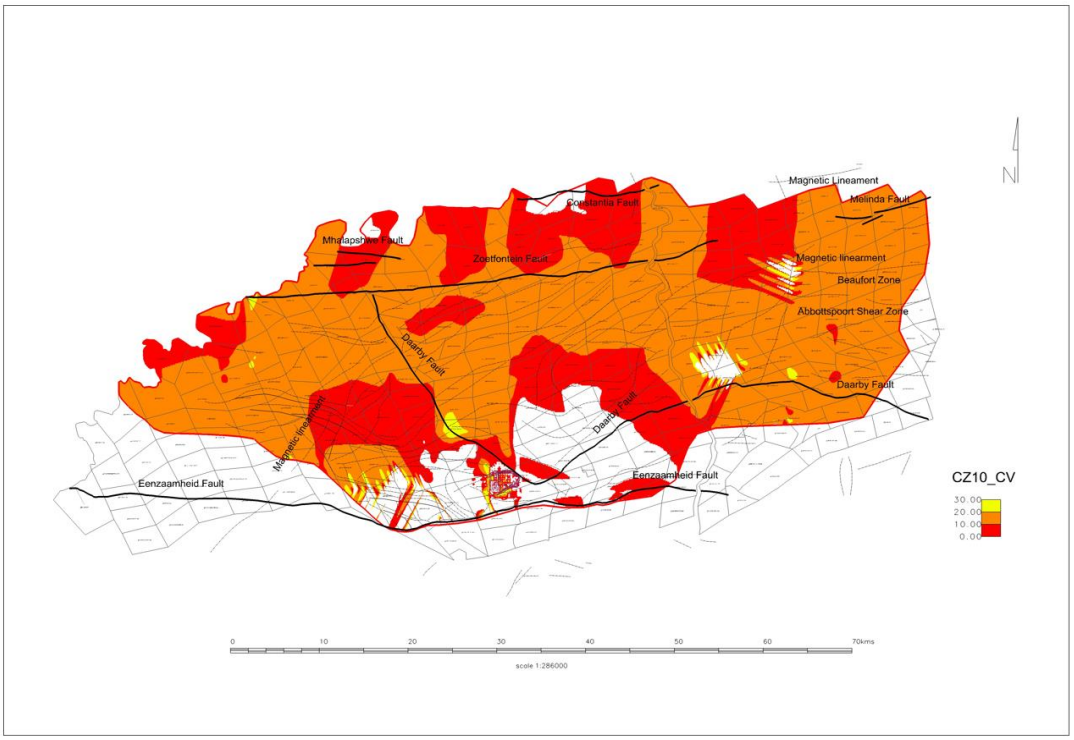

Figure B 10: CZ10_Calorific Value (CV)

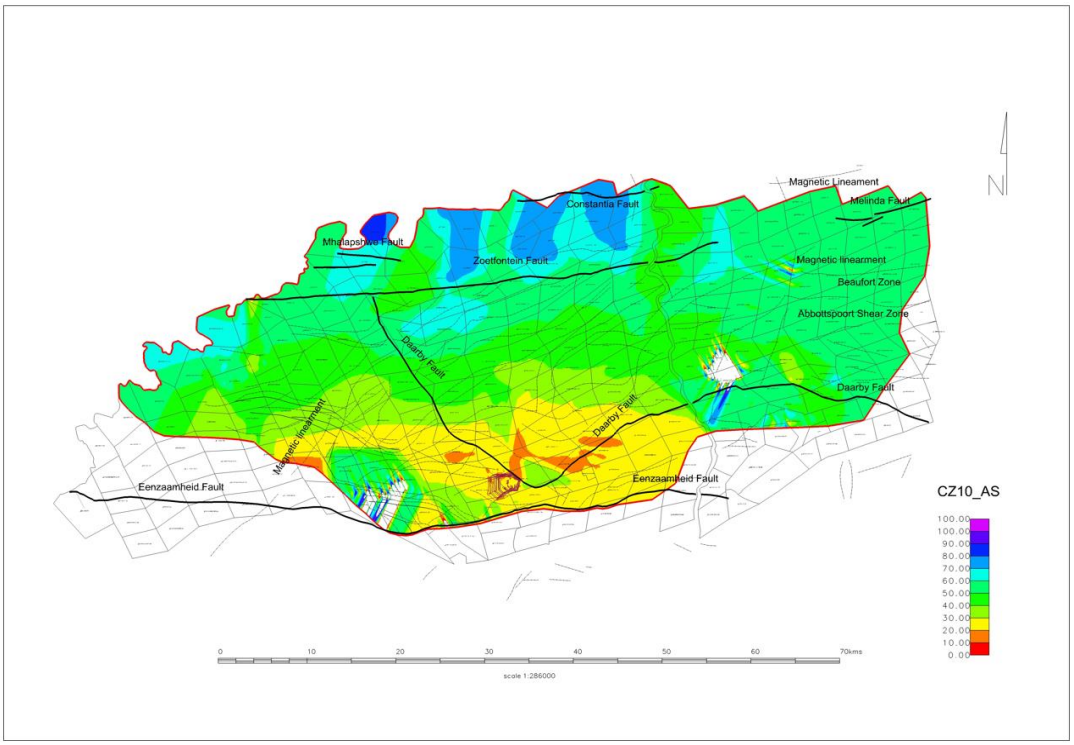

Figure B 11: CZ10_Ash (AS)

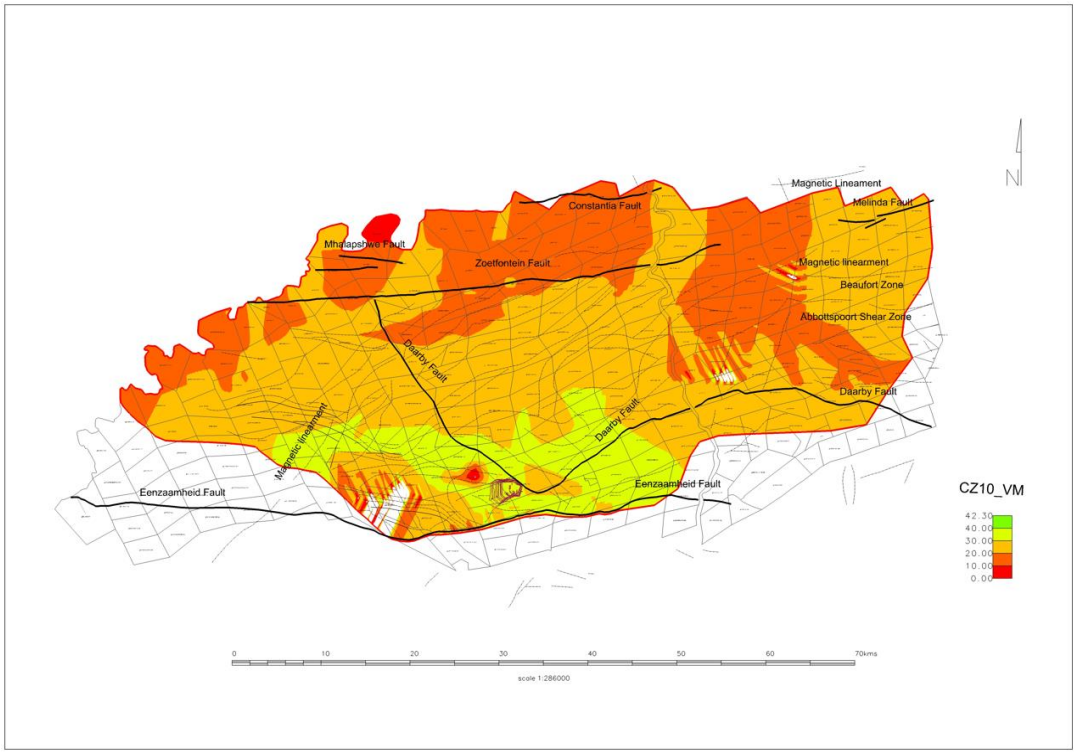

Figure B 12: CZ10_Volatile Matter (VM)

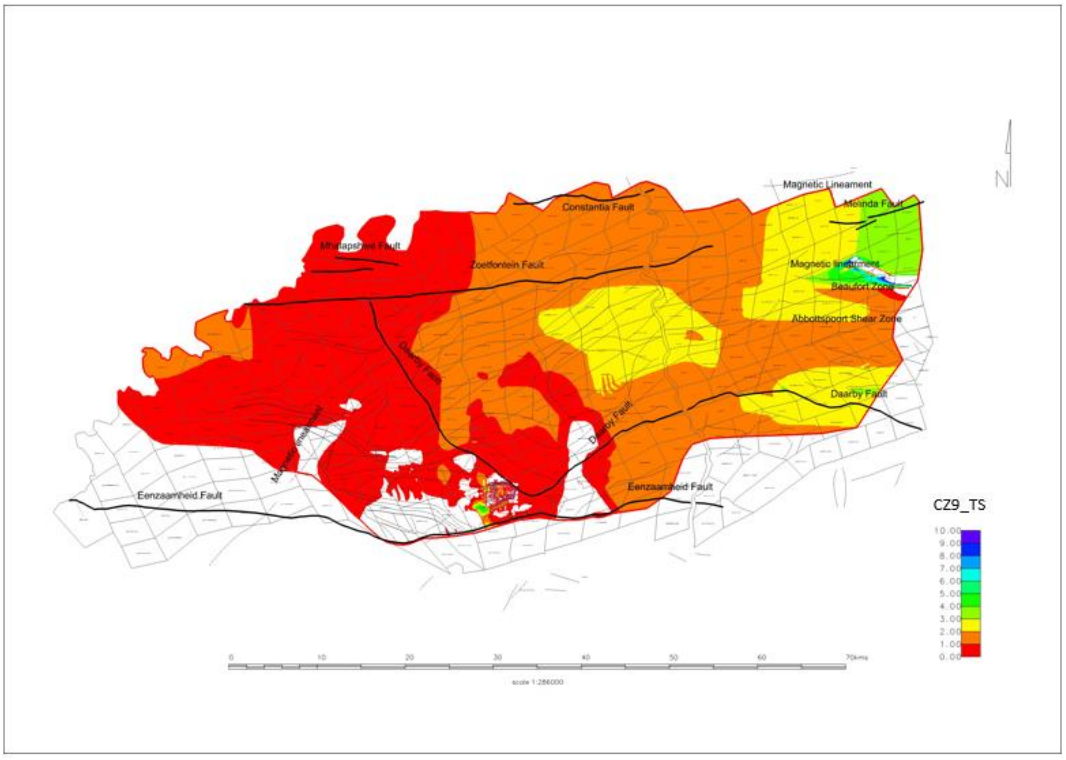

Figure B 13: CZ9_Total Sulphur (TS)

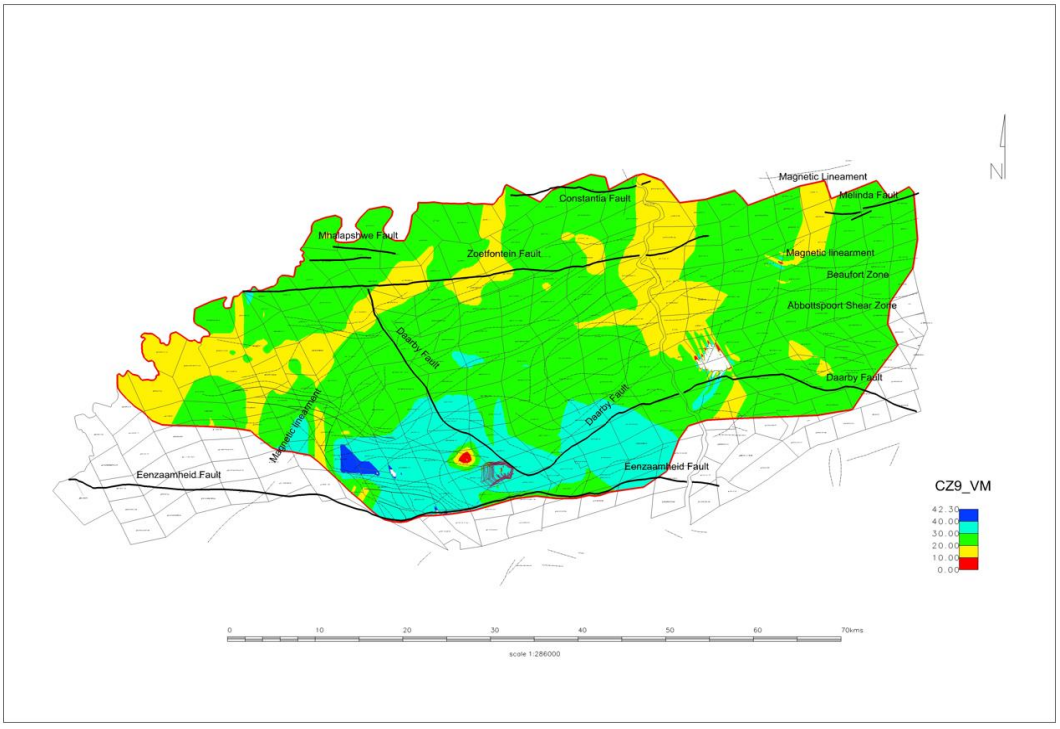

Figure B 14: CZ9_Volatile Matter (VM)

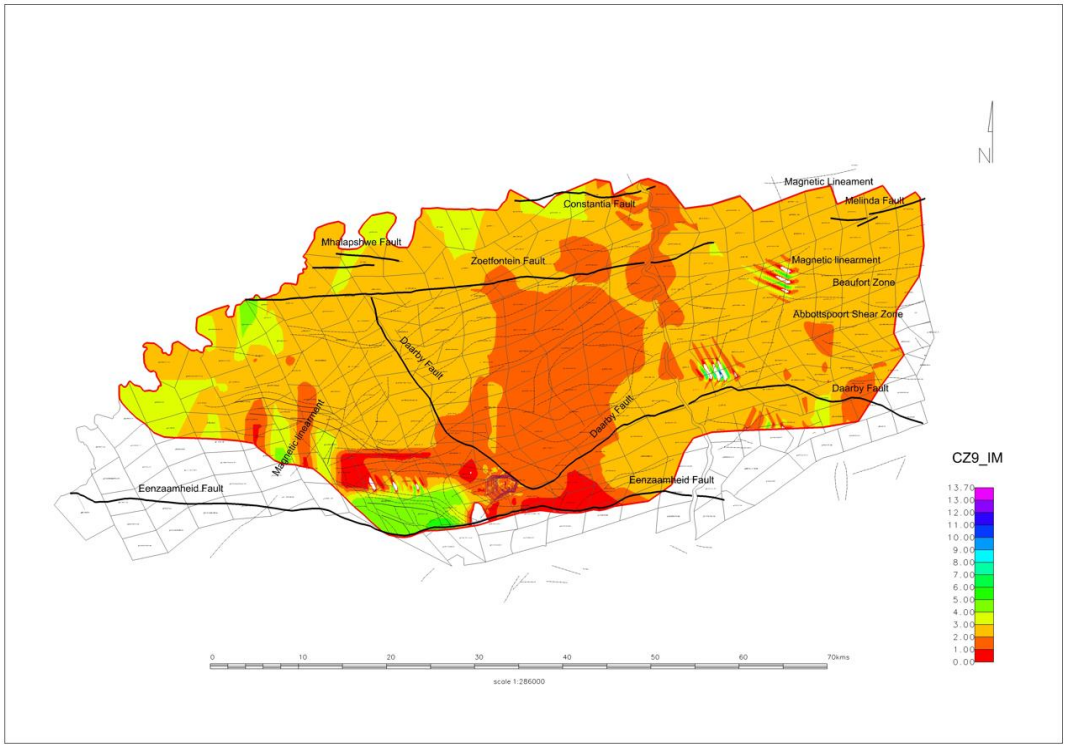

Figure B 15: CZ9_Inherent Moisture (IM)

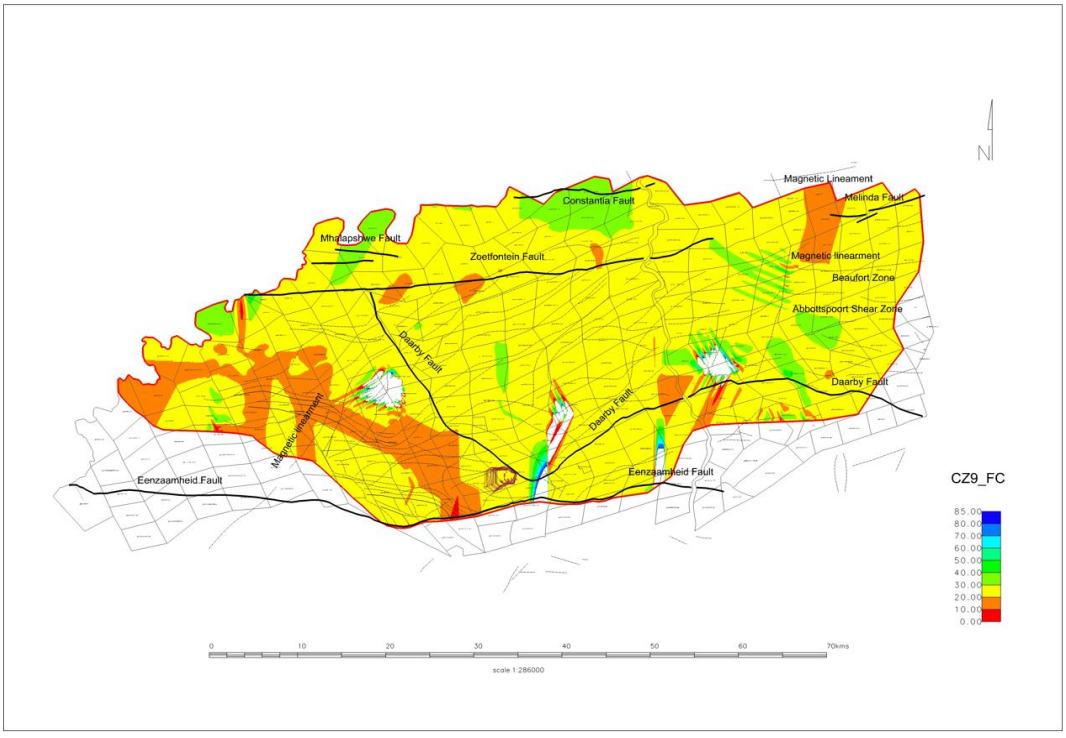

Figure B 16: CZ9_Fixed Carbon (FC)

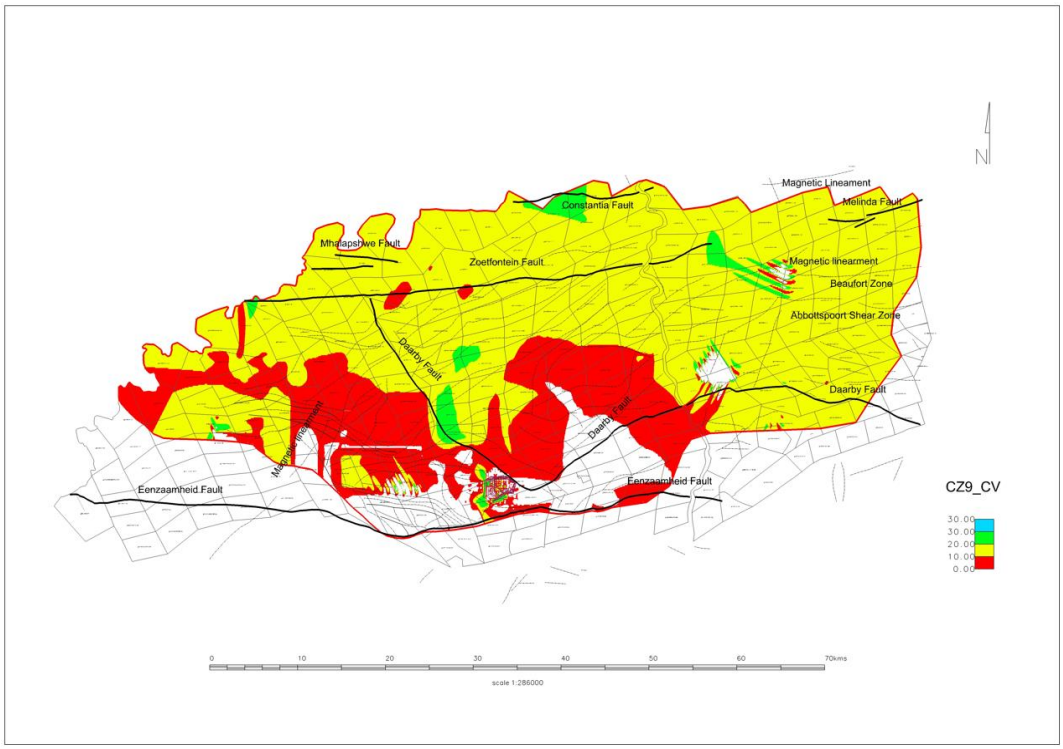

Figure B 17: CZ9_Calorific Value (CV)

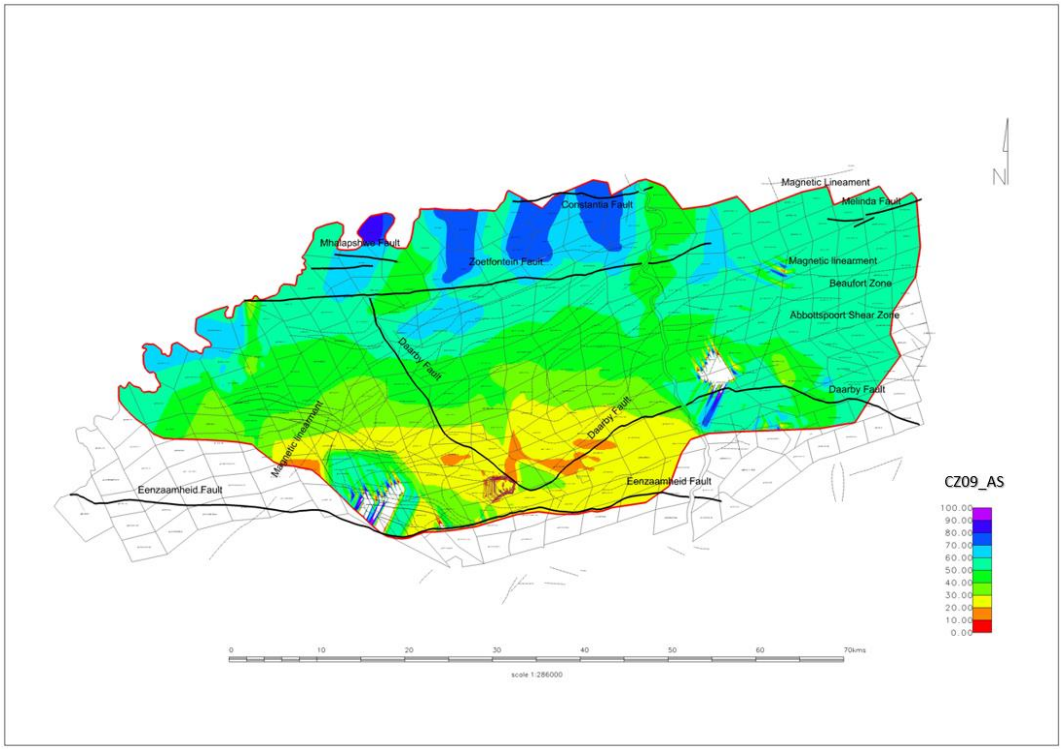

Figure B 18: CZ9_Ash (AS)

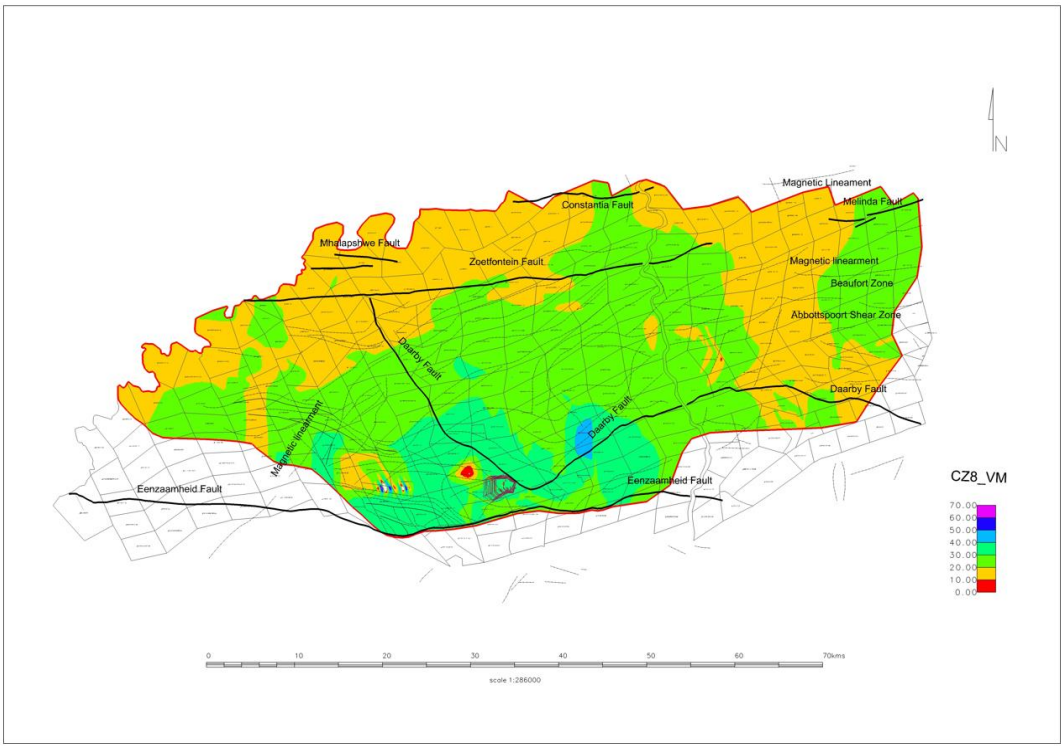

Figure B 19: CZ8_Volatile Matter (VM)



Figure B 20: CZ8_Total Sulphur (TS)

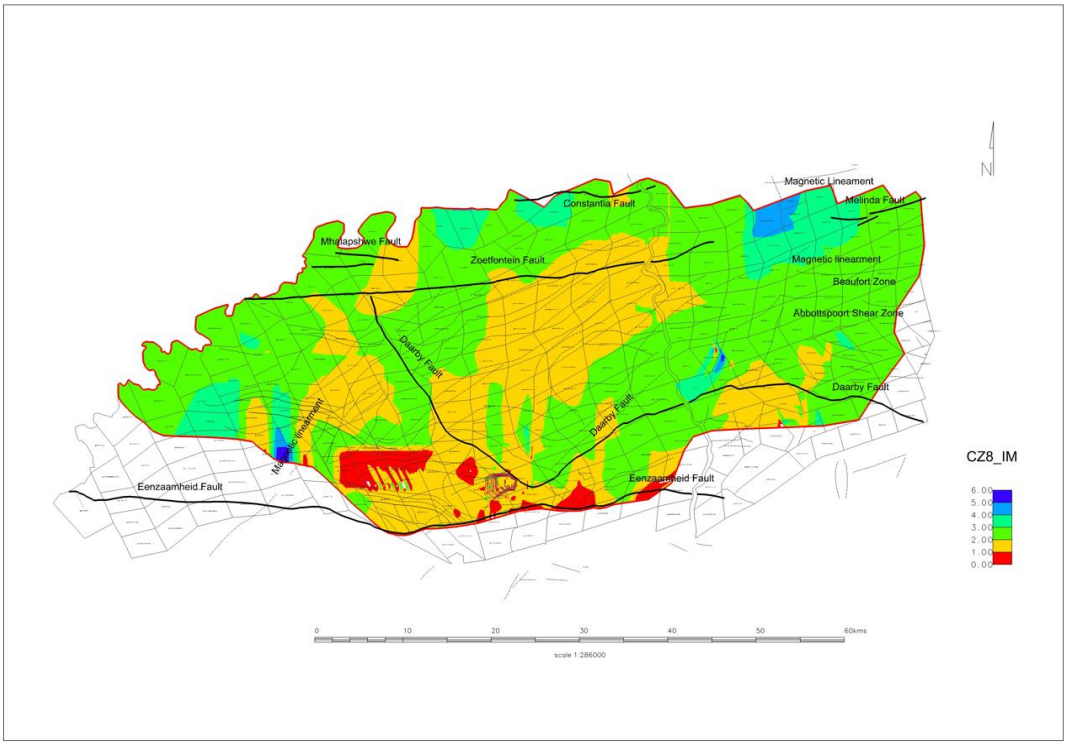

Figure B 21: CZ8_Inherent Moisture (IM)

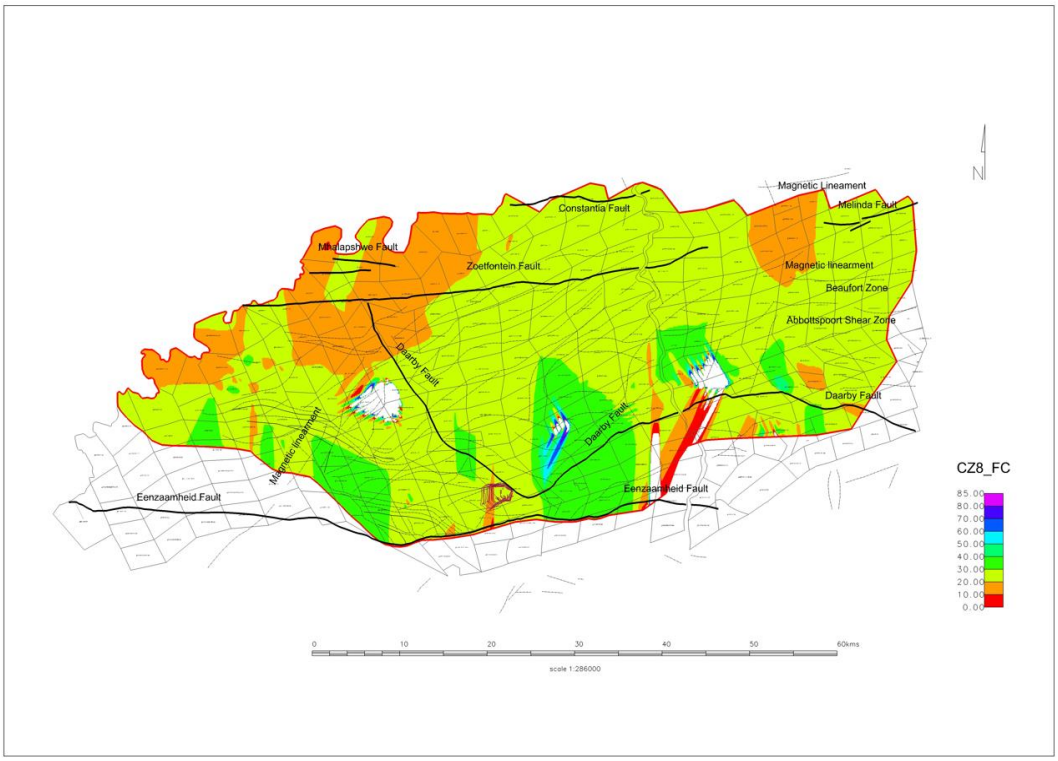

Figure B 22: CZ8_Fixed Carbon (FC)

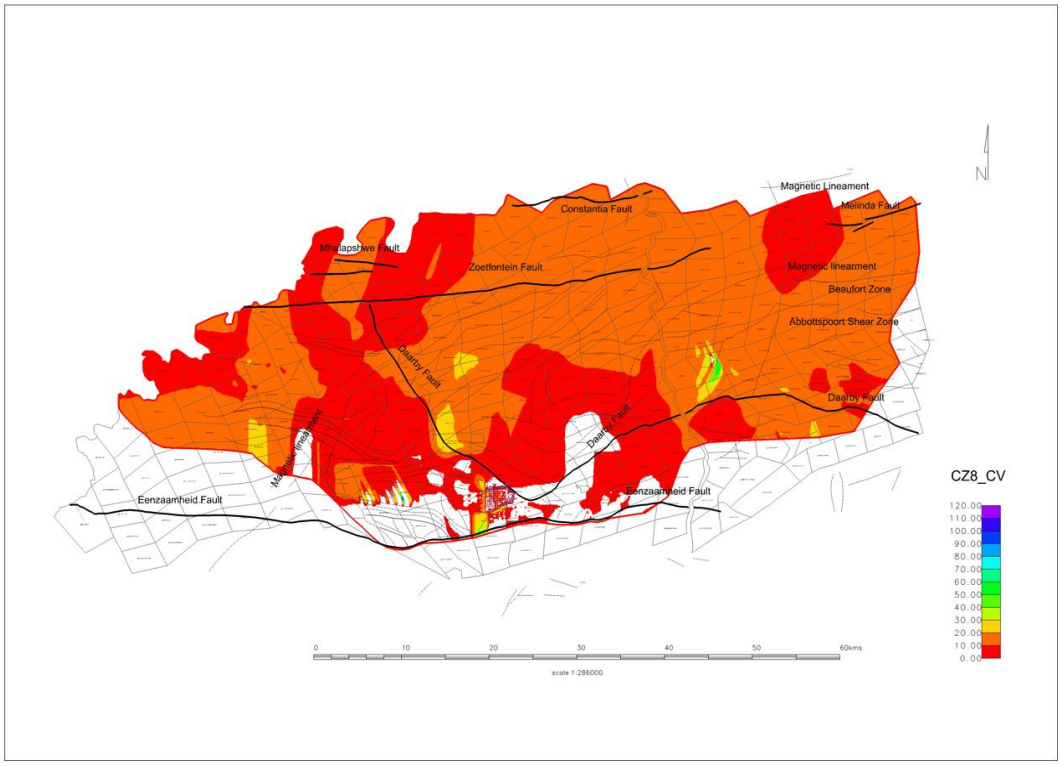

Figure B 23: CZ8_Calorific Value (CV)

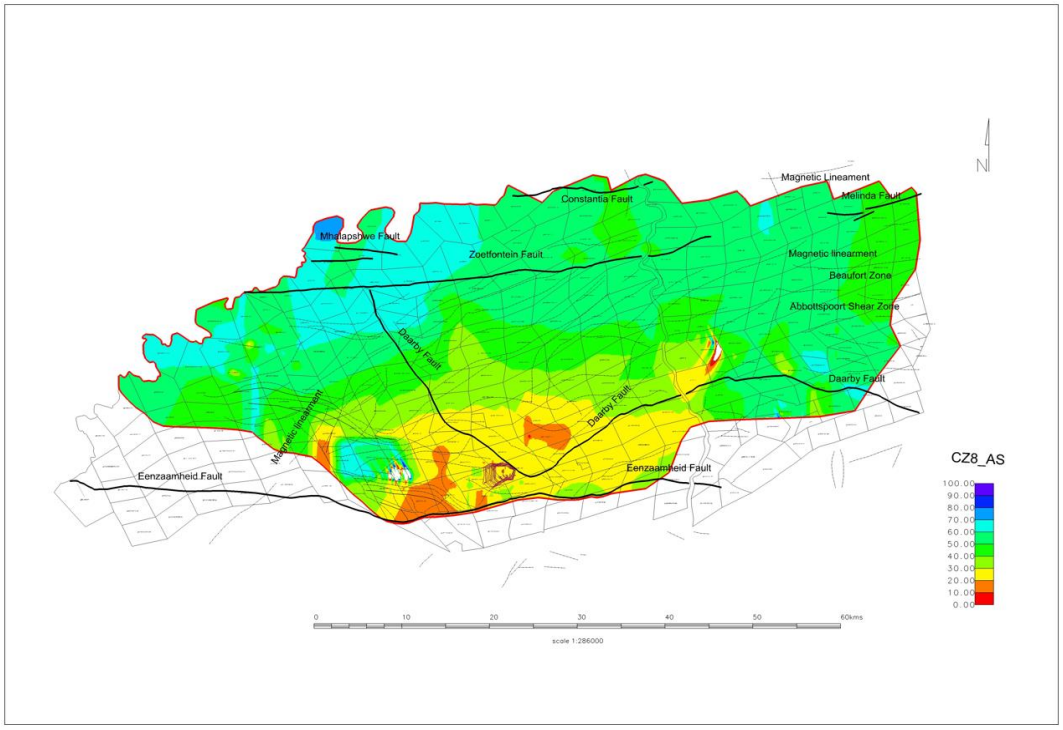

Figure B 24: CZ8_Ash (AS)

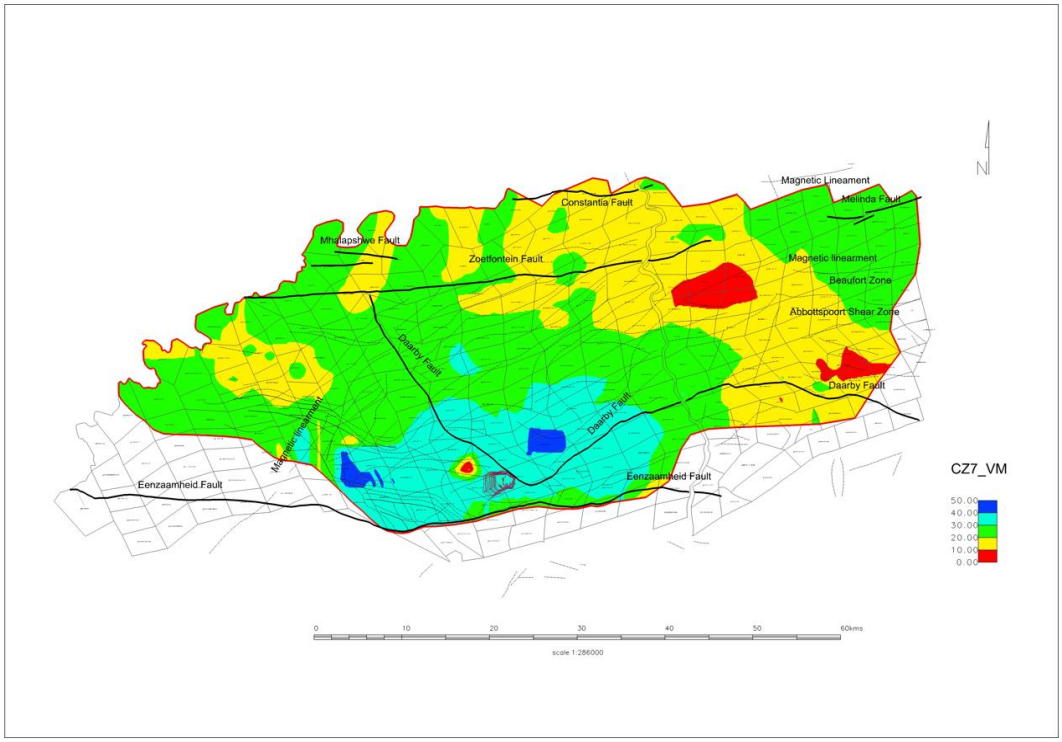

Figure B 25: CZ7_Volatile Matter (VM)

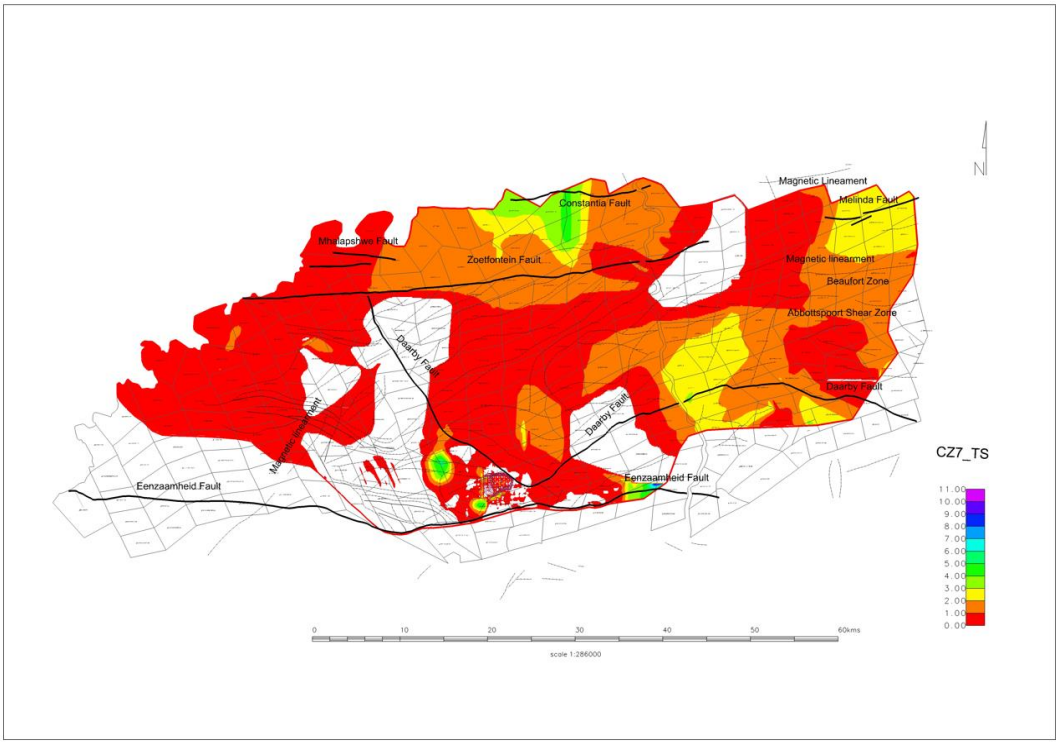

Figure B 26: CZ7_Total Sulphur (TS)

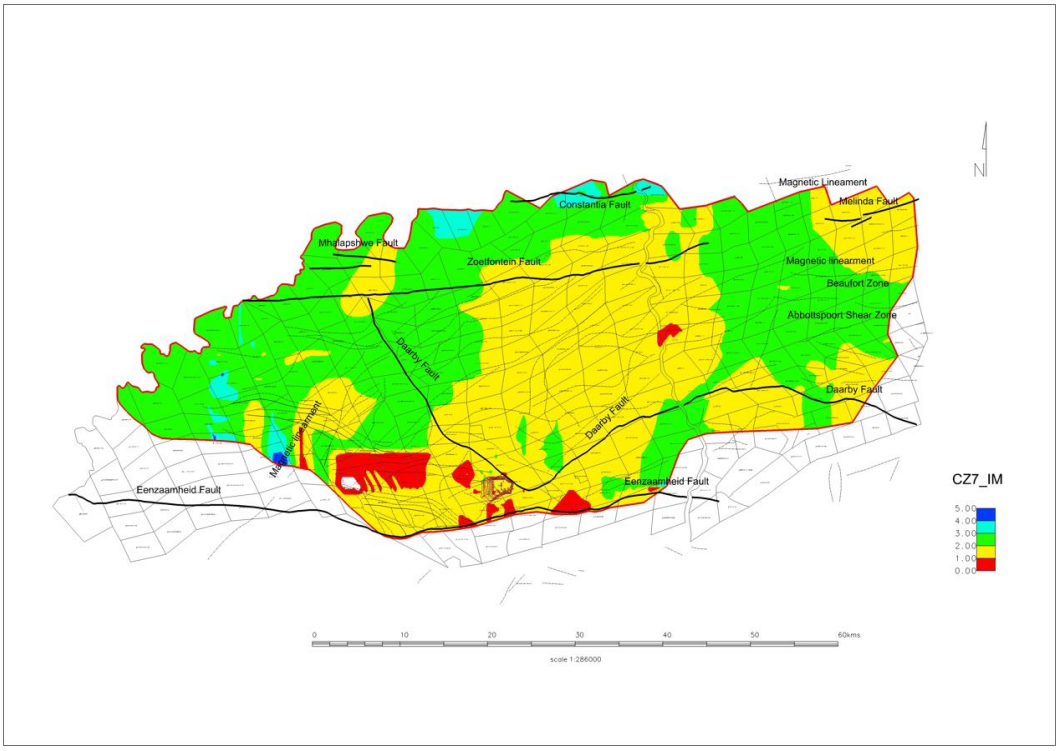

Figure B 27: CZ7_Inherent Moisture (IM)

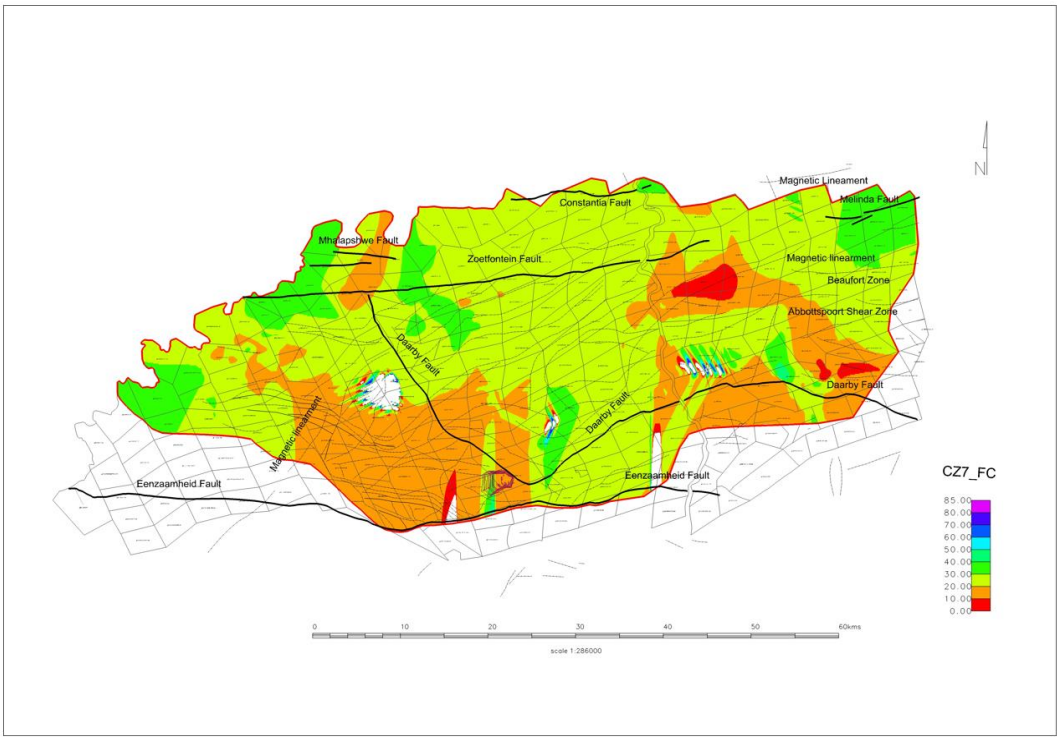

Figure B 28: CZ7_Fixed Carbon (FC)

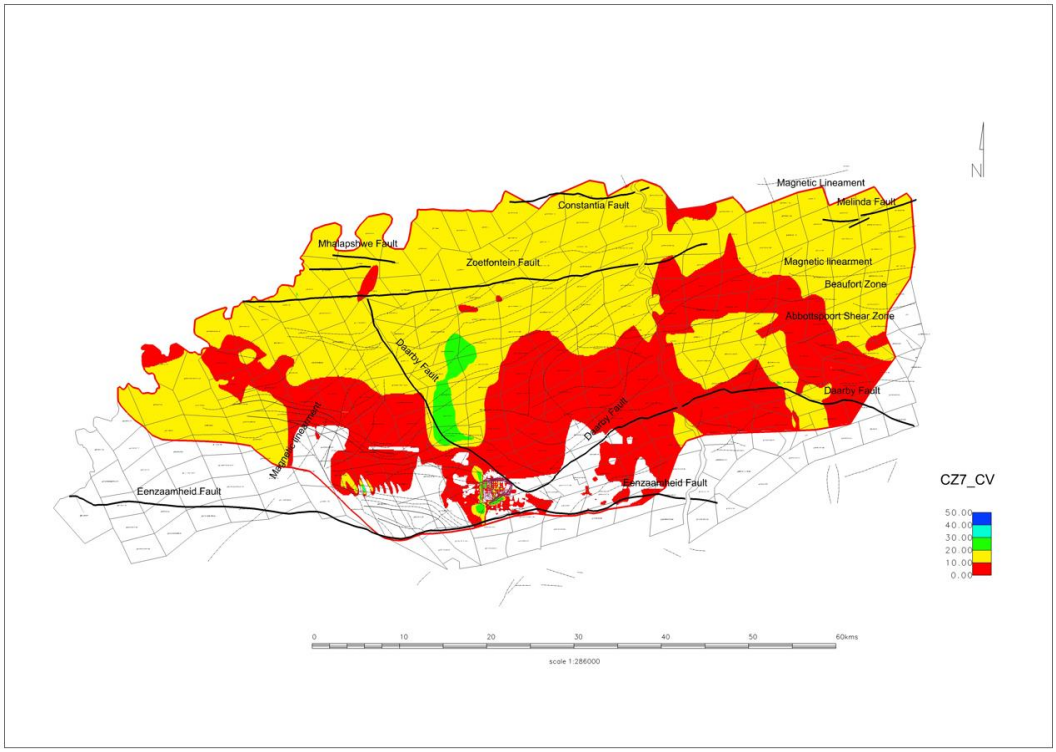

Figure B 29: CZ7_Calorific Value (CV)

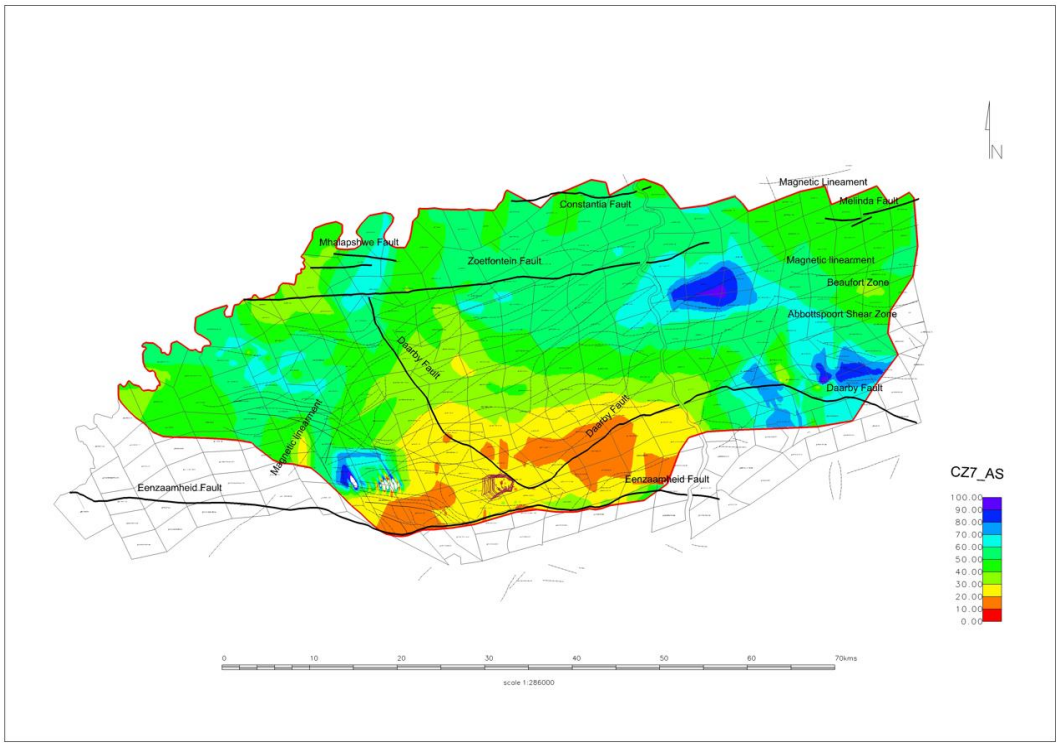

Figure B 30: CZ7_Ash (AS)

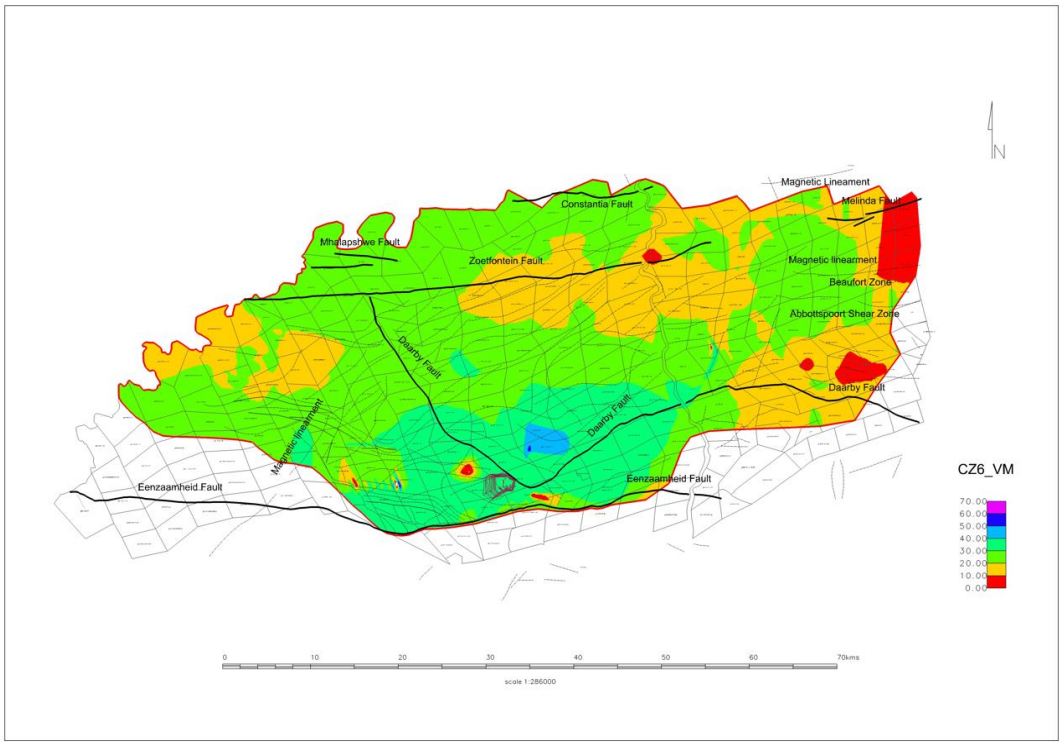

Figure B 31: CZ6_Volatile Matter (VM)

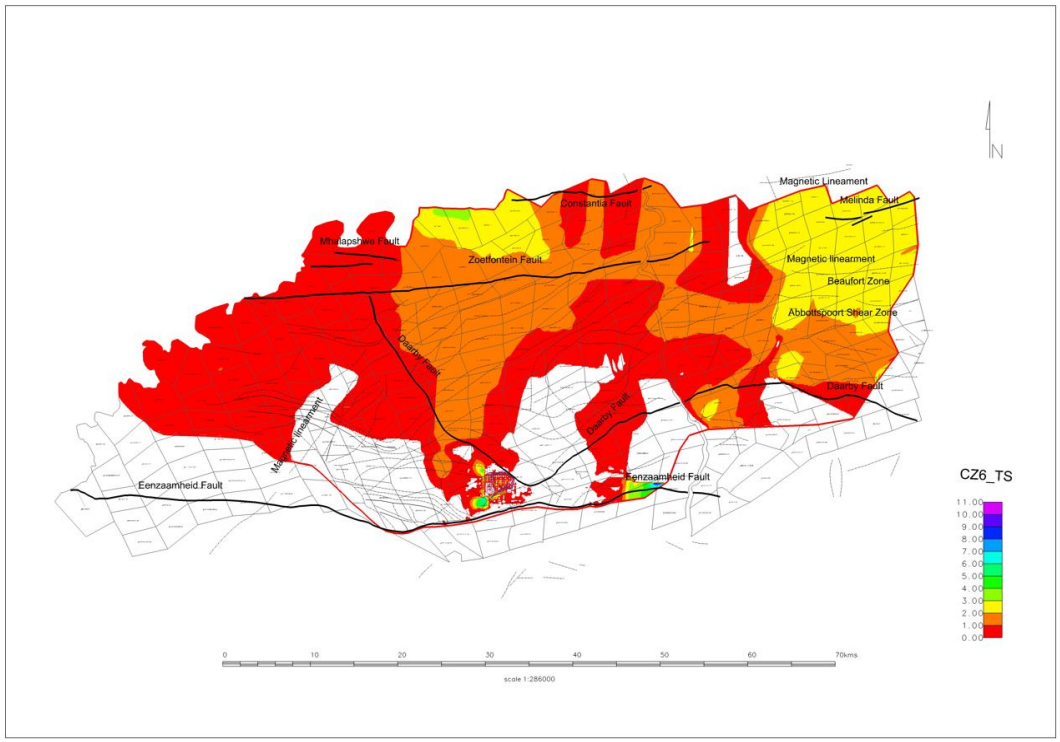

Figure B 32: CZ6_Total Sulphur (TS)

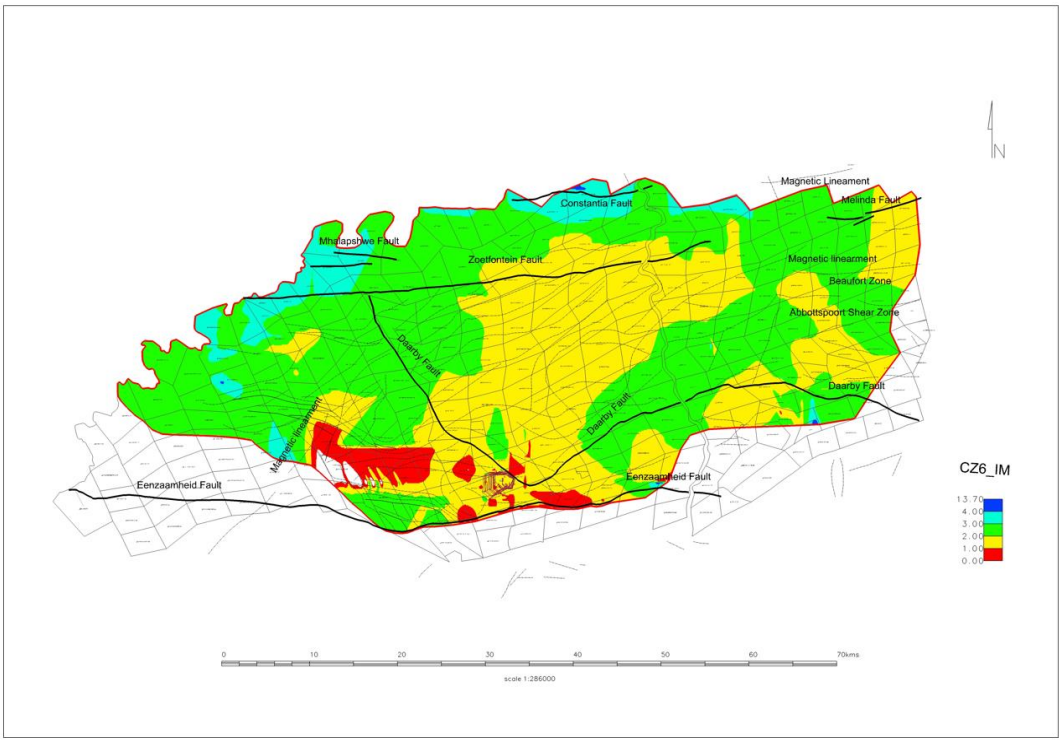

Figure B 33: CZ6_Inherent Moisture (IM)

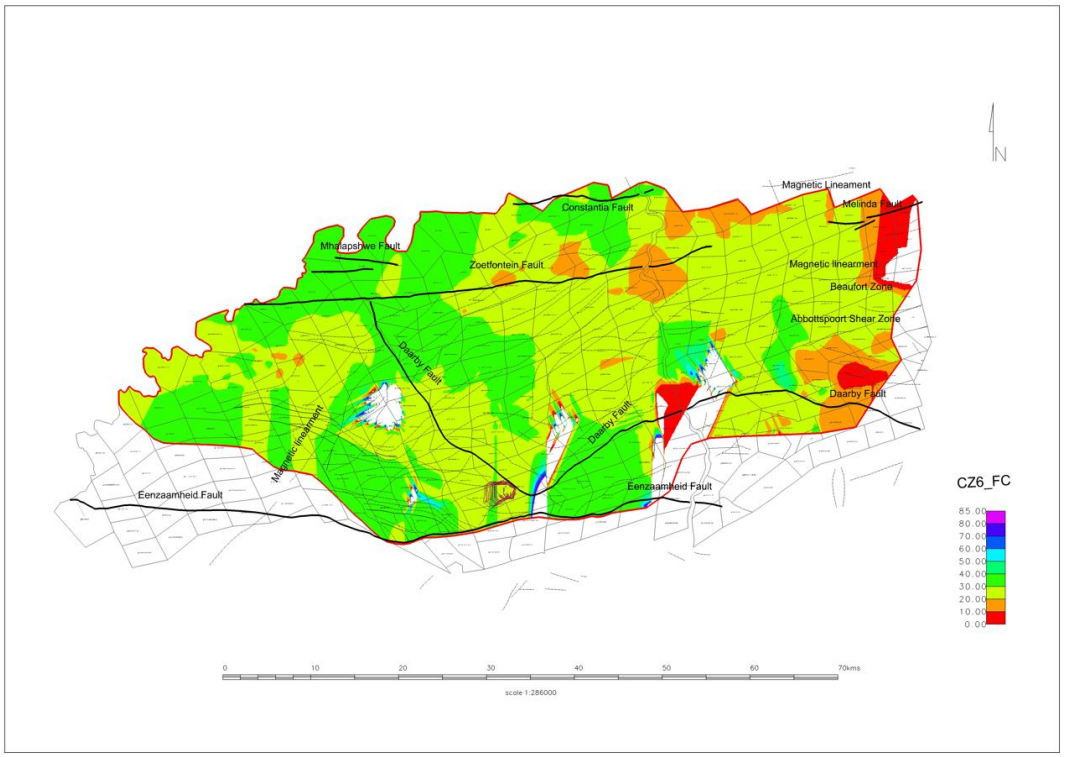

Figure B 34: CZ6_Fixed Carbon (FC)

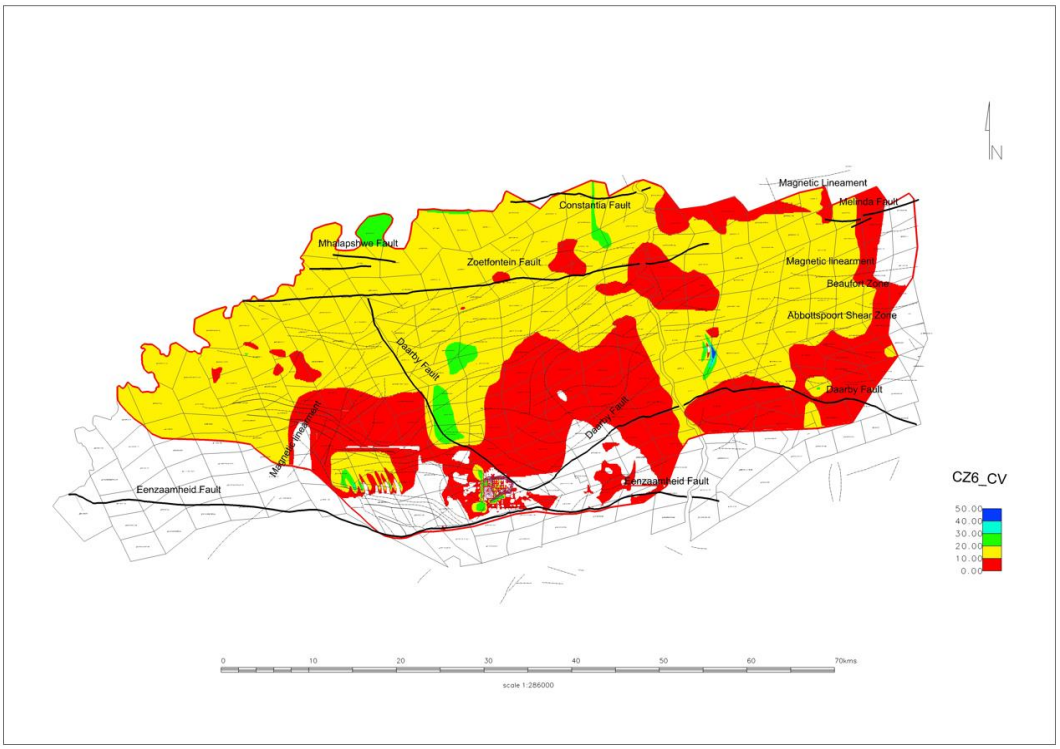

Figure B 35: CZ6_Calorific Value (CV)

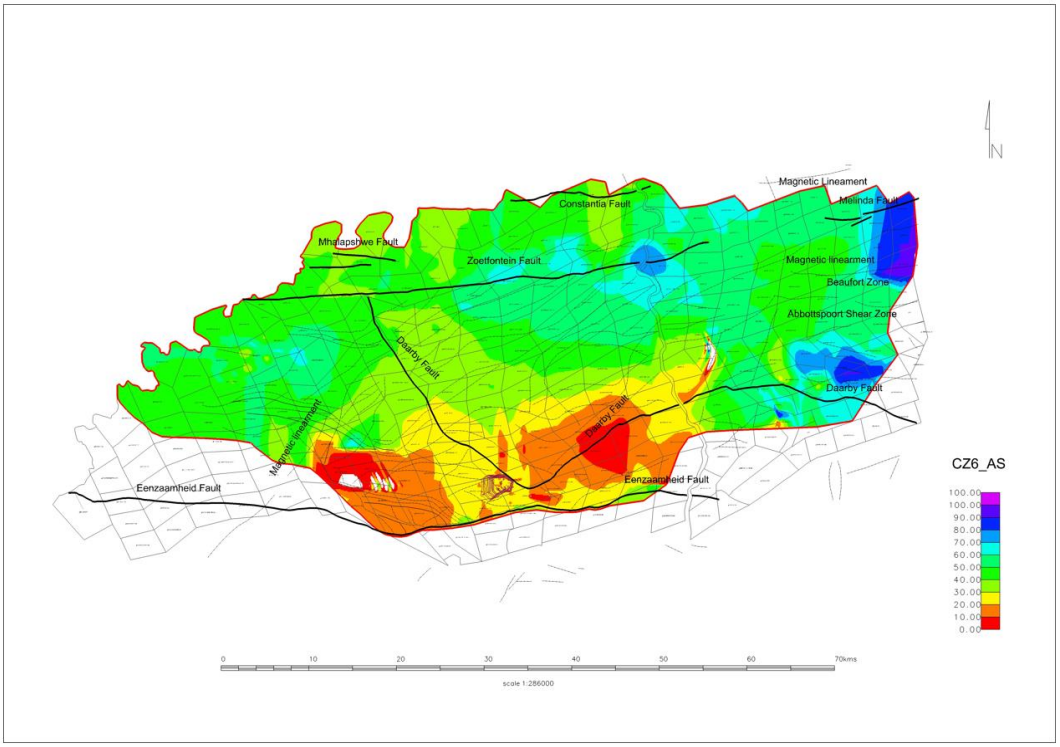

Figure B 36: CZ6_Ash (AS)

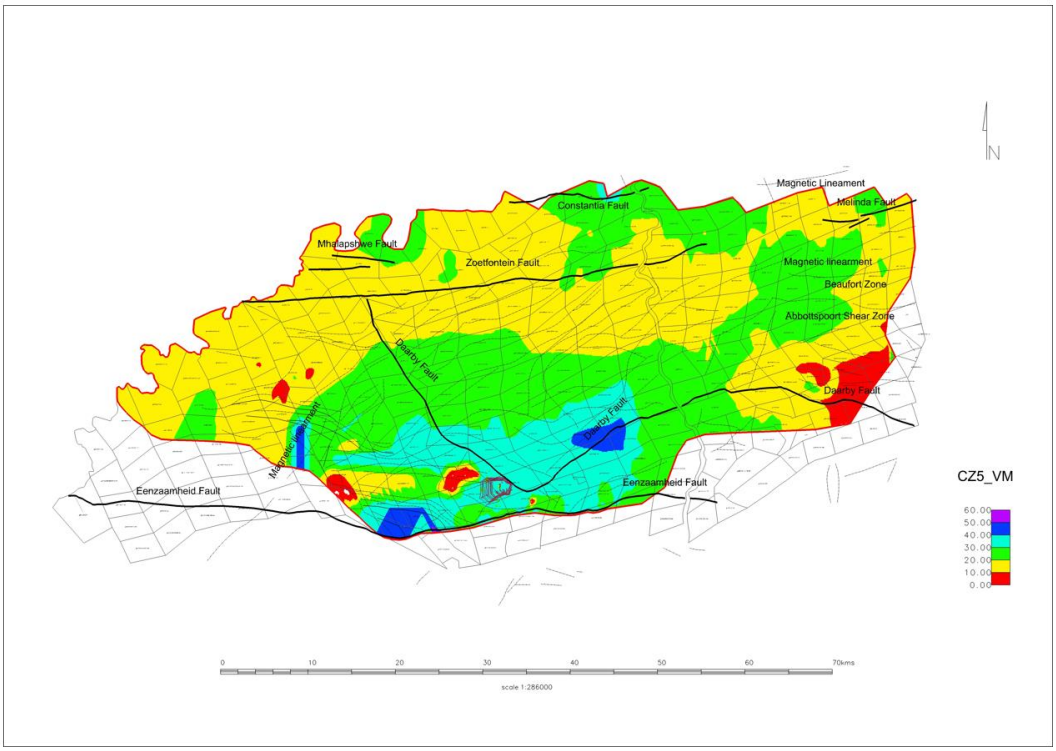

Figure B 37: CZ5_Volatile Matter (VM)

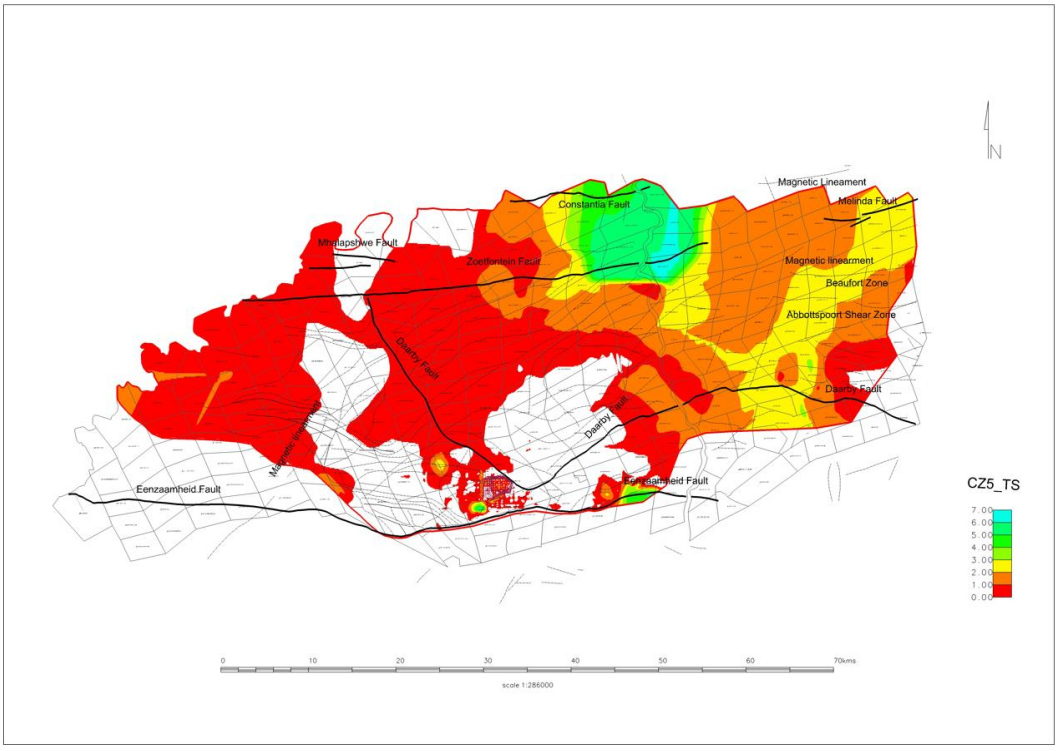

Figure B 38: CZ5_Total Sulphur (TS)

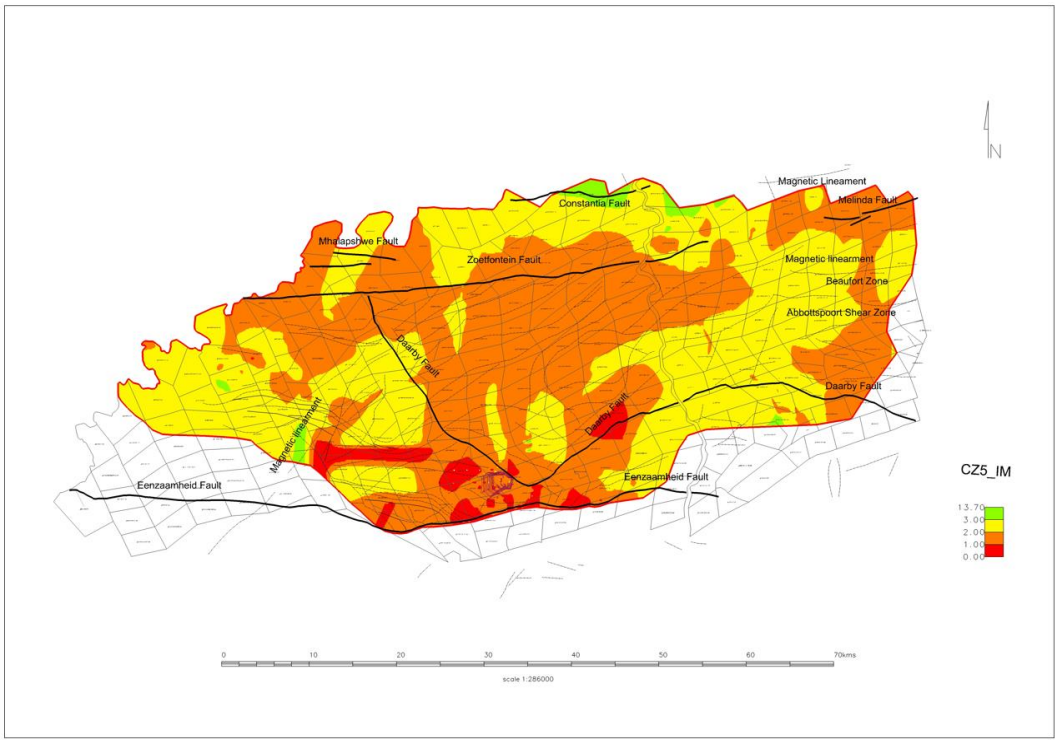

Figure B 39: CZ5_Inherent Moisture (IM)

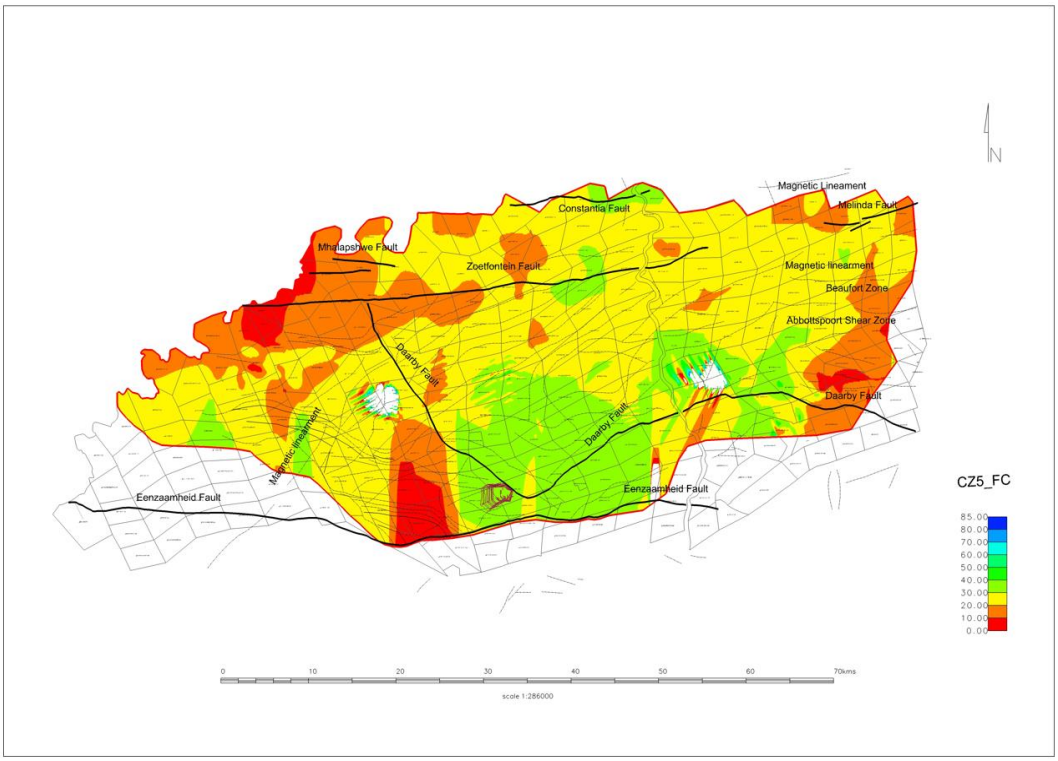

Figure B 40: CZ5_Fixed Carbon (FC)

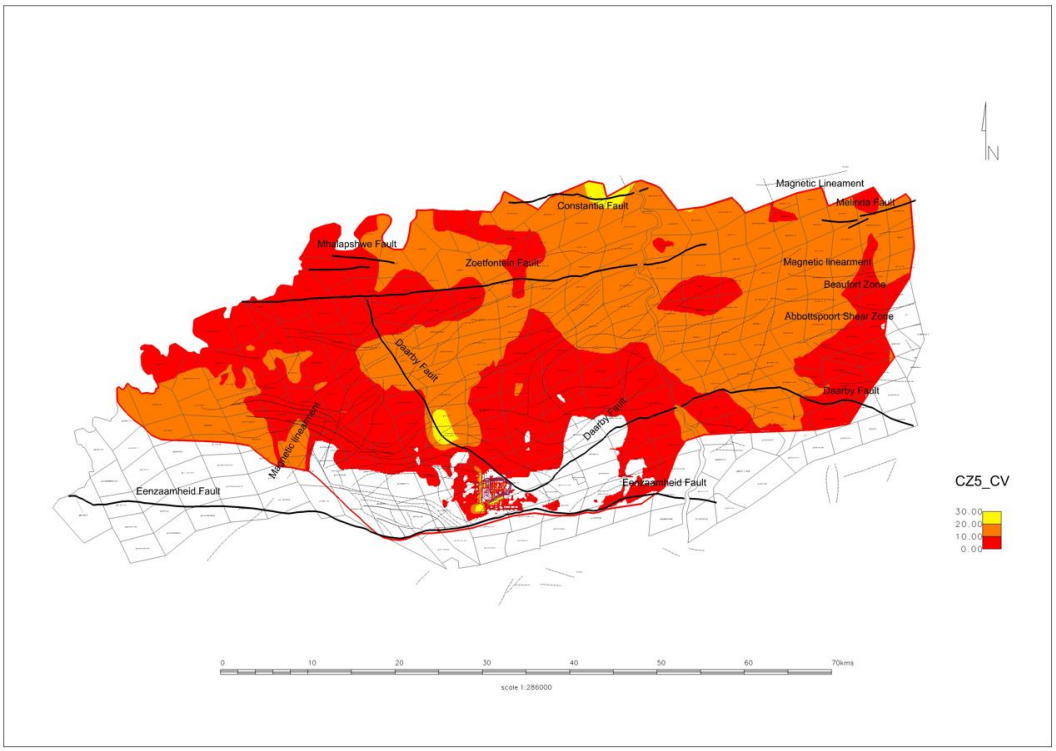

Figure B 41: CZ5_Calorific Value (CV)

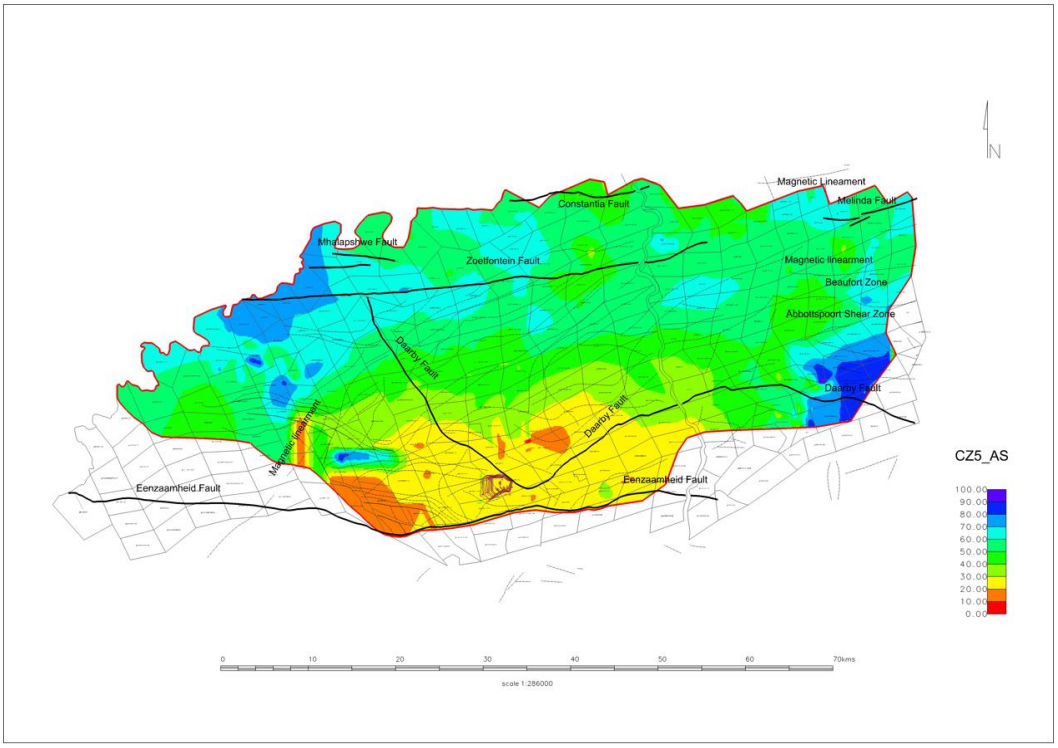

Figure B 42: CZ5_Ash (AS)

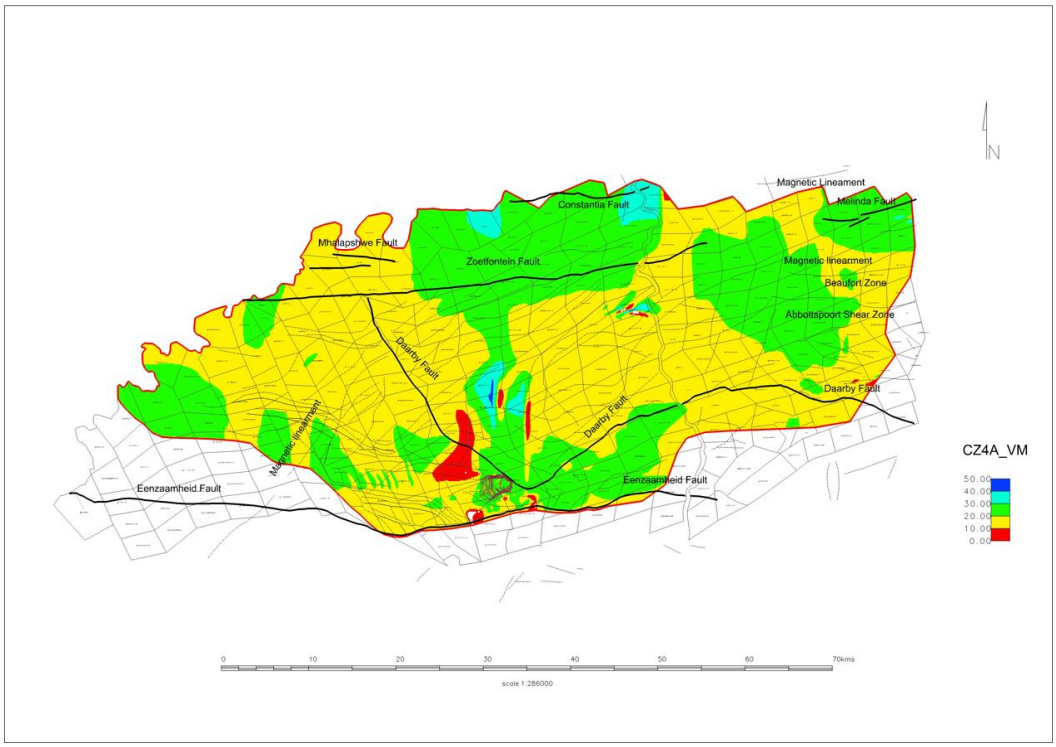

Figure B 43: CZ4A_Volatile Matter (VM)

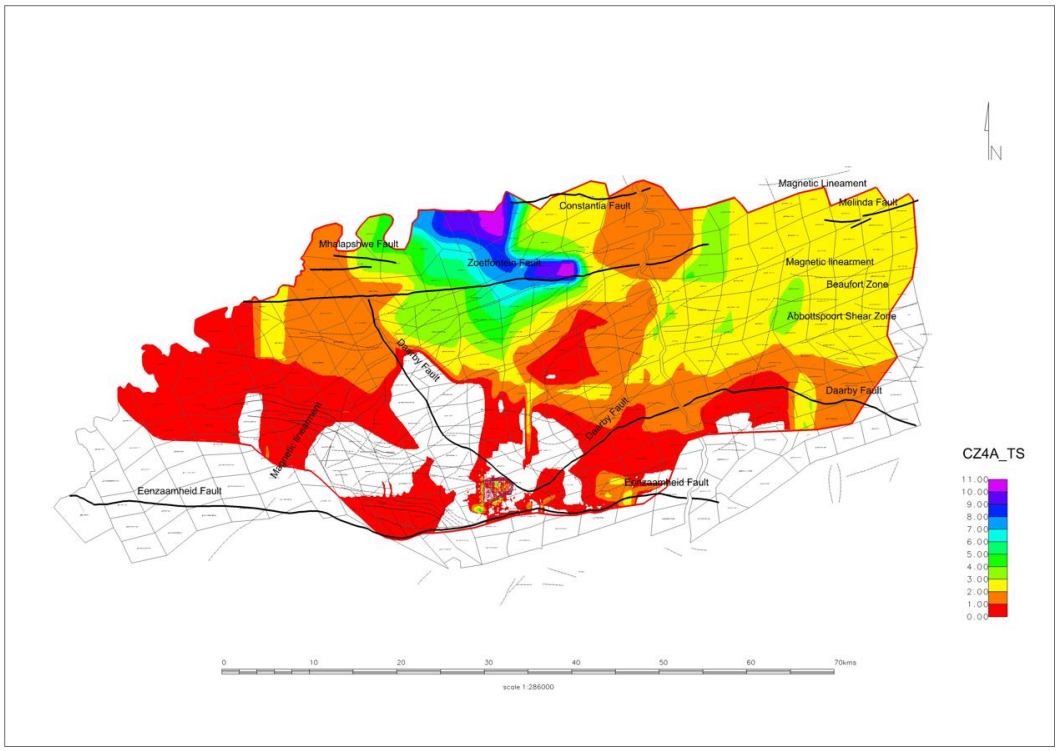

Figure B 44: CZ4A_Total Sulphur (TS)

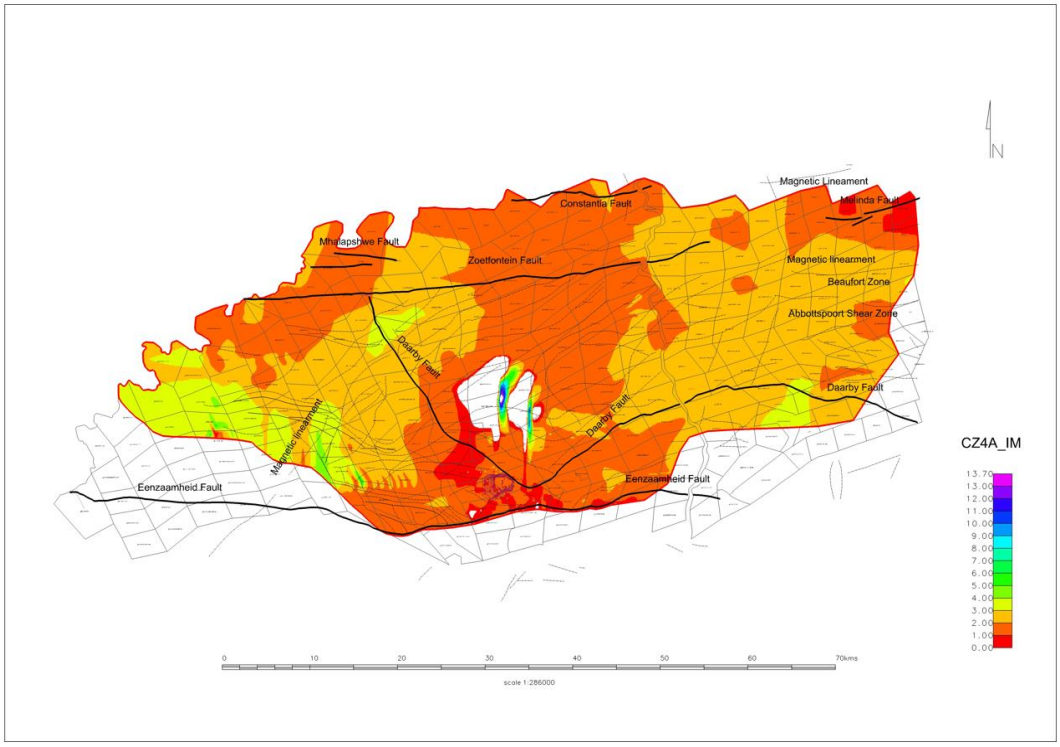

Figure B 45: CZ4A_Inherent Moisture (IM)

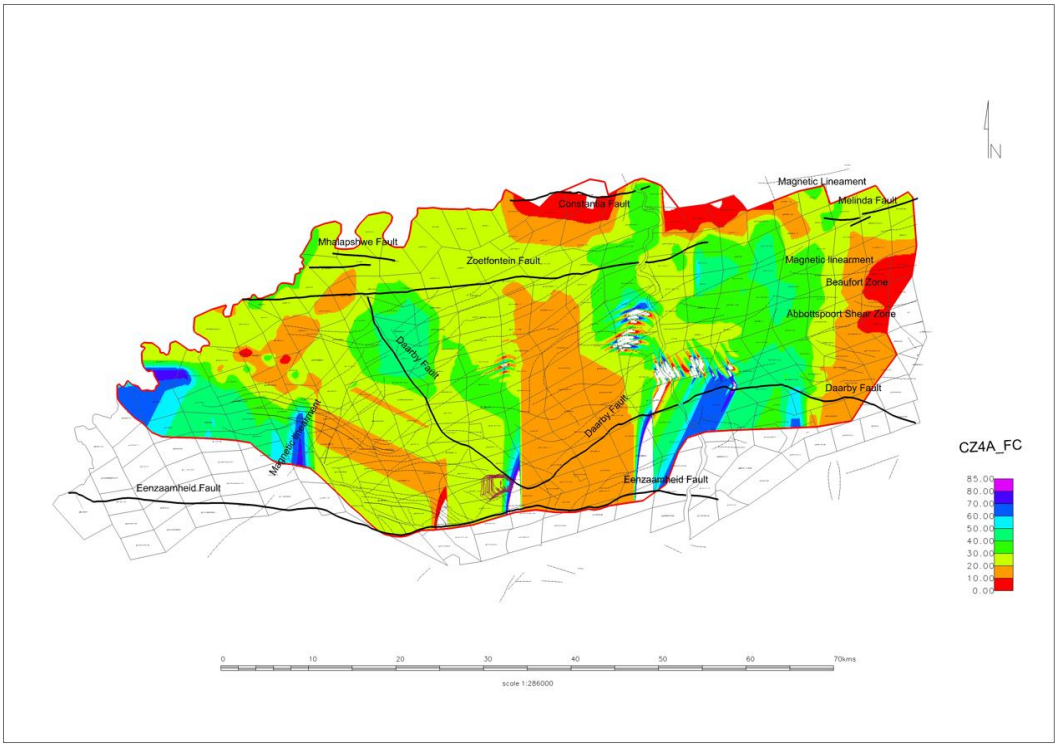

Figure B 46: CZ4A_Fixed Carbon (FC)

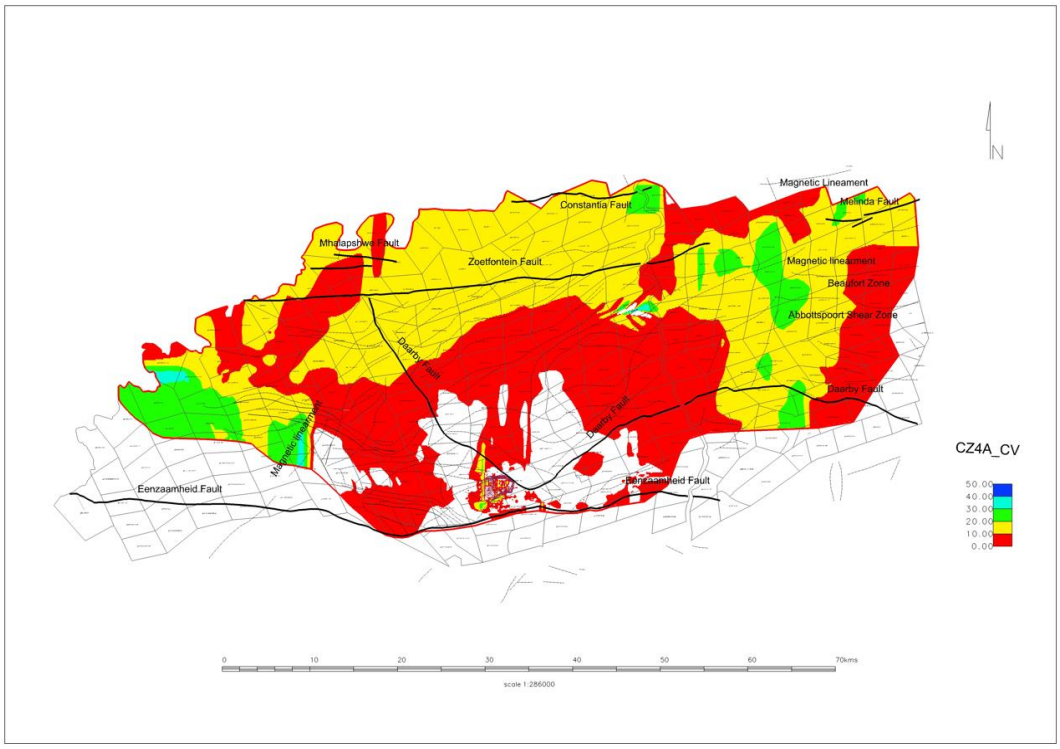

Figure B 47: CZ4A_Calorific Value (CV)

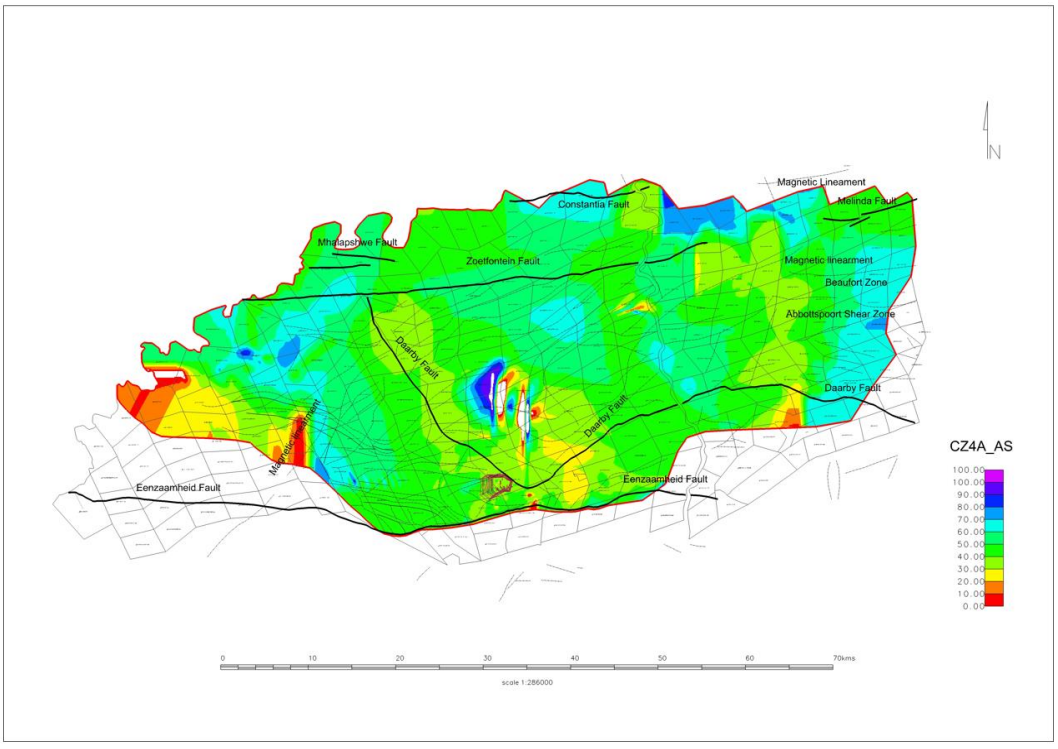

Figure B 48: CZ4A_Ash (AS)

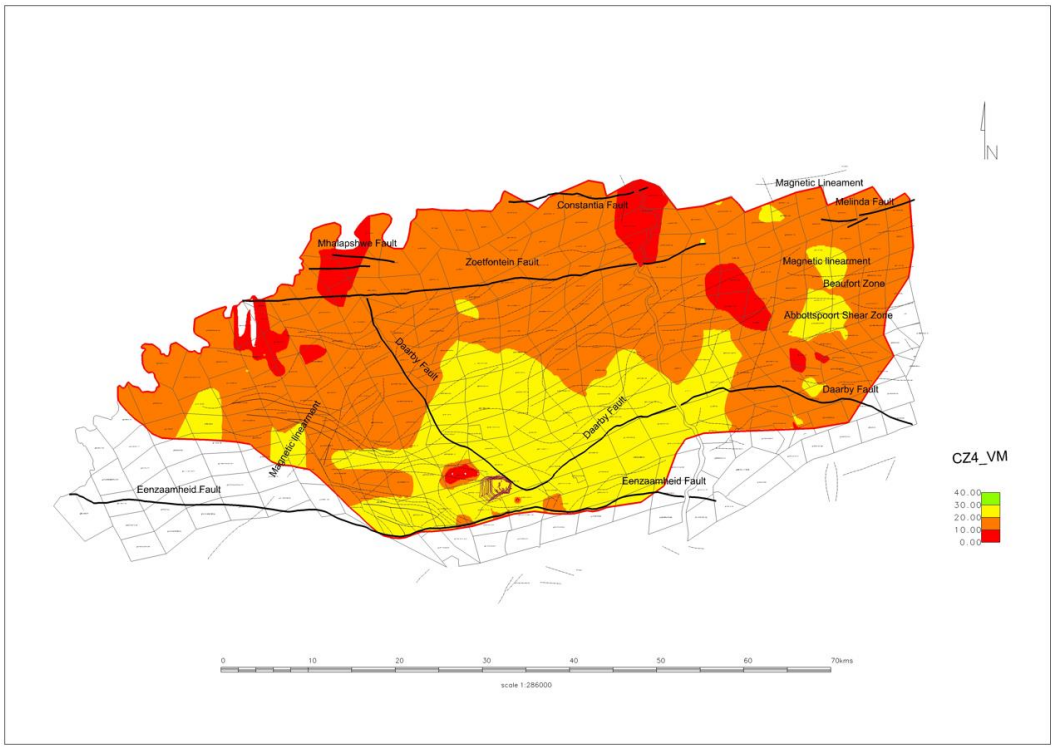

Figure B 49: CZ4_Volatile Matter (VM)

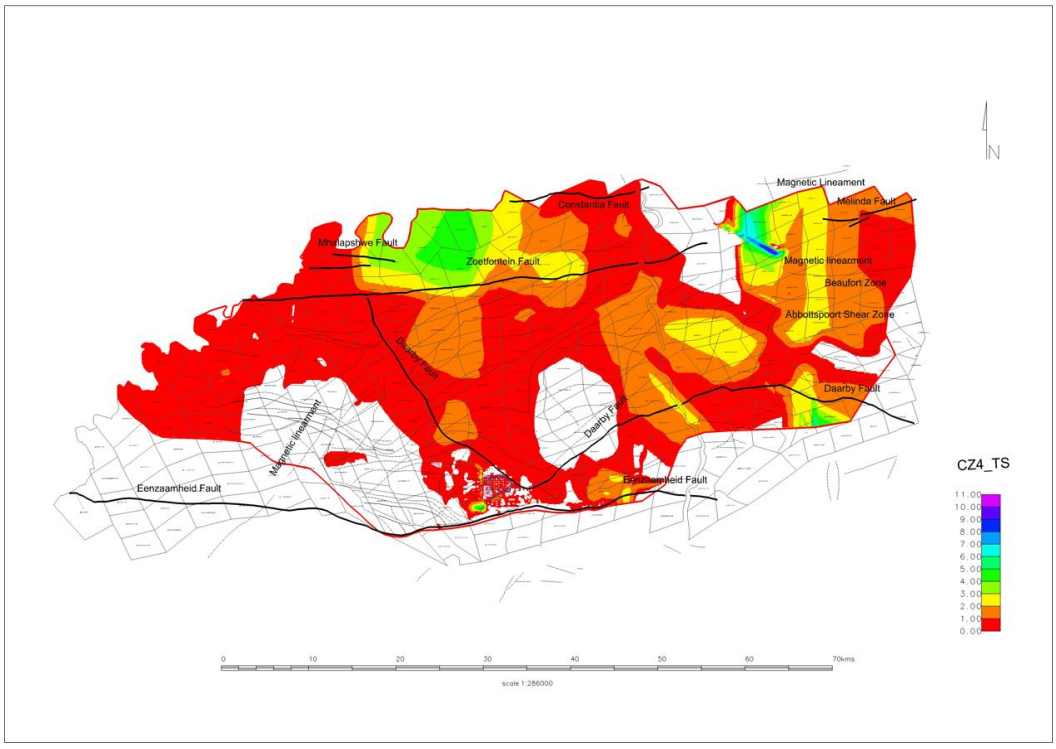

Figure B 50: CZ4_Total Sulphur (TS)

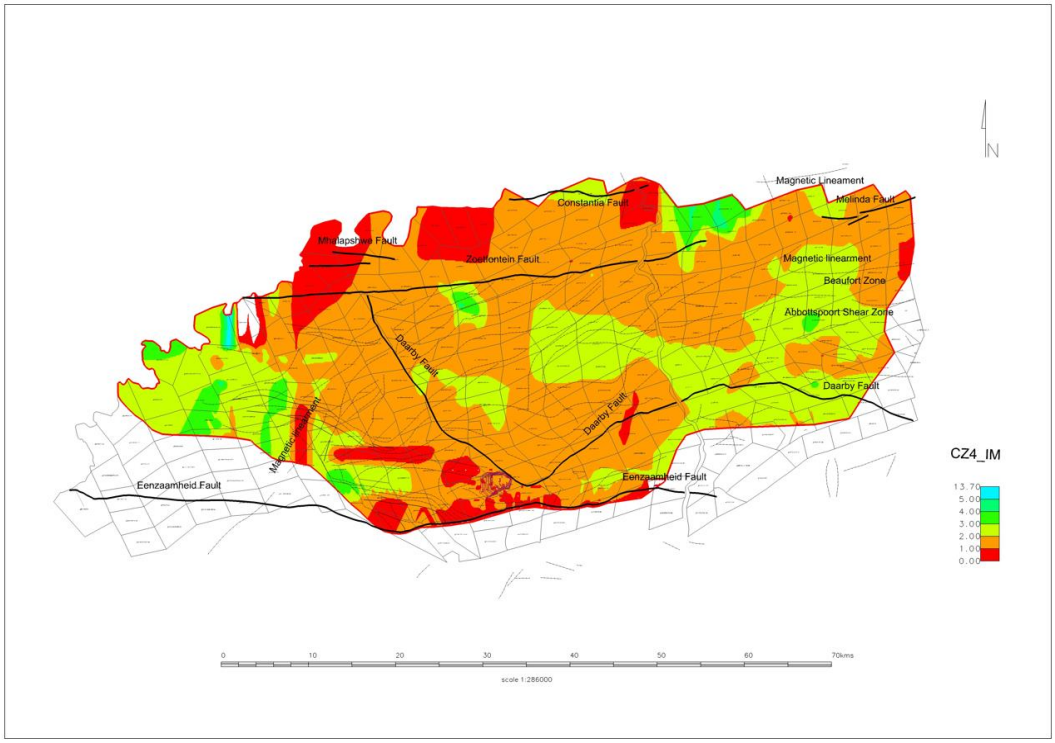

Figure B 51: CZ4_Inherent Moisture (IM)

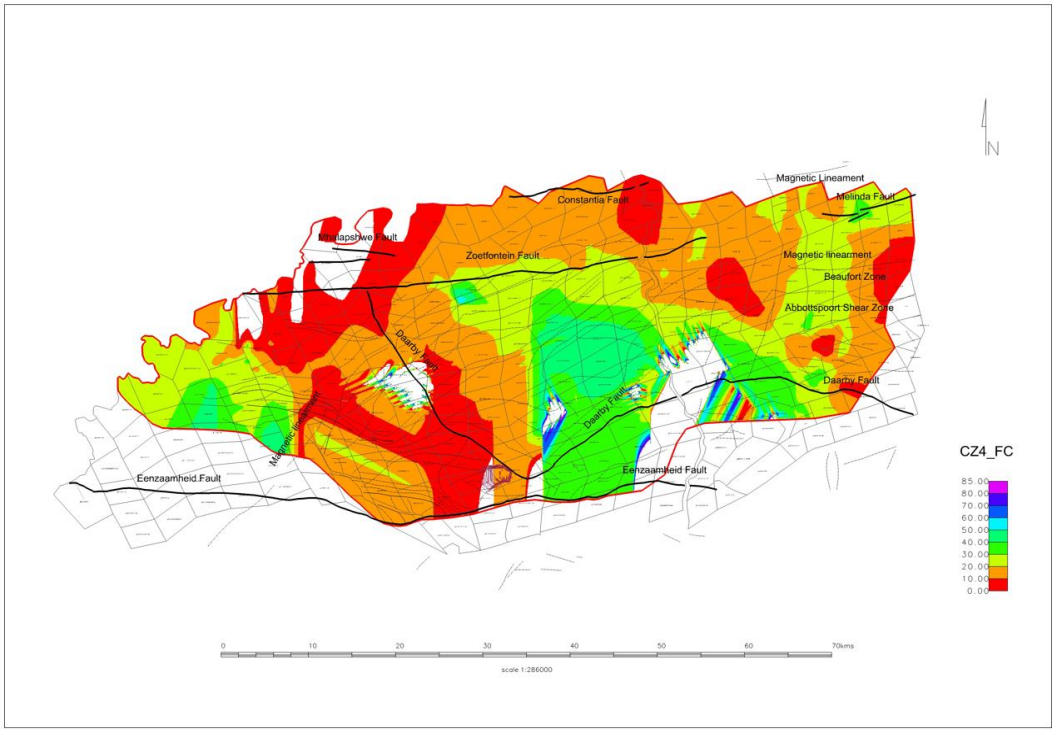

Figure B 52: CZ4_Fixed Carbon (FC)

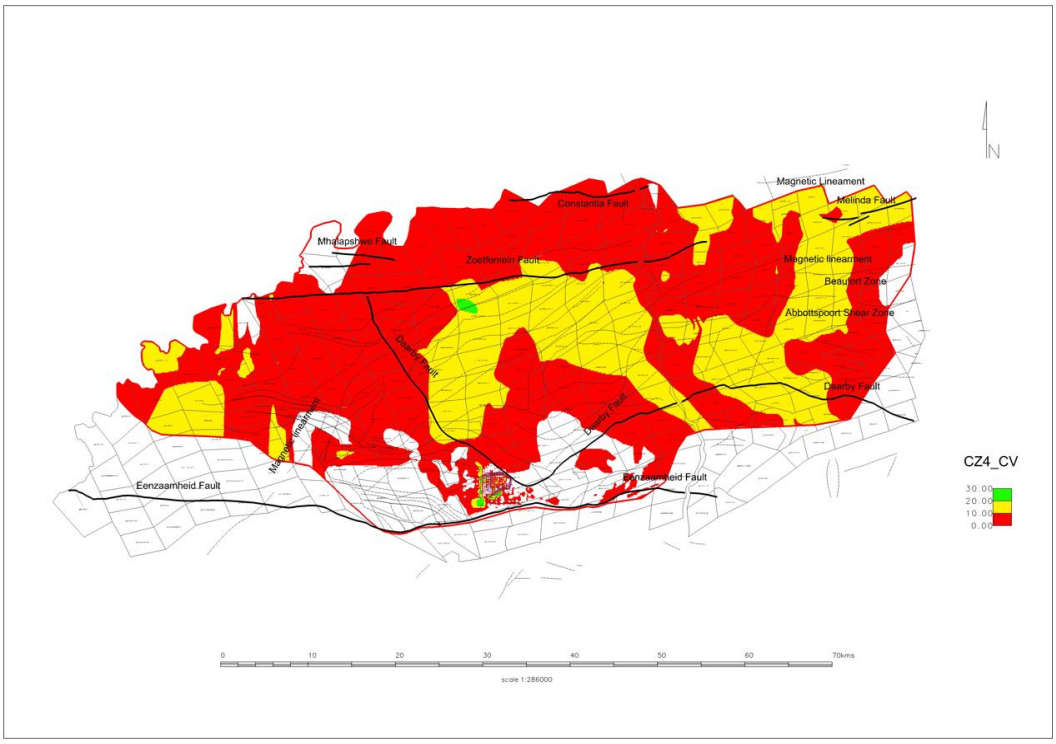

Figure B 53: CZ4_Calorific Value (CV)

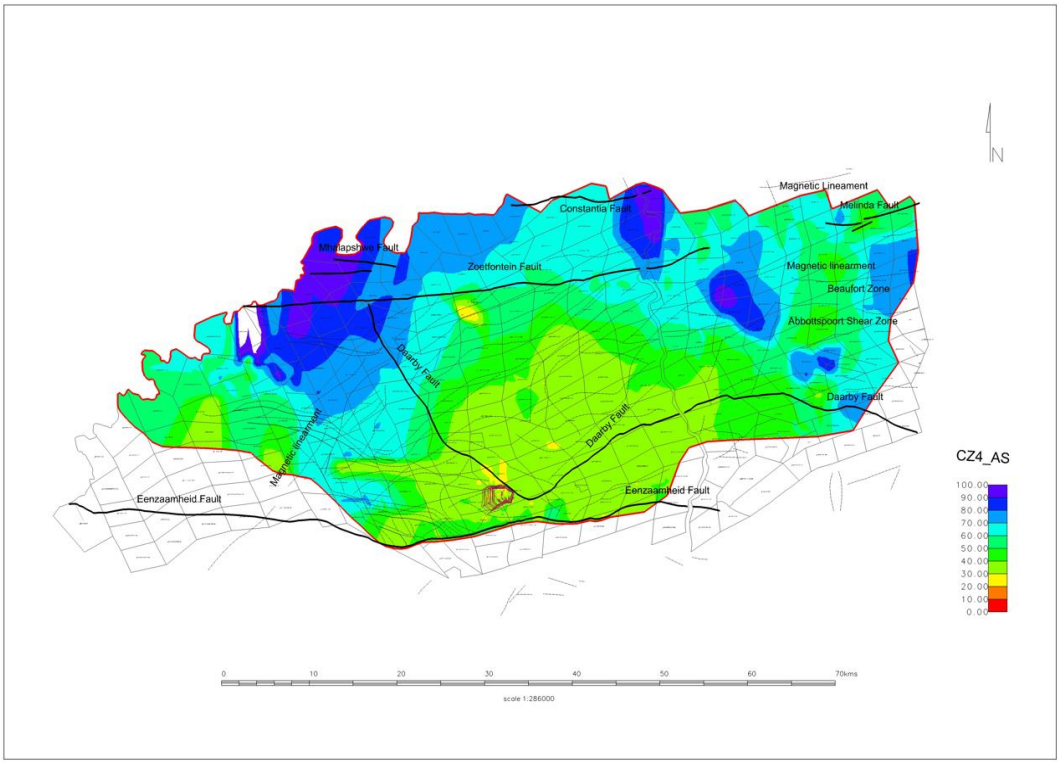

Figure B 54: CZ4_Ash (AS)

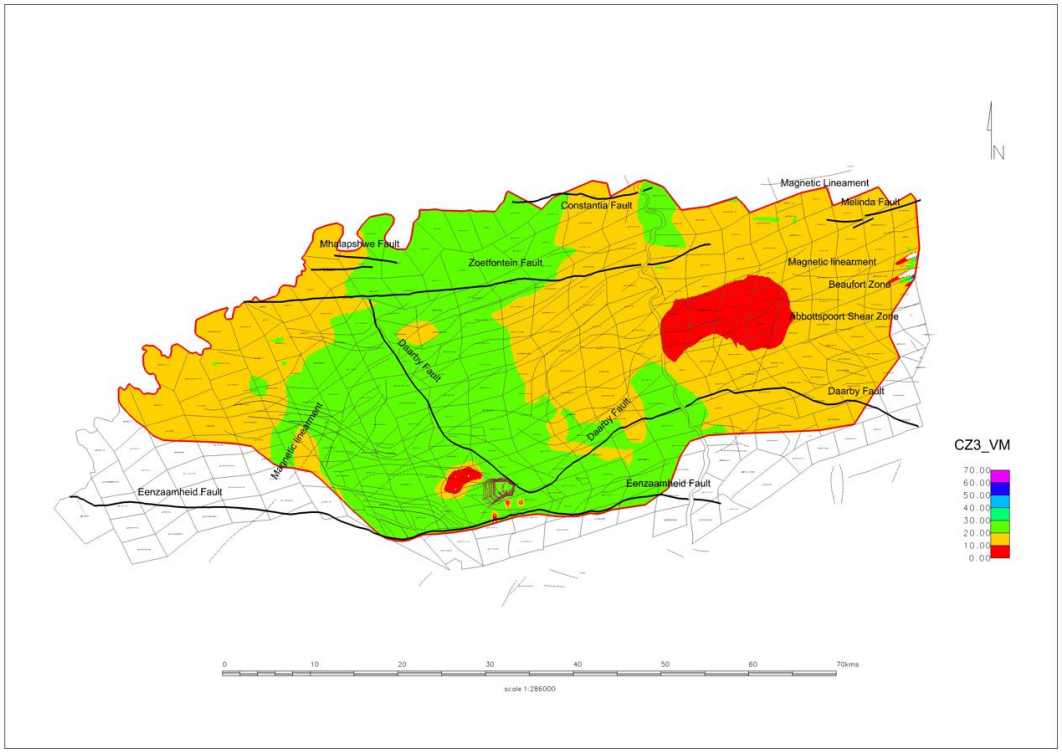

Figure B 55: CZ3_Volatile Matter (VM)

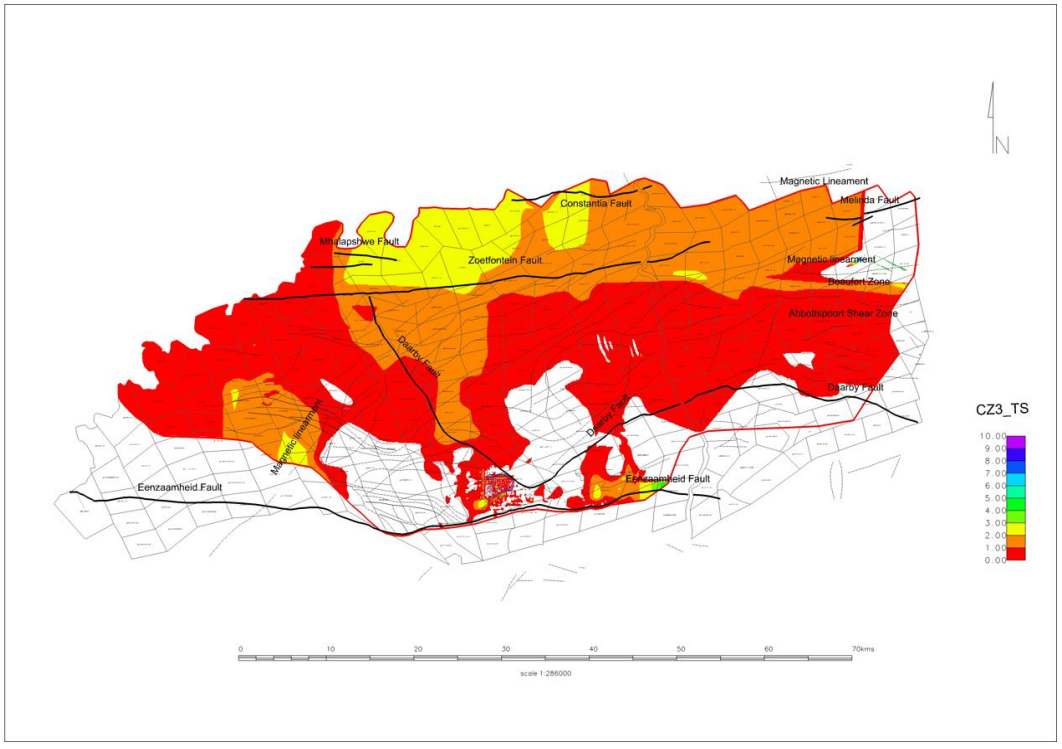

Figure B 56: CZ3_Total Sulphur (TS)

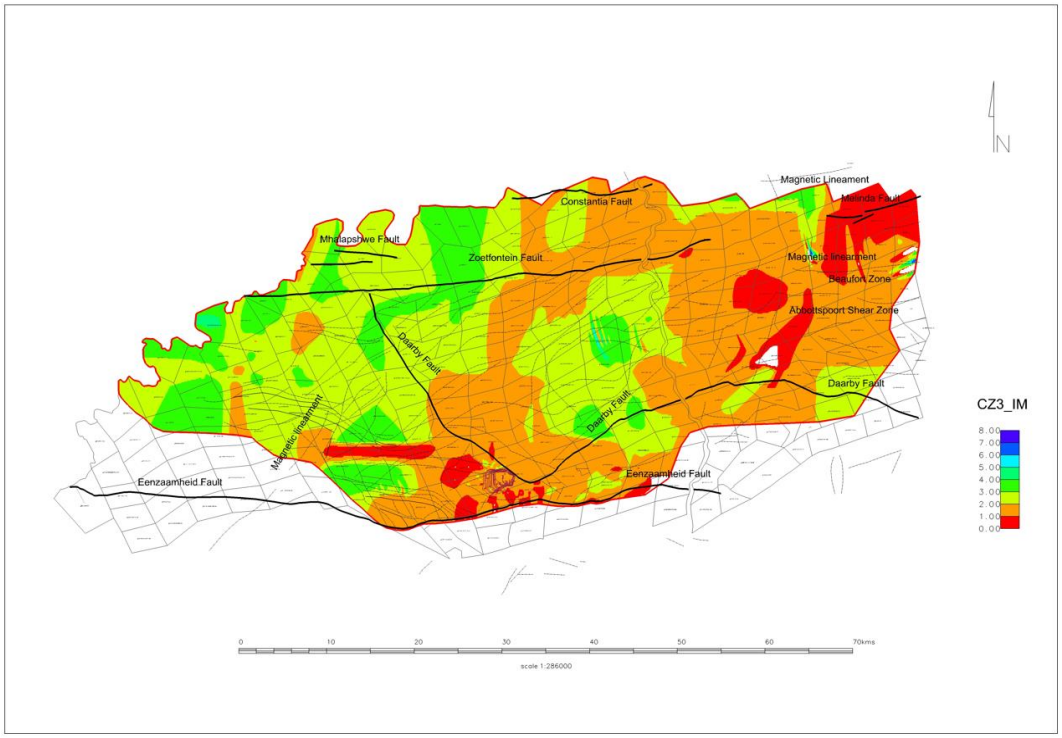

Figure B 57: CZ3_Inherent Moisture (IM)



Figure B 58: CZ3_Fixed Carbon (FC)

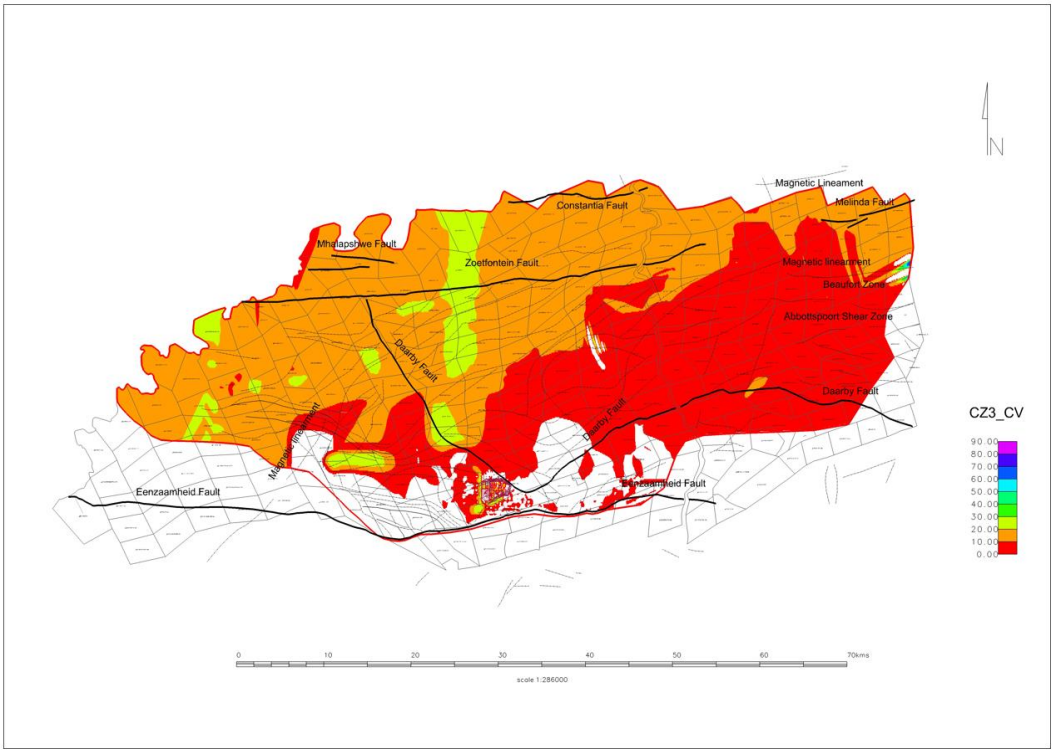

Figure B 59: CZ3_Calorific Value (CV)

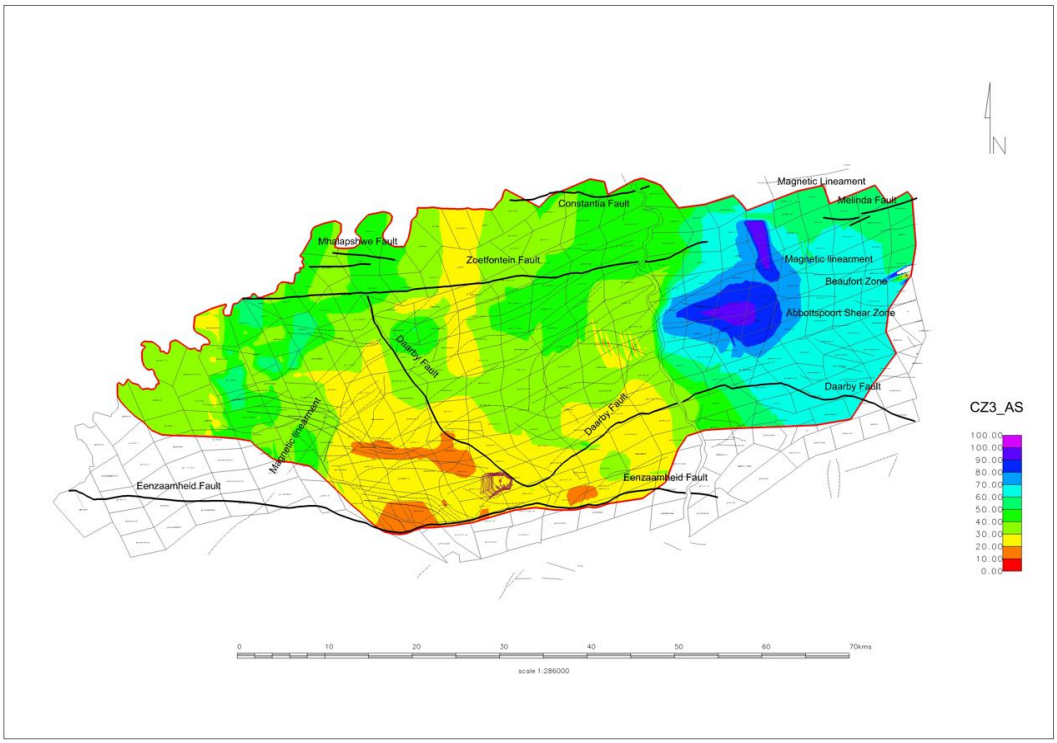

Figure B 60: CZ3_Ash (AS)

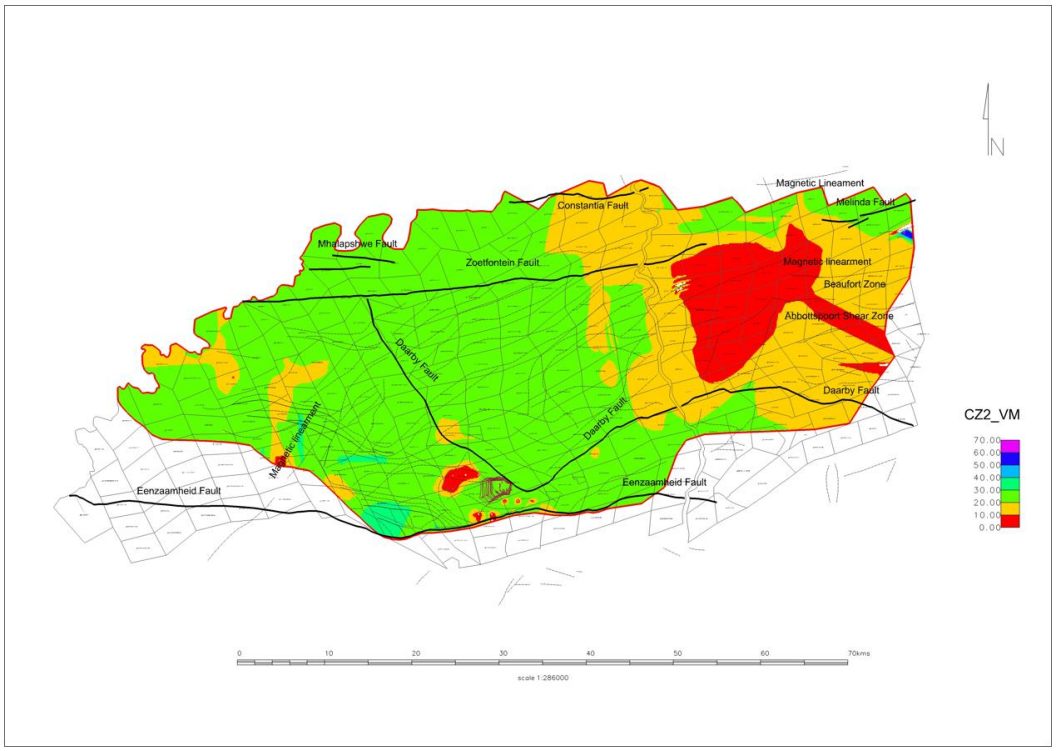

Figure B 61: CZ2_Volatile Matter (VM)

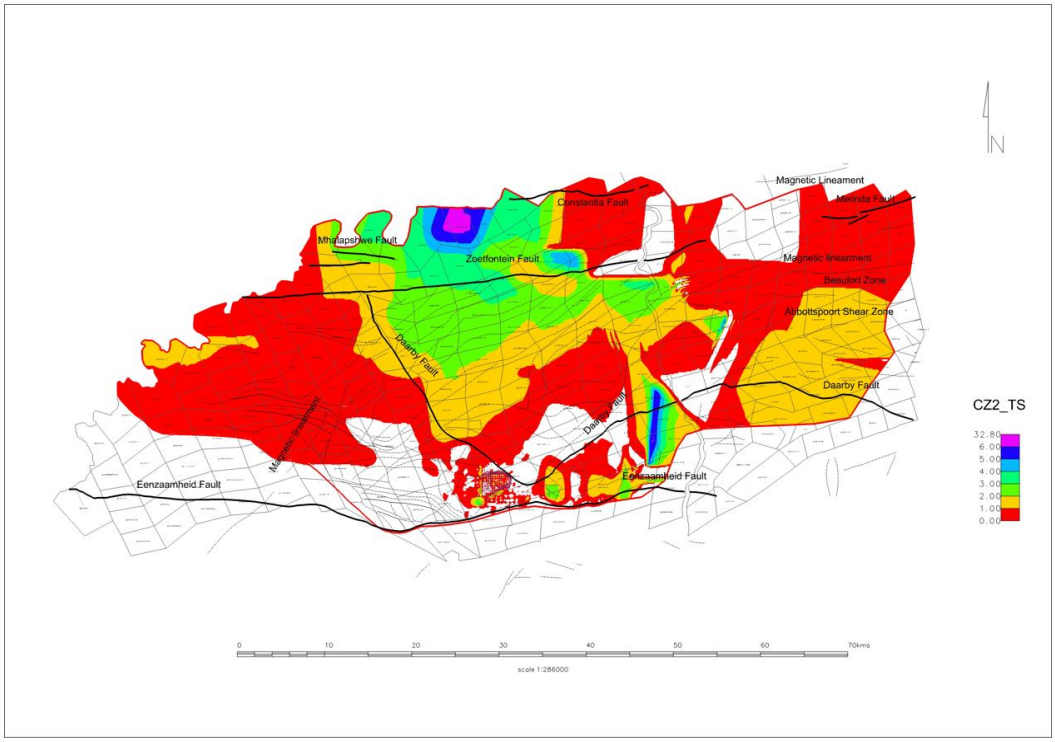

Figure B 62: CZ2_Total Sulphur (TS)

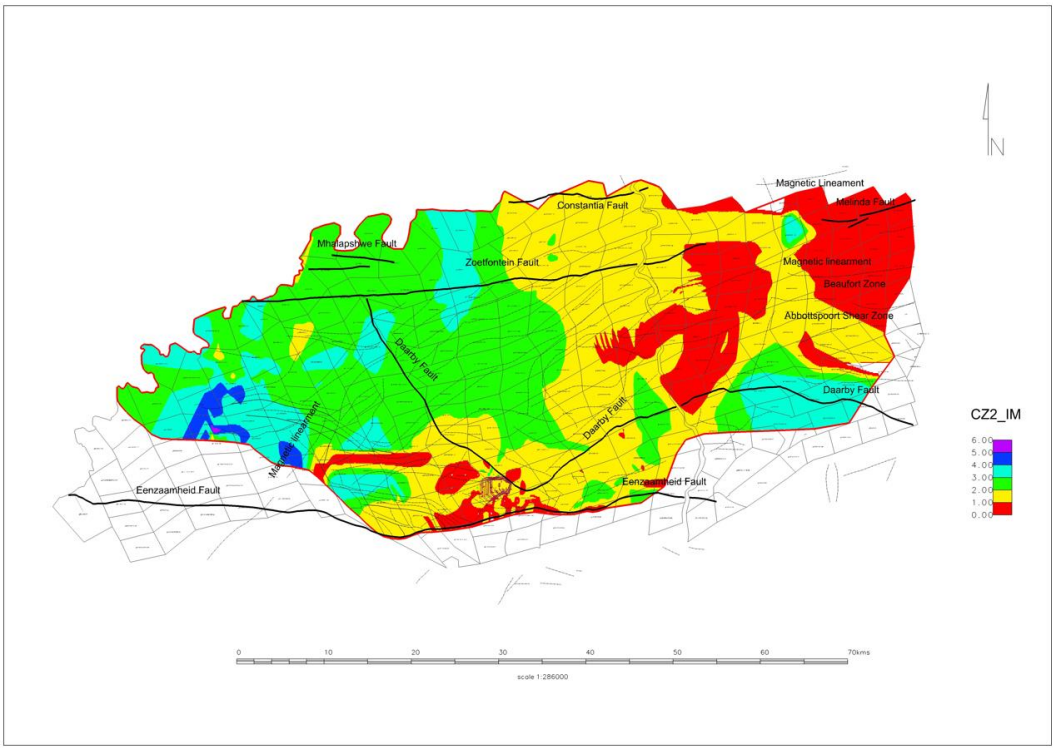

Figure B 63: CZ2_Inherent Moisture (IM)

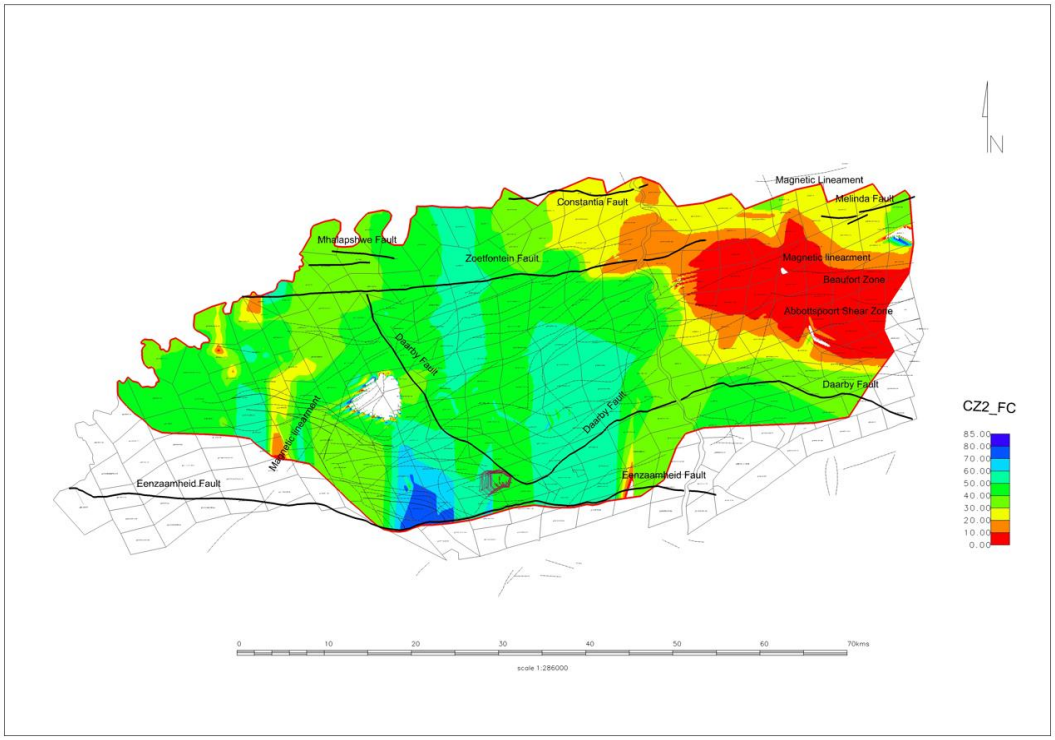

Figure B 64: CZ2_Fixed Carbon (FC)

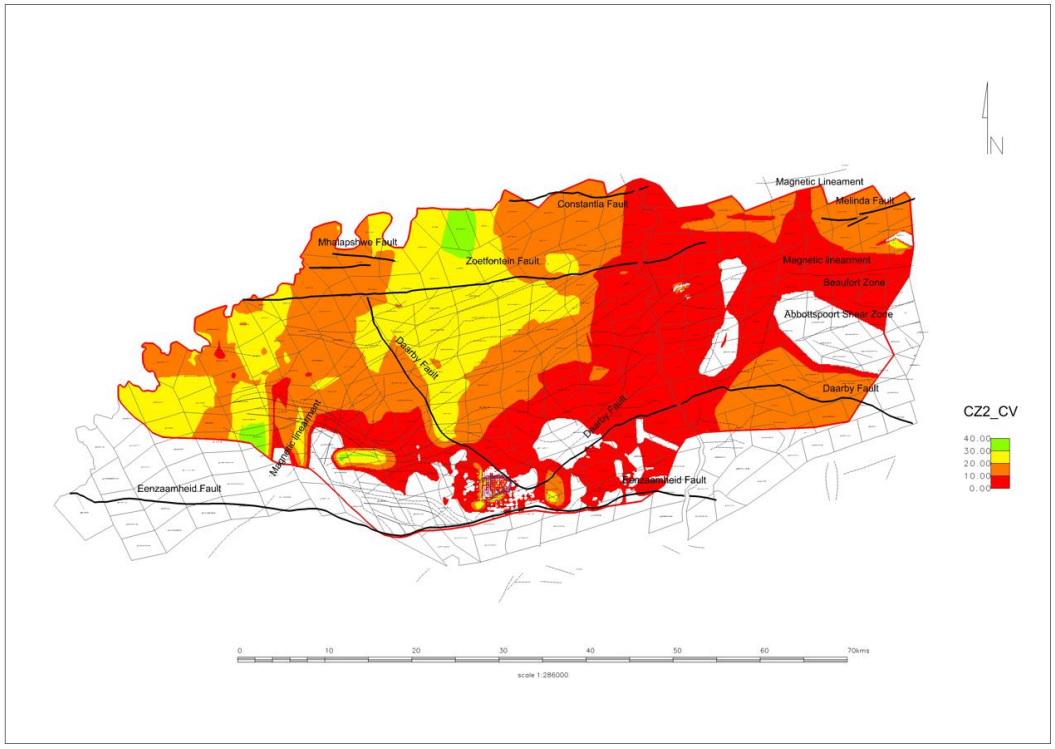

Figure B 65: CZ2_Calorific Value (CV)

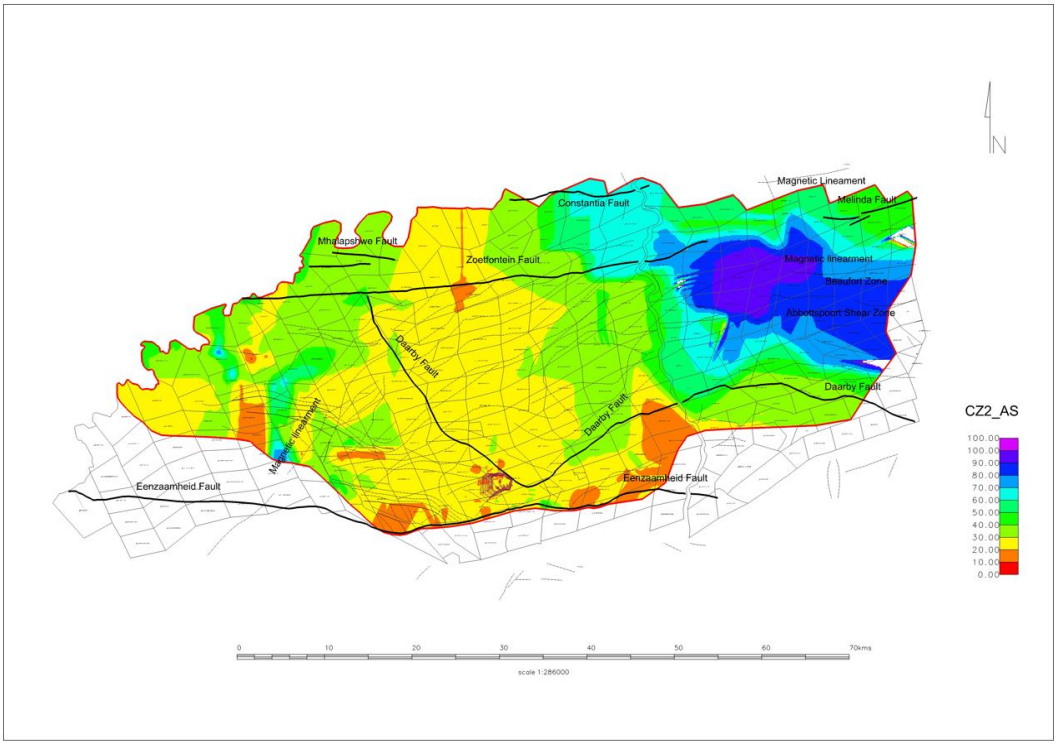

Figure B 66: CZ2_Ash (AS)

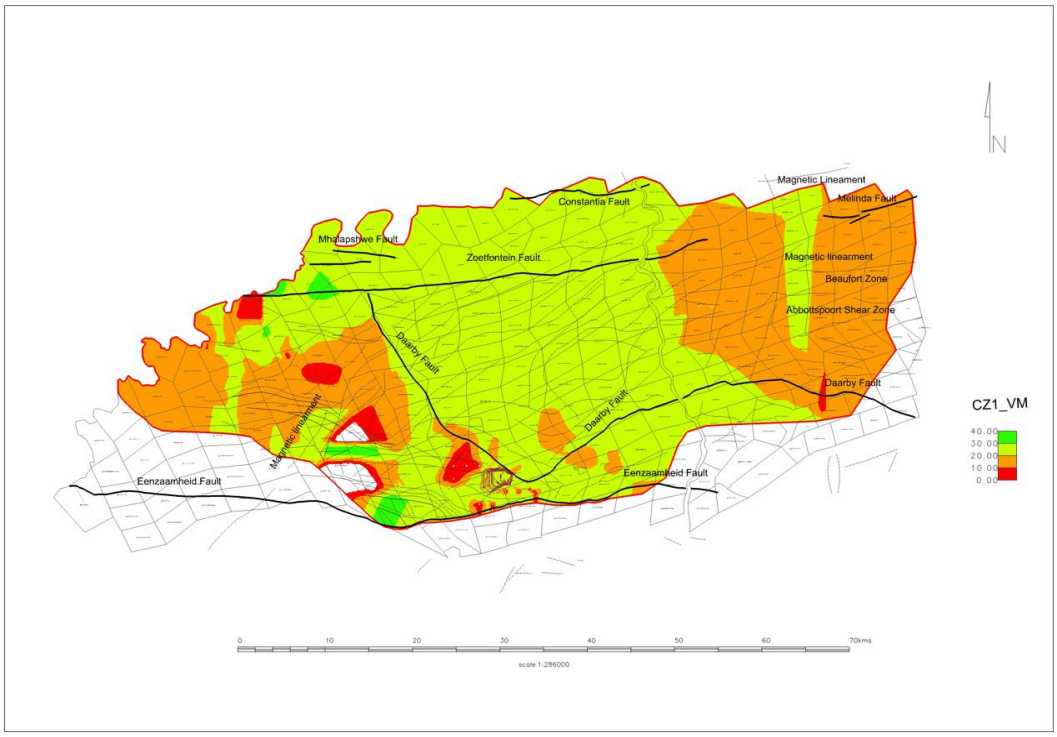

Figure B 67: CZ1_Volatile Matter (VM)

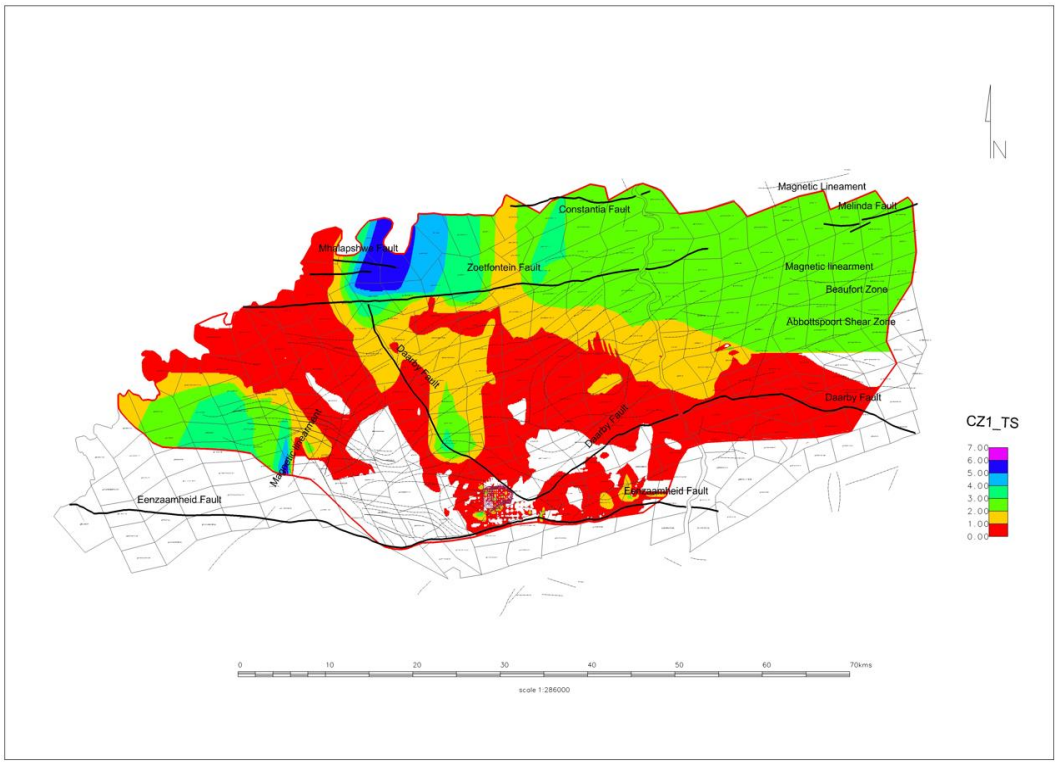

Figure B 68: CZ1_Total Sulphur (TS)

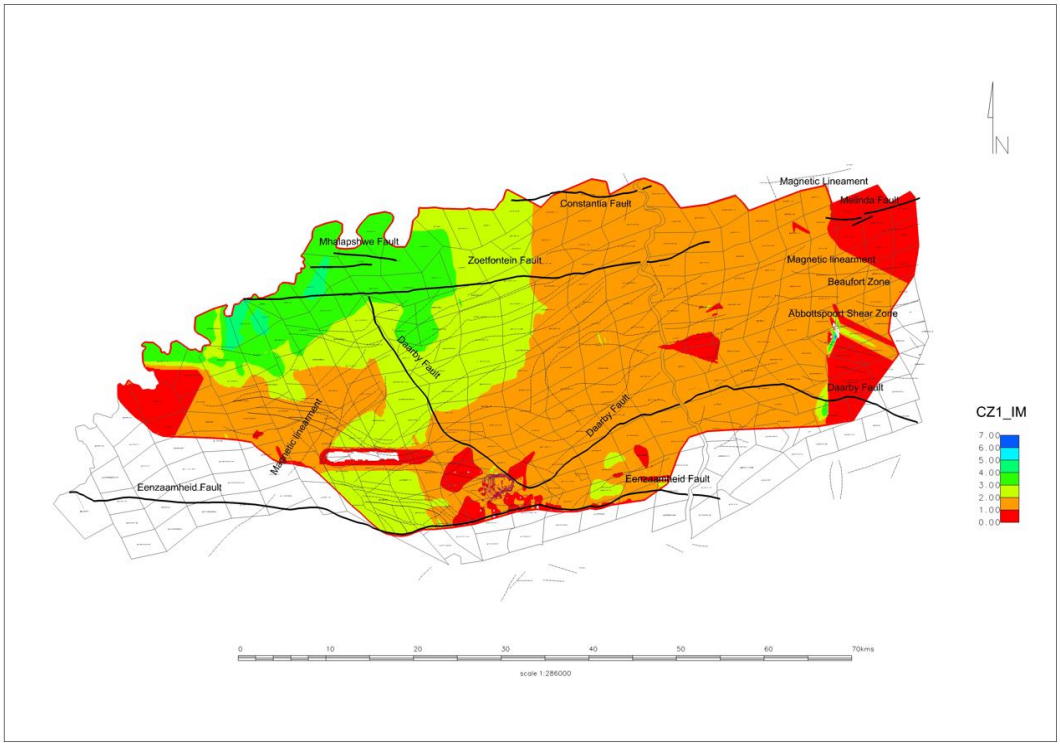

Figure B 69: CZ1_Inherent Moisture (IM)

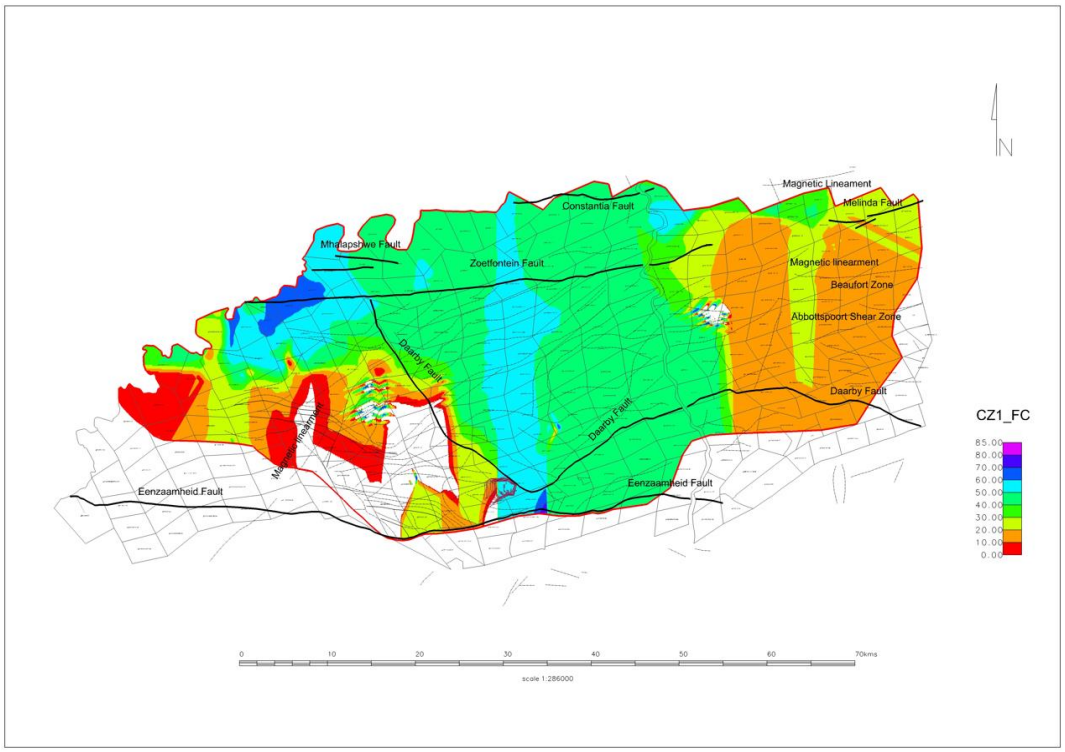

Figure B 70: CZ1_Fixed Carbon (FC)

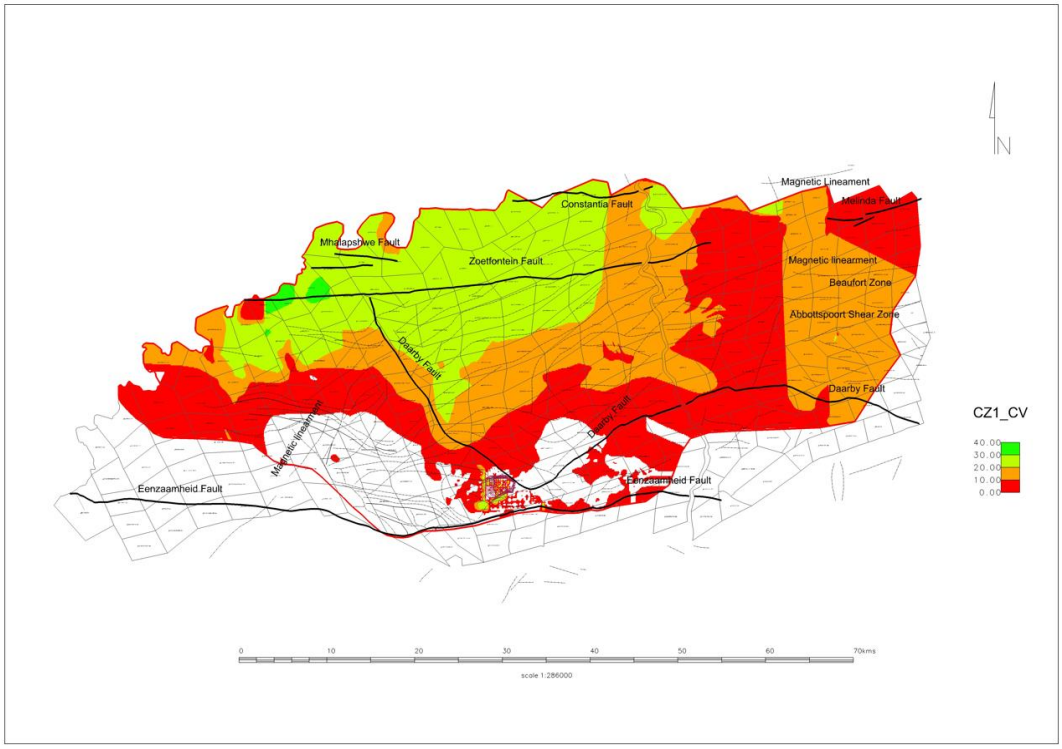

Figure B 71: CZ1_Calorific Value (CV)

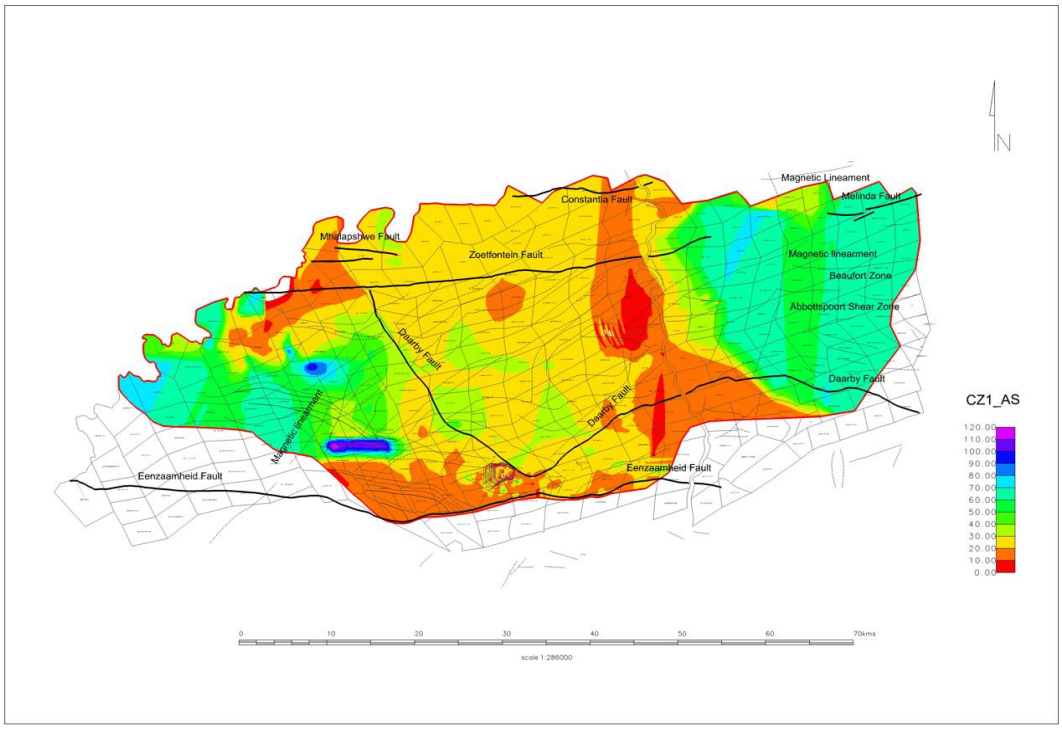

Figure B 72: CZ1_Ash (AS)

APPENDIX C: ISOPACH FLOOR GRIDS FOR THE OVB AND THE COAL ZONES ACROSS

The Waterberg Coalfield (from top to bottom).

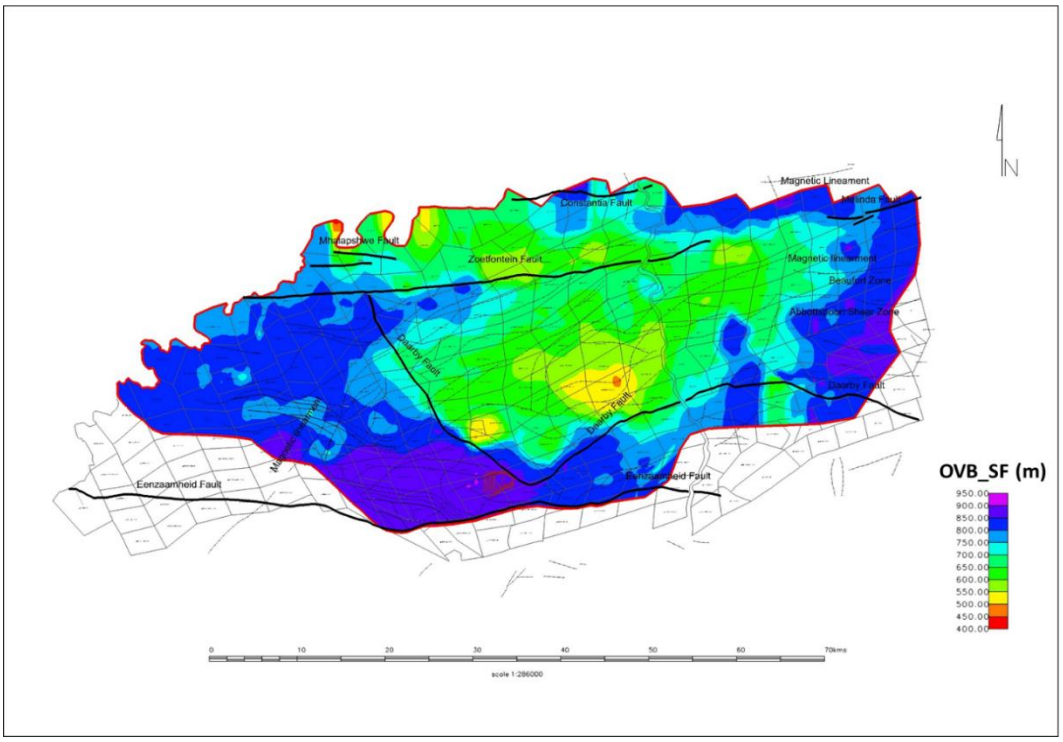

Figure C 1: Isopach floor map for the overburden (OVB)

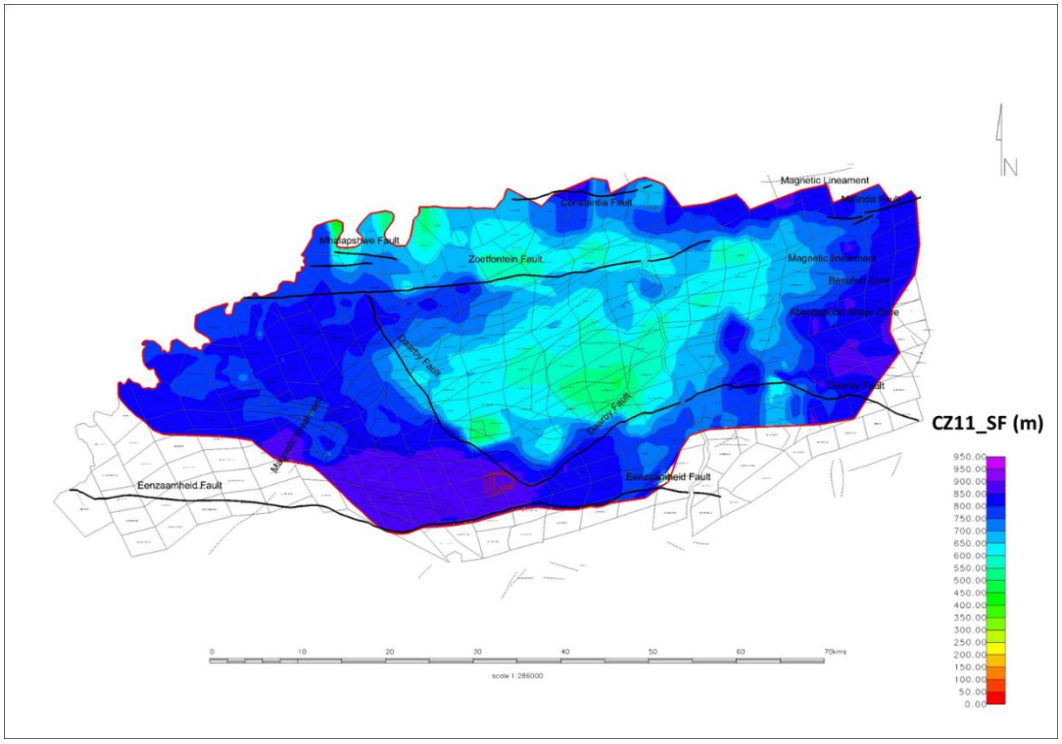

Figure C 2: Isopach Floor map for Coal Zone 11 (CZ11)

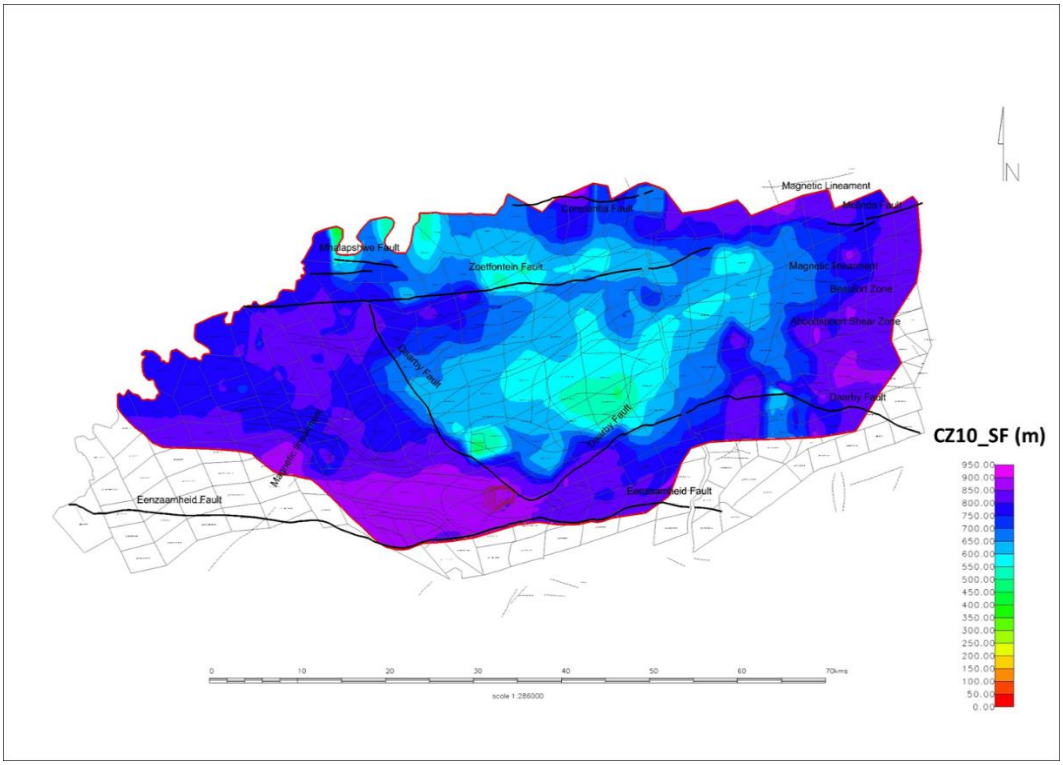

Figure C 3: Isopach Floor map for Coal Zone 10 (CZ10)

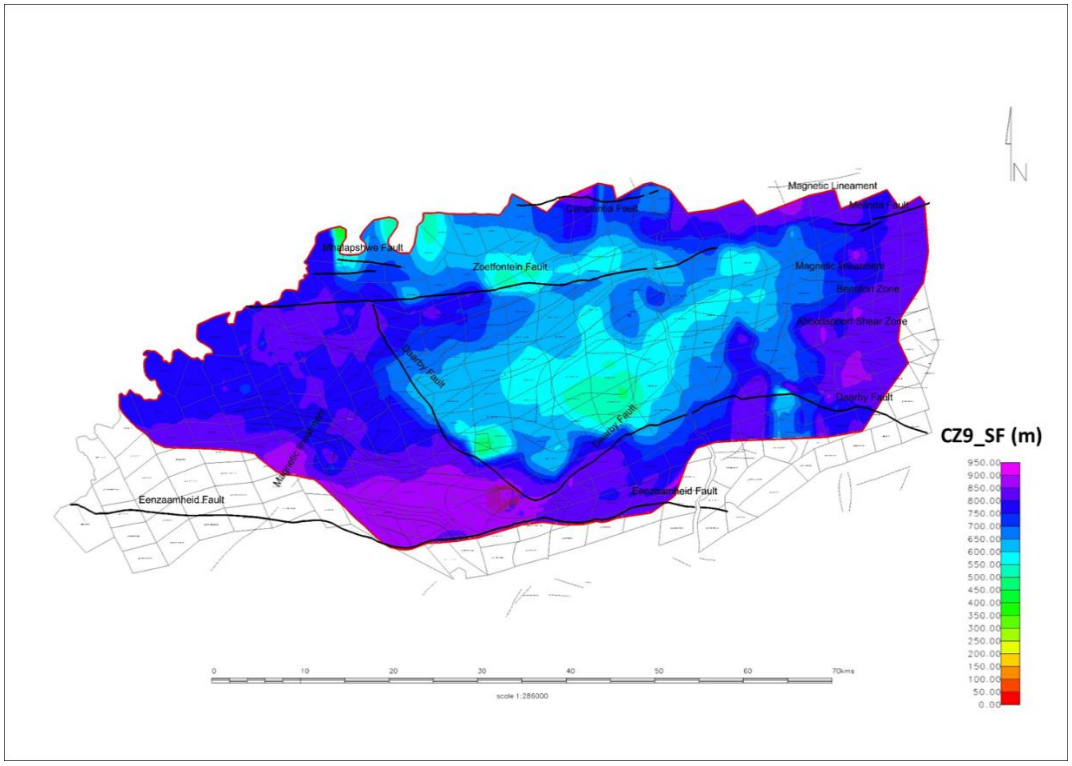

Figure C 4: Isopach Floor map for Coal Zone 9 (CZ9)

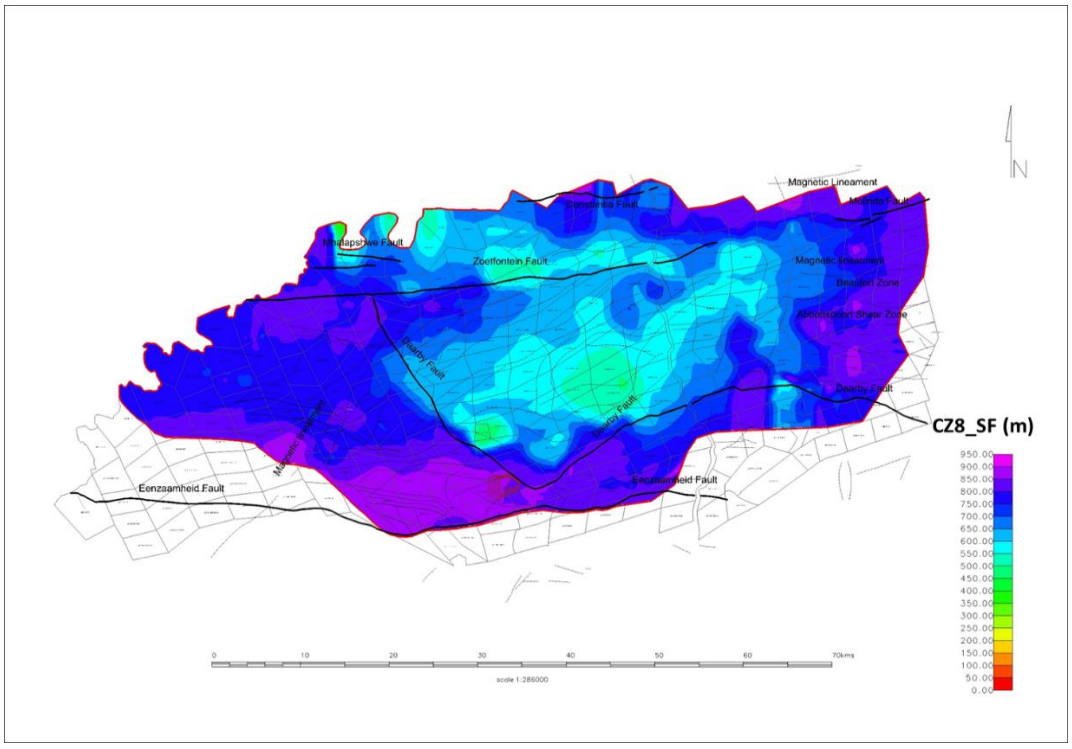

Figure C 5: Isopach Floor map for Coal Zone 8 (CZ8)

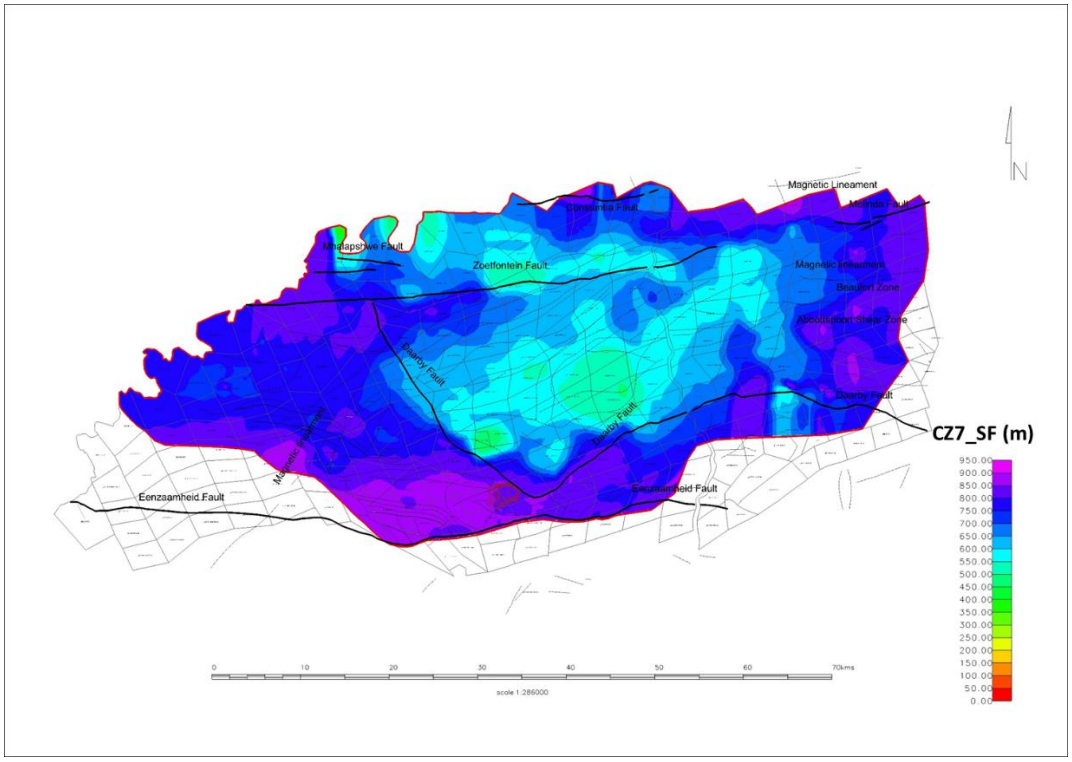

Figure C 6: Isopach Floor map for Coal Zone 7 (CZ7)

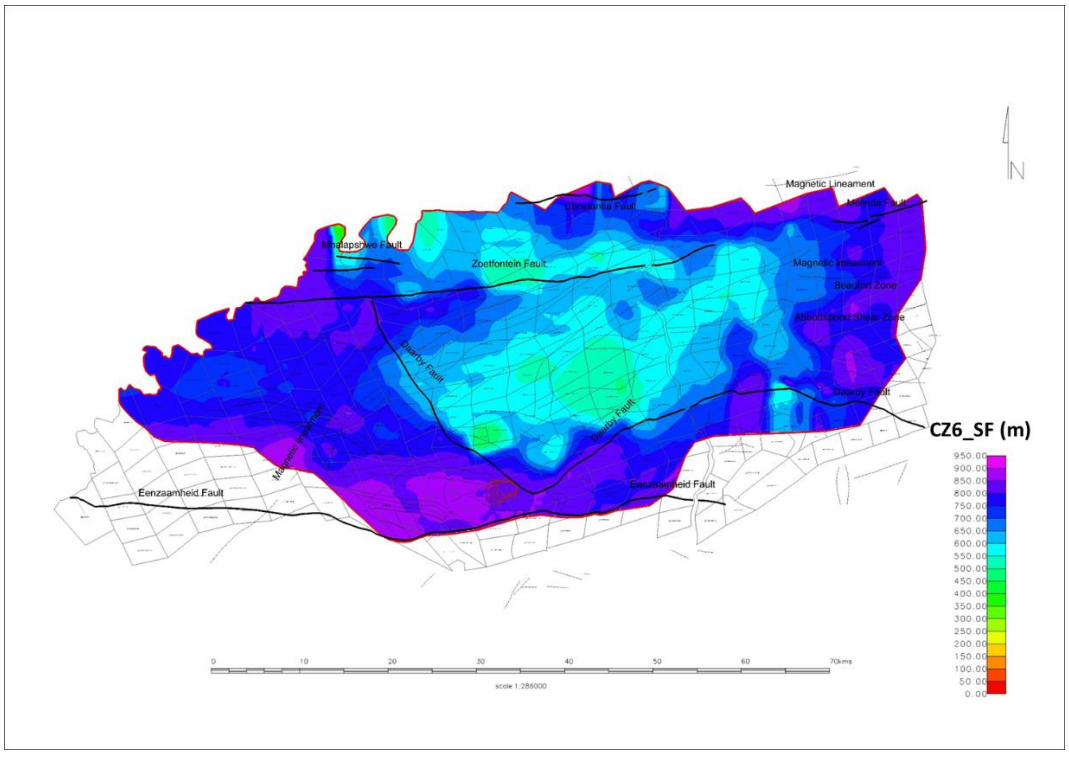

Figure C 7: Isopach Floor map for Coal Zone 6 (CZ6)

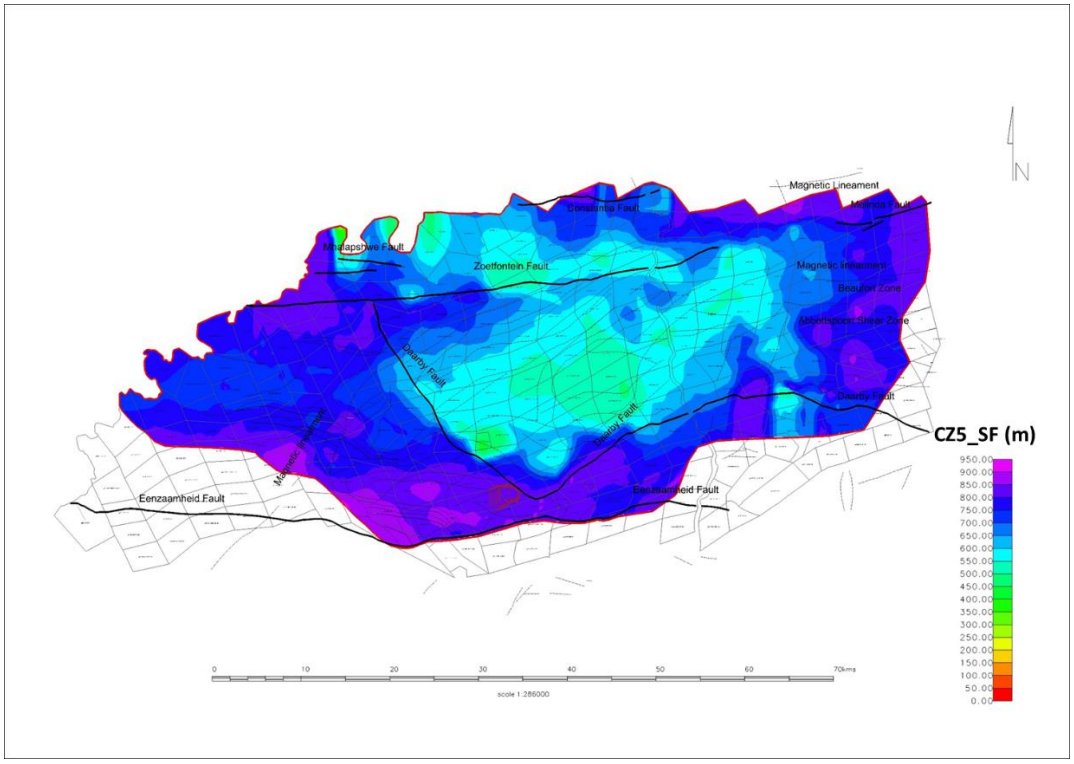

Figure C 8: Isopach Floor map for Coal Zone 5 (CZ5)

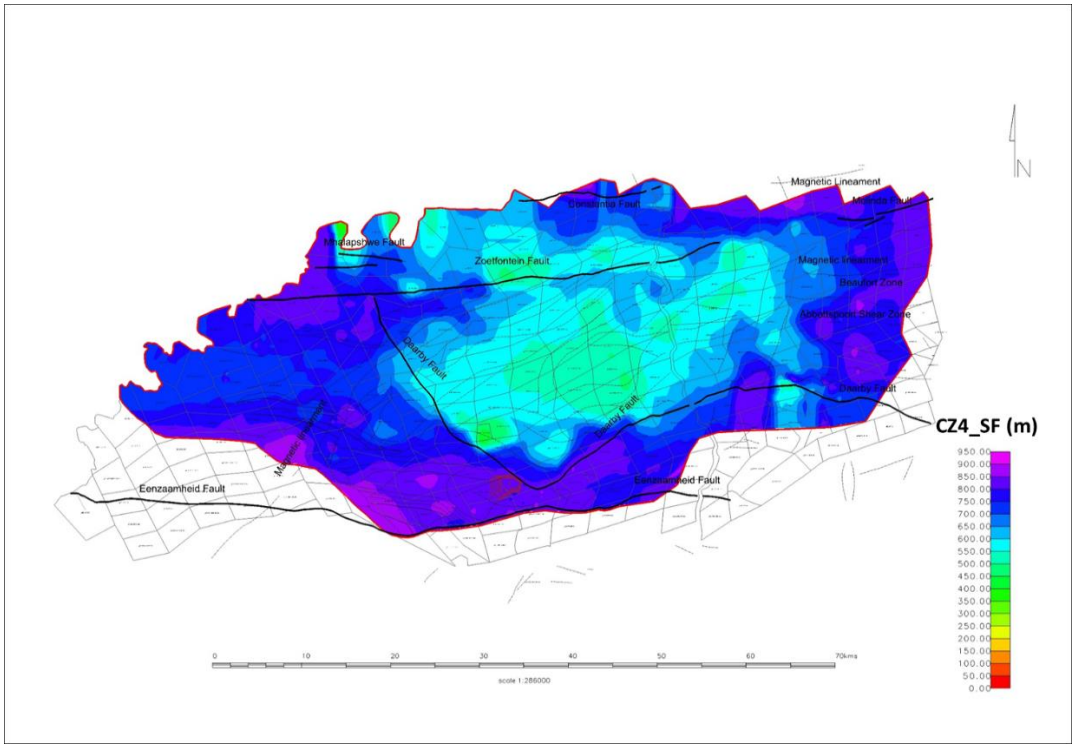

Figure C 9: Isopach Floor map for Coal Zone 4 (CZ4)

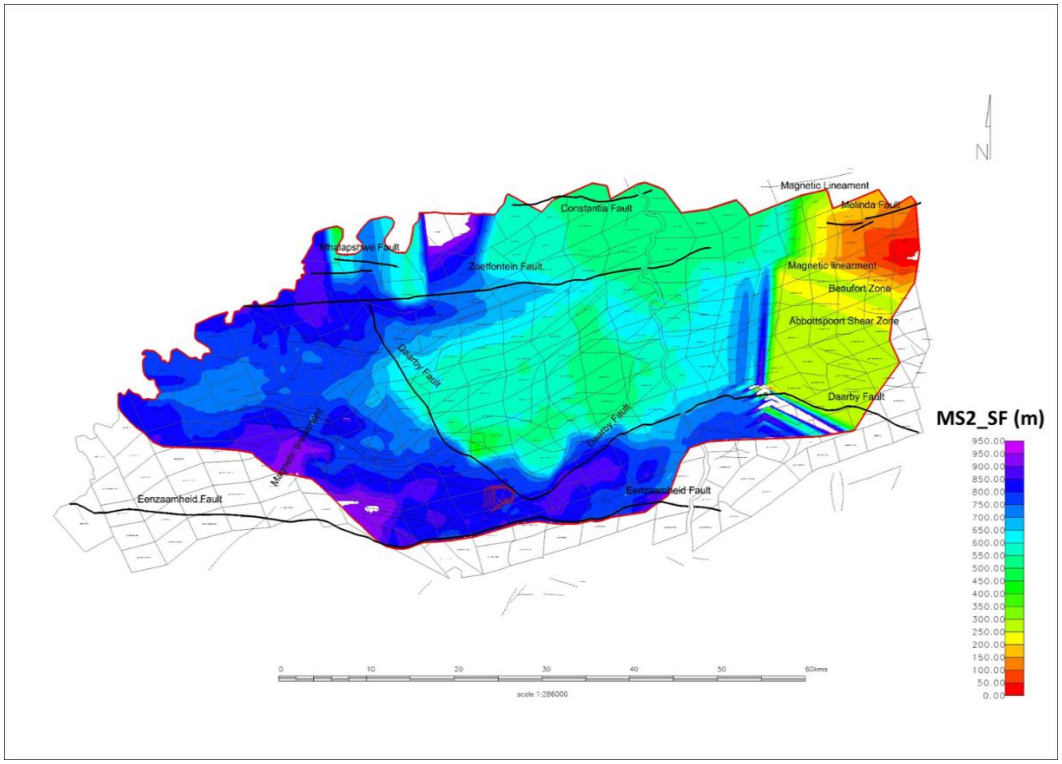

Figure C 10: Isopach Floor map for Mudstone Interburden_2 (MS2)

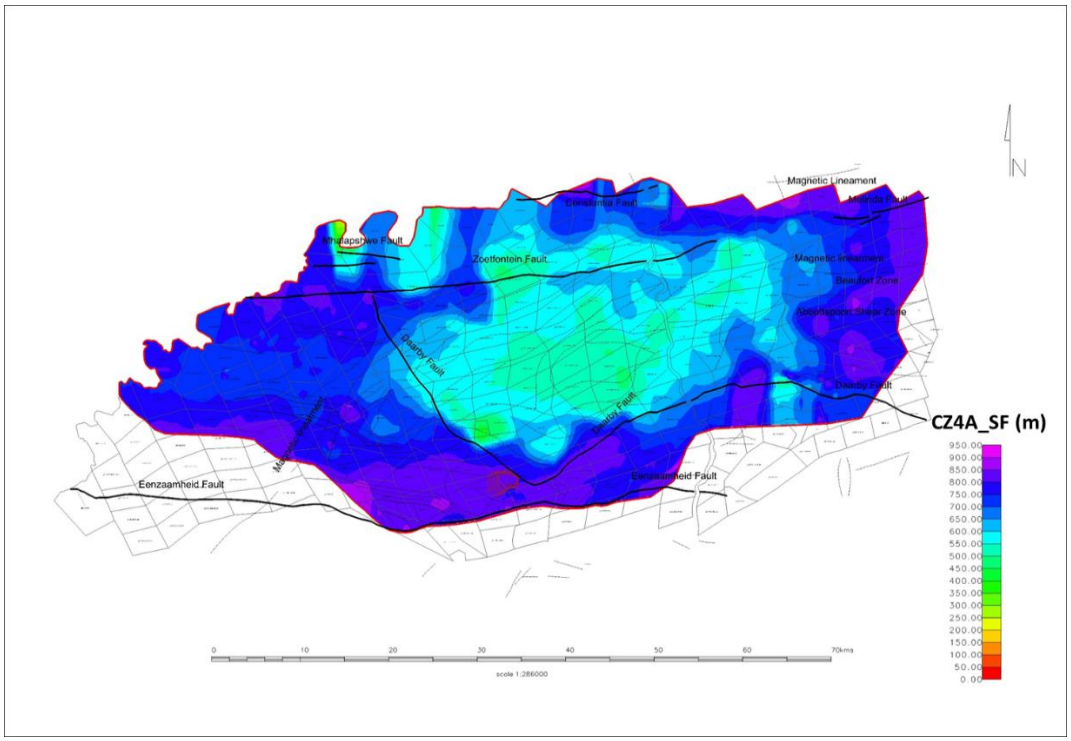

Figure C 11: Isopach Floor map for Coal Zone 4A (CZ4A)

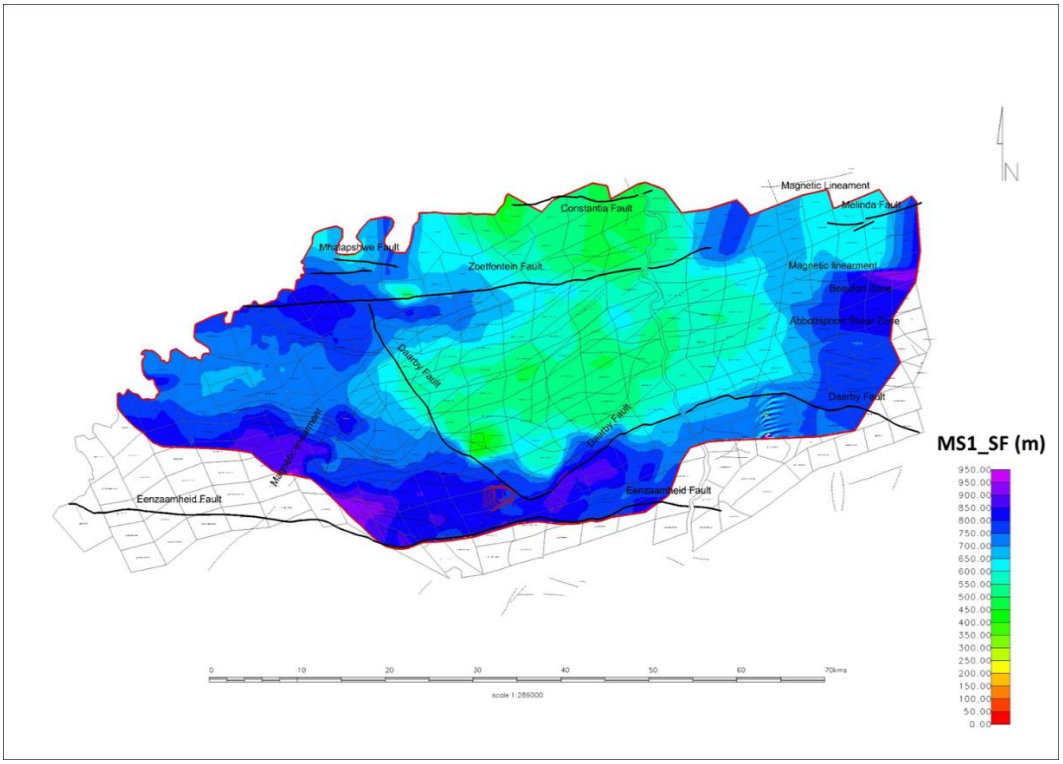

Figure C 12: Isopach Floor map for Mudstone Interburden_1 (MS1)

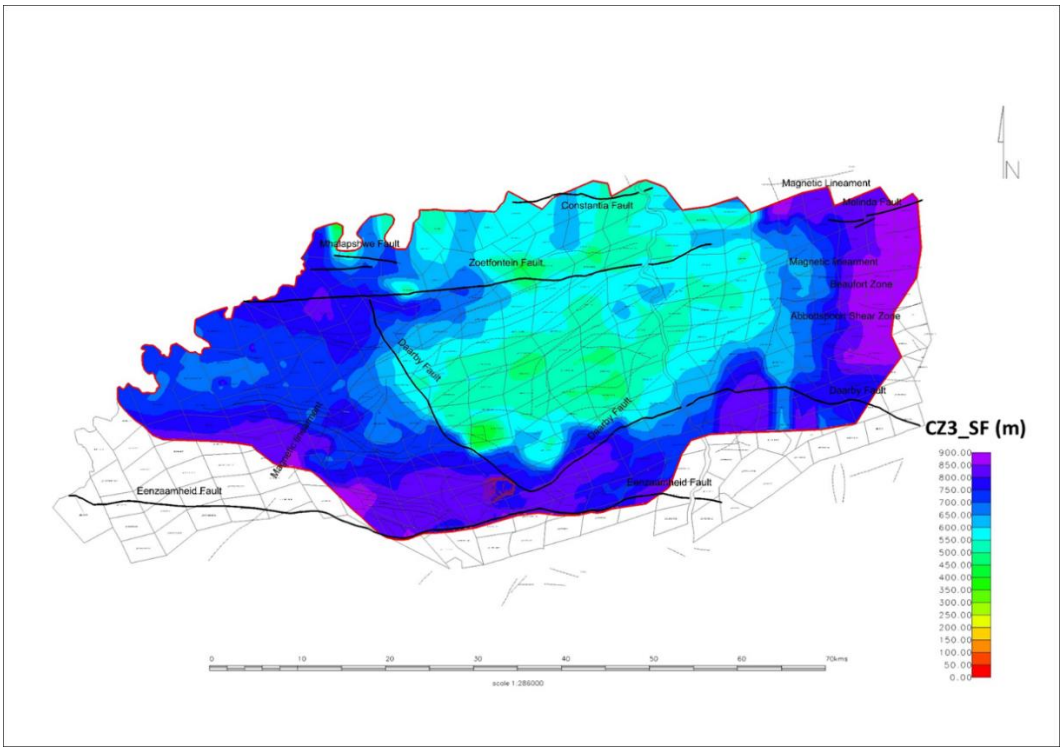

Figure C 13: Isopach Floor map for Coal Zone 3 (CZ3)

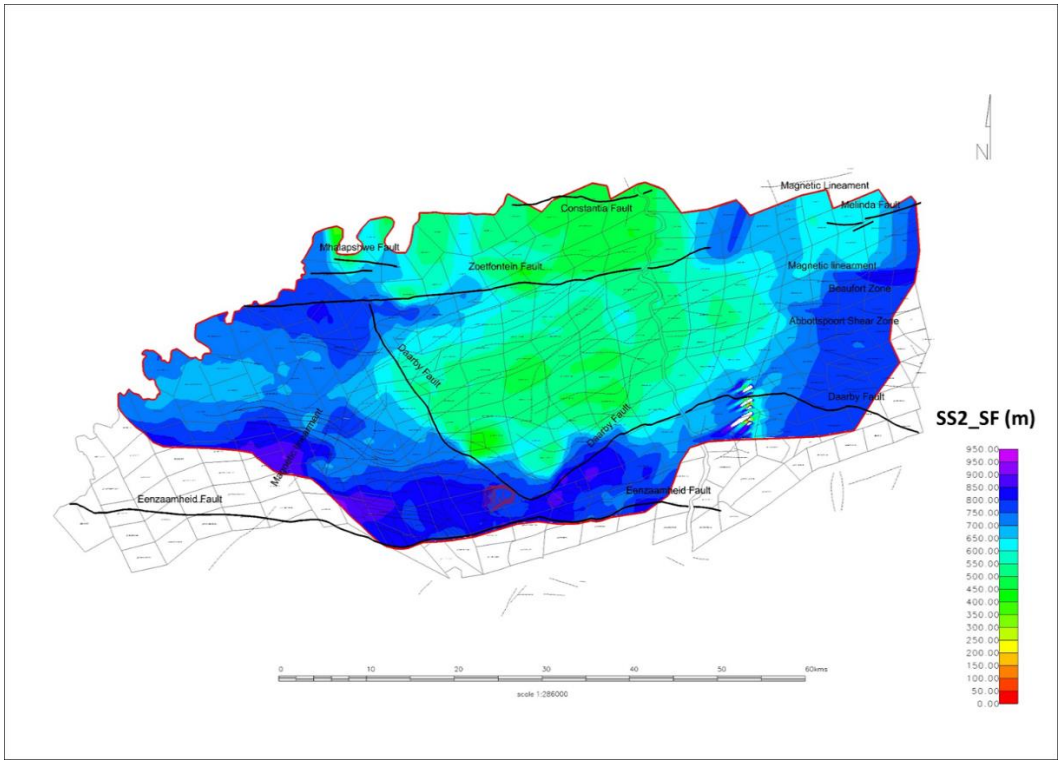

Figure C 14: Isopach Floor map for Sandstone Interburden_2 (SS2)

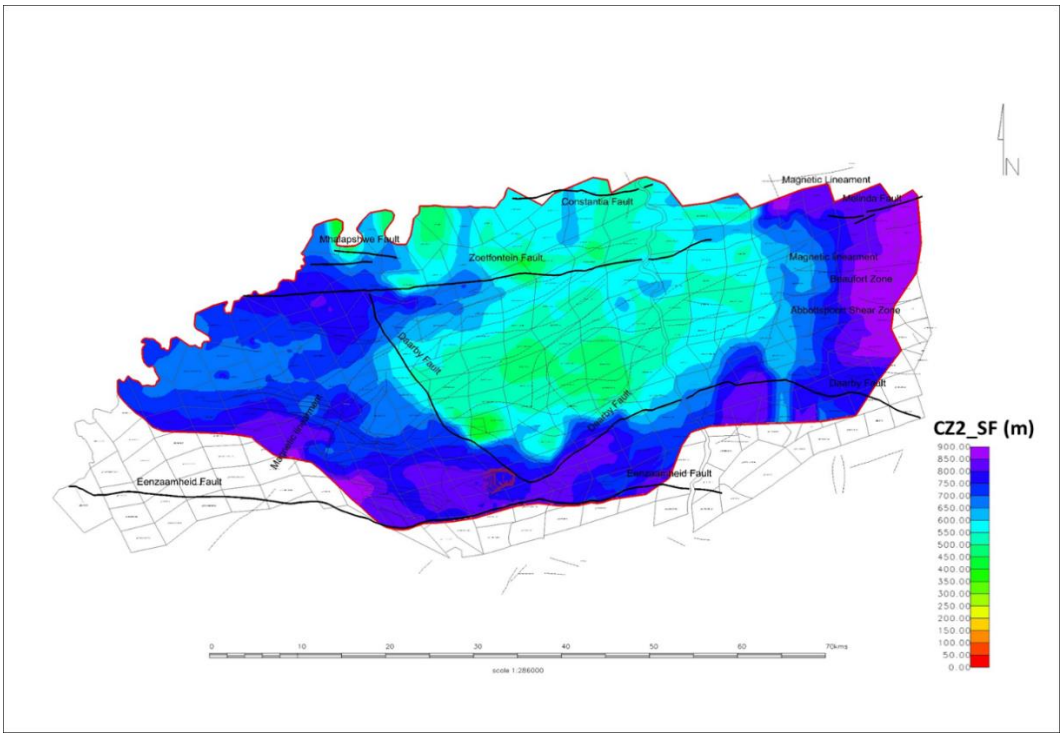

Figure C 15: Isopach Floor map for Coal Zone 2 (CZ2)

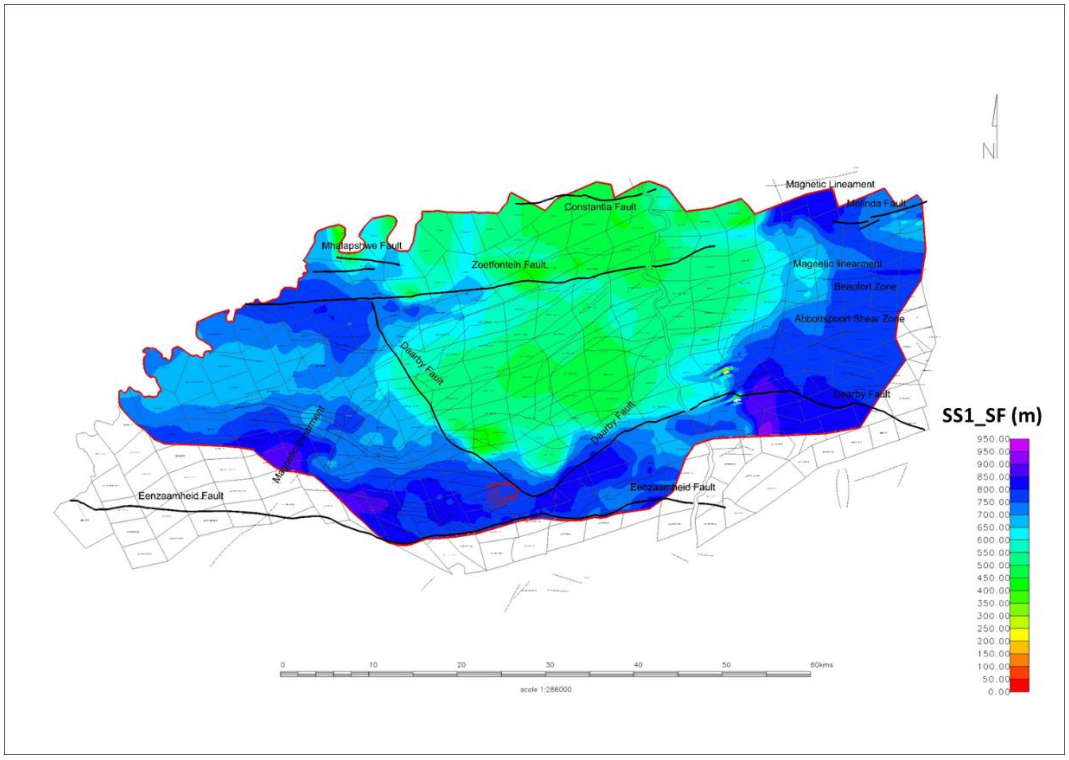

Figure C 16: Isopach Floor map for Sandstone Interburden_1 (SS1)

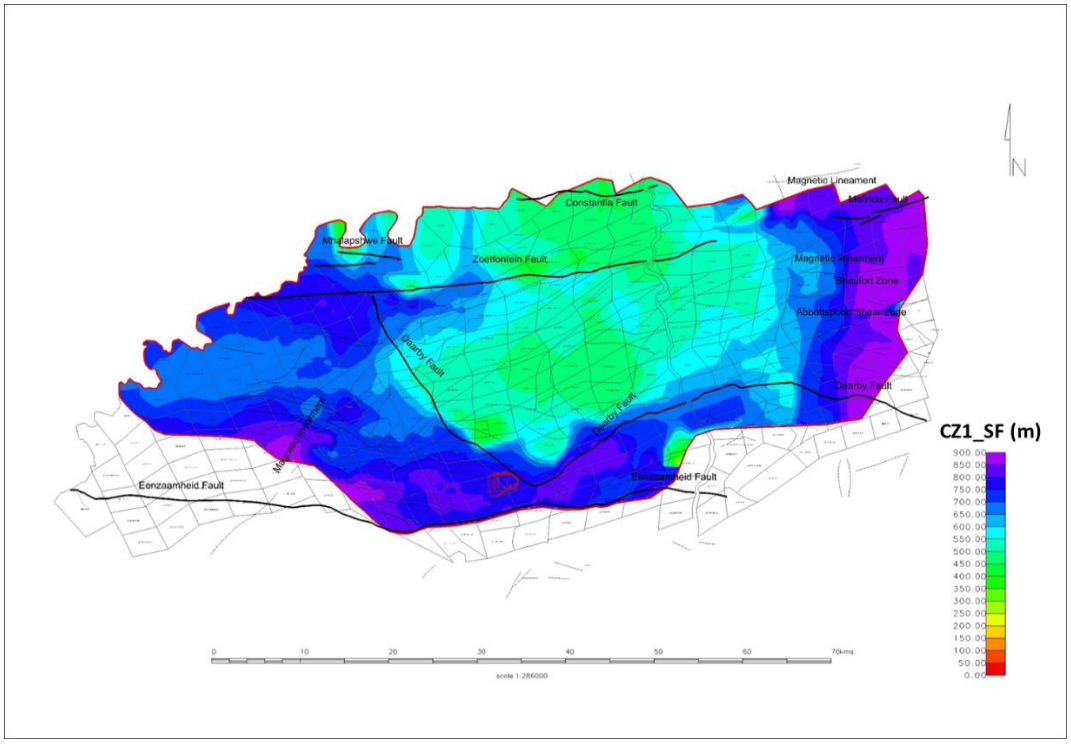

Figure C 17: Isopach Floor map for Coal Zone 1 (CZ1)

APPENDIX D: WATERBERG COALFIELD COLUMNAR SECTIONS

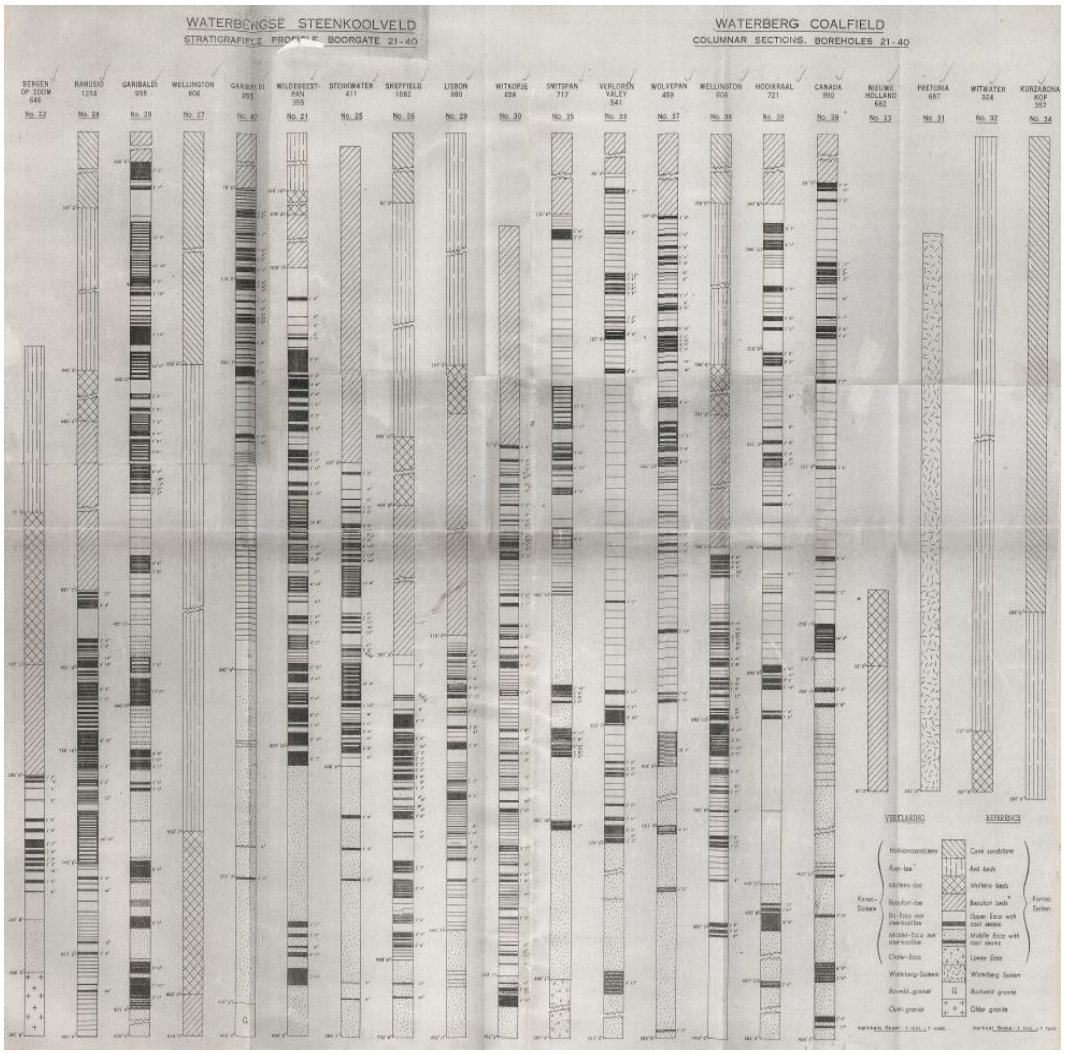

Figure D 1: Waterberg Coalfield columnar sections boreholes 21-40

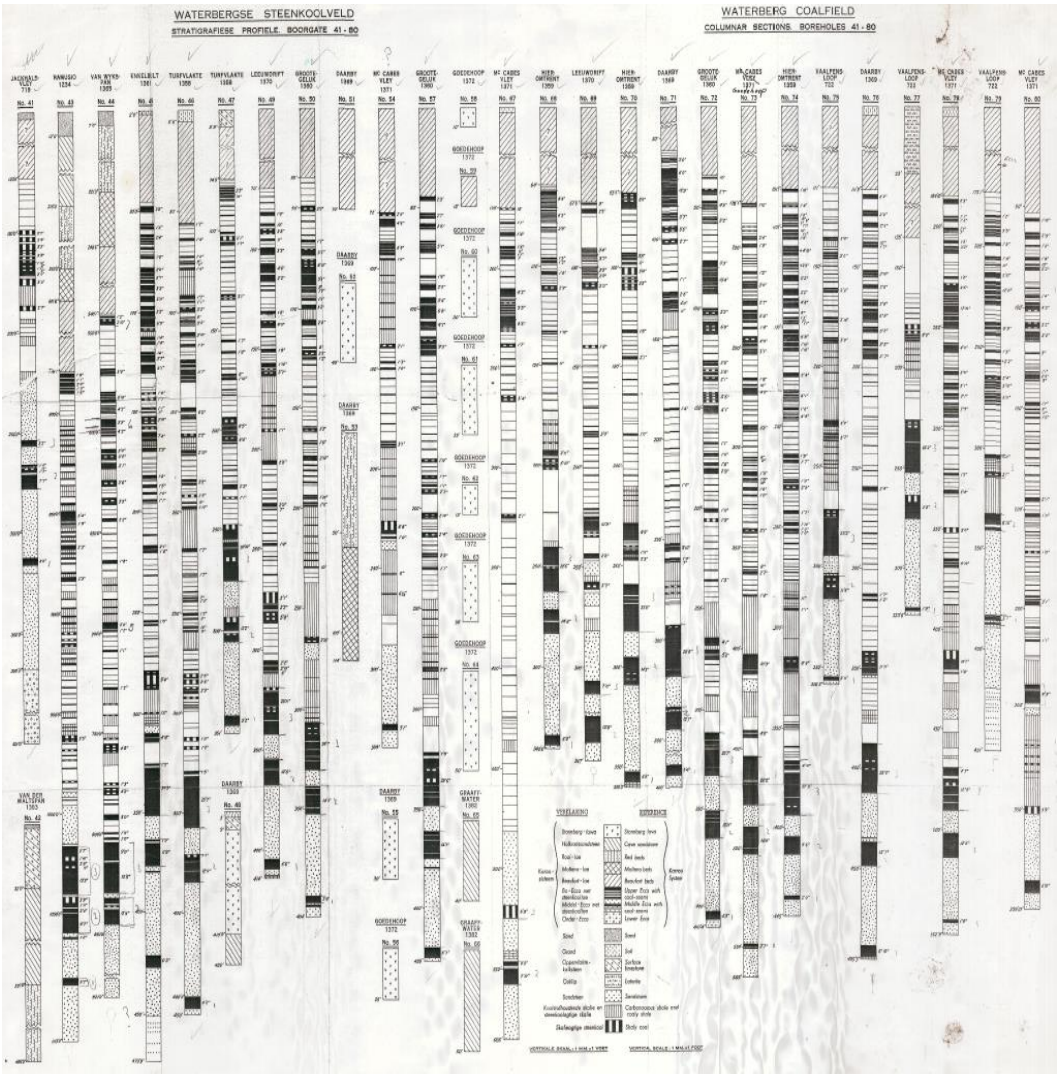

Figure D 2: Waterberg Coalfield columnar sections boreholes 41-80

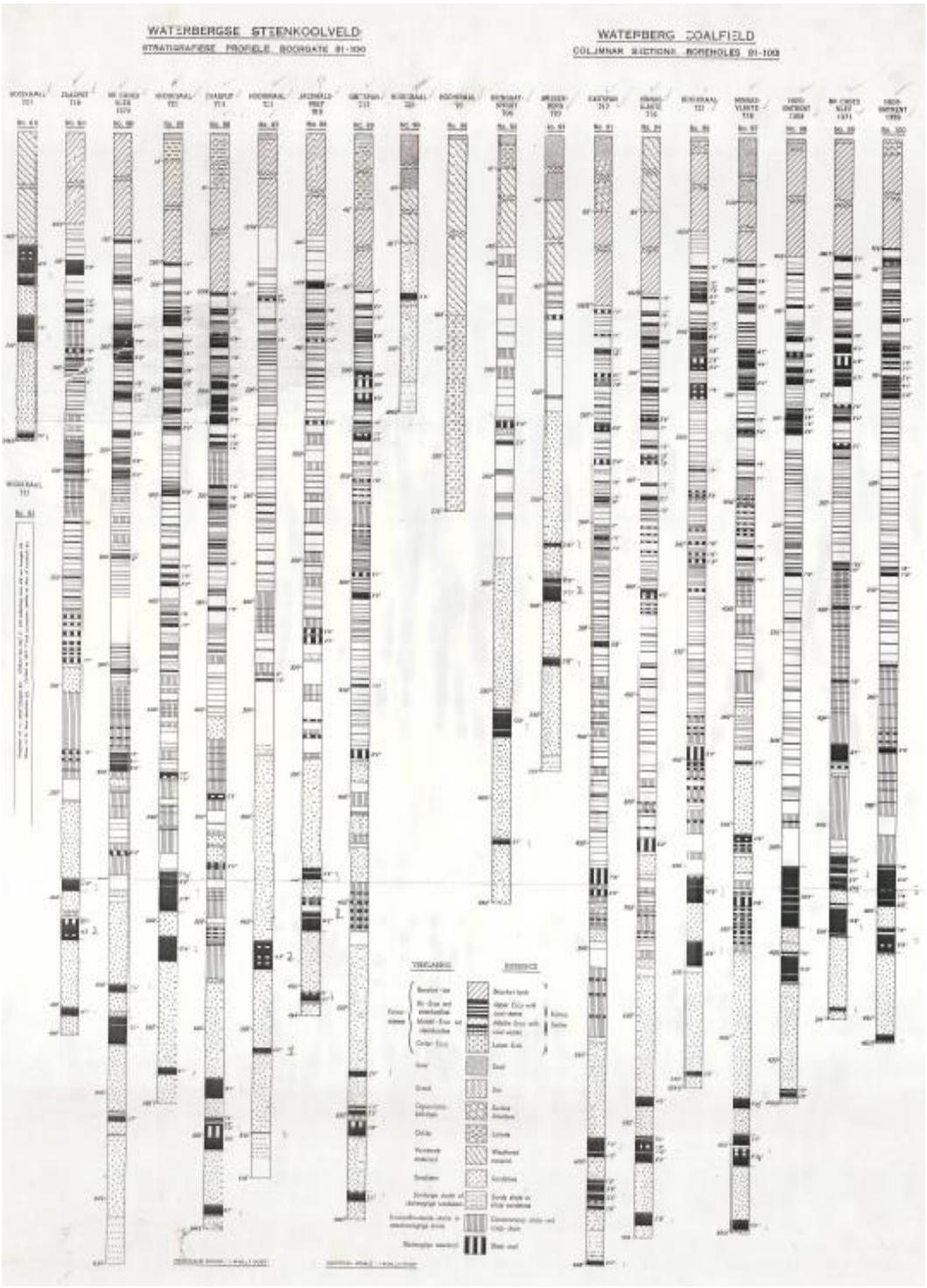

Figure D 3: Waterberg Coalfield columnar sections boreholes 81-100

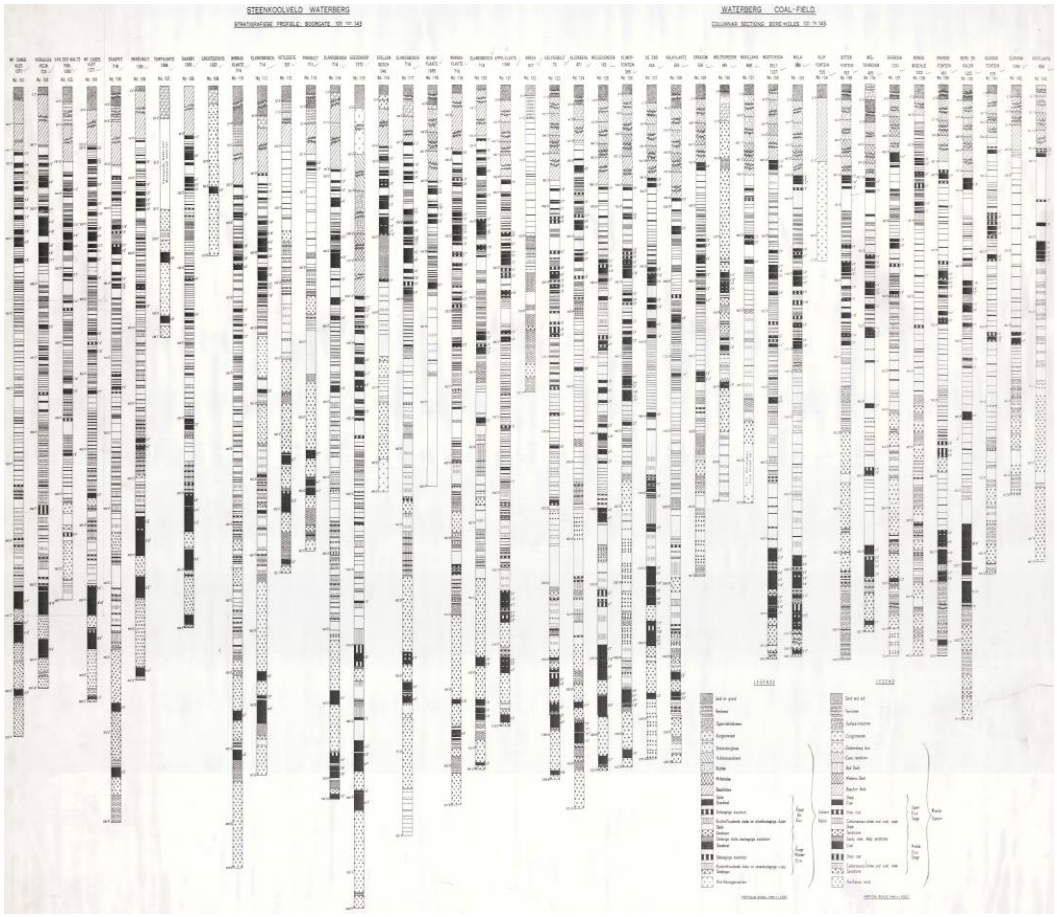

Figure D 4: Waterberg Coalfield columnar sections boreholes 101-143